Impact of Water Quality on Biofilm in Drinking Water Distribution Systems

Chen, L.

DOI
10.4233/uuid:9200ff23-ae62-48be-874b-033118bc3fea

Publication date
2024

Document Version
Final published version

Citation (APA)
Chen, L. (2024). *Impact of Water Quality on Biofilm in Drinking Water Distribution Systems*. [Dissertation (TU Delft), Delft University of Technology]. https://doi.org/10.4233/uuid:9200ff23-ae62-48be-874b-033118bc3fea

Impact of Water Quality on Biofilm in Drinking Water Distribution Systems

Dissertation

For the purpose of obtaining the degree of doctor

at Delft University of Technology,

by the authority of the Rector Magnificus, prof.dr.ir. T.H.J.J. Van der Hagen,

chair of the Board for Doctorates,

to be defended publicly on

Wednesday 1 May 2024 at 12:30 o'clock

by

Lihua CHEN

Master of Engineering in Environmental Engineering, University of Chinese Academy of Sciences, China

Born in Jiyuan, China

This dissertation has been approved by the promotors.

Composition of the doctoral committee:

Rector Magnificus,	Chairperson
Prof.dr. G.J. Medema	Delft University of Technology, promotor
Prof.dr.ir. W.G.J. van der Meer	University of Twente/ Oasen Water Company, promotor
Prof.dr.ir. G. Liu	University of Chinese Academy of Sciences, China / Delft University of Technology, promotor

Independent members:

Prof.dr. J.P. van der Hoek	Delft University of Technology
Prof.dr. J. Boxall	University of Sheffield, UK
Dr. B. Cao	Nanyang Technological University, Singapore
Dr. E. Prest	PWN technologies, The Netherlands
Dr.ir. E.J.M. Blokker	Delft University of Technology
Prof.dr.ir. L.C. Rietveld	Delft University of Technology, reserve member

This research presented in this thesis was performed at the Sanitary Engineering Section, Department of Water management, Faculty of Civil Engineering, Delft University of Technology, The Netherlands. This research was funded by Oasen Water Company and the China Scholarship Council, and also partially supported by the Lamminga Fund.

Cover by: Lihua CHEN, Xin CHEN

Printed by: Proefschrift-aio.nl

ISBN: 978-94-6384-573-1

Email: lhchen91@gmail.com

An electronic version of this dissertation is available at https://repository.tudelft.nl/

Summary

Microbial drinking water quality is of great importance to human health. Drinking water distribution systems (DWDSs) are designed as the final barriers for delivering and maintaining the biosafety of drinking water. Though the drinking water produced is usually safe and clean, it is common that the water quality deteriorates during the distribution. Such deteriorations can be linked to the establishment of biofilm in DWDSs, where the majority of the biomass is residing (> 95%). The formed biofilms are reportedly leading causes of the undesired taste, odor, and color of the drinking water, corrosion of the pipes, decay of the disinfectants, and proliferation of pathogenic microbes, giving rise to public health concerns.

In the Netherlands, the control of the biofilm growth in DWDSs is achieved by producing biostable drinking water with extremely low nutrients (e.g., AOC < 10 µg C/l). On the other hand, water utilities in many countries usually apply chemical disinfectants (e.g., free chlorine, monochloramine) to control the biofilm growth in DWDSs. Nevertheless, biofilm formation is inevitable, regardless of the strategy. Additionally, there is no standard method to monitor the biofilm growth in DWDSs, which makes the understanding and management of DWDS biofilms more challenging. Efforts have been made to explore the biofilm formation and structure through pilot studies. However, most of these investigations have been conducted in a short time frame (e.g., within weeks to a max of 84 days), where the developed biofilms were far from mature and significantly different from those in the real DWDSs. To uncover how biofilm develops and what roles disinfectants play during the biofilm development, a newly-built pilot system was followed for a 64-weeks period under different disinfection regimes: no disinfectants (NC), free chlorine (FC), and monochloramine (MC) (**Chapter 2**). The results showed that residual disinfectants presented intensive suppression of the biofilm growth and shaped the biofilm communities. Specifically, MC exhibited stronger suppression of the biofilm activity (i.e., ATP), whereas FC expressed intense selection pressure on the microbes and established more homogenous and less complex biofilm community, with Proteobacteria comprising on average 82% of the relative abundance. The temporal trends highlighted the essential developmental stages in biofilm formation from initial colonization to accumulation and selection and stabilization, which occurred at different rates under each of the conditions, and were associated with significant dynamic changes in biofilm bacterial communities. Reaching stabilization took longest in the MC condition (> 64 weeks), followed by the NC (~ 36 weeks) and FC (~ 19 weeks) conditions. Holistically, the early stages in the biofilm formation in the NC condition were primarily dominated by stochastic processes where colonizers originating from treated water randomly attached to and settled on the pipes, while

deterministic processes progressively increased in their relative contributions at the end of the accumulation stage and became predominant at the later stages. In the MC condition, the biofilm succession was governed by stochastic processes during the entire test, even though some deterministic processes occurred during the accumulation stage. Conversely, in the FC condition the biofilm succession was driven by deterministic processes already from the initial development stage.

DWDSs are highly dynamic ecosystems, where the liquid (i.e., bulk water, suspended particles) and solid (i.e., biofilm, loose deposits) phases interact intensively during transport of the water from treatment to consumer. The cells and/or particles that were introduced with the treated water may attach to and/or settle on the pipes, forming biofilm/loose deposits when the hydraulic forces are weak. Conversely, the biofilm/loose deposits might release cells/particles to the bulk water during hydraulic disturbances, affecting the drinking water quality negatively. The hydraulic conditions in DWDSs are very complex and dynamic. They exhibit daily patterns, with high flow rates at high water demand periods (e.g., morning and/or evening hours) and long stagnancy or low flows during the night. However, most monitoring occurs using grab samples at one point in time. Thus, continuous online sampling is required to obtain a representative image of the particles and microbes in drinking water. In **Chapter 3**, a novel online monitoring and sampling system (OMSS) was developed to investigate the spatiotemporal variations of the planktonic and particle-associated bacteria in an unchlorinated DWDSs. The 16S rRNA gene sequencing combined with SourceTracker2 was used to trace and reveal the origin of the changes in the planktonic and particle-associated bacteria, assigning sampled biofilm and loose deposits as sources. The results showed that, spatially, the particle loads significantly increased from treatment plant within distribution networks, while the trend in the quantity of the particle-associated bacteria was the opposite. Similar to the trend of particle loads, the number of the observed OTUs in both planktonic and particle-associated bacteria increased from the treatment plant within the distribution network. The spatial results implied a dominant role of sedimentation of particles entering the DWDS from the treatment plant, while the observed increases in particles and the associated bacteria primarily originated from the distribution network, which were confirmed by the increased contributions from loose deposits and biofilm determined by SourceTracker2. Temporally, daily peaks in the water quality, including particle-associated bacterial quantity, observed operational taxonomic unit (OTU) number, and contributions of biofilm and loose deposits, were sensitively captured during the high water demand (morning/evening peaks). The temporal results revealed clear

dynamic interactions between the liquid (i.e., bulk water, suspended particles) and solid (i.e., biofilm, loose deposits) phases in DWDSs.

Driven by increasingly stringent drinking water regulations and challenges to drinking water quality, efforts are underway to further improve water quality. These initiatives include source water switching, upgrading treatment processes, and implementing changes to disinfectant strategies. Such actions change the quality and composition of the treated water that enters the DWDS. This may have transition effects, which in this thesis refers to the water quality deteriorations contributed by the release of cells and particles from biofilm and/or loose deposits due to the irregular changes in supply-water quality. It is largely unknown whether, where and when the transition effects will happen. In **Chapter 4**, transition effects were investigated through characterizing the particles before (T_0), during ($T_{3\text{-weeks}}$) and after ($T_{6\text{-months}}$) introducing additional treatment steps (softening, second rapid sand filtration and adding carbon dioxide) to the existing treatment. The results showed that the upgraded treatment significantly improved the water quality after 6 months' time. However, significant water quality deterioration was observed at the initial stage ($T_{3\text{-weeks}}$) when the quality-improved treated water entered into the network. This manifested as a significant increase in total suspended solids (TSS) by 50-260%, active biomass (ATP) by 95-230%, and Mn by 130-250%. Furthermore, pyrosequencing results revealed sharp differences in microbial community composition and structure of the bacteria associated with particles between T_0 and $T_{3\text{-weeks}}$, implying the potential contributions from biofilm or loose deposits in the DWDS. Interestingly, the domination of *Nitrospira* spp. and *Polaromona*s spp. in the distribution system at $T_{3\text{-weeks}}$, which were detected at rather low relative abundance at treatment plant, further confirmed the potential contributions from biofilm or loose deposits.

Though the study in **Chapter 4** confirmed the occurrence of the transition effects, the question how fast/how long the transition effects will occur/last, where the deteriorations originate from, and what actions can be carried out to minimize the transition effects is not clear. The sampling was conducted in a relatively short time frame (i.e., 6 months), with only a few time points (i.e., T_0, $T_{3\text{-weeks}}$, $T_{6\text{-months}}$) and without the collection of biofilm and loose deposit samples. Additionally, as what we can see from the results from **Chapter 3**, it could be imagined that the transition effects might be enhanced during high water demand when shear forces are high. In order to fill the knowledge gaps, the OMSS was applied, accompanied with SourceTracker2, in an unchlorinated DWDS where partial RO was introduced (**Chapter 5**). The study was conducted before (T_B), immediately after (T_0), one month (T_{1M}), two month (T_{2M}), one year

(T_{1Y}) and two years (T_{2Y}) after the partial RO introduction. Noticeably, significant transition effects in DWDS were captured right after the RO introduction, with increases in the particle loads, bacterial quantity, community diversity, and significant differences between bacterial communities in particles at treatment plant and distribution network. The disturbances lasted one month until T_{1M}, after which they ceased to be observable around T_{2M}. The captured deteriorations were confirmed by the increased contributions of loose deposits and biofilm (both the number of the immigrants and their abundance) at T_0 and T_{1M} determined by SourceTracker2 and neutral community model. While the peak transition window spanned about one month, it took considerably longer, until one year (T_{1Y}) and two years (T_{2Y}) later, for the microbial ecology to re-stabilize and for improvements in water quality to become noticeable. In addition, the peaks in the water quality deteriorations were enlarged during the high water demand (morning/evening peaks), which implies that current monitoring could potentially underestimate the extent of the quality deterioration. Remarkably, the observation that loose deposits contributed more to the transition effects than biofilm challenges the traditional standpoint, and provided new insights into the management of the transition effects, where the risks of the transition effects can be largely reduced by conducting flushing before the introduction of treatment changes to remove the loose deposits. In light of the destabilization caused by the changed water quality, flushing with new-quality water might be more rewarding.

To conclude, through conducting studies at both field and pilot scales, the effects of the (changes in) operational conditions on the microbial drinking water quality in DWDSs were comprehensively explored. The findings in the thesis offer novel insights into the drinking water quality management. The knowledge gained from investigating the biofilm succession dynamics under different disinfectant regimes has significantly deepened our understanding of managing drinking water biofilms. These insights serve as valuable information when making informed decisions about the appropriate strategies to employ. The implementation of the developed OMSS is capable of capturing both periodic and aperiodic changes in drinking water quality, making it an essential tool in minimizing assessment deviations and ensuring accurate evaluations of drinking water quality. Moreover, the established methodology holds promise for application in various systems, including those that utilize chlorination. By identifying and characterizing the transition effects resulting from changes in supply water quality, such as treatment upgrades or the introduction of reverse osmosis, the study highlights the significance of considering these effects in water management practices. These observations underscore the

importance of addressing the impact of transition effects on drinking water quality and provide practical implications for minimizing their negative consequences.

Table of Content

Summary I

Chapter 1: Introduction 1

Chapter 2: Long-term Succession Dynamics in Drinking Water Distribution System Biofilms with and without Residual Disinfectants 17

Chapter 3: Capturing and Tracing the Spatiotemporal Variations of Planktonic and Particle-Associated Bacteria in an Unchlorinated Drinking Water Distribution System 45

Chapter 4: Assessing the Transition Effects in a Drinking Water Distribution System Caused by Changing Supply Water Quality: An Indirect Approach by Characterizing Particles in the Bulk Water 81

Chapter 5: Transition Effects in an Unchlorinated Drinking Water System Following the Introduction of Partial Reverse Osmosis 113

Chapter 6: Conclusions and Outlook..... 163

Bibliography 179

Acknowledgement 190

List of Publications 192

Curriculum Vitae 194

Chapter 1

Introduction

1.1 Water quality in drinking water distribution systems (DWDSs)

The supply of chemically and microbiologically safe as well as aesthetically pleasing drinking water is a long-standing challenge worldwide. Drinking water distribution systems (DWDSs) are key components for guaranteeing safe drinking water, which are designed to act as a protective barrier to prevent the ingress and growth of microorganisms during the transportation (Bautista-de los Santos et al., 2016b). Though the majority of the pollutants (e.g., particles, microorganisms, metal elements) in raw water have been removed by multiple drinking water treatment processes, the water leaving the treatment plant is literally not sterile, entering the DWDSs associated with low concentrations of nutrients, particles, metal elements, and microorganisms (Liu et al., 2017b; Liu et al., 2018; Prest et al., 2016b).

Planktonic microbial cells and/or microbes attached to particles attach to and/or settle on the inner surfaces of pipes within DWDSs, leading to the formation of biofilm and/or loose deposits. These substrates, identified as microbial hotspots in previous studies, are closely tied to water quality deterioration. Biofilms and loose deposits have been found to impact drinking water characteristics, affecting turbidity, taste, odor, and color (Liu et al., 2016b). Additionally, they contribute to residual disinfectant decay, bacterial growth, act as a niche for waterborne pathogens, prolong pathogen survival, and promote pipe corrosion (Cruz et al., 2020; Gomez-Smith et al., 2015; Servais et al., 1995; Tang et al., 2006; Waak et al., 2019a; Wingender and Flemming, 2011). Differing from loose deposits that settle loosely on the pipe bottom, amenable to control by reducing particles in the treated water and removal through flushing once established (Carrière et al., 2005; Friedman et al., 2002), biofilm exhibits a distinct characteristic. Biofilm tightly attaches to pipe surfaces, rendering it resistant to easy removal by flushing once formed (Fish et al., 2017; Liu et al., 2016b). Hence, it is crucial to proactively inhibit the formation of biofilm and understand the effects of biofilm on microbial drinking water quality.

In practice, two fundamental approaches were adopted worldwide to control the biofilm growth in DWDSs, including limiting the nutrients in the supply water (Smeets et al., 2009) and maintaining a disinfectant residual (e.g., free chlorine or monochloramine) in DWDSs (Dai et al., 2020; Waak et al., 2019a). Given the high requirements to produce bio-stable drinking water, such as the substantial nutrient removal by drinking water treatment and well-developed choice of materials and maintenance conditions to DWDSs, most of the countries (e.g., China, the US) still apply residual disinfectants to limit the growth of the microbes in DWDSs, unlike several

European countries (e.g., the Netherlands, Denmark, parts of Germany, Austria, Switzerland) which distribute bio-stable drinking water without disinfectants. Nevertheless, none of the methods mentioned above possesses the capability to prevent biofilm formation in DWDSs. Biofilms have been widely found in both unchlorinated and chlorinated DWDSs, ranging from 10^4 to 10^8 cells/cm^2, and 10^2 to 10^4 pg ATP/cm^2 (Liu et al., 2020; Prest et al., 2016a). While endeavors have been undertaken to investigate biofilm formation and the impact of disinfection regimes (Fish and Boxall, 2018; Fish et al., 2020), a significant limitation arises from the fact that most studies have been confined to short durations. This limitation is noteworthy as biofilm formation is a protracted, long-term process, evolving over months or even years. Furthermore, the factors driving biofilm succession remain largely unknown, possibly attributable to the limited application of microbial ecology theory in the context of drinking water systems. These limitations impede our comprehension of biofilm growth in DWDSs and the development of effective strategies for biofilm management.

Under the regular water supply conditions, DWDSs function as complex dynamic ecosystems where liquid (i.e., bulk water, suspended particles) and solid (i.e., loose deposits, biofilm) phases interact ubiquitously and are in a semi-equilibrium. The water leaving from the treatment plant contains certain amount of cells, particle, and nutrients, leading to the formation of biofilm and loose deposits. Previous studies primarily focused on the bulk water and biofilm phases and their interactions, with particle-associated bacteria and loose deposits being long-term neglected. This may result in underestimations of water quality changes, as particles and loose deposits also carry a high amount of cells. Apart from the constant contributions (e.g., nutrients, cells, particles, elements) from the treated water leaving the treatment plant, the growth of bacteria in biofilm and water and/or the release of the attached bacteria from biofilm and/or loose deposits into the bulk water might occur during the distribution due to the long water residence time or changing hydraulics, resulting in the deterioration of the drinking water quality (Bautista-de Los Santos et al., 2016a; Douterelo et al., 2013; Lehtola et al., 2006). Conventionally, the monitoring of drinking water quality in DWDSs is commonly on the basis of grab sampling, which is low resolution and labor intensive. In this context, it is challenging to capture the biofilm (as this is only seen through the lens of the water samples) and the periodic changes in the drinking water quality and generate a comprehensive assessment of drinking water quality. Online monitoring tools are expected to overcome the above-mentioned challenges. While technologies, such as the online adenosine triphosphate (ATP) measurements and online flow cytometry, have been applied to uncover the spatial and temporal changes in

microbial water quality in drinking water systems (Favere et al., 2021), there remains a knowledge gap concerning the causes/sources of the water quality variations. There is a pressing need to develop a methodology with the potential to achieve real-time monitoring of drinking water quality, encompassing dynamic interactions among all the phases (i.e., bulk water, suspended particles, biofilm, and loose deposits), and to trace the sources of deteriorations.

Driven by the progressively strict drinking water regulations, many efforts have been made to further improve the drinking water quality, involving the upgrading of the treatment processes, the switching of the source water, the changing of the disinfectant regimes, etc.. For instance, efforts have been made to apply alternative source waters in the light of water costs or shortages. The most representative examples are the South-to-North Water Diversion project in 2008 in Beijing where the city switched to better source water transported 1400 km from southern China (Li et al., 2010) and the Flint water crisis in 2014 in US where Flint changed its water source from treated Detroit Water and Sewerage Department water (sourced from Lake Huron and the Detroit River) to the Flint River (Hanna-Attisha et al., 2016). However, these changes caused severe deteriorations of the drinking water quality, where discolorations were found in the majority of the taps in Beijing and high lead concentrations in the drinking water in Flint. It is worth noting that these deteriorations caused by the changes in source water might be difficult to be captured due to the inherent dynamics in drinking water quality and the dilution effects by the large volume of the drinking water in DWDSs. Therefore, there is an urgent need for new approaches that provide more representative monitoring and comprehensively characterize potential deteriorations resulting from alterations in source water quality or other changes in DWDSs.

1.2 Biofilms in DWDSs

1.2.1 Biofilm growth

Microbes are ubiquitous and abundant in DWDSs. In addition to existing in a planktonic state (i.e., in the bulk-water), microorganisms can be embedded in biofilms in DWDSs even in the presence of disinfectants and regardless of pipe materials (Figure 1-1A-D) (Liu et al., 2016b). In DWDSs, biofilms are the predominant mode of microbial growth (Flemming, 1998). The biofilm in DWDSs can reach a cell concentration of 10^8 CFU cm^{-2} (Batté et al., 2003), 10^7 cells cm^{-2} (Lehtola et al., 2006) or 10^3 pg ATP cm^{-2} (Lehtola et al., 2006). The formed biofilms can be problematic, posing public health concerns. It was reported that biofilms favored the

deposition of elements such as iron (Fe), manganese (Mn) and calcium (Ca) in DWDSs (Liu et al., 2017a; Sly et al., 1990), which is responsible for the occurrence of discoloration in extreme cases. The biofilms can also protect harbored bacteria from unfavourable environment (e.g. low nutrients, chlorination, high shear stress, etc.) due to the presence of the extracellular polymeric substances (EPS) matrix, affect the taste and odor of the water, contribute to the decay of residual disinfectants, and cause the corrosion of the pipes (Batté et al., 2003; Liu et al., 2017a). Noticeably, opportunistic pathogens (OPs), which commonly possess high adhesion traits to surfaces, were demonstrated to be ubiquitously harboured by biofilm (Xing et al., 2018b). For instance, *Legionella spp.*, (and the opportunistic pathogenic species *Legionella pneumophila*), which are the leading cause of Legionellosis, are frequently detected in drinking water biofilms (Richards et al., 2015). Besides serving as a reservoir for bacteria and OPs, biofilm was indicated to be a significant sink for antibiotic resistance genes in aquatic environments (Guo et al., 2018), where horizontal gene transfer might occur easily due to its high cell density and close cell-to-cell proximity.

The formation of biofilm is a succession process (Douterelo et al., 2018b; Martiny et al., 2003), initiated by adsorption of certain species to pipe surfaces as bulk water flow through the DWDSs (Figure 1-1E). This is followed by the production of EPS by these attached cells, bacterial proliferation, ultimately resulting in the development of mature biofilms. Subsequently, these mature biofilms undergo dispersion/detachment, entering a new life cycle (Liu et al., 2016b). Efforts have been undertaken to investigate the temporal dynamics of biofilm in DWDSs. For instance, studies have focused on monitoring the growth patterns, structural changes, and microbial compositions of biofilms over time to gain insights into their evolution within the distribution network (Chen et al., 2023; Douterelo et al., 2018b; Fish et al., 2015). However, most studies have been conducted over short durations (e.g., 12 weeks), while the maturation of biofilm may span months or even years. As reported, biofilm maturation can take up to 3 years (Martiny et al., 2003). To enhance our comprehension of biofilm behavior within these systems, it is essential to gather long-term series data on the attached microbial phase. Furthermore, there are no standard methods or regulations to control or monitor the biofilm growth in DWDSs.

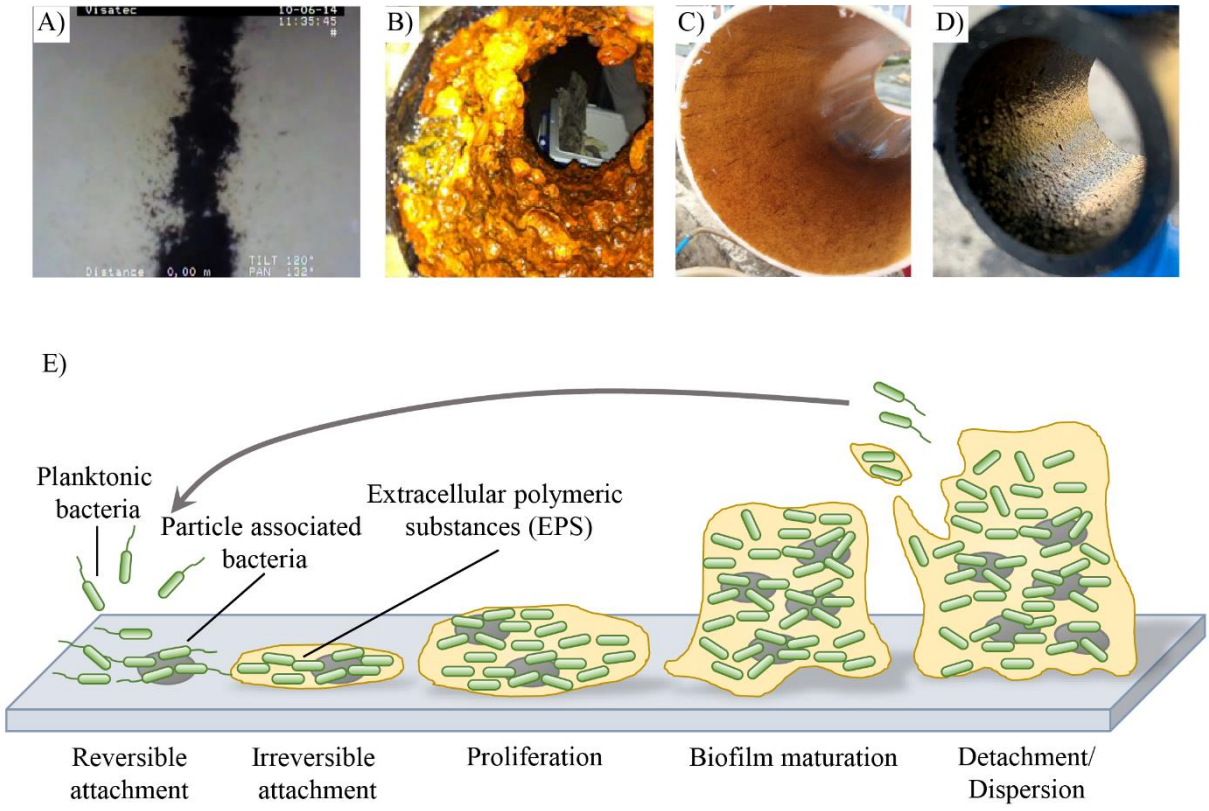

Figure 1-1. *Biofilm formed on pipes with different materials in drinking water distribution systems. (A) inner view of a distribution pipe under normal operation. The yellowish part represents biofilm, while the blackish part on the bottom represents loose deposits (Liu et al., 2017b); (B) cast iron pipe with scaling (Liu et al., 2017b); (C) PVC pipe with biofilm; (D) PE pipe with biofilm. (E) Biofilm life cycle in DWDSs. Modified based on the review from Liu et al. (Liu et al., 2016b).*

1.2.2 Effects of disinfection regimes on biofilm growth

Two fundamental approaches are used to limit the microbial growth in DWDSs, including i) distributing biologically stable drinking water without residual disinfectants (Smeets et al., 2009) and ii) maintaining residual disinfectants during the transportation (Dai et al., 2020; Waak et al., 2019a). Typically, countries mainly in Western Europe (e.g., Netherlands, Denmark, and Switzerland) distribute drinking water without residual disinfectants, given the production of harmful by-products during disinfection. The bacterial growth was inhibited by minimizing nutrient availability (AOC, < 10 µg/L) in DWDSs using high-quality source waters and/or multi-barrier treatments (Smeets et al., 2009). Alternatively, disinfectant residuals were commonly maintained during drinking water distribution to suppress the re-/post-growth of microorganisms in many countries including the US and China (Dai et al., 2020; Waak et al., 2019a). Free chlorine was the most popular disinfectant adopted worldwide in drinking water

industries (Dai et al., 2020; Liu et al., 2016b), owing to its low-cost and easy-get properties. Free chlorine is a highly reactive oxidizing agent, and it is known to be effective in permeabilizing bacterial membranes and causing lethal DNA damage. While effective in killing cells, chlorine is incapable of the complete elimination of the biofilms in DWDSs (Lee et al., 2018). Furthermore, it is noteworthy that the presence of chlorine may lead to the enrichment of chlorine/antibiotic-resistant bacteria in biofilms (Li et al., 2023; Miller et al., 2015; Shi et al., 2013; Zhu et al., 2014) and contribute to the formation of carcinogenic disinfection by-products (Fielding and Farrimond, 1999; Richardson, 2003). Monochloramine has been applied as an alternative to control the microbial growth in DWDS, given its less generation of disinfection by-products and better penetration into the biofilms in comparison to free chlorine application (Lee et al., 2018; Lee et al., 2011). Monochloramine can react slowly with DNA and RNA with little damage to bacterial membranes, but has the ability to penetrate deeper into the biofilm matrix (Lee et al., 2018; Lee et al., 2011; Liu et al., 2016b). However, monochloramine promotes nitrification in DWDS due to the presence of ammonia during the formation or decay of monochloramine (Cruz et al., 2020; Gomez-Alvarez et al., 2014), which in turn promotes the biofilm development and deteriorate the drinking water quality.

1.3 Spatiotemporal dynamics in water quality in DWDSs

DWDSs constitute intricate ecosystems comprising various phases, including bulk water, suspended particles, loose deposits, and biofilm (Ferrebee et al., 2023; Liu et al., 2017b; Prest et al., 2016a). Upon leaving the treatment plant, water carries certain amount of cells, nutrients, and particles. These cells or particles may attach to or settle on the pipe surfaces, thereby contributing to the formation of biofilm or loose deposits. Previous research predominantly focused on the water and biofilm phases (Douterelo et al., 2016; Prest et al., 2016b), overlooking the microbiology of suspended particles and loose deposits. Nonetheless, it has been documented that a single particle can transport 25 to 50 cells in bulk water (Liu et al., 2013a), and particle-associated bacteria exhibit higher activity and a more diverse community compared to planktonic bacteria (Bian et al., 2021; Ferrebee et al., 2023; Liu et al., 2013a). These particles may settle on the pipe surfaces during distribution, actively contributing to the formation of loose deposits (Liu et al., 2014; Prest et al., 2016a; Vreeburg et al., 2008). Loose deposits have been identified as hotspots for microbes, elements, and nutrients (Liu et al., 2017a; Ma et al., 2019; Rubulis et al., 2008; Zacheus et al., 2001). As reported in a previous study that over 98% of total bacteria within an unchlorinated DWDS were found within the pipe wall biofilm and loose deposits, with loose deposits contributing more biomass to the system than

biofilm (Liu et al., 2014). Additionally, loose deposits are widely acknowledged as contributors to water quality deterioration, including issues such as drinking water discoloration (Mussared et al., 2019; Poças, 2014; Vreeburg and Boxall, 2007). In contrast to biofilm, which attach to the pipe surfaces tightly, loose deposits, comprising materials such as mineral particles, organic matters, and other non-cohesive substances settling loosely on pipe surfaces, possess the characteristic of being removable and can be resuspended during hydraulic disturbances (Carrière et al., 2005; Rubulis et al., 2008). Neglecting the consideration of particle-associated bacteria and loose deposits may lead to underestimations of the variations or deteriorations in microbial drinking water quality and hinder effective water quality management.

There is a widely acknowledged consensus regarding the potential alteration of drinking water quality during distribution, primarily attributed to bacterial proliferation within the water and/or the potential release of bacteria attached to biofilm and/or loose deposits into the bulk water. This phenomenon may occur due to the extended water residence time or hydraulic disturbances within the distribution system (Bautista-de Los Santos et al., 2016a; Douterelo et al., 2013; Lehtola et al., 2006). For instances, increases in bacterial numbers and the establishment of a distance-decay relationship in bacterial communities in both planktonic and particle-associated bacteria have been observed during distribution (Bian et al., 2021; Potgieter et al., 2018). Furthermore, the drinking water quality may also change during distribution due to the complex network hydraulic conditions (Douterelo et al., 2013; Sekar et al., 2012), which vary with water demand and network locations, and commonly exhibit a diurnal pattern in flow driven by water consumption under normal operations. Studies have indicated that biofilm might detach from the pipe inner surfaces when the shear stress increases during the high water demand and overcome the biofilm internal cohesive strength (Paul et al., 2012), resulting in the increases in the concentration of planktonic cells, turbidity and materials related to discoloration (i.e. iron and magnesium) in water columns (Fish et al., 2022; Lehtola et al., 2006; Vreeburg and Boxall, 2007). On the other hand, low water demand is frequently detected at night as well as during the day in rural areas and at dead-ends, leading to long water residence times. The extended residence time or stagnation may contribute to increased bacterial concentrations and the proliferation of opportunistic pathogens (Lautenschlager et al., 2010; Ling et al., 2018; Zhang et al., 2021).

1.4 Effects of changes in operational conditions on DWDSs microbial water quality

To meet the increasingly strict drinking water regulations, many efforts have been made to

improve the drinking water quality, including the use of alternative source waters (Li et al., 2010; Zhang, 2009), the upgrade of drinking water treatment processes at water utilities (Lin et al., 2017), and the switching of disinfection strategies (Wang et al., 2014b). These approaches greatly improved the treated water quality regarding either physicochemical (e.g., TOC, turbidity, hardness) or microbiological (e.g., ATP, cell number) aspects (Chen et al., 2002; Sousi et al., 2020). The quality-improved drinking water, however, has to be delivered through the existing DWDSs before reaching to the customers, which might result in the transition effects refer to the water quality deteriorations caused by the release of the biofilm and/or loose deposits into bulk water during distribution under irregular changes in supply-water quality (Liu et al., 2017b).

A body of studies have reported the water quality deteriorations regarding the physicochemical (e.g., discoloration, lead release) and microbiological (e.g., the release of Legionella) aspects induced by the changes in operational conditions (Edwards and Dudi, 2004; Kim et al., 2011; Liu et al., 2017b; Preciado et al., 2021; Reiber and Dostal, 2000). The most well-known examples include the release of lead, arsenic, aluminium in bulk water in DWDSs due to the changes in coagulant in drinking water treatment in 2007 in Ontario, Canada (Kim et al., 2011), the discoloration in Midwestern U.S. when starting up chlorination (Reiber and Dostal, 2000), and the discoloration and lead crisis in 2001-2004 in Washington, DC when switching from chlorination to chloramination (Edwards and Dudi, 2004). These caused water quality deteriorations were highly related to the destabilizations of the harboured materials (e.g., biofilm, loose deposits) in DWDSs under the changes. However, due to the lack of accessibility of real DWDSs (Berry et al., 2006), the dilution effects of large volumes of water that flowing through the systems (Liu et al., 2017b), and the limitations on the application of source tracking methods, the knowledge on the water quality deterioration risks associated with biofilm and loose deposits destabilization in distribution systems during switching supply water quality is still limited. This significantly impedes comprehension of changes in water quality resulting from irregular operations, preventing water utilities from implementing the necessary monitoring and management measures to address disturbances caused by these irregular changes.

1.5 Approaches for the analysis of microbial water quality in DWDSs

1.5.1 Current microbial monitoring techniques

Monitoring microbial dynamics in DWDSs is a key step toward a better understanding on the

driving forces and consequences of changes in microbial drinking water quality. Conventionally, grab sampling is commonly used for regular assessments and statutory monitoring of drinking water quality in the DWDS. However, these conventional sampling strategies are basically water samples based, low-resolution, and labor-intensive, which makes it challenging to capture biofilms where most growth occurs in DWDSs and examine the spatiotemporal changes in the drinking water quality (Banna et al., 2014). In view of these constraints, online water quality monitoring progressively raised in popularity since the early 2000s (Hargesheimer et al., 2002). While, these techniques primarily referred to the physicochemical properties of the water quality, such as the online pH, chlorine sensors, and online particle counting devices (Storey et al., 2011). The application of online adenosine triphosphate (ATP) measurements and online flow cytometry allows the understandings on the changes in microbial drinking water quality (Farhat et al., 2020; Favere et al., 2021), acting as early warning tools for microbial water quality changes or contaminations (e.g., increases in cell numbers). However, it is impossible to clarify and track the origination of the water quality changes or contaminations in real DWDSs through these purely quantitative tools. The development of mathematical models such as Bayesian-based SourceTracker enables the tracking of contaminants or changes in water quality, which has been widely used across various scenarios. The integration of online sampling with SourceTracker represents a promising approach to overcome the above-mentioned challenges.

1.5.2 Techniques for microbial community analysis

The characterization of the microorganisms commenced since the beginning of the 20th century by means of the culture-based techniques (Eijkman, 1904). In drinking water industries, these culture-dependent methods were commonly applied to assess the microbial quality of drinking water, especially with a focus on the detection of the faecal coliforms. However, there are pronounced limitations with the application of these conventional approaches, as it was estimated that only 1% of the microorganisms is culturable, while the vast majority of the microorganisms remain unexplored because of the lacking of proper cultivation methods (Riesenfeld et al., 2004). The application of culture-independent techniques has overcome these limitations, allowing for a more detailed picture of the microbial communities in nature and engineered ecosystems. The culture-independent technology, refers to DNA sequencing based technology, was rapidly advanced from its inception in the 1970's by Frederick Sanger (Sanger et al., 1977). This technology is known as the Sanger sequencing, which is commonly called the first generation sequencing. The Sanger sequencing, however, only allows the sequencing

of one DNA fragment at a time, which challenges the exploration of the complex microbial communities in engineered ecosystems. Encouragingly, the advent of Next-Generation sequencing (NGS) technologies enables the need to sequence larger volumes of genetic materials faster and at a lower cost (Schuster, 2008; Shendure and Ji, 2008). In addition, NGS also offers greater discovery power to detect novel or rare variants with deep sequencing. The most frequently used NGS platforms include Roche 454 and Illumina. Nowadays, 454 pyrosequencing is largely overtaken by Illumina sequencing as the latter can provide higher output at a lower cost (Luo et al., 2012). This sequencing method has become a prevalent choice for characterizing microbial communities in drinking water systems, as evidenced by several studies (Chen et al., 2022b; Chen et al., 2020; Dai et al., 2020; Douterelo et al., 2018b; Ling et al., 2018; McDaniel et al., 2021).

The 16S rRNA gene serves as the predominant DNA barcode for prokaryote identification (Ntushelo, 2013), particularly in the context of drinking water microbial communities where bacteria play a pivotal role (Douterelo et al., 2018b). By means of Illumina 16S rRNA gene amplicon sequencing, the bacterial community composition within different phases in DWDSs (i.e., bulk water, suspended particles, loose deposits, biofilms) was integrally characterized in a series of studies (Liu et al., 2014; Liu et al., 2017a). These studies significantly contribute to our understanding of microbial ecology within DWDSs. Similarly, Ling et al. identified substantial changes in the bacterial community composition within municipal tap water following a 6-day stagnation period, providing insight into the deterioration of water quality associated with diurnal stagnation (Ling et al., 2018). While these studies greatly enhance our understanding of bacteriology in drinking water systems, it is crucial to acknowledge the presence of other microorganisms, such as archaea, viruses, fungi, and protozoa, which may raise public health concerns (Ashbolt, 2015; Buse et al., 2013; Douterelo et al., 2016). For instance, using both 16S and 18S rRNA gene sequencing, Douterelo et al. demonstrated that the biofilm in a chlorinated drinking water distribution system constitutes a mixed community of bacteria and fungi (Douterelo et al., 2018b). It is important to recognize that these DNA metabarcoding methods rely heavily on known species and are susceptible to amplification biases (Sze and Schloss, 2019; Walker et al., 2015). In response, the emergence of total DNA sequencing, also known as whole-genome shotgun metagenomics, offers a comprehensive alternative by sequencing the entire genomic content without targeting specific genes (Garner et al., 2021; Pérez-Cobas et al., 2020). This approach not only facilitates the identification of microbial taxa but also unveils the functional potential of the microbial community (Douterelo

et al., 2018a), providing insights into the complete genetic repertoire.

1.5.3 Microbial community assembly theory

Though the microbial communities within DWDSs have been considerably explored by means of various DNA sequencing technologies, the drivers in the microbial community assembly in DWDSs remain elusive. This is due to the difficulties in disentangling ecological drivers controlling microbial assembly in microbial ecology. Generally, there are two controversial theories, including the traditional niche-based theory and the neutral theory. According to the traditional niche-based theory, microbial communities are thought to be shaped by deterministic factors, such as environmental conditions, habitat heterogeneity and species interactions (Chesson, 2000; Tokeshi, 1990). On the contrary, neutral theory asserts that stochastic processes, such as birth, death, colonization, immigration, speciation and dispersal limitations are the main drivers for microbial community assembly (Bell, 2000; McGill et al., 2006). In fact, a body of studies supported that deterministic (niche-based) and stochastic (neutral) processes jointly contribute to the microbial community assembly (Dumbrell et al., 2010; Liebana et al., 2019; Niederdorfer et al., 2021; Ofiteru et al., 2010). However, the relative importance of deterministic and stochastic processes in community assembly varied across different temporal and spatial scales (Zhou and Ning, 2017). Explorations have been carried out extensively in natural and engineered systems, including river water and wastewater treatment. However, limited knowledge exists regarding drinking water systems, constraining our understanding of the factors driving microbial community changes in such systems.

1.6 Research objectives and questions

1.6.1 Research objectives

The overall goal of this thesis is to understand the formation of biofilm, the effects of disinfection regimes on biofilm development, and the dynamics in the intricate interactions between biofilm and bulk water phases under both regular and irregular conditions (i.e., introduction of additional softening and rapid sand filtration, introduction of partial reverse osmosis). The findings in this thesis are expected to contribute to a deeper understanding on the microbial drinking water quality and more efficient drinking water quality management.

1.6.2 Research questions

(1) Biofilm formation and the effects of disinfection regimes on biofilm development (Chapter 2)

How does biofilm form in DWDSs?

How do disinfection regimes affect the biofilm development in DWDSs?

(2) Dynamics in the interactions between biofilm and bulk water phases (Chapter 3, 4, and 5)

- Regular operational conditions (Chapter 3)

  What's the spatiotemporal dynamic in DWDSs microbial water quality under regular conditions?

- Irregular operational conditions (Chapter 4 & 5)

  Will transition effects (i.e., water quality deteriorations caused by contributions of biofilm/loose deposits) happen when treated water quality changes due to the changes in operational conditions?

  How to capture and characterise transition effects?

  When will the disturbed system be re-stabilized?

  How to manage the transition effects?

1.7 Thesis outline

Chapter 1 reviews current understandings on the (dynamics in) microbial water quality in DWDSs. The biofilm formation and prevention strategies have been reviewed. Furthermore, the spatiotemporal dynamics in drinking water quality and the effects of changes in operational conditions (e.g., treatment upgrading, source water switching, disinfection strategies changes) on the microbial water quality in DWDSs are discussed. Ultimately, the approaches to study the microbial water quality in DWDSs are described, with emphasis on the techniques for microbial water quality monitoring, microbial community analysis, and microbial community assembly theory.

Chapter 2 describes a long-term monitoring study (64 weeks) on the biofilm development in a newly-built pilot DWDS without and with residual disinfectants (i.e., free chlorine and monochloramine). The biofilm succession dynamics under different conditions and the ecological roles of residual disinfectants played during the biofilm development were explored.

Chapter 3 reveals the spatiotemporal dynamics in the microbial water quality in terms of the quantity and community of planktonic and particle-associated bacteria in an unchlorinated DWDS by means of a novel online monitoring and sampling system combined with the microbial fingerprint-based SourceTracker2. Specifically, the daily dynamics in the microbial water quality are emphasized.

Chapter 4 investigates the transition effects through indirectly characterizing the particles before, during and after the treatment upgrading. This study highlights the potential water quality deterioration risks associated with changing the supply water quality (for even better quality), which can be decisively captured and assessed by monitoring the suspended particles throughout distribution networks.

Chapter 5 characterizes the transition effects caused by supply water quality changes (i.e., RO introduction) using an online monitoring and sampling system through long-term and high-resolution (daily) observations spanning over 2 years. Specific attention is given to the microbial water quality changes contributed by biofilm and/or loose deposits in response to the supply water quality changes.

Chapter 6 summarizes the obtained results and describes the importance for drinking water practice and recommendation for future work.

Chapter 2

Long-term Succession Dynamics in Drinking Water Distribution System Biofilms with and without Residual Disinfectants

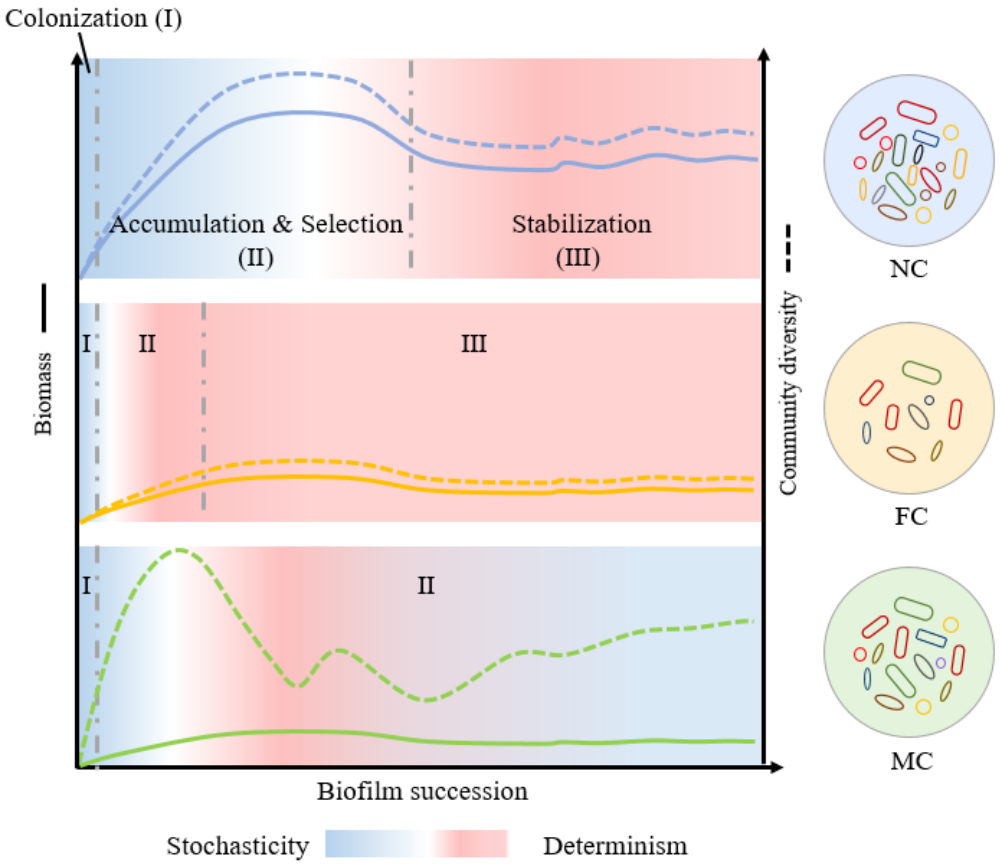

This chapter is based on: Chen, L., Shi, H., van der Meer, W., Medema, G., & Liu, G. Long-term succession dynamics in drinking water distribution system biofilms with and without residual disinfectants. To be submitted for publication.

Abstract

Biofilms are ubiquitous in drinking water distribution systems (DWDSs), even with the presence of residual disinfectants. The processes of succession and microbiome dynamics in biofilms, however, are not systematically understood. A pilot drinking water distribution system was thus followed for a 64-week period to comprehensively study the biofilm development in terms of microbial quantity, community composition, and community assembly, under different residual disinfectant regimes: no disinfectant (NC), free chlorine (FC, 0.1 mg/L), and monochloramine (MC, 0.4 mg/L). In comparison to the biofilms in the NC condition, the residual disinfectants suppressed biofilm growth throughout the entire developmental period and shaped the biofilm communities, with distinctive differences between the types of residual disinfectant. Remarkably, MC expressed stronger suppression effects on the biofilm activity (i.e., ATP), while FC resulted in a more homogenous and less complex biofilm community. The temporal results showed the developmental stages in biofilm formation, from initial colonization to accumulation and selection, and stabilization, at different rates under each of the conditions, associated with significant dynamic shifts in bacterial communities. The presence of MC significantly delayed the biofilm stabilization (> 64 weeks), while FC shortened the biofilm stabilization progress (~ 19 weeks), in comparison to the NC condition (~ 36 weeks). Altogether, this study highlighted the specificity of ecological processes at distinct biofilm development phases, highlighting the effects of residual disinfectants, advancing our understanding on the management of the biofilms in drinking water distribution systems.

Keywords: Pilot drinking water distribution system, long-term investigation, free chlorine, monochloramine, biofilm succession, microbial assembly

2.1 Introduction

Microbes are ubiquitous and abundant in drinking water distribution systems. It is widely recognized that the vast majority of the bacteria in drinking water distribution systems (DWDSs) reside in biofilms formed on the inner surface of the water mains, rather than present in bulk water (Flemming et al., 2002; Liu et al., 2017a; Liu et al., 2016b). These biofilms can be problematic, posing public health concerns. As documented, biofilms can serve as shelters for opportunistic pathogens (Gomez-Smith et al., 2015; Waak et al., 2019b; Wingender and Flemming, 2011), exacerbate corrosion of iron water pipes (Gomez-Smith et al., 2015; Tang et al., 2006), produce unpleasant tastes and odors (Servais et al., 1995), and promote disinfectant depletion and the resultant regrowth of the microbes (Cruz et al., 2020; Wang et al., 2014a).

Two fundamental approaches were ubiquitously applied to limit the microbial growth in DWDSs. Typically, in some European countries such as the Netherlands, the water utilities supply and distribute bio-stable drinking water with extremely low nutrients (e.g., AOC < 10 μg/L) to limit the microbial growth in DWDSs (Liu et al., 2017b; Smeets et al., 2009). On the other hand, disinfectant residuals are commonly maintained during drinking water distribution to suppress the re-/post-growth of microbes in many countries such as the US and China (Dai et al., 2020; Waak et al., 2019a). Free chlorine and monochloramine were the two most popular disinfectants adopted worldwide in drinking water industries (Dai et al., 2020; Liu et al., 2016b). Because it is cheap and easy-to-get, free chlorine is widely used. Nevertheless, concerns regarding to harmful disinfection by-products (Fielding and Farrimond, 1999; Richardson, 2003), low disinfection efficiency especially on biofilm (Lee et al., 2018), and selective chlorine-/antibiotic-resistant species enrichment (Li et al., 2023; Miller et al., 2015; Shi et al., 2013; Zhu et al., 2014) , result in reluctance to chlorine application. Monochloramine has been applied as alternative to control DWDS microbiomes since less disinfection by-products are generated and biofilm penetration is better (Lee et al., 2018; Lee et al., 2011). Conversely, monochloramine promotes nitrification in DWDS due to the presence of ammonia during the formation or decay of monochloramine (Cruz et al., 2020; Gomez-Alvarez et al., 2014), which further promotes the biofilm development and affects the drinking water quality during distribution.

Biofilm formation has been recognized as a long-term successional process (Martiny et al., 2003). The process begins with stochastic colonization and/or attachment of free-living microorganisms to pipe surfaces, that subsequently generate extracellular polymeric substances

(EPS) and establish a typical micro-environment in a way that supports other microorganisms to survive (Liu et al., 2016b). However, most of the studies report the microbiology of DWDSs over short-term frames (e.g., in 12 weeks) (Douterelo et al., 2018b; Zhou et al., 2009), where biofilm is far from being mature and stabilized, meaning our understanding on the biofilm development is incomplete. Additionally, the characterization of the biofilm succession is mainly focused on the bacterial quantity and community composition due to the difficulties in disentangling ecological drivers (deterministic versus stochastic processes) controlling microbial assembly in microbial ecology (Douterelo et al., 2018b; Roeder et al., 2010). Though there are some attempts, like in wastewater systems (Niederdorfer et al., 2021) and slow sand filtration (Chen et al., 2021), there is still very little information available in the literature concerning the community assembly mechanisms of biofilm bacteria in DWDSs.

A newly-built pilot drinking water distribution system was thus followed for a 64-week time period to integrally study the biofilm development in DWDSs from the perspectives of bacterial quantity, community composition, and community assembly, under different residual disinfectant regimes (i.e., no disinfectants, free chlorine, and monochloramine). The major objective of this study was to determine the effects of residual disinfectants on the development, microbial composition and long-term succession in drinking water biofilms.

2.2 Materials and Methods

2.2.1 Pilot drinking water distribution system

A new pilot system was built at one of the treatment plants of Oasen in the Netherlands. The pilot system consisted of 9 parallel pipelines with each of triplicate pipelines developed under unchlorinated (NC), free chlorine (FC, 0.1 mg/L) and monochloramine (MC, 0.4 mg/L) applied conditions, respectively (Figure 2-1). Each pipeline was constructed with 40 segments of new 20 cm PVC pipes (D = 32 mm) with a total length of ~ 12 m. The system was maintained at the flow velocity of 0.05 m/s (144 L/h, ~ 5 mins retention time) in a normal velocity in Dutch DWDSs (Prest et al., 2021) and the pressure of ~ 2 bar, with the water flowing continuously from the inlet to outlet and being discharged directly. The system was operated in a steady state to mitigate the impact of hydraulic conditions, as it is well-documented that biofilm development can be significantly influenced by the complex hydraulic conditions during distribution (Douterelo et al., 2013; Fish et al., 2017; Fish et al., 2022). The system was supplied with treated water with extremely low AOC (15-30 µg/L) from the treatment plant, where groundwater is used as the source water and treated by conventional treatment processes (i.e.,

spray aeration, rapid sand filtration, pellet softening, carry-over submerged rapid sand filtration, granular activated carbon filtration and UV disinfection) without disinfectants. The selection of concentrations for both free chlorine and monochloramine was based on the consideration of the low AOC content in the feed water (Ohkouchi et al., 2013). The system was maintained at 12~13 °C during the experiments, mirroring the usual temperature of treated water in the groundwater treatment plant (Agudelo-Vera et al., 2020) and the typical temperature in these locations near the treatment plant within the distribution system. Prior to the start, the pipelines were flushed with 20 mg/L sodium hypochlorite for 24h at the maximum flow rate (~ 0.24 m/s) and flushed afterwards with fresh treated water at the maximum flow rate until the chlorine was no longer detected. The physicochemical properties of the feed water were shown in table 2-S1.

The stock solution of free chlorine was prepared by directly diluting the commercial sodium hypochlorite (60 – 185 g/L active chlorine content), while monochloramine was prepared by the sequential addition of chlorine and ammonia at a Cl_2:N mass ratio of 4:1 and pH at 8 with slow stirs. The chemicals were prepared and refreshed every three days. The flow rate of dosing was controlled at 250-300 mL/min to obtain the target free (0.1 mg/L) and total chlorine (0.4 mg/L) concentration in the system (Figure 2-S1). A PVC mixer (~20 cm) was mounted in each pipeline right after the dosing point to completely mix the disinfectants and feed water. In addition, the free and total chlorine concentration was measured every 1-2 days to ensure the target concentration (Figure 2-S1). The system was operated for 16 months (64 weeks) during the experiments.

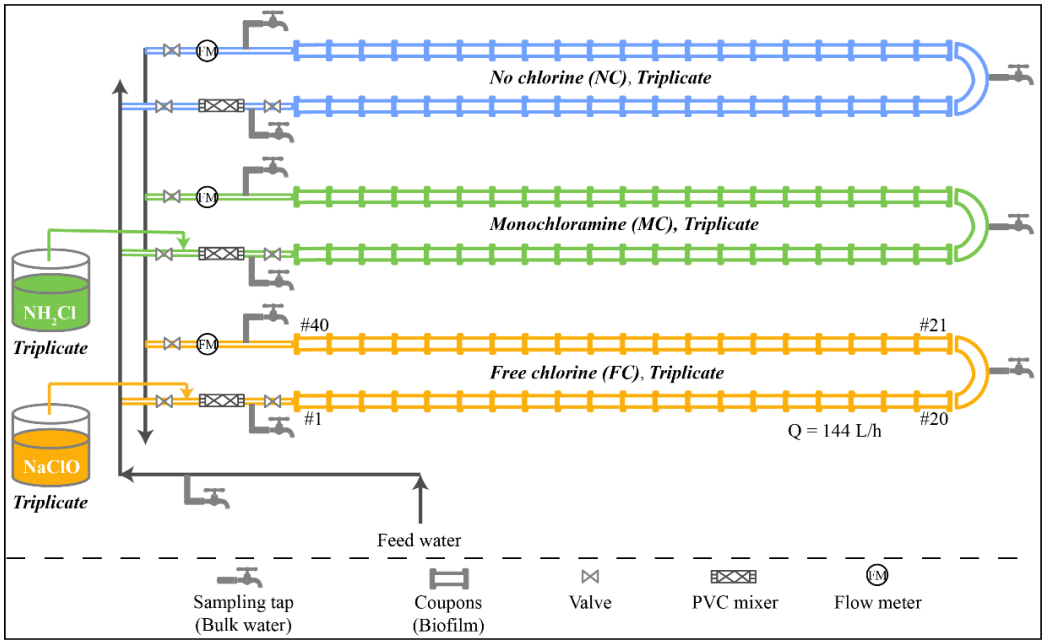

Figure 2-1. *The design of the pilot system*

2.2.2 Sample collection

After the sampling of the bulk water for physicochemical analysis, the system was drained at the maximum speed immediately for biofilm sampling. Biofilm samples were methodically collected by swabbing the inner surfaces of the pipe segments, progressing from the end (#40) to the front (#21), at regular intervals of every three or four weeks (Figure 2-1). The concentration of chlorine/chloramine was consistently maintained at the target level in pipe segments #21-40 (Figure 2-S1). Triplicate biofilm samples were collected at each time point under each condition, with each sample originating from one of the triplicate pipelines in each condition. This meticulous approach ensures the reliability and representativeness of the collected data. In addition, biofilm samples were swabbed in circles to avoid the uneven distribution of the biofilm on the inner pipes using sterile swabs in a short time (~ 5 mins). For each pipe segment, the surface area swabbed for ATP and ICC analysis was ~ 4 cm^2, while the rest of the surface area (~ 200 cm^2) was swabbed for DNA extraction.

2.2.3 Physicochemical and microbiological analysis

2.2.3.1 Water quality analysis

Free and total chlorine concentrations in the bulk water samples taken from feed, inlet, and outlet portal were determined by the N,N-diethyl-para-phenylenediamine (DPD) method using a Hach DR300 Pocket Colorimeter with a detection range of 0.02-2 mg/L Cl_2. Dissolved oxygen (DO), pH, temperature (T), and electrical conductivity (EC) were measured on site by WTW™ MultiLine™ 3420 Portable Digital Multiparameter. TOC was measured by TOC analyzer. The concentrations of ammonia, nitrite and nitrate were measured by Ion chromatography (IC).

2.2.3.2 Adenosine triphosphate and intact cell counts measurements

All the biofilm samples were pre-treated through a low energy ultrasonic treatment performed 3 times, for 2 min each (Branson ultrasonic water bath, 43 kHz, 180 W power output, 10 L sonication chamber) before the adenosine triphosphate (ATP) content and intact cell count (ICC) measurements. Subsequently, the ATP within the obtained suspensions from the above-mentioned pre-treatment was firstly released from cells by nucleotide-releasing buffer (NRB, Celsis), then measured by the intensity of the emitted light in a luminometer (Celsis Advance™) calibrated with solutions of free ATP (Celsis) in autoclaved tap water following the standard procedure given by the manufacturer (Magic-Knezev and Van Der Kooij, 2004). The ICC was measured by using the Bactosense flow cytometry in manual mode (Manickum, 2020).

2.2.4 DNA extraction and 16S rRNA gene amplicon sequencing

The DNA across all the samples was extracted through the FastDNA Spin Kit for Soil (Q-Biogene/MP Biomedicals, Solon, OH, USA) following the manufacturer's instructions. The V3-V4 hypervariable regions of the 16S rRNA genes were amplified before sequencing using the 341F-785R primer set (341F: 5′-CCTACGGGNGGCWGCAG-3′; 785R: 5′-GACTACHVGGGTATCTAATCC-3′). Paired-end sequencing of the amplicons (2 × 300 bp) was performed on an Illumina Miseq platform by BaseClear (Leiden, the Netherlands). The sequencing data have been deposited in the NCBI database, with reference code PRJNA966936.

2.2.5 Sequencing analysis

The bacterial 16S rRNA gene amplicons were processed using the Quantitative Insights Into Microbial Ecology (QIIME2, v2020.11) pipeline with default settings (Caporaso et al., 2010). DADA2 was used for filtering, dereplication, sample inference, chimera identification, and merging of paired-end reads (Callahan et al., 2016). As a consequence, unique amplicon sequence variants (ASVs) that were equivalent to 100% similarity operational taxonomic units (OTUs) in the conventional practice were generated. The taxonomy assignment was complemented using the q2-feature-classifier with Silva SSU database release 132 (Quast et al., 2012). Multiple sequence alignment and phylogenetic tree construction were performed using the QIIME 2 plugin q2-phylogeny. Alpha and beta diversity analyses were performed using the QIIME 2 plugin q2-diversity with a threshold of 6095. Principal coordinates analysis (PCoA) was conducted based on Bray-Curtis distance to assess community dissimilarity within biofilm across sampling time periods and conditions. Specifically, a community dissimilarity index of 1 indicates that the communities are entirely different. Significant differences in biofilm communities across different groups were assessed using PERMANOVA (Permutational multivariate analysis of variance) with 999 permutations calculated per test. The differences were considered significant when the p-value was lower than 0.05 ($P < 0.05$).

2.2.6 Null model analysis

To disentangle the relative importance of deterministic and stochastic processes underlying microbial community assembly, Raup-Crick (RC) based on Bray−Curtis dissimilarities were calculated (Stegen et al., 2013). The RC index values range between −1 and 1. $|Values| > 0.95$ represents that the community assembly was dominated by deterministic processes, whereas $|values| < 0.95$ indicates that stochastic processes dominated in the community assembly. The

modified index-normalized stochasticity ratio (MST) was determined to further quantify the relative contributions of deterministic and stochastic processes in the community assembly, with 0.5 as the boundary point between more deterministic (< 0.5) and more stochastic (> 0.5) assemblies (Ning et al., 2019). The MST analysis was conducted in R using the package "NST".

2.3 Results

2.3.1 Physicochemical water quality

The physicochemical water quality from feed to outlet under unchlorinated (NC), monochloramine (MC), and free chlorine (FC) applied conditions was regularly monitored (i.e., every 3 weeks). In summary, there were no significant differences in the physicochemical parameters among these three conditions and from different sampling points (i.e., feed , inlet, outlet), with the exception of the concentration of ammonia (Table 2-S1). Particularly, TOC, water temperature, and pH were maintained at 6 mg/L, 12~13 ℃, and 8, respectively, during distribution under each condition for the entire experiments. In addition, nitrite and nitrate concentrations were 0.002 and 13.7 mg/L on average in the systems regardless of conditions. However, the ammonia concentration under the MC condition was significantly higher (29 times) than the other two conditions, with the increase observed immediately after the addition of monochloramine.

2.3.2 Variations in ATP and ICC during biofilm development with and without residual disinfectants

The results showed that the ATP and ICC concentration within biofilm differed between the three conditions (Figure 2-2). Specifically, during the 64-week development period, the highest values were detected under the NC condition (on average 216.6 pg/cm^2 and 1.2×10^6 cells/cm^2 for ATP and ICC), followed by the FC (on average 73.4 pg/cm^2 and 2.0×10^5 cells/cm^2 for ATP and ICC) and MC (on average 8.6 pg/cm^2 and 1.2×10^5 cells/cm^2 for ATP and ICC) conditions. Similar to the trends in ATP and ICC, the highest DNA concentration within biofilm was observed under the NC condition, followed by the FC and MC conditions (Figure 2-S2). The biomass in the biofilm accumulated over the course of the time, but with different trends under the different conditions. In the NC condition, the ATP, ICC and DNA concentrations in biofilm consistently increased up to week 32, then slightly decreased to week 36, and remained relatively stable thereafter with the exception of a peak observed at week 60. In the FC condition, a large increase in ATP concentration was found from week 0 to 11, after which the increase was slight but consistent until week 36, then decrease was observed at week 44, whereafter the

ATP concentration remained at a relatively low level. In addition, the trends in ICC and DNA concentration in biofilm under the FC condition were similar to that of ATP concentration. Differently, in the MC condition, the increases in ATP, ICC and DNA concentrations in biofilm were inconspicuous, with only a small peak in ICC concentration detected at week 44.

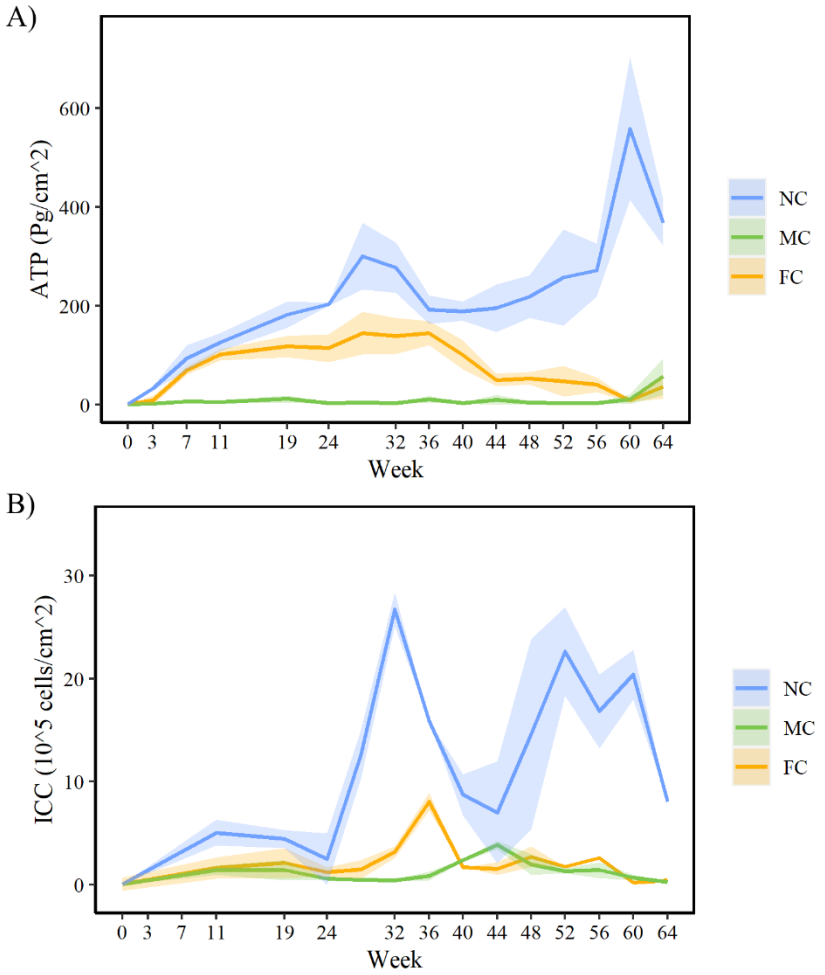

Figure 2-2. *Variations in ATP (A) and ICC (B) concentration within biofilm across the time under unchlorinated (NC), monochloramine (MC), and free chlorine (FC) applied conditions. Line plots represent mean values with error bands (mean ± s.d., n = 6).*

2.3.3 Succession dynamics in biofilm communities during biofilm development with and without residual disinfectants

A total of 3,482,410 sequences were obtained across all the 135 biofilm samples. Rarefication was performed prior to the alpha and beta diversity analysis by subsampling at an even sampling depth of 6095 sequences. The rarefication curves reached a plateau after 3000 sequences, indicating sufficient sample coverage was obtained in this study (Figure 2-S3).

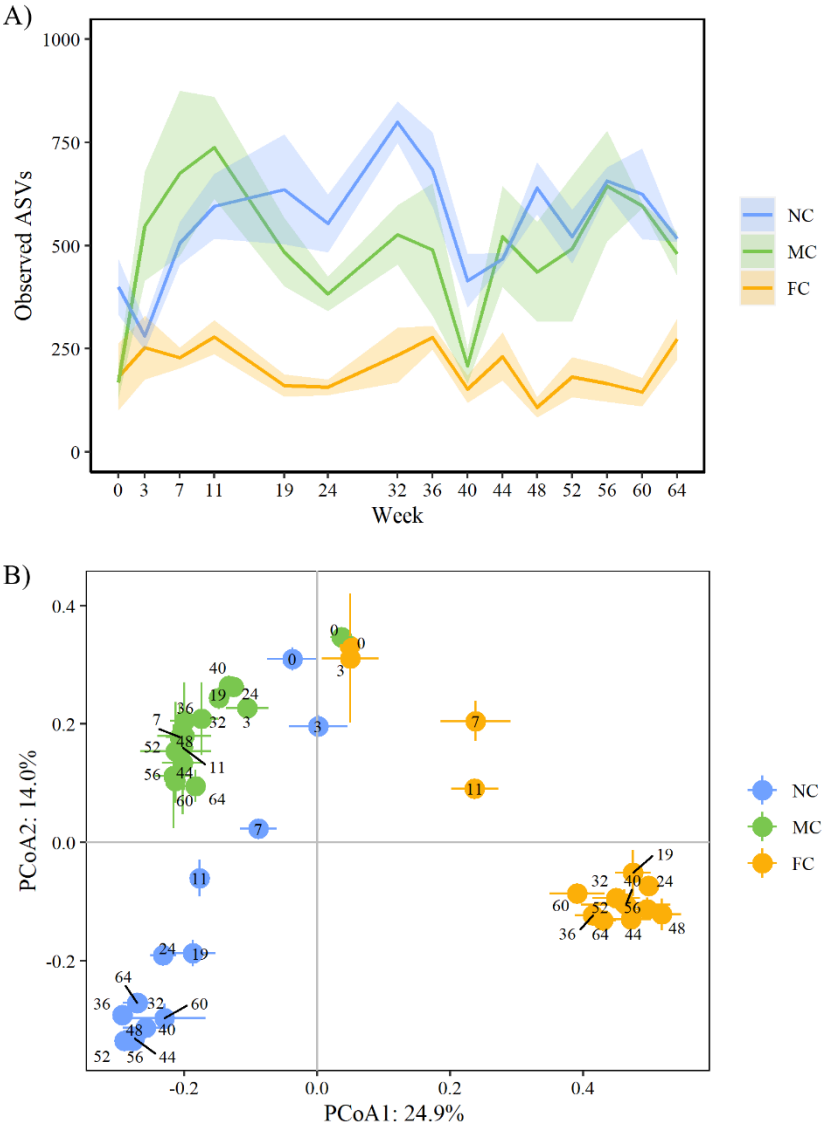

Figure 2-3. *Alpha and beta diversity within biofilm samples across time under unchlorinated (NC), monochloramine (MC), and free chlorine (FC) conditions. A) alpha diversity variations within biofilm samples over time under different conditions; B) PCoA plot based on Bray-Curtis distances (mean ± s.d., n = 3) showing the distribution of biofilm samples over time developed under different conditions (numbers indicate the sample week). Line plots represent mean values with error bands (mean ± s.d., n = 3).*

Alpha diversity. The number of observed ASVs was used as an indicator to represent the alpha diversity. Differences in the number of observed ASVs were observed in biofilm developed under the NC, MC, and FC conditions (Figure 2-3A). During the entire development period, the number of observed ASVs within biofilm under the NC, MC, and FC condition was at a level of 553 ± 140 ASVs, 493 ± 178 ASVs, and 202 ± 66 ASVs, respectively. Over time, the number of observed ASVs in biofilm behaved differently under these three conditions.

Specifically, rapid initial increases in the number of observed ASVs were found in both NC (up to 595 ± 79 ASVs at week 11) and MC (up to 675 ± 200 ASV at week 11) conditions, indicating the elevated diversity of the biofilm communities during the initial development periods in both systems. In contrast, the increase in the number of observed ASVs was not significant in the FC condition during the initial stage. Noticeably, differences in the temporal trends of the biofilm community diversity were more pronounced under different conditions with time. In the NC condition, a second peak in the number of observed ASVs was observed at week 32, followed by a rapid decrease until week 40 and waves during week 44 to 64. Distinctively, in the MC condition, strong decreases were found from week 11 to 24, followed by waves thereafter, with comparable community diversity to the NC condition at the end of the development. In the FC condition, only slight decreases were detected during week 11 to 24, followed by waves thereafter.

Beta diversity. As illustrated by the PCoA plot based on the Bray-Curtis distances, the biofilm communities started similarly under the three conditions, reflecting the relatively undiversified biofilm communities established at the early stage of the development. In week 3, the communities started to move into three distinct directions. Most of the movements occurred between week 0 and 3 for the MC system and between week 0 and 19 for the NC and FC systems. The diversification resulted in three clear clusters, with samples from the MC condition clustered closer to those from the NC condition than those from the FC condition (Figure 2-3B and 2-S4A). Furthermore, the biofilm community dissimilarities within samples from each two successive time points were progressively decreased over time regardless of conditions (Figure 2-S4B).

Community composition. Consistent with the trends in community structure, the community composition within biofilm under the three conditions was clearly different. At phylum level, during the observation period, Proteobacteria (41% on average) and Pastecibacteria (23% on average) were the two dominant phyla in the biofilm under the NC condition, while Proteobacteria dominated the biofilm communities in the MC (57% on average) and FC condition (82% on average), but with different proportions (Figure 2-4A). The temporal trends showed distinct succession dynamics in community composition under different conditions (Figure 2-4A). In the NC condition, Proteobacteria dominated at the early stage, whereas Pastecibacteria progressively became dominant at the later stages. In the MC and FC condition, Proteobacteria dominated consistently over time, where in the FC condition they increased in dominance in the first three weeks and maintained this dominance during the study period.

At ASV level, the same ASVs started the biofilm in each condition, but were succeeded by different ASVs under different conditions over time (Figure 2-4B). Specifically, in the NC condition, *Sphingobium* spp. (ASV14034 and ASV15480), *Rhodococcus* spp. (ASV7224), and *Ferribacterium* spp. (ASV14567) dominated during the first 7 weeks, followed by o_Saccharomidales (ASV21218) and *Pseudonocardia* spp. (ASV14716) since week 19, which were succeeded by other o_Saccharomidales (ASV15845, ASV4436, ASV8695, and ASV16443) since week 44. Differently, in the MC condition, *Massilia* spp. (ASV18454 and 14515), *Nocardioides* spp. (ASV14572), and f_Sphingobacteriaceae (ASV17454) predominated during the early stage until week 11, whereas *Sphingobium* spp. (ASV4223) and o_Saccharimonadales (ASV1622) became dominated since week 19, with ASV14572 and ASV17454 consistently dominated at the later stages. In the FC condition, *Sphingobium* spp. (ASV14034 and ASV4223), f_Sphingomonadaceae (ASV7759), f_Burkholderiaceae (ASV17026), and *Blastomonas* spp. (ASV15488) dominated during the initial stage (until week 11), while *Rhizobacter* spp. (ASV1125) and *Hyphomicrobium* spp. (ASV2103) became dominant together with ASV17026 and ASV7759 until week 48. Thereafter, ASV2103 and ASV7759 disappeared progressively, with ASV17026, *Rhizobacter* spp. (ASV1125 and ASV6093), and *Pseudomonas* spp. (ASV24582) dominated. The detailed taxonomy information of the dominant ASVs is shown in Table 2-S2.

2.3.4 Succession dynamics in ecological processes in biofilm community assembly with and without residual disinfectants

Null model analysis based on the modified Raup-Crick (RC) dissimilarity metrics and modified stochasticity ratio (MST) was conducted to uncover and quantify the relative importance of deterministic and stochastic processes in shaping the biofilm communities (Figure 2-5). Specifically, in the NC condition, it was observed that the stochastic processes played greater roles until week 36 with RC values < |0.95| and MST values > 0.5, while the deterministic processes progressively dominated thereafter with most of RC values < -0.95 and MST values < 0.5. It should be noted that, though the community assembly was largely driven by stochastic processes until week 36 in the NC condition, increases in the relative contributions of deterministic processes were observed since week 19. Differently, in the MC condition, stochastic processes remained relatively high throughout (RC values < |0.95| and MST values > 0.5), but with more deterministic processes occurred since week 19 (RC values < -0.95 and MST values < 0.5). Interestingly, in the FC condition, deterministic processes consistently dominated throughout the entire development period (RC values < -0.95 and MST values < 0.5),

although some stochastic processes were detected during week 3 to 11 (RC values < |0.95| and MST values > 0.5).

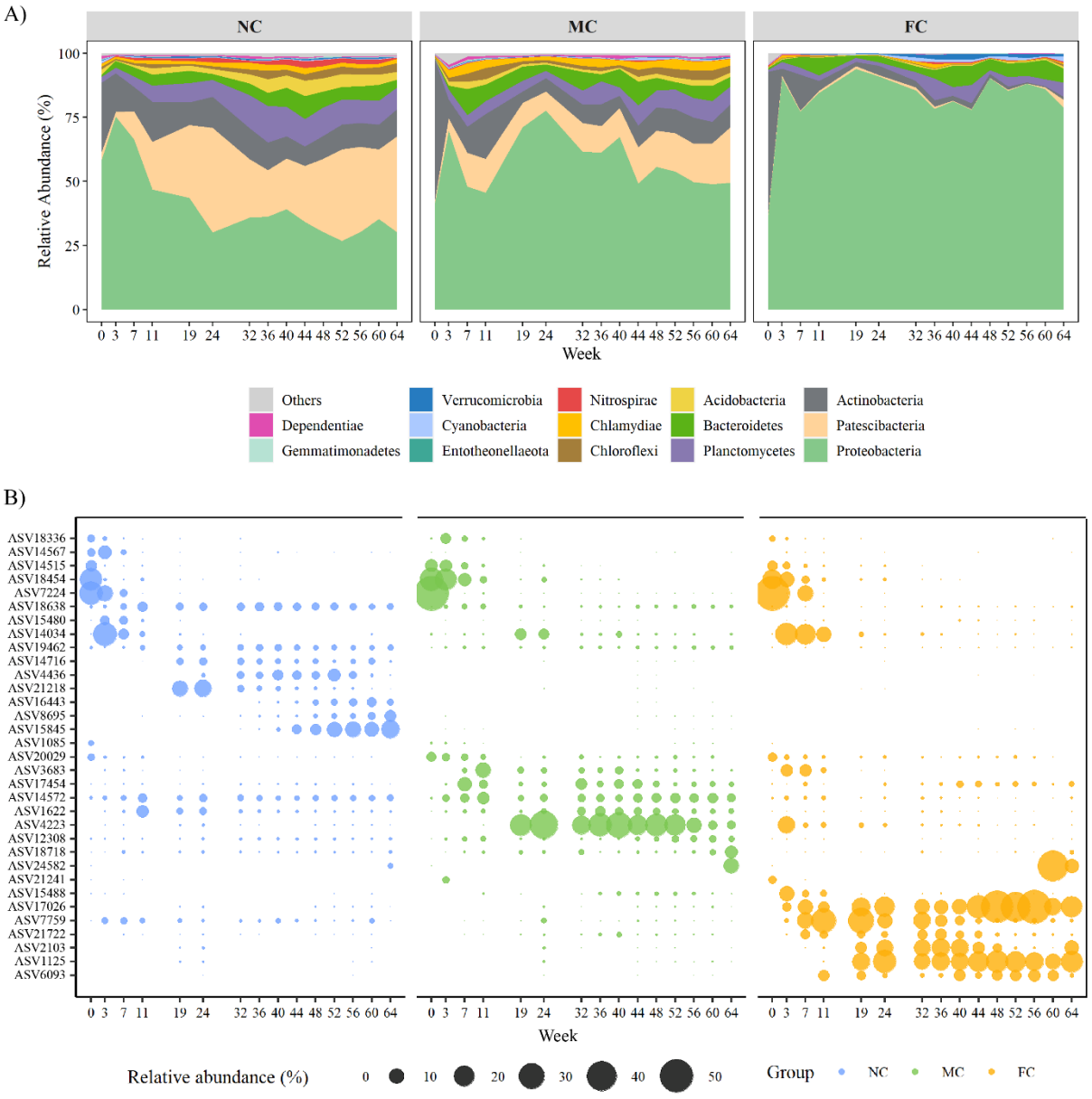

Figure 2-4. *(A) Variations in community composition within biofilms over the course of time under unchlorinated (NC), monochloramine (MC), and free chlorine (FC) conditions at phylum level; (B) Variations in dominant community populations within biofilms over the course of time under the three conditions (i.e., NC, MC, FC) at ASV level. The dominant populations were the top 15 ASVs within biofilms under each condition (totally 33 ASVs). The detailed taxonomy information of these ASVs were shown in table 2-S2.*

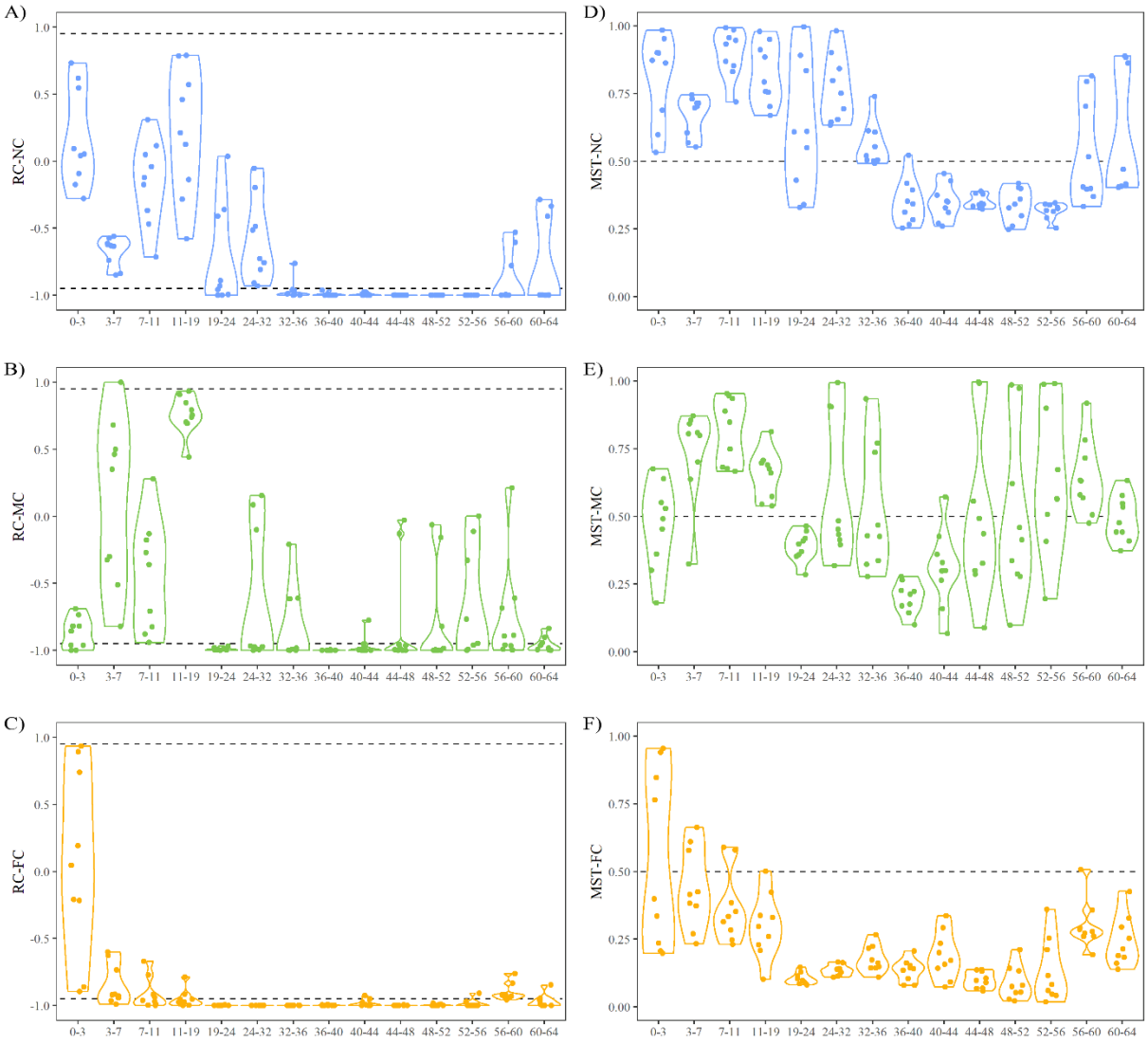

Figure 2-5. *Dynamics in Raup-Crick dissimilarity (RC, A-C) and modified stochastic ratio (MST, D-F) based on Bray-Curtis distances under different conditions over time generated through the comparisons between two successive sample points. Different conditions were colored, with blue represents unchlorinated (NC) condition, while green and orange represents monochloramine (MC) and free chlorine (FC) conditions. Horizontal dotted lines indicate thresholds for significant deviations from the null expectation, −0.95 and +0.95 for RC and 0.5 for MST.*

2.4 Discussion

In the present study, the DWDS biofilm development was monitored over a 64-week period without and with disinfectants (i.e., no disinfectants - NC, free chlorine - FC, and monochloramine - MC). To our knowledge, the present study is the first to reveal the biofilm development in terms of bacterial quantity, community structure and composition, and

community assembly from a long-term perspective under different disinfection regimes. The findings in this study provide novel insights into our understanding of biofilm development and strategies for biofilm management.

2.4.1 Ecological effects of residual disinfectants on drinking water biofilm development

Integrally, FC and MC both exhibited fairly strong suppression effects on the biofilm growth and significantly shaped the biofilm community. The observations were unsurprising, as the ability of FC and MC to suppress the growth of drinking water biofilms have been confirmed extensively (Clayton et al., 2021; Shen et al., 2017). But less is known about their effects on biofilm community development and composition. The suppression effects and selection appeared already in the early colonization stage and went through the entire observation period, but with distinctive behaviors for the presence/type of disinfectants. The biofilm in the MC condition harbored higher community diversity than that in the FC condition, suggesting FC exhibited a more powerful selective pressure on biofilm communities. The observed deviations might be attributed to the distinctive inherent disinfection mechanisms of FC and MC. As documented, FC, known as a potent oxidizer, has the ability to permeabilize bacterial membranes causing lethal DNA damage (Lee et al., 2018; Lee et al., 2011; Liu et al., 2016b). The powerful oxidizing property of FC might lead to a strong selection pressure on the biofilm community members where only a limited number of chlorine-resistant members dominated. This can be directly confirmed by the results from null model analysis, where much lower RC and MST values were observed in the FC condition compared with the MC condition. While, the relatively higher biofilm activity in the FC condition might have resulted from the oxidation of organic matter in drinking water (biofilm) to more readily biodegradable compounds that serve as nutrient sources since free chlorine can kill cells by destroying the cell walls (Huang et al., 2020; Polanska et al., 2005). Not as potent an oxidizer as FC, MC would not increase the biodegradable organic compounds in drinking water as much as FC. MC reacts slowly with DNA and RNA with little damage to bacterial membranes, allowing it to penetrate deeper into biofilm matrix (Lee et al., 2018), which renders MC as a better suppression reagent for biofilm growth. In addition, instead of destroying cells membrane, MC might lead cells to enter into a dormancy state (persistent or viable but non-culturable state), resulting in lower biofilm activity but still higher community diversity (Chen et al., 2018; Ng et al., 2021).

The significant changes in microbial community structure under different disinfection strategies and developmental stages are likely to be derived from the different bacterial sensitivity to

disinfectants, where chlorine/monochloramine-resistant species outcompeted others in biofilms. In the FC condition, the biofilm community was rapidly dominated by the phylum Proteobacteria, wherein mainly Gammaproteobacteria (i.e., f_Burkholderiaceae, *Rhizobacter* spp., *Pseudomonas* spp.) and Alphaproteobacteria (*Hyphomicrobium* spp.) dominated. Likewise, the genus *Pseudomonas* was recognized as the dominant genus in a biofilm development spanning 84 days under chlorinated conditions (Douterelo et al., 2018b). The chlorine-resistant properties of other species have also been confirmed in previous studies (Gomez-Alvarez et al., 2012; Mi et al., 2015; Williams et al., 2004). Differently, the dominant biofilm community members in the MC condition were significantly different and more diverse from/than that in the FC condition, with ASVs affiliated to Alphaproteobacteria (*Sphingobium* spp.), Actinobacteria (*Nocardioides* spp.), and Patescibacteria (o_Saccharimonadales) dominant. Some of these monochloramine-resistant species have been reported previously (Gomez-Alvarez et al., 2012). For instance, it was reported that *Sphingobium* spp. were commonly present coincident with *Nitrosomomas* spp., which was ubiquitously found in monochloraminated drinking water induced by the increased ammonia concentration through the addition/decay of MC in DWDSs (Liao et al., 2015; Potgieter et al., 2020; Revetta et al., 2013). Likewise, the high concentration of ammonia observed in the MC condition in the present study likely acted as a driving factor for the dominance of *Sphingobium* spp.. Noticeably, though the selection pressure of disinfectants (especially for FC) on biofilm communities has presented since the early colonization stage, the representative species under each of the conditions (e.g., *Rhizobacter* spp. in the FC condition, *Sphingobium* spp. in the MC condition) were dominant after around 3 months' operation when multi-layer aggregates were probably formed, hinting that the selection on biofilm communities is a chronical and complex process and is likely affected by many abiotic and/or biotic factors (e.g., disinfectants, micro-environment in biofilm matrix, bacterial interactions).

2.4.2 Succession dynamics in drinking water biofilm development

Stage I: Initial colonization. The biofilm formation was initiated by the attachment of a consortium of heterotrophic bacteria, with members mainly affiliated to the phylum Proteobacteria (e.g., *Massilia spp.*) and Actinobacteria (e.g., *Rhodococcus* spp.), regardless of conditions. These microbes were commonly found as primary and initial colonizers in drinking water biofilms attributing to their ability of auto- or co-aggregation and high adaptability to the extreme oligotrophic environment (Biggs et al., 2013; Douterelo et al., 2018b; Fish and Boxall, 2018). Presumably, these pioneer microorganisms originated from the treated water non-

specifically and randomly attached/settled to/on the pipe surfaces, irrespective of competitiveness.

Stage II: Accumulation and selection. After successful surface attachment the accumulation stage starts, cells multiply and produce essential EPS matrix components, modifying the pipe surfaces for the recruitment of new immigrants from the bulk water (Martiny et al., 2003). This is especially true in the NC condition, where significant and consistent increases in biofilm biomass and community diversity were observed until week 32. The dominant stochastic processes at this stage (up to week 32) determined by the null model analysis further implied that the biofilm community assembly during the accumulation stage in the NC condition was most likely driven by the random dispersal of species from the bulk water. The presence of residual disinfectants considerably suppressed the biofilm growth and affected the biofilm succession, with different behaviors regarding the types of the residual disinfectants. Specifically, the biofilm community diversity in the MC condition was constantly increased up to week 11 to an even higher level than that in the NC condition though the biofilm quantity remained at extremely low levels, suggesting the presence of MC was less deterministic. This is coalesce with the observation that stochastic processes dominated during this stage in the MC condition determined by null model analysis. The deviations between the biofilm community between the MC and NC condition might be attributed to the suppression effects of MC which generated different niches in biofilms. Distinctively, FC exhibited strong selective pressure on the biofilm communities, where no significant increases in the biofilm quantity and community diversity were found during the accumulation. This conformed the observation that deterministic processes were dominant since week 3 in the FC condition.

Further biofilm development may yield reduced community diversity where bacterial competition in biofilms might occur due to the limited resources in the biofilm matrix. This hypothesis could explain the significant decreases in the biofilm biomass and community diversity after their peaks under each of the conditions (week 36, 19, 19 in the NC, MC, and FC condition, respectively). In this context, species well-adapted to the biofilm environment (e.g., f_Rhizobiales Incertae Sedis in the NC condition, *Sphingobium* spp. in the MC condition, *Rhizobacter* spp. and f_Burkholderiaceae in the FC condition) dominated, while others (e.g., *Sphingobium* spp., *Ferribacterium* spp., *Rhodococcus* spp. in the NC condition, *Massilia* spp. in the MC condition, *Sphingobium* spp. in the FC condition) might be outcompeted and disappeared progressively in the biofilm community during the development. The dominant roles of deterministic processes at week 19 in the FC and MC condition and week 36 in the NC

condition determined by the null model analysis expressively confirmed the selection pressure (e.g., starvation, disinfectants) on the biofilm community assembly at the end of the accumulation stage.

Stage III: Stabilization. The further reduced community dissimilarities in biofilm revealed convergence of the biofilm towards a relatively stable community at the last stage of the experimental period, which might start around week 19 (FC) to week 36 (NC). In the light of the established concepts of biofilm life cycles, it can be imagined that cells disperse from the established biofilm, revert to a planktonic state and start a new cycle of biofilm establishment (Liu et al., 2016b; Sauer et al., 2022). At this point, the community has established over a long time succession, and species well adapted to the oligotrophic environment and FC sustain their presence in the biofilm (e.g, o_Saccharimonadales in the NC condition, and f_Burkholderiaceae and *Pseudomonas* spp. in the FC condition). This is in line with the observations from the null model analysis, which showed deterministic processes dominated during the last stage of the biofilm development in the FC and NC condition. Interestingly, the biofilm community assembly in the MC condition was still largely driven by stochastic processes during the last stage of the biofilm development. This implies that the presence of monochloramine might extend the duration required for biofilm stabilization. Similarly, in a prior investigation, a steady state in biofilm development was not achieved within a 12-month period when the biofilm developed under monochloramine conditions with low AOC (Pick et al., 2021).

2.4.3 Practical implications

In the present study, a newly-built pilot system was monitored over a 64-week period under various disinfection regimes (i.e., no disinfectants - NC, free chlorine - FC, and monochloramine - MC) to investigate the biofilm succession dynamics. To the best of our knowledge, this is the first study to examine the long-term effects of disinfection regimes on biofilm succession dynamics. The suppression effects of FC and MC on biofilm growth were confirmed in this study. Importantly, the presence of FC and MC significantly shaped the biofilm communities and exhibited strong effects on the biofilm succession. Remarkably, the presence of FC resulted in a reduction in biofilm diversity and shortened the biofilm stabilization, while the presence of MC led to a higher biofilm diversity and significant delay in the biofilm stabilization. These findings indicated that FC may contribute to more predictable biofilm dynamics and improved system performance compared to MC, ultimately enhancing the stability and manageability of the system. From a sustainability and safety perspective, it is

highly advantageous to minimize the reliance on residual disinfectants. In certain countries like the Netherlands, biofilm growth is effectively controlled by delivering highly stable drinking water. However, achieving such bio-stable drinking water requires strict prerequisites, including access to high-quality source water, advanced treatment technologies, and meticulous management practices. Thus, in scenarios where the necessary prerequisites for producing bio-stable drinking water cannot be achieved, the use of residual disinfectants becomes essential. The findings of this study emphasized the advantages of using FC over MC in predicting biofilm dynamics and improving biofilm management in DWDSs. However, it is important to acknowledge that when formulating disinfection strategies, additional factors in DWDSs should be taken into account, including the generation of disinfection by-products, the decay of residual disinfectants, and the potential enrichment of specific pathogens and antibiotic resistance genes.

Furthermore, the results in the present study indicated that the biofilm formation is a long-term successional process, which might take at least 5-9 months toward a stable state. Hence previous studies on the investigations of DWDS biofilms over short-term frames may lead incorrect assessment of the risks of biofilms (Douterelo et al., 2018b), as the resistance/response to operation conditions (e.g., disinfectants, hydraulics) of young and old (mature) biofilms is supposed to be significantly different. It is essential to take the age of the biofilms into account in further relevant studies. Additionally, while complete eradication of bacteria from distribution systems is impractical, it may be more beneficial to focus on manipulating the composition of the bacterial community to achieve desirable outcomes. This can be accomplished through gaining a deeper understanding of the microbial composition at each stage of biofilm development. Consequently, comprehending the dynamics of biofilm succession is essential for the development of future strategies for monitoring and managing biofilms, as well as protecting against water-borne health risks.

Notably, the monitored DWDS in the present study was fed with Dutch drinking waters without residual disinfectants and low nutrient content, which allows for a unique assessment of disinfectant-induced effects on the drinking water microbiomes that have not previously been exposed to disinfection-based selection pressures. Nonetheless, the pathogenicity and antibiotic resistance of chlorine/monochloramine-resistant species identified solely through 16S rRNA sequencing data remains unknown (Dai et al., 2020; Sevillano et al., 2020). To address these concerns, future research should focus on metagenomics and proteomic analysis for a more comprehensive understanding. Furthermore, it is noteworthy that the EPS, a significant

component of the biofilm's physical structure, were not characterized in this study. Subsequent research endeavors could explore the impact of disinfection regimes on EPS within the biofilm, as this aspect is closely linked to water quality deteriorations, including issues such as discoloration in drinking water distribution systems (Fish et al., 2017). In addition, the present investigation was carried out in a pilot system under steady-state conditions. Given the potential influences of complex hydraulic conditions in field distribution networks (Douterelo et al., 2013; Fish et al., 2017; Fish et al., 2022), forthcoming research on biofilm development should also take these effects into consideration.

2.5 Conclusions

A newly-built pilot drinking water distribution system was monitored over 64 weeks to comprehensively study the biofilm development in terms of bacterial quantity/activity, community composition, and community assembly, under different disinfectant regimes (i.e., no disinfectants - NC, free chlorine - FC, and monochloramine - MC). The following conclusions can be drawn from this study:

- The residual disinfectants exhibited strong suppression effects on the biofilm growth and significantly shaped the biofilm communities, but were notably different in the presence of MC and FC. Specifically, MC expressed better suppression effects on the biofilm activity, while FC presented more intense selection pressure on the microbes, yielding a more homogenous and less complex biofilm community.
- Specifically, Gammaproteobacteria (i.e., f_Burkholderiaceae, *Rhizobacter* spp., *Pseudomonas* spp.) were abundant in the presence of FC, while biofilm developed under MC harbored more diverse species, including Alphaproteobacteria (*Sphingobium* spp.), Actinobacteria (*Nocardioides* spp.), and Patescibacteria (o_Saccharimonadales).
- Biofilm formation is successional dynamic, undergoing several stages: initial colonization, accumulation and selection and stabilization. These stages differed in community structure and community assembly processes (deterministic versus stochastic processes) over time and across different conditions. Reaching the stabilization stage took longest in the MC condition and shortest in the FC condition.
- Specifically, in the NC condition, the early development stage was driven by the stochastic processes where colonizers originated from the bulk water consistently contributed to the biofilm community, while deterministic processes increased in their relative contributions at the end of the accumulation stage, and became dominant at the

stabilization stages where competitive ones dominated. In the MC condition, the biofilm succession was largely represented by stochastic processes across time, while the biofilm succession in the FC condition was strongly driven by deterministic processes since the early developmental stage.

Supporting information

Table 2-S1. The physicochemical water quality in unchlorinated (NC), monochloramine (MC), and free chlorine (FC) applied conditions.

	NC			MC			FC		
	Feed	In	Out	Feed	In	Out	Feed	In	Out
pH	8.2±0.1	8.1±0.1	8.2±0.3	8.2±0.1	8.1±0.1	8.1±0.1	8.2±0.1	8.1±0.1	8.2±0.1
EC	739±29	760±24	749±33	743±27	757±18	754±22	748±19	758±19	756±18
DO (mg/L)	8.88±0.50	9.03±0.30	8.96±0.48	9.10±0.32	8.91±0.43	8.95±0.49	8.98±0.39	8.99±0.44	8.99±0.41
T (°C)	13.1±0.8	12.1±0.9	12.4±1.1	12.7±0.9	12.3±0.7	12.5±0.9	12.6±0.8	12.3±0.7	12.5±1.0
TOC (mg/L)	6.1±0.6	6.1±0.5	6.1±0.6	6.1±0.6	6.0±0.6	6.2±0.6	6.0±0.6	6.0±0.6	6.0±0.6
NH_4^+ (mg/L)	0.003±0.002	0.003±0.001	0.003±0.003	0.005±0.004	0.142±0.044	0.145±0.013	0.005±0.002	0.007±0.003	0.008±0.005
NO_2^- (mg/L)	0.002±0.003	0.002±0.003	0.002±0.003	0.001±0.002	0.002±0.002	0.002±0.002	0.001±0.002	0.001±0.002	0.001±0.002
NO_3^- (mg/L)	13.96±0.48	13.85±0.30	13.90±0.57	13.63±0.54	13.71±0.54	13.77±0.57	13.77±0.67	13.80±0.63	13.81±0.67

Table 2-S2. The taxonomy information of the top 15 ASVs under each condition (unchlorinated, chloramine and free chlorine applied conditions, totally 33 ASVs), respectively.

ASVs	Phylum	Class	Order	Family	Genus	Species
ASV18336	Proteobacteria	Gammaproteobacteria	Pseudomonadales	Pseudomonadaceae	Pseudomonas	
ASV14567	Proteobacteria	Gammaproteobacteria	Betaproteobacteriales	Rhodocyclaceae	Ferribacterium	
ASV14515	Proteobacteria	Gammaproteobacteria	Betaproteobacteriales	Burkholderiaceae	Massilia	
ASV18454	Proteobacteria	Gammaproteobacteria	Betaproteobacteriales	Burkholderiaceae	Massilia	
ASV7224	Actinobacteria	Actinobacteria	Corynebacteriales	Nocardiaceae	Rhodococcus	
ASV18638	Proteobacteria	Gammaproteobacteria	PLTA13			
ASV15480	Proteobacteria	Alphaproteobacteria	Sphingomonadales	Sphingomonadaceae	Sphingobium	
ASV14034	Proteobacteria	Alphaproteobacteria	Sphingomonadales	Sphingomonadaceae	Sphingobium	
ASV19462	Proteobacteria	Alphaproteobacteria	Rhizobiales	Rhizobiales Incertae Sedis	uncultured	Ambiguous_taxa
ASV14716	Actinobacteria	Actinobacteria	Pseudonocardiales	Pseudonocardiaceae	Pseudonocardia	
ASV4436	Patescibacteria	Saccharimonadia	Saccharimonadales	uncultured soil bacterium	uncultured soil bacterium	uncultured soil bacterium
ASV21218	Patescibacteria	Saccharimonadia	Saccharimonadales	uncultured bacterium	uncultured bacterium	uncultured bacterium
ASV16443	Patescibacteria	Saccharimonadia	Saccharimonadales			
ASV8695	Patescibacteria	Saccharimonadia	Saccharimonadales	uncultured bacterium	uncultured bacterium	uncultured bacterium
ASV15845	Patescibacteria	Saccharimonadia	Saccharimonadales			
ASV1085	Proteobacteria	Gammaproteobacteria	Betaproteobacteriales	Burkholderiaceae	Limnohabitans	
ASV20029	Proteobacteria	Gammaproteobacteria	Betaproteobacteriales	Burkholderiaceae	Ralstonia	
ASV3683	Proteobacteria	Alphaproteobacteria	Sphingomonadales	Sphingomonadaceae	Blastomonas	
ASV17454	Bacteroidetes	Bacteroidia	Sphingobacteriales	Sphingobacteriaceae		
ASV14572	Actinobacteria	Actinobacteria	Propionibacteriales	Nocardioidaceae	Nocardioides	uncultured bacterium
ASV1622	Patescibacteria	Saccharimonadia	Saccharimonadales			
ASV4223	Proteobacteria	Alphaproteobacteria	Sphingomonadales	Sphingomonadaceae	Sphingobium	
ASV12308	Patescibacteria	Saccharimonadia	Saccharimonadales			
ASV18718	Patescibacteria	Parcubacteria	Candidatus Nomurabacteria	uncultured bacterium	uncultured bacterium	uncultured bacterium
ASV21241	Epsilonbacteraeota	Campylobacteria	Campylobacterales	Arcobacteraceae	Arcobacter	
ASV15488	Proteobacteria	Alphaproteobacteria	Sphingomonadales	Sphingomonadaceae	Blastomonas	
ASV17026	Proteobacteria	Gammaproteobacteria	Betaproteobacteriales	Burkholderiaceae		
ASV7759	Proteobacteria	Alphaproteobacteria	Sphingomonadales	Sphingomonadaceae		
ASV21722	Proteobacteria	Alphaproteobacteria	Rhizobiales	Beijerinckiaceae	Bosea	
ASV2103	Proteobacteria	Alphaproteobacteria	Rhizobiales	Hyphomicrobiaceae	Hyphomicrobium	
ASV1125	Proteobacteria	Gammaproteobacteria	Betaproteobacteriales	Burkholderiaceae	Rhizobacter	
ASV6093	Proteobacteria	Gammaproteobacteria	Betaproteobacteriales	Burkholderiaceae	Rhizobacter	

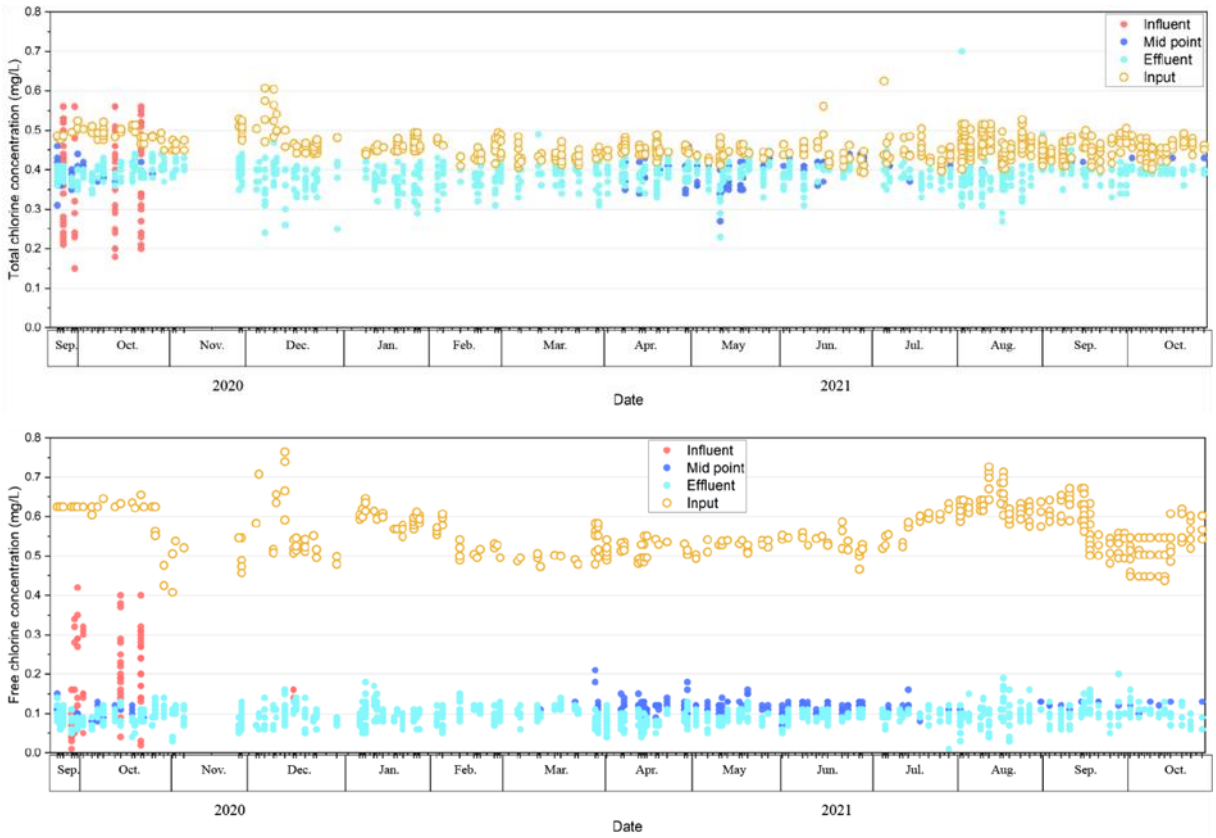

Figure 2-S1. Monochloramine (top) and free chlorine (bottom) concentration over time

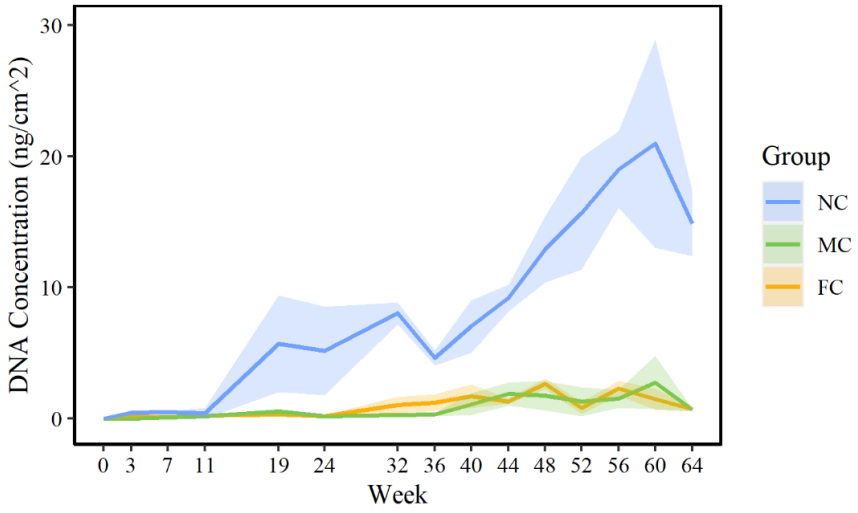

Figure 2-S2. DNA concentration in biofilm under different conditions over the course of the time. Line plots represent mean values with error bands (mean ± s.d., n = 3).

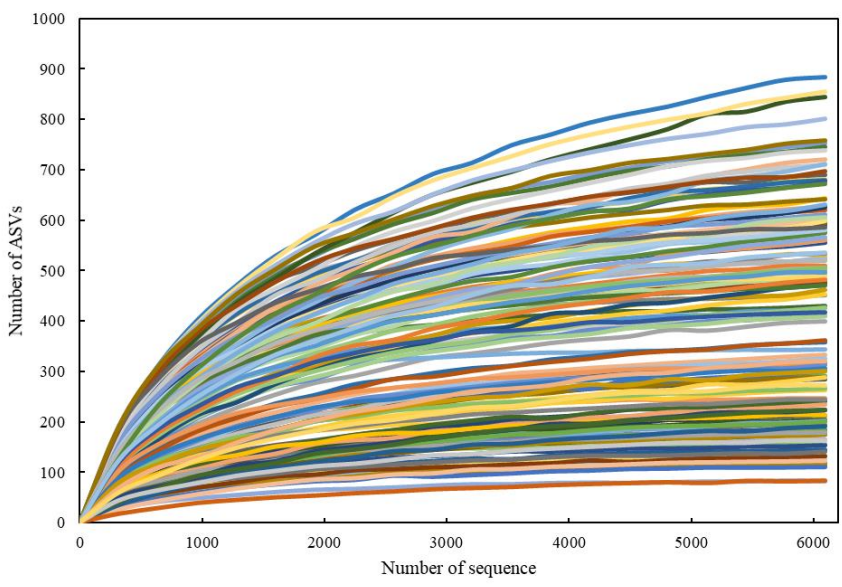

Figure 2-S3. Rarefaction curves. Different colours represent different samples.

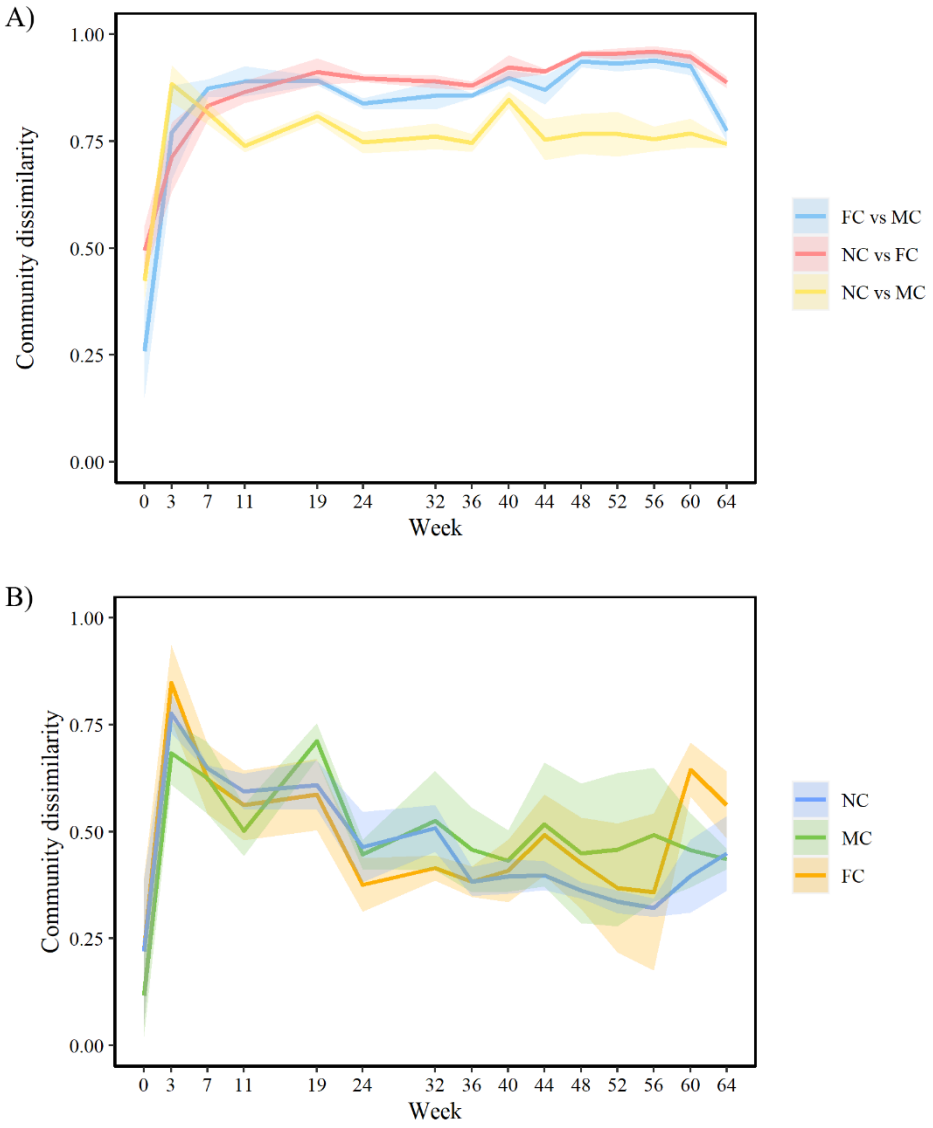

Figure 2-S4. A) Community dissimilarities between biofilm samples collected under different conditions over time based on Bray-Curtis distances; B) Community dissimilarities based on Bray-Curtis distances between two successive sample points under each condition. NC, MC, and FC stand for unchlorinated, monochloramine, and free chlorine applied conditions, respectively. Line plots represent mean values with error bands (mean ± s.d., n = 3).

Chapter 3

Capturing and Tracing the Spatiotemporal Variations of Planktonic and Particle-Associated Bacteria in an Unchlorinated Drinking Water Distribution System

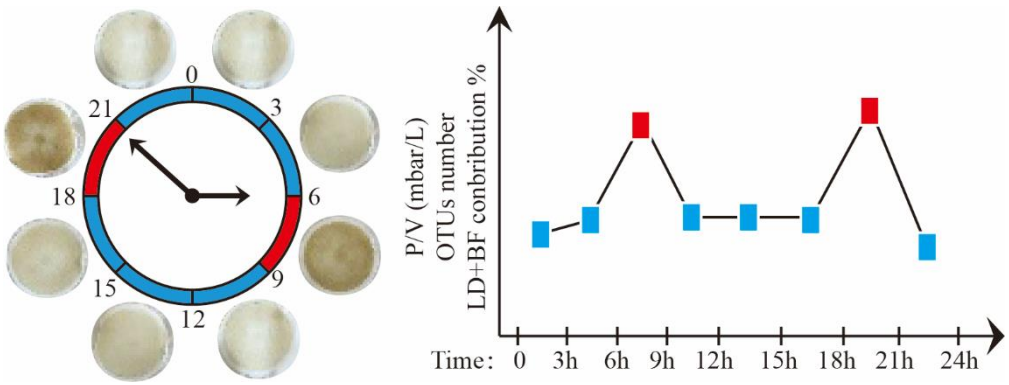

This chapter is based on: Chen, L., Li, X., van der Meer, W., Medema, G., & Liu, G. (2022). Capturing and tracing the spatiotemporal variations of planktonic and particle-associated bacteria in an unchlorinated drinking water distribution system. *Water Research, 219,* 118589.

Abstract

The aperiodic changes in the quantity and community of planktonic and particle-associated bacteria have hampered the understanding and management of microbiological water quality in drinking water distribution systems. In this study, online sampling was combined with the microbial fingerprint-based SourceTracker2 to capture and trace the spatiotemporal variations in planktonic and particle-associated bacteria in an unchlorinated distribution system. Biofilm and loose deposits at corresponding locations were sampled as sources for the planktonic and particle-associated bacteria within the distribution system. The distribution of particle load, particle-associated metal elements, particle-associated ATP, and contributions of biofilm and loose deposits to both planktonic and particle-associated bacteria during distribution were quantitatively evaluated in eight three-hour sampling periods in 24h. The spatial results indicate the dominant role of sedimentation of particles from the treatment plant during distribution, while the observed increases in particles and the associated bacteria mainly originated from the distribution network, which were confirmed directly by the increased contributions of loose deposits and biofilm. Temporally, the daily peaks of particle-associated bacterial quantity, particle-associated metal elements, observed OTU number, and contributions of loose deposits and biofilms were captured at 18-21 h. The temporal results reveal clear linkages between the distribution system harboring bacteria (e.g., within loose deposits and biofilms) and the planktonic and particle-associated bacteria flowing through the distribution system, which are dynamically connected and interact. This study highlights that the spatiotemporal variations in planktonic and particle-associated bacteria are valuable and unneglectable for the widely on-going sampling campaigns required by water quality regulations and/or drinking water microbiological studies.

Keywords: Drinking water distribution system (DWDS); Online monitoring sampling system (OMSS); SourceTracker2; Spatiotemporal variations; Planktonic and particle-associated bacteria

3.1 Introduction

There is a consensus that the microbiological quality of drinking water changes during distribution (Prest et al., 2014), which could be caused by the growth of planktonic bacteria in the water and/or the release of attached bacteria from established biofilms and loose deposits in drinking water distribution systems (DWDS) (Chen et al., 2020; Kooij, 1992; Liu et al., 2017a; Liu et al., 2018). Studies have found that stagnation time and water demand are important factors influencing both the quantity and community of bacteria in DWDSs (Ling et al., 2018). For example, high bacterial concentrations and the growth of opportunistic pathogens in drinking water supply systems have been observed after long-term stagnation (Chan et al., 2019; Zhang et al., 2021; Zlatanovic et al., 2017). Hydraulic disturbances may cause water quality deterioration, such as increases in particle counts, water turbidity, and the concentrations of heavy metals and/or bacteria (Lehtola et al., 2006). All of the abovementioned water quality deteriorations pose public health concerns, especially regarding the biosafety of drinking water.

Worldwide, grab sampling is commonly used for regular assessments and statutory monitoring of drinking water quality in the DWDS. However, such low-resolution and labor-intensive sampling strategies can neither capture the aperiodic changes nor reveal the origination of physiochemical and microbiological contamination events (Banna et al., 2014). Online monitoring of particulate matter in the DWDS has been introduced since the early 2000s (Hargesheimer et al., 2002). Studies by online particle counting/sampling and pairwise monitoring of hydraulic parameters and turbidity have clearly illustrated the daily variations in particulate profiles, but their application has been preliminarily limited to physiochemical aspects (Matsui et al., 2007; Verberk et al., 2006), such as discolorations (Mounce et al., 2015; Vreeburg et al., 2008). Recently, online flow cytometry was developed for counting total and intact bacterial cells (Hammes et al., 2012) and applied in DWDS (Prest et al., 2021). By combining online particle counts, intact cell counts (ICCs) and adenosine triphosphate (ATP) measurements, Prest et al. (2021) observed a weak correlation between ATP and flow velocity, which was attributed to the release of particle-associated bacteria from biofilms or loose deposits. However, assessing only quantitative data on water samples could neither explain the source of contamination nor offer enlightenments on effective solutions.

The understanding of the microbial ecology in DWDS has been substantially expanded by the rapid development and application of high-throughput sequencing (Zhang and Liu, 2019). This

is especially true when the generated high-throughput sequencing data are combined with microbial ecology theory and mathematic modelling. For example, using an island biogeography model, Ling et al. found that pipe diameter drove the changes in the tap water bacterial community in building plumbing (Ling et al., 2018). By using the bacterial community fingerprint-based Bayesian SourceTracker, the authors quantified the contribution of biofilm and loose deposits to the bacteria present in tap in unchlorinated DWDS (Liu et al., 2018). However, in the study, the authors only collected three sets of samples in the distribution system, and capturing and tracing the aperiodic daily variations remains a critical knowledge gap. Therefore, the objective of this study is to capture and trace the aperiodic spatiotemporal variations in planktonic bacteria (PB) and particle-associated bacteria (PAB) in drinking water distribution systems. More specifically, based on the investigations of the spatial and temporal variations in the distribution system, the critical questions of what the local dominant processes are, when the peaks would occur, and why the changes may occur and where the changes may come from will be addressed. As an approach to this goal, an online sampling and monitoring system was developed, which was used and combined with the bacterial community fingerprint-based Bayesian SourceTracker. The findings obtained from this study advance the current understanding of the dynamics of aperiodic planktonic and particle-associated bacteria in drinking water distribution systems, which will be a powerful tool for water utilities to diagnose water quality problems and develop effective strategies for managing biological water quality.

3.2 Materials and methods

3.2.1 Drinking water treatment plant and sampling locations

The study was conducted in one of the drinking water supply systems of Oasen, the Netherlands. The drinking water treatment plant produces drinking water from anaerobic groundwater (340 m^3/h) through conventional treatment processes. In short, the water was treated by spray aeration, rapid sand filtration, pellet softening, carry-over submerged rapid sand filtration, granular activated carbon filtration and UV disinfection. The drinking water is distributed to customers without chlorine.

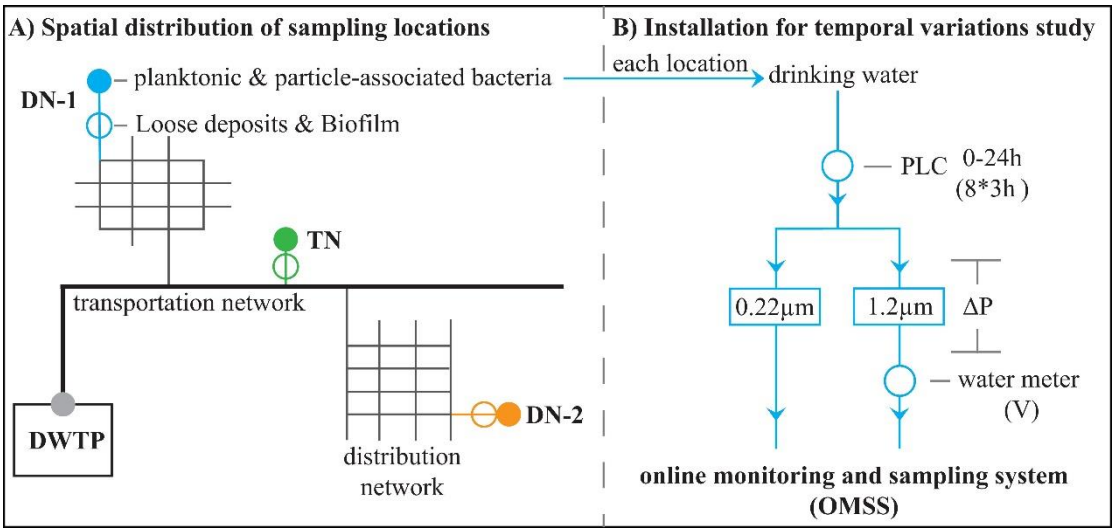

Figure 3-1. *A) Spatial distribution of sampling locations. DWTP stands for drinking water treatment plant, DN stands for locations in distribution network, TN stands for location in the transportation network. At each location, water, particles, biofilm and loose deposits were sampled. B) Illustration of the installation for temporal variation study, named the online monitoring and sampling system (OMSS), which runs continuously for 24 hours (8 × 3 hours) to capture the daily variations. The planktonic bacteria were sampled by filtrating drinking water through 0.22 µm filters, and particle-associated bacteria were sampled by filtrating drinking water through 1.2 µm filters. ΔPressure (ΔP) was recorded online.*

As illustrated in Figure 3-1A, the sampling locations were selected at the treatment plant before the water entered the distribution system (referred to as DWTP), at the transportation network before the water was distributed into communities (referred to as TN), and at distribution network locations (referred to as DN-1 and DN-2). More specifically, DN-1 and DN-2 were located at the distal part of the secondary distribution network (DN), while TN was located at the proximal part of the secondary distribution network that is connected to the transportation network (TN). The distribution pipe material is PVC-U in the study area. The diameter in TN is 110 mm, while the diameter in DN is 63 mm. In total, 147 samples were collected from the four locations, including 62 water samples (planktonic bacteria, PB), 63 suspended particles (particle-associated bacteria, PAB), 10 biofilms (BF), and 12 loose deposits (LD).

3.2.2 Online monitoring and sampling of water and suspended particles

A novel online monitoring and sampling system (OMSS) was developed to conduct online monitoring of water quality and continuous sampling of water and particles in DWDSs (Figure 3-1B). Briefly, the system integrated water quality monitoring sensors, data loggers, water

sampling bottles and particle sampling filters (Whatman, 1822-047, 1.2 μm), which were controlled and run by a preprogramed PLC for 24 hours. The filter pore size of 1.2 μm was selected based on the results of a previous study (Liu et al., 2013a). The online monitored physicochemical parameters included temperature, conductivity, and pH. Water and suspended particles were sampled every 3 hours. Suspended particles were sampled by filtrating tap water for 3 hours with particle sampling filters. Particle sampling filters were collected in triplicate 8 times a day automatically (n = 3 × 8, 24 samples) at sampling time periods of 0-3 h, 3-6 h, 6-9 h, 9-12 h, 12-15 h, 15-18 h, 18-21 h, and 21-24 h. The transmembrane pressure was monitored and recorded online, and the pressure differences per volume of water (ΔPressure/Volume, ΔP/V) were used as an index of particle load in water. The particle load reflects the degree of particle accumulation per volume of water but cannot be directly equated to turbidity. The filters and water bottles were kept in refrigerator to guarantee the sample quality for the downstream microbiological analysis. Samples were collected and transported on ice and processed in the lab immediately after the 24 hour sampling was performed. The OMSS was connected to the hydrants and operated at a flow of 2 L/min, resulting in a total of ~120 L per filter for suspended particle sampling. The flow was measured and recorded online by a digital flow meter. All data were logged every 5 minutes and visualized on a screen. The sampling was carried out in April and May. At each location, the OMSS ran for two consecutive working days to obtain reliable and representative samples. The sampling was conducted during the middle of the week (Tuesday and Wednesday) to mitigate the potential impact of low weekend demand on the water quality (Sekar et al., 2012).

3.2.3 Biofilm and loose deposit sampling

At each location, after the two days of running the OMSS, the loose deposits and biofilm were sampled as previously described (Vreeburg et al., 2008). In short, loose deposits were sampled at corresponding hydrants by fully opening the fire hydrant. Afterward, sections of the flushed pipes with biofilm were cut in duplicate from the network, PVC-U, D = 110 or 63 mm, length = 30 cm. During the cutting process, chlorine spray was used to disinfect both the exposed cleaned pipes and cutting tools to minimize the potential for contaminations. After cutting, the pipe section was closed with sterile caps and filled with DNA-free water to keep the inner surface wet. All samples were stored in sterile plastic containers on ice and transported to the lab within 2 hours. To detach the bacteria and materials from particles (filters), loose deposits (suspensions) and pipe surfaces (pipe section), the samples were pretreated by ultrasonication for 3 × 2 minutes at 42 KHz in a water bath (Liu et al., 2017a). The obtained suspensions were

used for downstream physicochemical and microbiological analyses.

3.2.4 Physicochemical analysis

The concentrations of metal elements in all samples, including iron (Fe), manganese (Mn), calcium (Ca), aluminum (Al), and arsenic (As), were determined by inductively coupled plasma-mass spectrometry (ICP-MS). Quality control samples, including laboratory-fortified blanks and laboratory-fortified samples, were performed for every 10 samples.

3.2.5 ATP measurement

ATP content measurements were used to determine the active biomass across all samples. The ATP content was measured using the Luciferene Luciferase method (Magic-Knezev and Van Der Kooij, 2004). In brief, the ATP released from cells by nucleotide-releasing buffer (NRB, Celsis) was measured by the intensity of the emitted light in a luminometer (Celsis AdvanceTM) calibrated with solutions of free ATP (Celsis) in autoclaved tap water following the procedure given by the manufacturer.

3.2.6 DNA extraction and sequencing

The DNA was extracted from all samples using the FastDNA Spin Kit for Soil (Q-Biogene/MP Biomedicals, Solon, OH, USA) according to the manufacturer's instructions. The extracted DNA was amplified with a primer set (341F: 5′-CCTACGGGNGGCWGCAG-3′ and 785R: 5′-GACTACHVGGGTATCTAATCC-3′) targeting the V3-V4 hypervariable regions of sequences from both bacterial and archaeal domains. The primer set was modified for the Illumina MiSeq platform (Illumina, Inc., San Diego, CA, USA) by appending the Illumina sequencing adaptors on the 5′ end. Paired-end sequencing of the amplicons (2 × 300 bp) was performed by BaseClear (Leiden, the Netherlands). The sequencing data have been deposited in the NCBI database (accession number PRJNA715925).

3.2.7 Sequence data processing

The sequences generated from the Illumina MiSeq analysis of the 16S rRNA gene amplicons were processed using the Quantitative Insights Into Microbial Ecology (QIIME2, v2020.11) pipeline with the default settings (Bolyen et al., 2018; Caporaso et al., 2010). Raw sequences were first processed using DADA2 (Callahan et al., 2016), including quality filtering, denoising, paired-end sequence merging, and chimera filtering. Unique amplicon sequence variants that were equivalent to 100% similarity operational taxonomic units (OTUs) in conventional

practice were consequently generated through DADA2. Taxonomy was assigned using the q2-feature classifier (Bokulich et al., 2018), customized for the primer set used in this study with Silva SSU database release 132 (Quast et al., 2012). Multiple sequence alignment and phylogenetic tree construction were performed using the QIIME 2 plugin q2-phylogeny. Alpha and beta diversity analyses were performed using the QIIME 2 plugin q2-diversity. Principal coordinate analysis (PCoA) was conducted based on weighted UniFrac distance matrices (Liu et al., 2014). The major OTUs are defined as OTUs with a defined cutoff of relative abundance (> 1%) within each sample category. The statistical analysis was performed in Past and Qiime2. Significant differences were identified when the p value was lower than 0.05 ($p < 0.05$).

3.2.8 SourceTracker analysis

The Bayesian-based SourceTracker method was performed to quantify the contribution of potential sources to the sinks (Henry et al., 2016). In the present study, the planktonic bacteria (PB) and particle-associated bacteria (PAB) at each location in the network (TN, DN-1, DN-2) were identified as sinks, while the PB and PAB at DWTP and the biofilm and loose deposits at corresponding locations in the network were defined as potential sources. SourceTracker analysis was conducted using default settings with a rarefaction depth of 1000, burn-in 100, restart 10, alpha (0.001) and beta (0.01). The analysis was performed three times, and the average was calculated as previously described (Henry et al., 2016; McCarthy et al., 2017).

3.3 Results

In general, clear spatial and temporal variations in the physiochemical and microbiological parameters in the DWDS were captured by the online monitoring and sampling system (OMSS). Spatially, the particle load ($\Delta P/V$) increased significantly from 1.98 ± 0.93 mbar/L in the DWTP to 3.15 ± 2.49 mbar/L in the primary transportation network (TN) and 21.36 ± 5.25 and 24.79 ± 7.24 mbar/L in the secondary distribution networks DN-1 and DN-2, respectively ($P < 0.001$, Figure 3-S1A). Temporally, peaks in particles and microbes were observed corresponding to the water demand peaks in the morning (06-09:00) and/or in the evening (18-21:00) (Figure 3-S2). In this section, the results will be presented with an emphasis on capturing and tracing the dynamics of quantity and community of the planktonic bacteria (PB) and particle-associated bacteria (PAB).

3.3.1 Spatial variations in PB and PAB

Quantity. Considering the active biomass, the ATP concentrations in water were stable ($8.1 \pm$

0.9 ng/L) among the sampling times and locations, while the particle-associated ATP (P-ATP) decreased from 1.10 ± 0.40 ng/L at DWTP to 0.09 ± 0.03 ng/L at TN and then slightly increased to 0.23 ± 0.15 ng/L and 0.13 ± 0.06 ng/L at DN-1 and DN-2, respectively ($P < 0.001$, Figure 3-2A). A weak negative correlation was observed between particle load and particle-associated ATP ($R^2 = 0.17$, $P = 0.001$, Figure 3-2B).

Community. In total, 2,655,227 sequences were obtained for 147 samples, including 62 water (PB), 63 particles (PAB), 10 biofilms (BF), and 12 loose deposits (LD), which were assigned as 18,308 OTUs. The rarefication curves reached a plateau after 3000 sequences, indicating that enough sample coverage was obtained in the present study (Figure 3-S3). Alpha and beta diversity scores were generated after verification to an even sampling depth of 5670. For PB, the number of observed OTUs followed the same changes as P-ATP, which decreased first from DWTP (457 ± 171 OTUs) to TN (331 ± 50 OTUs) and increased in DN (636 ± 205 at DN1, 646 ± 251 OTUs at DN2) ($P < 0.001$, Figure 3-3A). Similarly, for PAB, the number of observed OTUs decreased from DWTP (456 ± 59 OTUs) to TN (381 ± 38 OTUs) and then increased in DN (803 ± 101 OTUs at DN-1, 939 ± 152 OTUs at DN-2) ($P < 0.001$, Figure 3-3B). A strong positive correlation was observed between the number of observed OTUs in PAB and particle load ($R^2 = 0.69$, $P < 0.001$, Figure 3-3C).

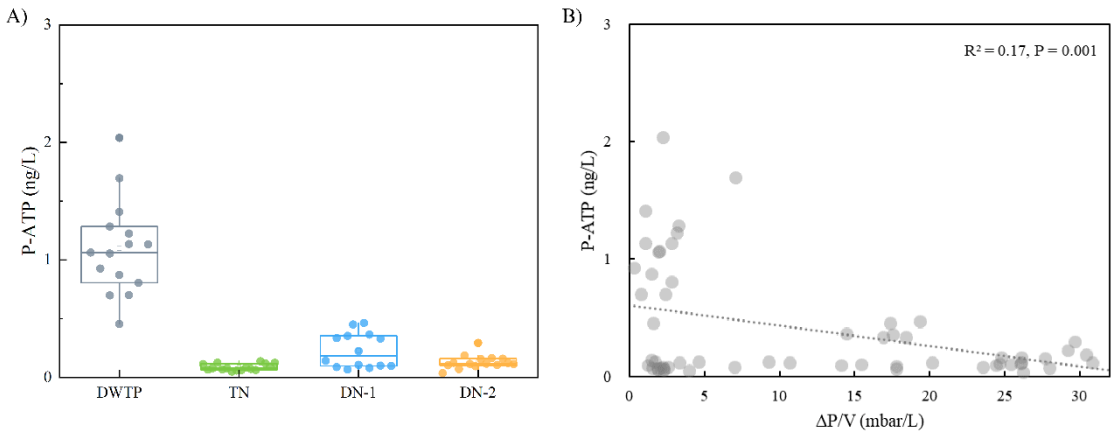

Figure 3-2. *Variations in particle-associated ATP (P-ATP) during distribution from DWTP to DWDS (A) and the correlation between the particle-associated ATP (P-ATP) and particle load (ΔP/V) (B). Box plots show median values (middle line), 25th and 75th percentiles (boxes) and 5th and 95th percentiles (whiskers) with individual data points overlaid. Outliers, if present, are shown as individual points beyond the whiskers.*

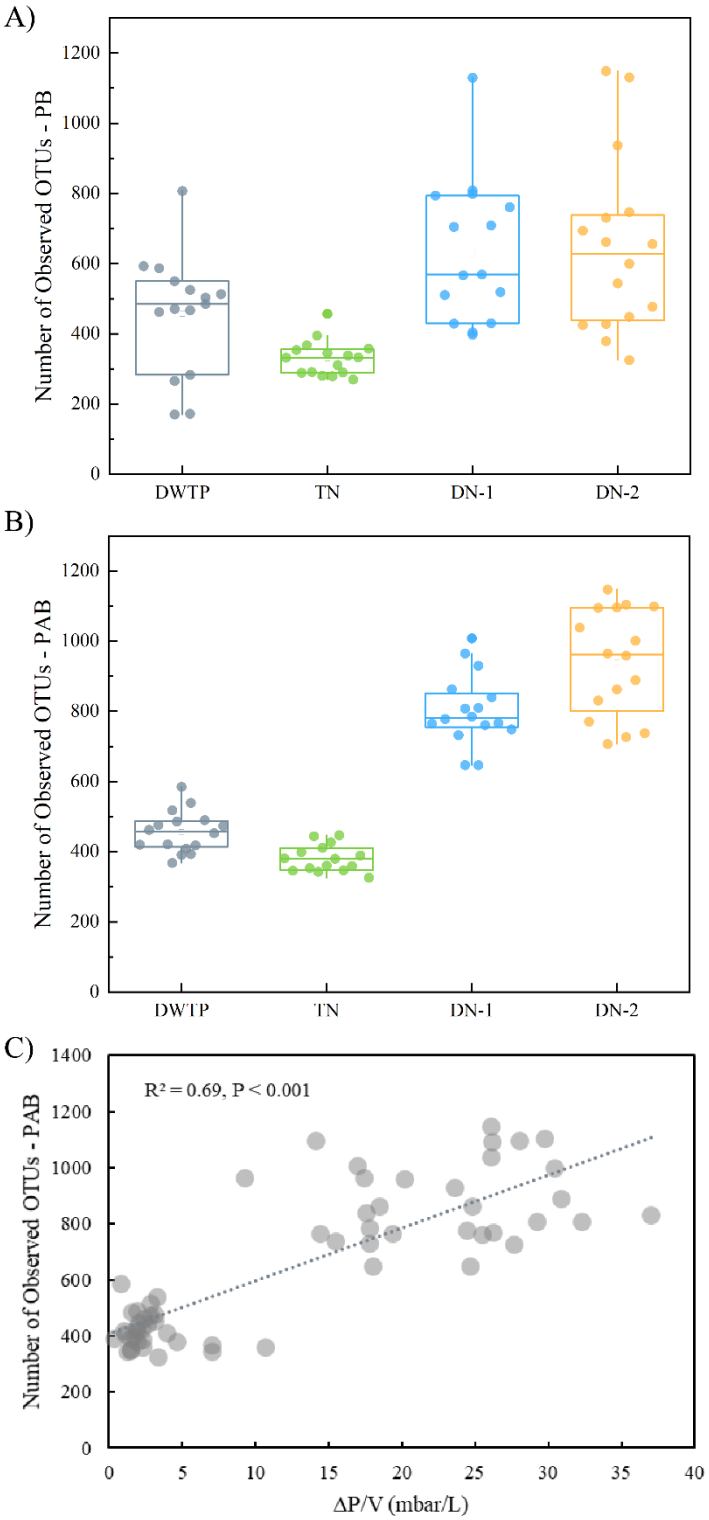

Figure 3-3. *The numbers of observed OTUs for A) PB and B) PAB at different locations; and C) the correlation between the number of observed OTUs for PAB and particle load (ΔP/V). Box plots show median values (middle line), 25th and 75th percentiles (boxes) and 5th and 95th percentiles (whiskers) with individual data points overlaid. Outliers, if present, are shown as individual points beyond the whiskers.*

Regarding beta diversity, the PCoA plot showed that the PB community was highly similar among all locations. For the PAB community, TN clustered together with DWTP, which was different from DN-1 and DN-2 (Figure 3-S4). At the phylum level, both PB and PAB were dominated by Proteobacteria and Patescibacteria across all locations (Figure 3-S5A and 3-S5B). The relative abundance of Proteobacteria decreased from the DWTP to locations in the distribution system, while the relative abundance of Patescibacteria showed the reverse trend. At the genus level, the relative abundance of OTU1525, assigned as *Polaromonas* spp., decreased dramatically from DWTP to distribution sites for both PB and PAB (Figure S6A and 3-S6B). In contrast, the relative abundances of OTU903 (assigned as the order *Candidatus Kaiserbacteria*) and OTU1540 (assigned as the family *Burkholderiaceae*) increased from DWTP to DWDS for PB, and the relative abundances of OTU1137 (assigned as *Caulobacter* spp.) and 1657 (assigned as the family *Methylomonaceae*) increased from DWTP to DWDS for PAB.

Compared to PB and PAB, higher OTU numbers were observed in loose deposits (LD, 980 ± 96) and biofilms (BF, 806 ± 302) (Table 3-S1). According to the beta diversity shown as the PCoA plot in Figure S4, the bacterial communities of LD and BF were highly similar regardless of phase and location. For the bacterial community composition, Proteobacteria was the dominant phylum in both LD (41.6 ± 4.0%) and BF (54.9 ± 10.4%), followed by Planctomycetes, Acidobacteria, Chloroflexi, Nitrospirae, Patescibacteria, Bacteroidetes and Gemmatimonadetes (Figure 3-S5C). The taxonomic profile at the OTU level is shown in Figure S6C and Table 3-S2.

3.3.2 Daily variations in PB and PAB

At the DWTP, the particle load was relatively stable (1.98 ± 0.93 mbar/L), while clear daily patterns were observed in the DWDS, with peak hours occurring at different times, e.g., 8.82 mbar/L between 6-9 h at TN, 25.34 mbar/L between 18-21 h at DN-1, and double peaks at DN-2 between 6-9 h (31.57 mbar/L) and between 18-21 h (30.64 mbar/L) (Figure 3-S2A). The peaks of particle load were positively correlated with the concentrations of five selected elements but not with the concentrations of PB (ATP) or PAB (P-ATP), indicating that the particles might have mainly consisted of nonbiomass (Figure 3-2B and 3-S7).

Considering the bacterial community, no clear peak in OTU number was found for PB at either DWTP or TN. Remarkably, the peak numbers were observed between 18-21 h at DN-1 (804 OTUs) and DN-2 (813 OTUs), which was exactly the time of peak particle loads at the location

(Figure 3-4A and 3-S2A). Although it was not reflected in the beta diversity analysis results, significant daily variations in bacterial community composition were observed at the OTU level at DN-1 and DN-2. For example, the relative abundance of OTU903 reached its peak between 18-21 h at DN-2 (Figure 3-4C).

For PAB, there were no significant daily variations in alpha and beta diversity analysis (Figure 3-4B and 3-S4), whereas differences in bacterial community composition were observed over the course of the day at each location (Figure 3-4D). For example, peaks of certain OTUs were observed during the particle load peaks at TN (OTU1526, assigned as *Polynucleobacter* spp.) and DN-2 (OTU1498, assigned as *Aquabacterium* spp.) (Figure 3-4D). In particular, taking location TN as an example, when comparing the peak hour 6-9 h with other sampling hours, many OTUs (i.e., OTU1526, OTU899, OTU892) were significantly enriched (Figure 3-S8).

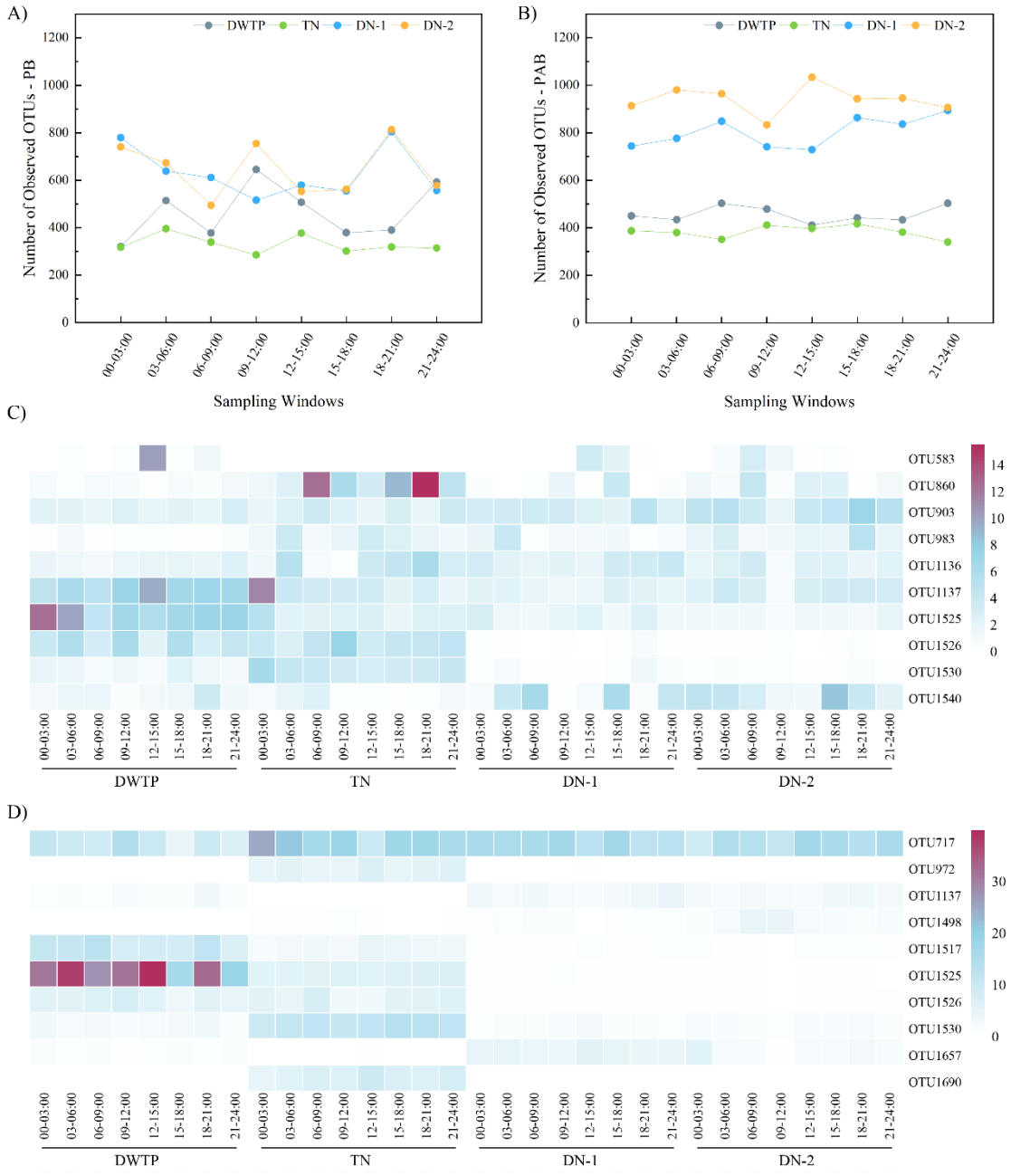

Figure 3-4. *The daily variations in the number of observed OTUs and the top 10 dominant OTUs over time and space in DWDS: A) the daily variations in observed OTU numbers for PB; B) the daily variations in observed OTU numbers for PAB; C) the heatmap showing the top 10 dominant OTUs in PB; and D) the heatmap showing the 10 dominant OTUs in PAB. The line plots show the averaged values in the number of observed OTUs from triplicate samples at each time point, while the heatmaps illustrate the averaged relative abundance within each species from triplicate samples at each time point.*

3.3.3 Microbial source tracking of the PB and PAB variations

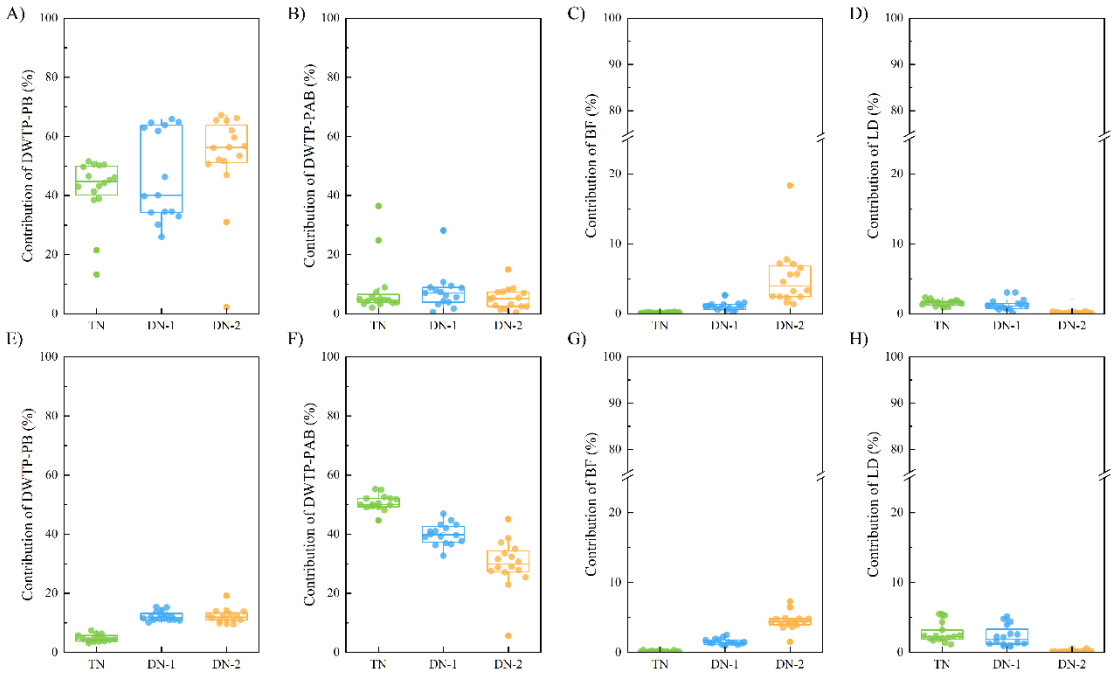

Figure 3-5. *The percentages of contributions from different sources (PB and PAB at DWTP, BF and LD) to PB and PAB in the DWDS at different locations. A) the percentage of contributions from PB at DWTP to PB in DWDSs across different locations; B) the percentage of contributions from PAB at DWTP to PB in DWDSs across different locations; C) the percentage of contributions from BF to PB in DWDSs across different locations; D) the percentage of contributions from LD to PB in DWDSs across different locations; E) the percentage of contributions from PB at DWTP to PAB in DWDSs across different locations; F) the percentage of contributions from PAB at DWTP to PAB in DWDSs across different locations; G) the percentage of contributions from BF to PAB in DWDSs across different locations; H) the percentage of contributions from LD to PAB in DWDSs across different locations. BF stands for biofilm, while LD stands for loose deposits. Box plots show median values (middle line), 25th and 75th percentiles (boxes) and 5th and 95th percentiles (whiskers) with individual data points overlaid. Outliers, if present, are shown as individual points beyond the whiskers.*

Spatially, the PB at the DWTP was the major contributor to the PB in water in the DWDS (47.3 ± 14.0%), the contribution of which increased slightly from 42.2 ± 10.6% at TN to 46.9 ± 15.2% at DN-1 and 52.7 ± 16.2% at DN-2 (Figure 3-5A). Similarly, the PAB at DWTP was the main contributor to the PAB in the distribution system (40.2 ± 4.4%), but the exact contribution decreased from 50.7 ± 1.2% at TN to 40.0 ± 3.6% at DN-1 and 29.9 ± 8.5% at DN-2 (Figure 3-5F). Noticeably, the contributions of BF and LD to the PB and PAB in DWDS increased along

the distance from TN (PB,1.8 ± 0.5%; PAB 2.8 ± 3.4%) to DN-1 (PB, 2.3 ± 1.3%; PAB, 3.8 ± 1.9%) and further increased to DN-2 (PB, 5.3 ± 4.2%; PAB, 4.7 ± 1.4%) (Figure 3-5C, 3-5D, 3-5G, and 3-5H). In addition, a large fraction of the contribution was from unknown sources, which may be because some possible sources were not covered in the sampling campaign.

Temporally, significant peak contributions of BF and LD to PB and PAB in DWDS were captured. The contributions from BF and LD were well correlated with the trend of the daily particle loads (Figure 3-S9, $R^2 = 0.22$ and $P < 0.001$ for PB, $R^2 = 0.34$ and $P < 0.001$ for PAB), suggesting the potential sporadic release of BF- and LD-harbored microbes and contaminants during regular water demand fluctuations. This is especially true after the secondary distribution at DN-1 and DN-2, where multiple peaks of BF and LD contributions were observed. For example, peak contributions of BF and LD to PAB at DN-1 were captured at 6-9 h (BF, 1.8 ±1.0%; LD, 3.1 ± 1.3%), 18-21 h (BF, 1.9 ± 0.1%; LD, 3.3 ± 1.5%), and 21-24 h (BF, 1.9 ± 0.6%; LD, 5.0 ± 0.3%) (Figure 3-S10), while peak contributions of BF and LD to PB at DN-2 were captured at 3-6 h (BF, 6.7 ± 1.5%; LD, 0.2 ± 0.1%), 6-9 h (BF, 4.5 ± 3.0%; LD, 0.3 ± 0.1%), and 18-21 h (BF, 5.3 ± 2.7%; LD, 0.2 ± 0.2%) (Figure 3-S11).

3.4 Discussion

An online monitoring and sampling system (OMSS) was combined with SourceTracker to assess the spatial and temporal variations in the quantity and community of planktonic bacteria (PB) and particle-associated bacteria (PAB) in a drinking water distribution system (DWDS). The spatial variations revealed a dominant process during distribution, which allowed for the understanding of general biological water quality changes. In addition, online sampling and monitoring at certain locations makes it possible to have reliable comparisons among different locations, which also uncovers the local circumstances and contributions of the DWDS to daily water quality variations.

3.4.1 Spatial variations in PB and PAB reveal the dominant process in the DWDS

Water quality is determined by complicated physiochemical and biological processes in DWDSs, such as the sedimentation and resuspension of particles with the associated bacteria (Vreeburg and Boxall, 2007) and the attachment and detachment of bacteria to/from pipe wall biofilms (Liu et al., 2018). However, conventional sampling methods (e.g., a single collection time-point) and analysis parameters (e.g., heterotrophic plate count with insufficient sensitivity) can hardly reveal the dominant processes (Banna et al., 2014). In the present study, the results

obtained from different locations by the combination of online monitoring and sampling, integral analysis, and bacterial community fingerprint-based source tracking make it possible to explore the detailed processes that occur during water distribution. For all parameters analyzed, the newly developed online monitoring and sampling outlined the ranges of variation at each location, based on which a rational spatial comparison could be made with high resolution. In this manner, the mismatched comparison of randomly single time-point grabbed samples and any potential misunderstanding on distribution processes could be avoided, such as comparing a valley value from one location with a peak value of another location.

The newly introduced parameter 'ΔP/V' captured particle load variations (not revealed by turbidity, results not shown), which increased significantly from DWTP to DWDS, especially after the secondary network at DN-1 and DN-2. The observed increase in particle load in DWDS complied with a previous study in chlorinated (filtration, quantified offline by TSS) (Matsui et al., 2007) and unchlorinated systems (online particle counting) (Verberk et al., 2009). Considering other newly introduced measures, the decrease in active PAB (P-ATP), the decrease of PAB_{-DWTP}'s contributions to PAB_{-DWDS}, and the increase in PAB_{-DWDS}'s diversity (observed OTU numbers), it is reasonable to argue that particles supplied by DWTP were dominated by the sedimentation process, while new particles were released from loose deposits (LD) and biofilms (BF) in the secondary network. This was directly confirmed by the increases in LD and BF contributions to PB and PAB from TN to DN-1 and DN-2, which also agree with the findings of a previous study assessing the origins of PB and PAB in unchlorinated DWDS (Liu et al., 2018). In addition, it was observed that the changes of physicochemical and microbiological parameters in the primary distribution network (TN) was statistically different from that of the secondary network (DN-1 and DN-2). More specifically, there were no visible changes from DWTP to TN, but significant increases at DN-1 and DN-2 of the particle load, particle-associated elements and the number of OTUs of both PB and PAB. This could be attributed to the longer residence time, smaller diameter (bigger surface/volume ratio), and more variable local hydraulics in the secondary network than primary network, which have been reported as factors influencing either the interactions between pipe wall and water (e.g. release of biofilm, pipe scale, loose deposits) (Ling et al., 2018; Liu et al., 2017b; Tsvetanova and Hoekstra, 2010), and/or the reactions within bulk water itself (e.g. bacterial growth, particle aggregation, disinfectant decay if applicable) (AWWA, 2002; Scharfenaker, 2002).

3.4.2 Daily dynamics of PB and PAB uncover the local circumstances of DWDS

There were no significant daily variations for any parameters measured at the DWTP, suggesting a stable input from the treatment plant into the DWDS. In the DWDS, clear daily variations were observed, which were captured as peaks of particle loads, observed OTU numbers (PB), and certain members of the PB and PAB communities. Similar morning/evening peaks of turbidity and cell numbers in DWDSs were reported previously (Besmer and Hammes, 2016; Matsui et al., 2007; Sekar et al., 2012). In addition, another study found daily patterns of PB community richness in chlorinated systems, but the peak periods varied among locations (e.g., 8-12 h and 0-4 h) (Bautista-de Los Santos et al., 2016a). In the same study, the authors also reported significant differences in PB community structure and composition between 8-12 h and 16-20 h. Likewise, Sekar et al. found temporal variations in the microbial community of drinking water between 06:00 and 09:00 am (Sekar et al., 2012). However, no significant difference in the bacterial community was observed among the different periods for either PB or PAB in the present study. This might be because the present study was conducted in unchlorinated DWDS, where the flocculation of chlorine decay associated with water demand and usage shaping the bacterial community would not occur (Ling et al., 2018).

Considering that the feed from the DWTP is stable, it is reasonable to hypothesize that the captured daily peaks at each site were contributed by local DWDS circumstances (e.g., level of harbored contaminants and hydraulic turbulences), which can be well illustrated by characterizing PB and PAB. This is especially true for the increase in PB OTU numbers between 18-21 h at DN-1 from 636 OTUs on average to 804 OTUs and at DN-2 from 646 OTUs on average to 813 OTUs. Such increases in OTU number were positively correlated with the increase in particle load, which may be because local water demand peaks lead to variable hydraulic regimes in pipes and cause different levels of BF and LD release (Carragher et al., 2012; Douterelo et al., 2013; Lucas et al., 2010; Sekar et al., 2012). Previous studies also found that the increased flow rate accompanied by increases of shear stress and scouring forces caused the release of particles and cells into water from biofilm and loose deposits (Choi and Morgenroth, 2003; Husband et al., 2008; Paul et al., 2012). In the present study, the peaks of loose deposits and biofilm contributions to PB and PAB in the DWDS (calculated by SourceTracker) during the evening and morning hours offered direct and solid evidence to for this hypothesis. Notably, the increase in PB OTU numbers did not lead to significant changes in PB community structure because the contributions of LD and BF to PB were 5.3%, which were lower than the previously reported threshold (20%) in the same DWDS (Liu et al., 2017a).

3.4.3 Practical implications

The present study sensitively captured the spatial and temporal variations in PB and PAB in a DWDS, which is important to consider for both routine sampling campaigns required by the water quality regulations and the widely conducted random collection sampling campaigns for research purposes. Ignoring such aperiodic variations would lead to mismatched comparisons of spatiotemporal series data and misunderstandings of DWDS microbial ecology. In addition, it was demonstrated that the quantitative and qualitative characterizations of PB and PAB could be valuable messengers for determining local dominant processes within DWDS. However, to understand the origin of captured variations and develop an effective management strategy accordingly, high-resolution integral sampling campaigns are required to cover all potential sources. It would be even more powerful if other online microbiological analyses could be used together with OMSS, such as the commercially available automated ATP (de Vera and Wert, 2019) and the online flow cytometers (Besmer et al., 2014).

This study was conducted in an unchlorinated distribution system under regular water supply conditions. For chlorinated distribution systems subjected to supply-water changes and/or hydrological disturbances, the proposed methodology of combining OMSS with SourceTracker based on microbial community fingerprints would also be valuable for investigating water quality dynamics and transition effects. In chlorinated systems, the dynamic changes in PB and PAB because of water demand, stagnation and chlorine decay could be investigated with high resolution. For example, critical questions such as daily spatiotemporal variations of chlorine residual, its correlation with PB and PAB changes, and the local interactions among water, biofilm and loose deposits could be answered. Moreover, the methodology involves continuous online monitoring and sampling, as well as large volume preconcentration. These advantages allow it to overcome the challenges of transition effect studies, e.g., its contingency and the dilution of released bacteria when it takes place. Therefore, as suggested previously, using OMSS will significantly increase the success rate of capturing the release events and transition effects compared to offline sampling (Chen et al., 2020). Future application of such a method is highly recommended both for studying the mechanism of water quality deterioration during water distribution and for preventing esthetic and health risks at customers' ends, especially if the distribution system is subject to supply-water quality changes (e.g., switching source water, upgrading treatments) and/or hydraulic disturbances (e.g., long-term stagnation during the pandemic, postrepair flushing, firefighting).

3.5 Conclusions

In the present study, an online monitoring and sampling system (OMSS) was developed to investigate the daily variations in planktonic and particle-associated bacteria in an unchlorinated drinking water distribution system. The microbial fingerprint-based SourceTracker was used for capturing and source tracking the daily bacterial peaks, using planktonic and particle-associated bacteria in treated water and the biofilm and loose deposits in the distribution system as potential sources. The following conclusions can be drawn from this study regarding the daily variations in particle and bacterial load, changes in the diversity and composition of bacterial communities, and the sources of increased particles and cells during hydraulic peaks:

- Spatially, the particle load slightly increased from the treatment plant to the transportation network and then sharply increased in the distribution network. In contrast, the quantity of particle-associated bacteria decreased from the treatment plant to the transportation network and the distribution network. For both planktonic and particle-associated bacteria, the number of observed OTUs first slightly decreased from the treatment plant to the transportation network and then sharply increased in the distribution network. According to the SourceTracker results, the planktonic and particle-associated bacteria in the produced water are the main contributors to bacteria in the distribution system. Along the distribution distance, the contribution of planktonic bacteria from the treatment plant increased, while the contribution of particle-associated bacteria from the treatment plant deceased.
- Temporally, clear daily patterns were observed, especially at the two locations in the distribution network (DN-1, DN-2). More specifically, the quantitative peaks of particle-associated bacteria were captured at morning (6-9h) and/or evening (18-21h) hours during the day. According to the SourceTracker results, the contributions of biofilm and loose deposits to the planktonic and particle-associated bacteria in the drinking water distribution system (DN-1 and DN-2) spiked during the morning (6-9h) and/or evening (18-21h) hours, accounting for 5.3 ± 2.7% and 6.7 ± 1.5%, respectively.
- Methodologically, it was demonstrated that the combination of an online monitoring and sampling system (OMSS) and the microbial fingerprint-based SourceTracker is a powerful tool for studying spatiotemporal water quality variations in an unchlorinated drinking water distribution system. The particles and bacteria can be valuable messengers revealing physiochemical and microbiological processes occurring in

distribution systems. To better understand and manage the microbiological quality of drinking water during distribution, future investigations are recommended to apply such a method in chlorinated systems and/or transition effect studies.

Supporting information

Table 3-S1. The number of observed OTUs in biofilm and loose deposits across all locations

Phase	Location	The number of observed OTUs
Biofilm	DN-1	960 ± 294
	DN-2	795 ± 266
	TN	523 ± 305
Loose deposits	DN-1	1000 ± 96
	DN-2	951 ± 46
	TN	990 ± 143

Table 3-S2. The taxonomy information of OTUs in all heatmaps

OUT ID	Phylum	Class	Order	Family	Genus
OTU32	Acidobacteria	Blastocatellia (Subgroup 4)	Blastocatellales	Blastocatellaceae	JGI 0001001-H03
OTU52	Acidobacteria	Subgroup 17	metagenome	metagenome	metagenome
OTU85	Acidobacteria	Subgroup 6	__	__	__
OTU263	Bacteroidetes	Bacteroidia	Cytophagales	Microscillaceae	uncultured
OTU323	Bacteroidetes	Bacteroidia	Sphingobacteriales	env.OPS 17	__
OTU382	Chloroflexi	Anaerolineae	Anaerolineales	Anaerolineaceae	uncultured
OTU455	Chloroflexi	Dehalococcoidia	S085	metagenome	metagenome
OTU480	Chloroflexi	JG30-KF-CM66	uncultured bacterium	uncultured bacterium	uncultured bacterium
OTU506	Cyanobacteria	Melainabacteria	Obscuribacterales	uncultured bacterium	uncultured bacterium
OTU531	Dadabacteria	Dadabacteriia	Dadabacteriales	uncultured candidate division SBR1093 bacterium	uncultured candidate division SBR1093 bacterium
OTU578	Entotheonellaeota	Entotheonellia	Entotheonellales	Entotheonellaceae	Candidatus Entotheonella
OTU583	Epsilonbacteraeota	Campylobacteria	Campylobacterales	Thiovulaceae	Sulfuricurvum
OTU642	Gemmatimonadetes	BD2-11 terrestrial group	__	__	__
OTU644	Gemmatimonadetes	Gemmatimonadetes	Gemmatimonadales	Gemmatimonadaceae	uncultured
OTU672	Latescibacteria	__	__	__	__
OTU693	Nitrospirae	Nitrospira	Nitrospirales	Nitrospiraceae	Nitrospira
OTU717	Omnitrophicaeota	uncultured bacterium	uncultured bacterium	uncultured bacterium	uncultured bacterium
OTU860	Patescibacteria	Parcubacteria	Candidatus Adlerbacteria	metagenome	metagenome

Table 3-S2. Continued.

OUT ID	Phylum	Class	Order	Family	Genus
OTU903	Patescibacteria	Parcubacteria	Candidatus Kaiserbacteria	__	__
OTU972	Patescibacteria	Saccharimonadia	Saccharimonadales	Saccharimonadaceae	uncultured bacterium
OTU983	Patescibacteria	Saccharimonadia	Saccharimonadales	__	__
OTU1010	Planctomycetes	OM190	uncultured bacterium	uncultured bacterium	uncultured bacterium
OTU1021	Planctomycetes	Phycisphaerae	CCM11a	uncultured Planctomycetaceae bacterium	uncultured Planctomycetaceae bacterium
OTU1036	Planctomycetes	Phycisphaerae	Phycisphaerales	Phycisphaeraceae	SM1A02
OTU1074	Planctomycetes	Planctomycetacia	Gemmatales	Gemmataceae	uncultured
OTU1083	Planctomycetes	Planctomycetacia	Pirellulales	Pirellulaceae	Pir4 lineage
OTU1086	Planctomycetes	Planctomycetacia	Pirellulales	Pirellulaceae	uncultured
OTU1101	Planctomycetes	Planctomycetacia	Planctomycetales	uncultured	__
OTU1136	Proteobacteria	Alphaproteobacteria	Caulobacterales	Caulobacteraceae	Brevundimonas
OTU1137	Proteobacteria	Alphaproteobacteria	Caulobacterales	Caulobacteraceae	Caulobacter
OTU1142	Proteobacteria	Alphaproteobacteria	Caulobacterales	Hyphomonadaceae	SWB02
OTU1182	Proteobacteria	Alphaproteobacteria	Rhizobiales	A0839	__
OTU1187	Proteobacteria	Alphaproteobacteria	Rhizobiales	Beijerinckiaceae	Methylocystis
OTU1200	Proteobacteria	Alphaproteobacteria	Rhizobiales	Methyloligellaceae	uncultured
OTU1209	Proteobacteria	Alphaproteobacteria	Rhizobiales	Rhizobiales Incertae Sedis	uncultured
OTU1248	Proteobacteria	Alphaproteobacteria	Rhodospirillales	uncultured	__

Table 3-S2. Continued.

OUT ID	Phylum	Class	Order	Family	Genus
OTU1285	Proteobacteria	Alphaproteobacteria	Sneathiellales	Sneathiellaceae	uncultured
OTU1315	Proteobacteria	Alphaproteobacteria	uncultured	uncultured bacterium	uncultured bacterium
OTU1316	Proteobacteria	Alphaproteobacteria	uncultured	__	__
OTU1373	Proteobacteria	Deltaproteobacteria	Myxococcales	Haliangiaceae	Haliangium
OTU1398	Proteobacteria	Deltaproteobacteria	Myxococcales	bacteriap25	uncultured Syntrophobacterales bacterium
OTU1405	Proteobacteria	Deltaproteobacteria	Myxococcales	bacteriap25	__
OTU1476	Proteobacteria	Deltaproteobacteria	__	__	__
OTU1498	Proteobacteria	Gammaproteobacteria	Betaproteobacteriales	Burkholderiaceae	Aquabacterium
OTU1517	Proteobacteria	Gammaproteobacteria	Betaproteobacteriales	Burkholderiaceae	Limnohabitans
OTU1525	Proteobacteria	Gammaproteobacteria	Betaproteobacteriales	Burkholderiaceae	Polaromonas
OTU1526	Proteobacteria	Gammaproteobacteria	Betaproteobacteriales	Burkholderiaceae	Polynucleobacter
OTU1530	Proteobacteria	Gammaproteobacteria	Betaproteobacteriales	Burkholderiaceae	Rhodoferax
OTU1540	Proteobacteria	Gammaproteobacteria	Betaproteobacteriales	Burkholderiaceae	__
OTU1564	Proteobacteria	Gammaproteobacteria	Betaproteobacteriales	Nitrosomonadaceae	IS-44
OTU1565	Proteobacteria	Gammaproteobacteria	Betaproteobacteriales	Nitrosomonadaceae	MND1
OTU1579	Proteobacteria	Gammaproteobacteria	Betaproteobacteriales	Rhodocyclaceae	Sulfuritalea
OTU1593	Proteobacteria	Gammaproteobacteria	Betaproteobacteriales	TRA3-20	__

Table 3-S2. Continued.

OUT ID	Phylum	Class	Order	Family	Genus
OTU1649	Proteobacteria	Gammaproteobacteria	Methylococcales	Methylomonaceae	IheB2-23
OTU1651	Proteobacteria	Gammaproteobacteria	Methylococcales	Methylomonaceae	Methyloglobulus
OTU1657	Proteobacteria	Gammaproteobacteria	Methylococcales	Methylomonaceae	__
OTU1666	Proteobacteria	Gammaproteobacteria	PLTA13	__	__
OTU1690	Proteobacteria	Gammaproteobacteria	Tenderiales	Tenderiaceae	Candidatus Tenderia

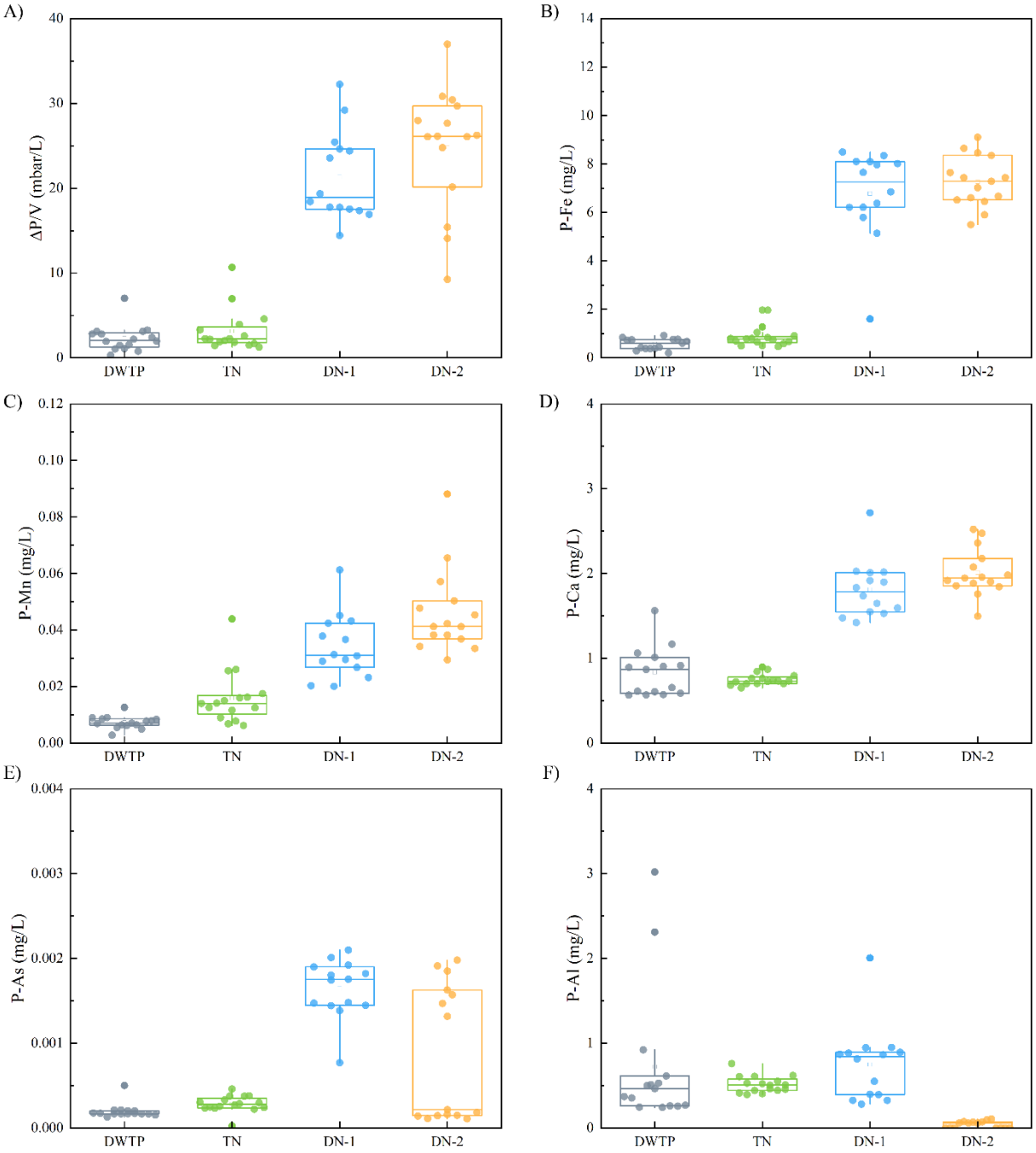

Figure 3-S1. The spatial variations in particle loads (ΔP/V, A) and particle-associated Fe (P-Fe, B), Mn (P-Mn, C), Ca (P-Ca, D), As (P-As, E), and Al (P-Al, F). Box plots show median values (middle line), 25th and 75th percentiles (boxes) and 5th and 95th percentiles (whiskers) with individual data points overlaid. Outliers, if present, are shown as individual points beyond the whiskers.

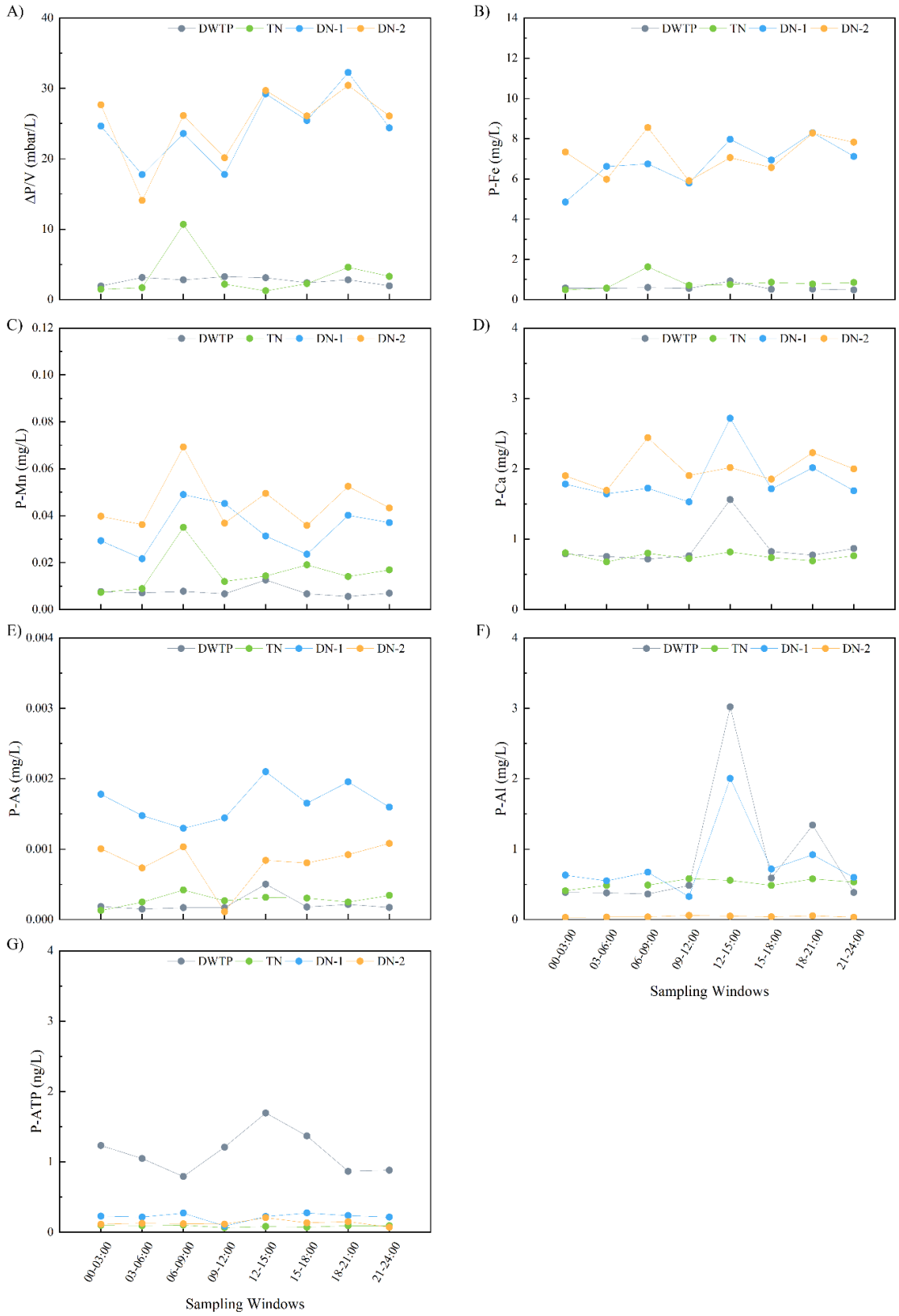

Figure 3-S2. The daily variations in particle loads (ΔP/V, A) and particle-associated Fe (P-Fe, B), Mn (P-Mn, C), Ca (P-Ca, D), As (P-As, E), Al (P-Al, F) and ATP (P-ATP, G). The line plots show the averaged values in each parameter from triplicate samples at each time point.

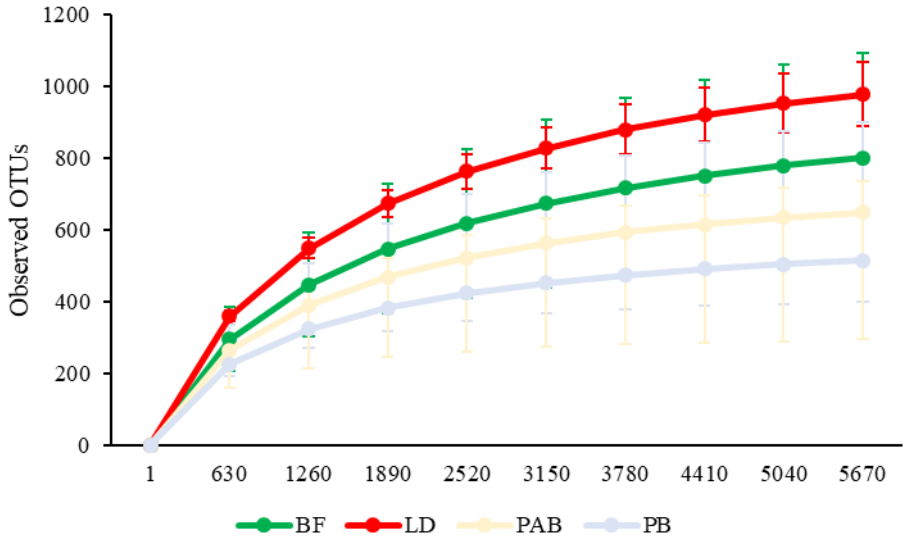

Figure 3-S3. Rarefaction curves

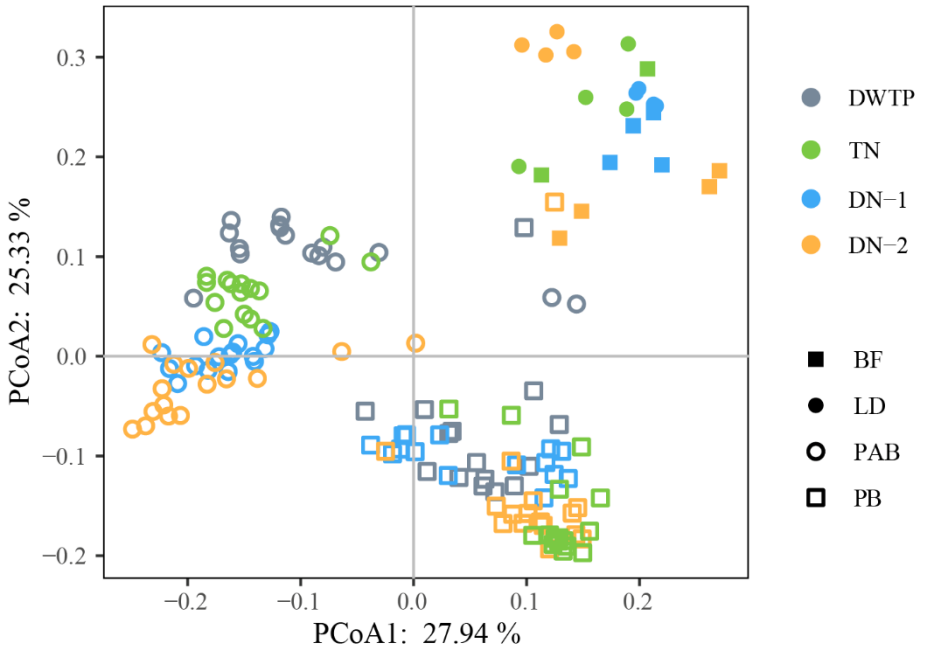

Figure 3-S4. The PCoA plot showing the dissimilarity of all samples from different phases and locations based on weighted Unifrac distance. BF represents biofilm, while LD represents loose deposits.

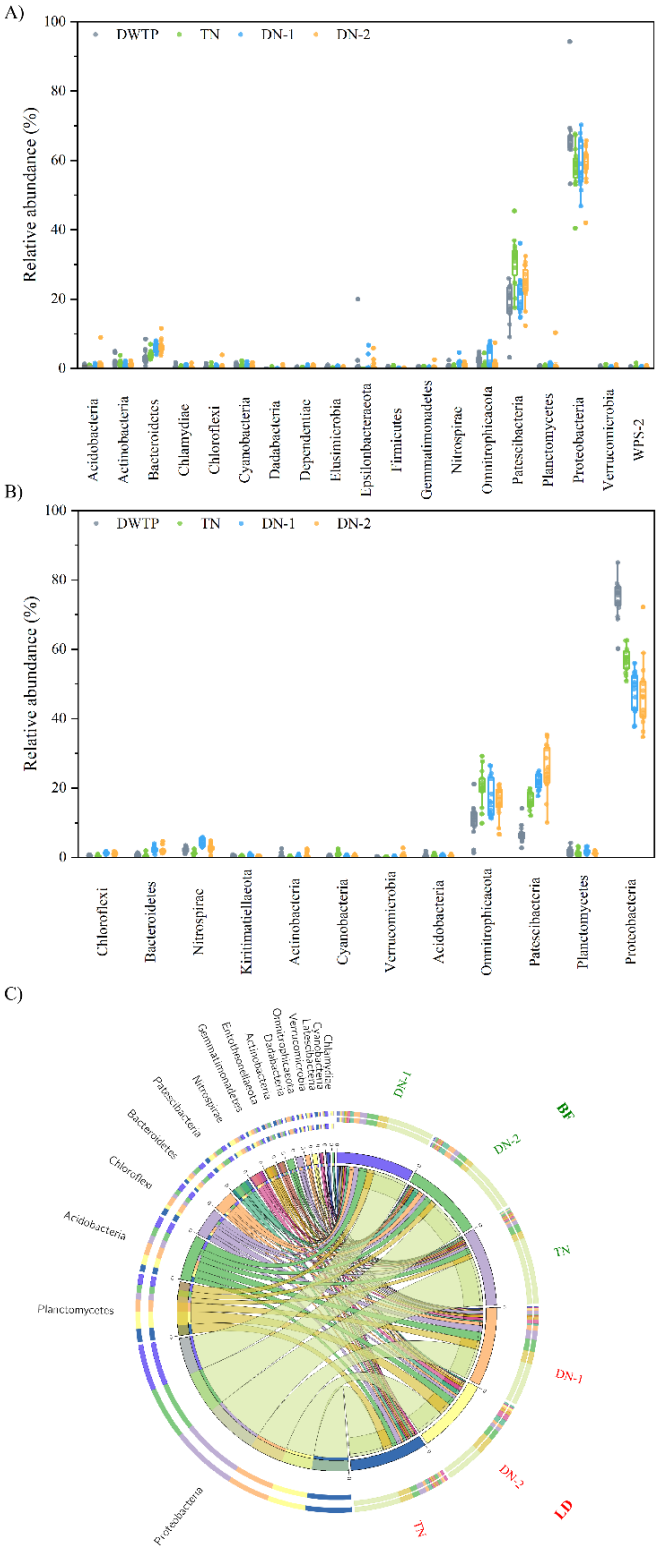

Figure 3-S5. Major phylum (relative abundance > 1%) within water (A), particles (B), biofilm (BF) and loose deposits (LD, C) samples across all locations. Box plots show median values (middle line), 25th and 75th percentiles (boxes) and 5th and 95th percentiles (whiskers) with individual data points overlaid. Outliers, if present, are shown as individual points beyond the whiskers.

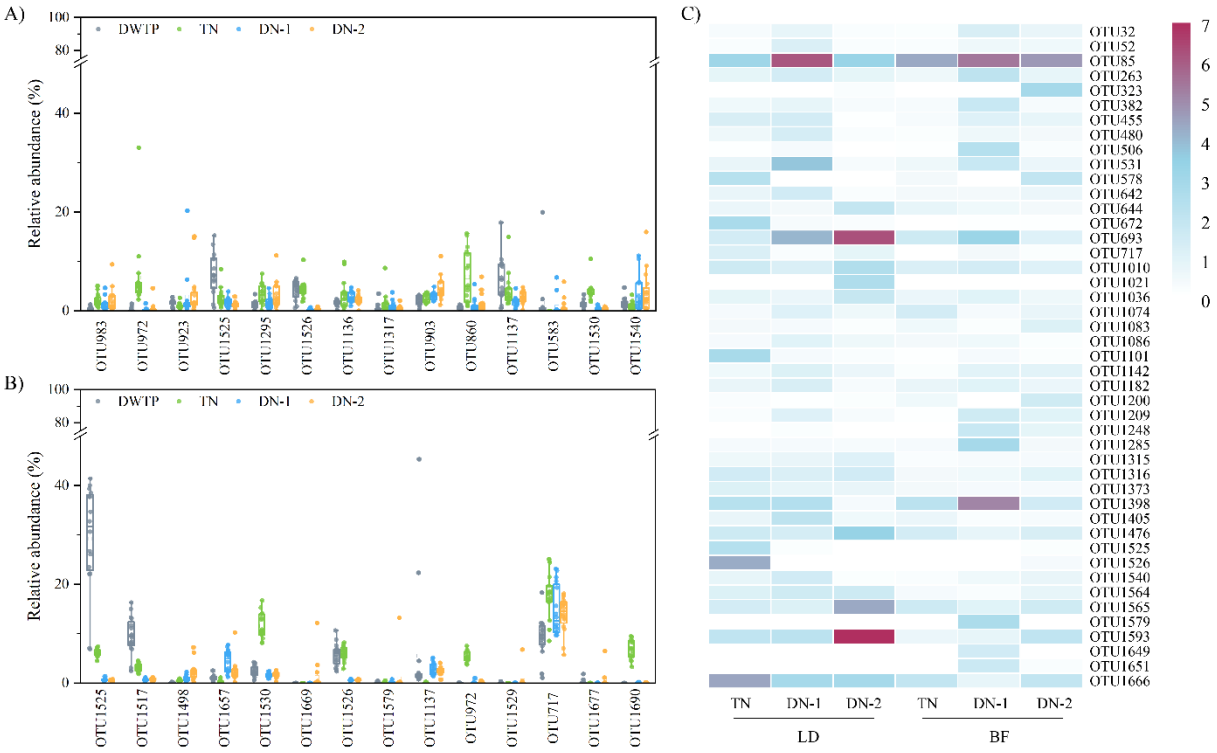

Figure 3-S6. Dominant OTUs (the top 14 OTUs with relative abundance > 8%) within water (A) and particles (B), and major OTUs (relative abundance > 1%) within biofilm (BF) and loose deposits (LD) samples (C) across all locations. Box plots show median values (middle line), 25th and 75th percentiles (boxes) and 5th and 95th percentiles (whiskers) with individual data points overlaid. Outliers, if present, are shown as individual points beyond the whiskers.

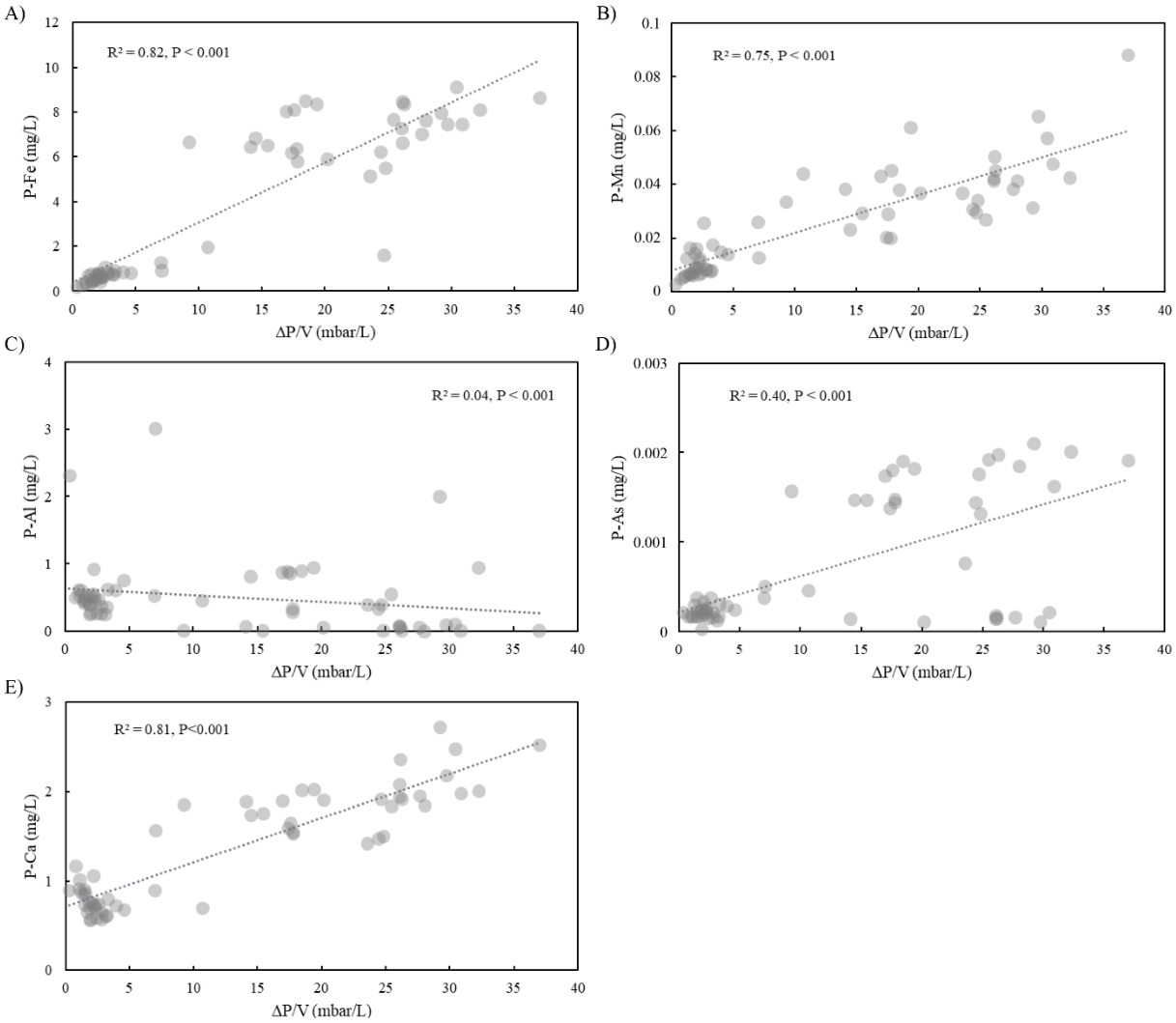

Figure 3-S7. Scatterplot depicting the correlations of Δ P/V (Δ Pressure/Volume, mbar/L) and particle-associated Fe (A), Mn (B), Al (C), As (D) and Ca (E) within particles.

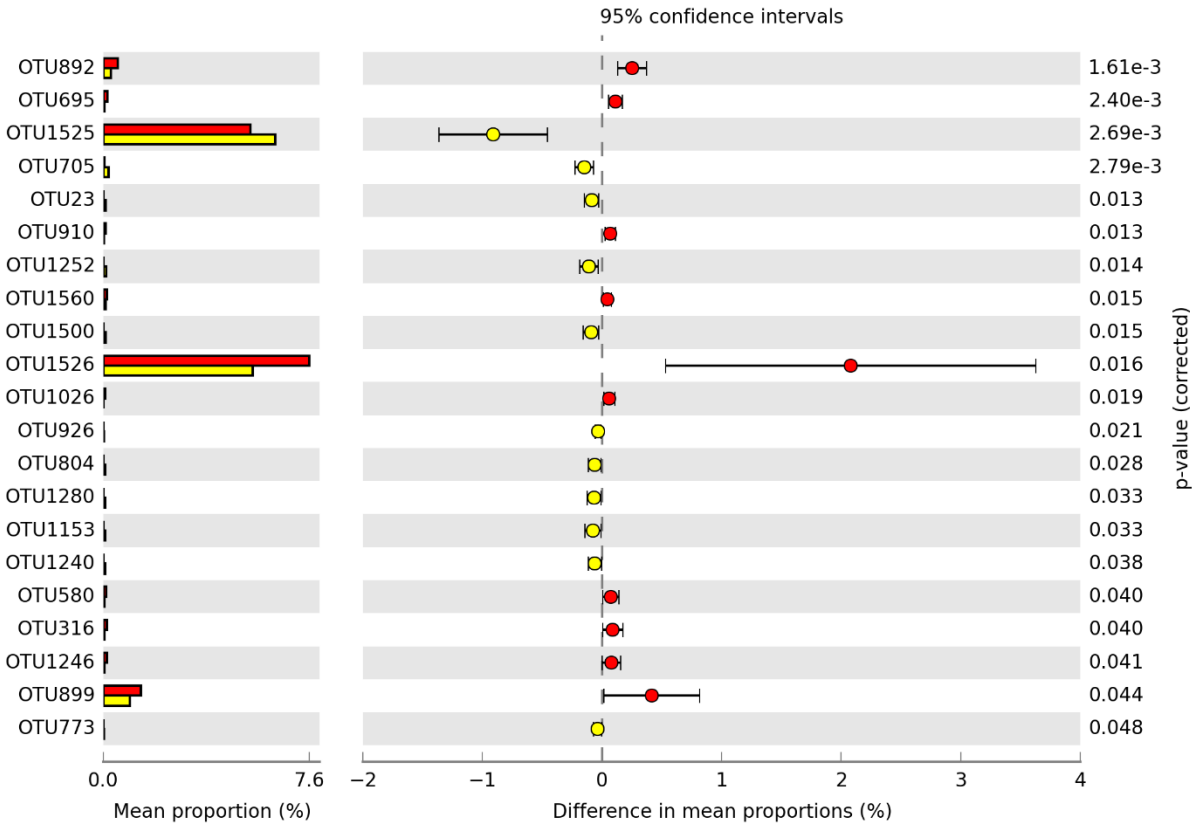

Figure 3-S8. Extended error plot showing the significant OTUs enriched in the particles at 6-9h (red) and other sampling time periods (yellow) at TN (Welch's t-test, two-sided, Benjamin FDR method, 95% confidence interval, $p < 0.01$).

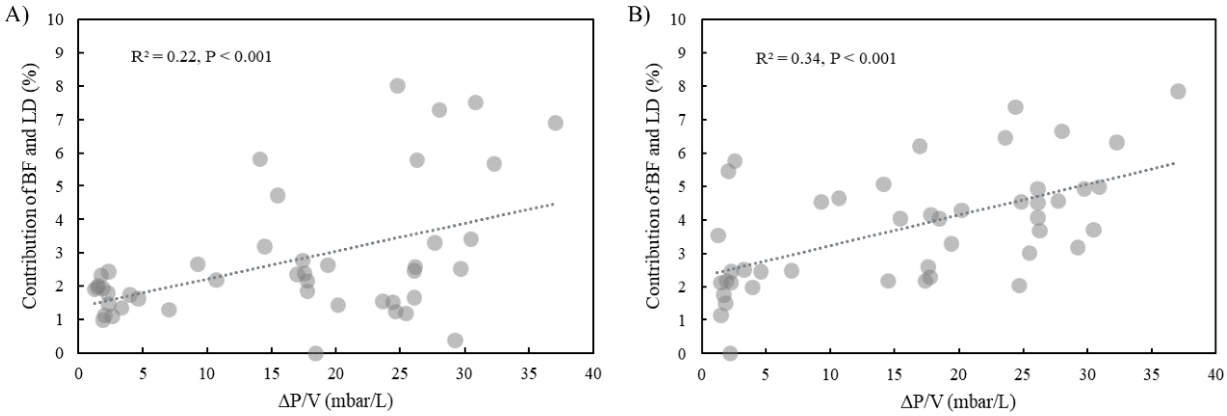

Figure 3-S9. The correlations between particle load (ΔP/V) and the contribution of biofilm (BF) and loose deposits (LD) to PB (A) and PAB (B).

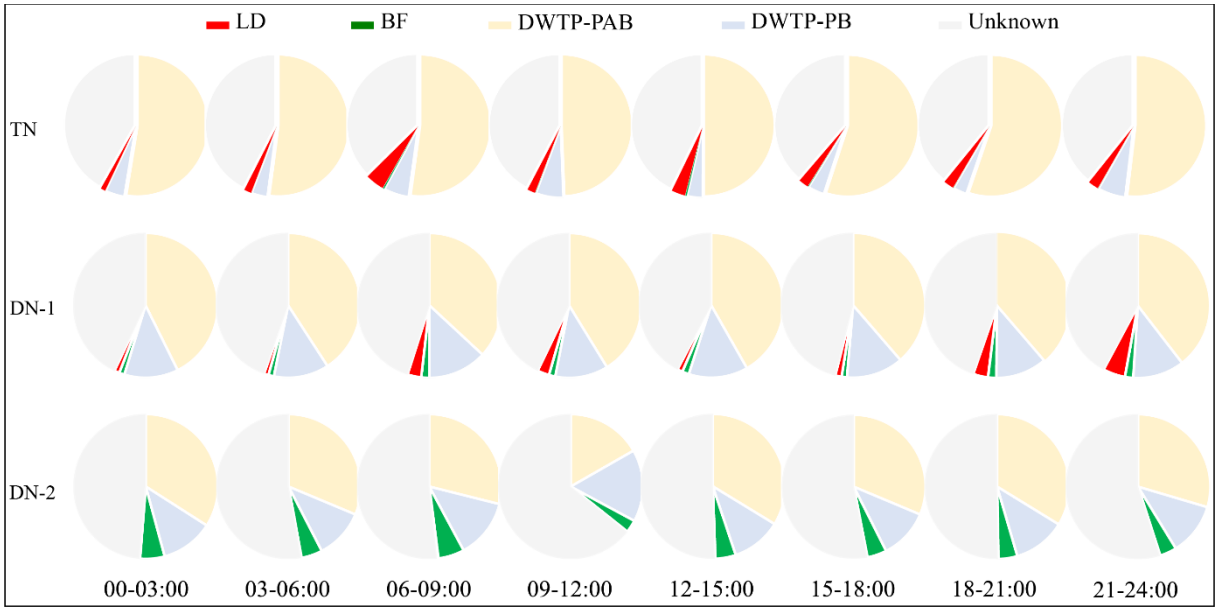

Figure 3-S10. The daily variations in mean percentage of contributions from different sources to the communities within all particles samples at different locations.

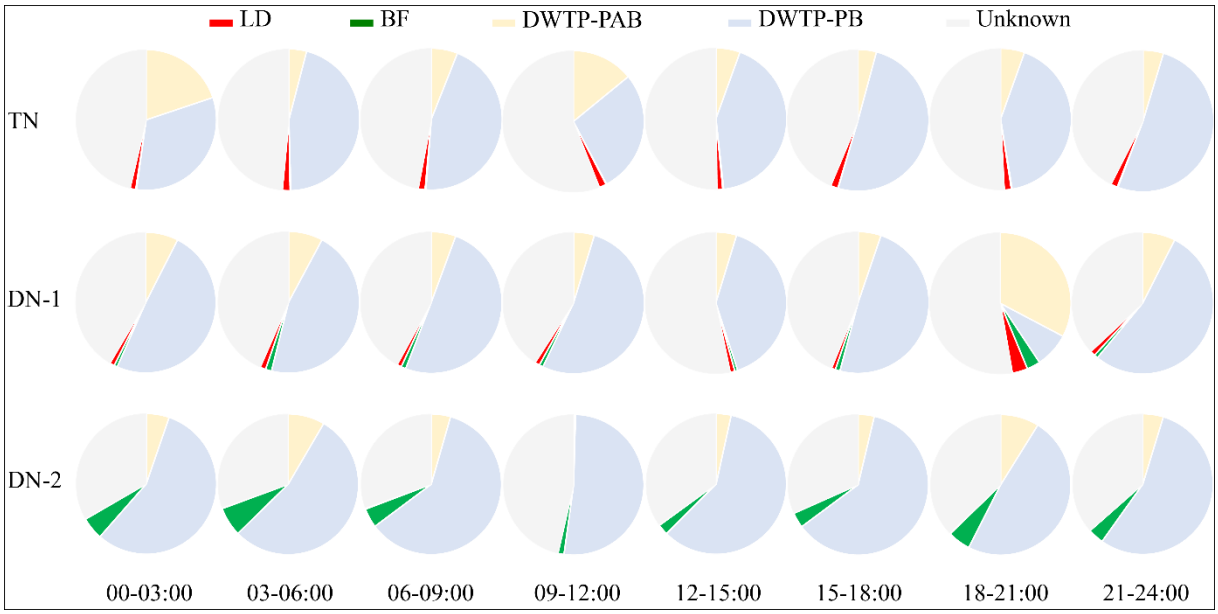

Figure 3-S11. The daily variations in mean percentage of contributions from different sources to the communities within all water samples at different locations.

Chapter 4

Assessing the Transition Effects in a Drinking Water Distribution System Caused by Changing Supply Water Quality: An Indirect Approach by Characterizing Particles in the Bulk Water

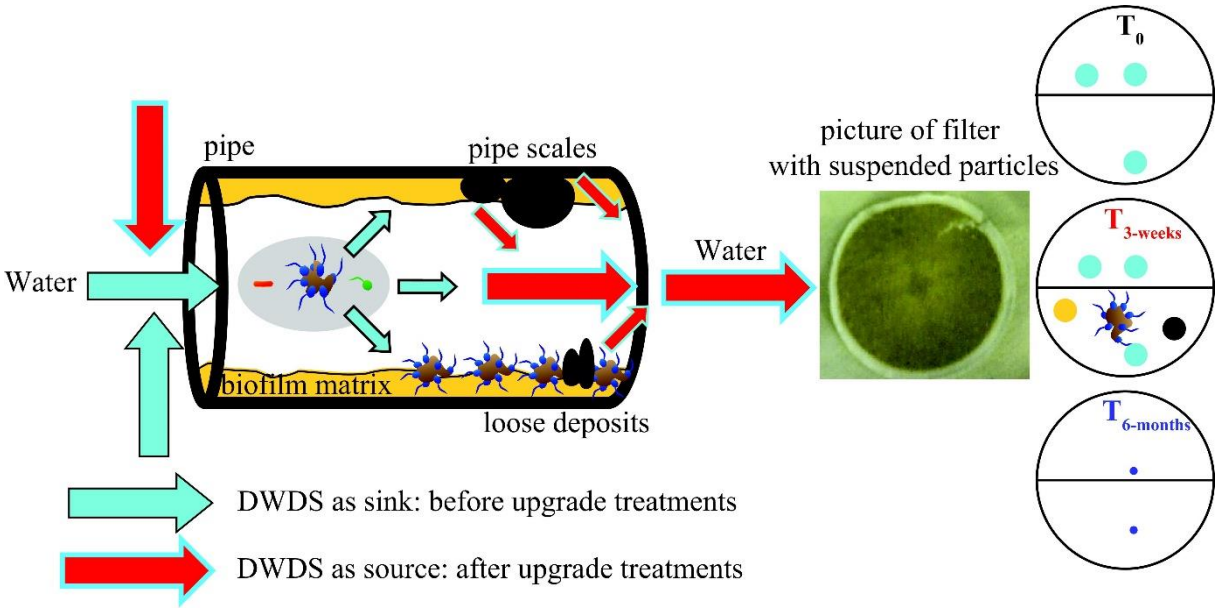

This chapter is based on: Chen, L., Ling, F., Bakker, G., Liu, W. T., Medema, G., van der Meer, W., & Liu, G. (2020). Assessing the transition effects in a drinking water distribution system caused by changing supply water quality: an indirect approach by characterizing particles in the bulk water. *Water research, 168,* 115159.

Abstract

Worldwide, it is common that the drinking water distribution systems (DWDSs) may be subjected to changes of supply water quality due to the needs of upgrading the treatment processes or switching the source water. However, the potential impacts of quality changed supply water on the stabilized ecological niches within DWDSs and the associated water quality deterioration risks were poorly documented. In the present study, such transition effects caused by changing the supply water quality that resulted from destabilization of biofilm and loose deposits in DWDS were investigated by analyzing the physiochemical (i.e., TSS, elements) and microbiological (i.e., ATP, microbial community) characteristics of particles in the bulk water before (T_0), during ($T_{3\text{-weeks}}$) and after upgrading the treatments ($T_{6\text{-months}}$) in an unchlorinated DWDS in the Netherlands. The results demonstrated that after 6 months' time the upgraded treatments significantly improved the water quality. Remarkably, water quality deterioration was observed at the initial stage when the quality-improved treated water distributed into the network at $T_{3\text{-weeks}}$, observed as a spike of total suspended solids (TSS, 50-260%), active biomass (ATP, 95-230%) and inorganic elements (e.g. Mn, 130-250%). Furthermore, pyrosequencing results revealed sharp differences in microbial community composition and structure for the bacteria associated with suspended particles between T_0 and $T_{3\text{-weeks}}$, which re-stabilized after 6 months at $T_{6\text{-months}}$. The successful capture of transition effects was especially confirmed by the domination of *Nitrospira* spp. and *Polaromona*s spp. in the distribution system at $T_{3\text{-weeks}}$, which were detected at rather low relative abundance at treatment plant. Though the transitional effects were captured, this study shows that the introduction of softening and additional filtration did not have an effect on the water quality (e.g., no customer complaints regarding the water color, taste, and odor), nor water safety (no pathogenic species detected), which improved considerably after 6-months' period. The methodology of monitoring particles in the bulk water with multiple particle filtration systems (MuPFiSs) and additional analysis is capable of detecting transitional effects by monitoring the dynamics of particles and its physiochemical and microbiological composition.

Keywords: upgrading treatments, drinking water distribution system, transition effects, particles, water quality deterioration risks

4.1 Introduction

Drinking water treatments remove contaminants present in source water to make water potable. In both developing and industrialized nations, a growing number of contaminants are entering water supplies from human activity: from pathogen/virus, heavy metals to micropollutants (Shannon et al., 2008; Ternes et al., 2015). Consequently, public health, environmental concerns and growing constraint to optimize the esthetical and comfort quality for the consumers (e.g. drinking water without chlorine taste and low in hardness) drive efforts to further treat waters previously considered clean, which has greatly promoted the development of water treatment science and technology over past decades (Shannon et al., 2008). In practice, the developments have been focusing on the upgrades of treatments and improvements of supply water quality regarding physiochemical and microbiological parameters, e.g. the concentrations of elements composition, nutrients concentration, cell number and microbial community (Liu et al., 2019; Xing et al., 2018b). However, the quality-changed drinking water still has to be delivered to customers' taps through the old distribution systems in which biofilm and loose deposits have been established for decades (Liu et al., 2013c).

In drinking water distribution systems (DWDSs), over 98% of the total biomass was found to be contributed by the bacteria accumulated within loose deposits and biofilm (Liu et al., 2014). In particular, the biofilm in DWDSs has been widely documented because of its potential health risks (Batté et al., 2003; Chaves Simões and Simões, 2013; Flemming et al., 2002; Van Der Wende et al., 1989; Wingender and Flemming, 2011). As reported, biofilm can be as much as 10^8 CFU cm^{-2} (Batté et al., 2003), 10^7cells cm^{-2} (Lehtola et al., 2006) or 10^3 pg ATP cm^{-2} (Lehtola et al., 2006) depending on the measuring methods. The presence of biofilm promoted the deposition of elements such as manganese (Mn) and calcium (Ca) in a distribution system (Liu et al., 2017a; Sly et al., 1990). Similarly, loose deposits, reported to be reservoirs for inorganic elements, organic nutrients and bacteria (Gauthier et al., 1999; Lehtola et al., 2004; Liu et al., 2017a; Zacheus et al., 2001), can be as much as 24.5 g m^{-1} in a full-scale distribution system (Carrière et al., 2005) and harbor comparable biomass (671-3738 ng m^{-1} ATP) to biofilm (534 ± 23 ng m^{-1} ATP) (Liu et al., 2014).

Under the regular water supply conditions, there is an equilibrium between the water and the solid phases in the network (e.g. loose deposits and biofilm). It is a common sense that water quality may deteriorate during distribution; the typical cases have been observed and reported as manganese-related "dirty water" problems (Sly et al., 1990) and discoloration (Vreeburg and

Boxall, 2007; Xing et al., 2018a). For distribution of quality-changed water through old pipes, the equilibrium will be disturbed, and material harbored by distribution pipes (e.g. pipe scales, biofilm and loose deposits) will be destabilized and released into water column which can be potentially harmful (Feazel et al., 2009; Li et al., 2010; Liu et al., 2017b; Torvinen et al., 2004). As previously defined, such destabilization may be caused by physiochemical and microbiological water quality changes that break the established forces balance in pipe scales, biofilm and loose deposits, such as physical destabilization (e.g. reducing the weight of particles causing loose deposits resuspension), chemical destabilization (e.g. changes of pH, redox and ion composition can remobilize contaminants bound by pipe scales on metal pipes via desorption and/or dissolution), and microbiological destabilization (e.g. changes of nutrients concentration and composition can influence the microbial community and function in biofilm) (Liu et al., 2017b). It has been quantified that the release of 20% of either biofilm or loose deposits will cause significant changes in the bulk water bacterial community (Liu et al., 2017a). In practice, one example is the occurrence of red water in large areas of Beijing in 2008 when the city switched to better source water transported 1400 kilometers from southern China, where increased sulfate in supply-water caused microbial community composition changes revealed by increase in sulfur oxidizing bacteria, sulfate reducing bacteria and iron oxidizing bacteria and red water events associated with high iron concentrations (Li et al., 2010). Recently, in the Flint drinking water crisis in Michigan, U.S., elevated blood lead levels were detected in children after water source changes (Hanna-Attisha et al., 2016), which has been attributed to the missing of orthophosphate corrosion inhibitor and lead leaching from the aging pipes into water column.

However, until now, our understanding of the water quality deterioration risk associated with biofilm and loose deposits destabilization in distribution systems during switching supply water quality is limited. This has been mainly attributed to the lack of accessibility of real distribution systems for study (Berry et al., 2006) and the dilution effects of large volumes of water that keep flowing through the system increasing the difficulty of detection (Liu et al., 2017b). The particles in the bulk water, especially the associated bacteria, have been used to study the effects of mixing water on bacterial community (Liu et al., 2016a) and used as SourceTracker to study the contribution of biofilm detachment and loose deposits resuspension to the tap water bacteria (Liu et al., 2018). To overcome the above-mentioned difficulties, monitoring the variations of the characteristics of the particles in the bulk water can be used as an indirect approach without deconstructing distribution pipes or interrupting water supply services, while still being able to

detect the changes with serious implications for health risks and esthetical water quality. This study followed the upgrade of treatments in an unchlorinated drinking water supply system in the Netherlands, monitored the particles in treated and distributed water before (T_0), during ($T_{3\text{-weeks}}$) and after the treatment upgrade ($T_{6\text{-months}}$). The objective was to capture and study the potential release of elements and biomass caused by biofilm and loose deposits destabilization subjected to the changes in the supply water quality caused by the introduction of new softening and rapid sand filtration steps (for example: decrease of hardness and particle load) through monitoring and characterizing particles in the drinking water leaves treatment plant and distributed water at the customers' taps.

4.2 Material and Methods

4.2.1 Treatment plant and sampling locations

The drinking water treatment plant produces drinking water from anoxic groundwater (3,8 Mm^3/year). Before introducing new treatment steps (softening, second rapid sand filtration and adding carbon dioxide), the water was treated by aeration and rapid sand filtration before being pumped into the distribution system. The sampling locations were selected at the treatment plant before the water entered the distribution system (TP, 0km): locations at customers' taps at DN1 (5km to TP), DN2 (11km to TP), and DN3 (17km to TP). The lengths are determined by the distances from the treatment plant to the distribution sites. The distribution networks in the study area is 110 mm PVC-U pipes (water main pipe). The treatment processes and sampling locations are illustrated in Figure 4-S1. The produced water quality before and after treatment changes is given in Table 4-1. Generally, the water quality clearly improved after upgrading the treatments (Table 4-1): turbidity was decreased with 50% ($P < 0.05$), meanwhile TOC, Ca ($P < 0.05$) and Mg were decreased with 15%, 35%, and 7%, respectively. The NH_4^+, Fe and Mn that were detected before were under the detection limit after upgraded treatments ($P < 0.05$). About 20% extra active biomass reduction ($P < 0.05$), as quantified by both ATP and TCC, was achieved by the introduction of additional treatments. A stable pH was maintained by CO_2 dosing. The most noticeable water quality improvement is the Ca concentration reduction.

Table 4-1. *Water quality in finished water before and after changing the treatments*

Parameters	Before treatment changes	After treatment changes	
	(n = 6)	3 weeks (n = 6)	6 months (n = 6)
Turbidity (NTU)	0.20 ± 0.09	0.15 ± 0.06	0.10 ± 0.03
pH	7.41 ± 0.03	7.53 ± 0.04	7.65 ± 0.02

ATP (ng l^{-1})	4.0 ± 0.9	3.6 ± 0.4	3.2 ± 0.2
TCC (cells ml^{-1})	$1.6 \times 10^5 \pm 1.5 \times 10^4$	$1.5 \times 10^5 \pm 3.5 \times 10^3$	$1.2 \times 10^5 \pm 4.1 \times 10^3$
TOC (mg l^{-1})	1.7 ± 0.3	1.7 ± 0.2	1.5 ± 0.1
Ca (µg l^{-1})	84.1 ± 2.8	78.4 ± 0.8	55.2 ± 0.3
Mg (µg l^{-1})	10.4 ± 1.5	10.78 ± 0.7	10.1 ± 0.4
NH_4^+ (mg l^{-1})	0.04 ± 0.02	<0.01	<0.01
SO_4^{2-} (mg l^{-1})	22 ± 0.5	<0.01	<0.01
Fe (mg l^{-1})	0.012 ± 0.004	<0.002	<0.002
Mn (mg l^{-1})	0.014 ± 0.007	<0.005	<0.005

4.2.2 Sampling of particles in the bulk water

The particles were sampled by multiple particle filtration systems (MuPFiSs) as previously described (Liu et al., 2013a). In short, the system has four filtration lines in parallel with water meters in each line to measure the volume of water flow filtrated. The SS were sampled by filtering approximately 200 L of water through glass fiber filters (Whatman, 1822-047, 1.2 µm) over a period of 3 hours under tap pressure (~2.0 bar). The filter pore size was selected according to a previous study (Liu et al., 2013a). Before each sampling, the water tap was flushed until a constant temperature at the tap to make sure the water from distribution system was taken (~5mins for a typical Dutch household).

The sampling of particles was conducted over three time periods: before (1 month, T_0, in March), during (at the 1st, 2nd and 3rd week immediately after the introduction of new treatment steps, $T_{3\text{-weeks}}$, in April), and stabilized after treatment upgrades (6 months, $T_{6\text{-months}}$, in October). Comply with the stable climate temperature in the three different sampling periods at the study area in the Netherlands, the temperature in the distribution system were also comparable (~ 11-15 °C). Therefore, given the stability of the source ground water and the minor influence of biofilm and loose deposits to bulk water under normal conditions, the quality of the distributed water collected at T_0 and $T_{6\text{-months}}$ showed minimal impact from seasonal temperature fluctuations.

For each period, triplicate samples were obtained by running MuPFiSs on the same day of the week for three consecutive weeks at all sampling locations. For each run of MuPFiSs, four filters were collected in parallel, three of which were sent for TSS, elements and ATP/DNA

analysis, respectively. The 4th filter was set as back up in case of any filter broken during the sampling. For $T_{6\text{-months}}$ the third time-sampling was contaminated, therefore results from duplicate samples were presented. In total, 32 samples were collected for the whole period of this study at each location ($3 \times 4 = 12$ from T_0, $3 \times 4 = 12$ from $T_{3\text{-weeks}}$, $2 \times 4 = 8$ from $T_{6\text{-month}}$), which resulted in 128 filters from all locations ($32 \times 4 = 128$). For each parameter of TSS, elements and ATP/DNA sequencing, 32 filters have been analyzed. Every time, water samples were collected together with the MuPFiS run from the nearest tap (32 water samples along with the filter samples).

4.2.3 Sample preparation

Four samples can be obtained by each MuPFiS run for different analyses. The filters for particle-associated bacteria analysis were inverted and submerged into 5 ml of autoclaved tap water with glass beads immediately after filtration. As described previously (Liu et al., 2016a; Liu et al., 2013a), all of the samples were maintained in a cooling box and transported to the laboratory within 2 hours after sampling; the bacteria were detached from the particles by a low energy ultrasonic treatment performed 3 times, for 2 min each (Branson ultrasonic water bath, 43 kHz, 180W power output, 10L sonication chamber). The obtained suspensions were used for particle-associated bacteria (PAB) quantification and DNA extraction. The other filters were kept for total suspended solids (TSS) and elemental composition analyses.

4.2.4 Sample analysis

4.2.4.1 Total and volatile suspended solids analysis (TSS and VSS)

Suspended material is collected on the filter for mass measurement. Prior to filtration, filters were pre-dried in the oven for two hours at 105 ºC. Gravimetric analyses were conducted by weighing the filters before and after filtration (drying at 105 ºC), providing the TSS, and after a second filtration (combusting in a muffle furnace at 550ºC) for two hours, providing the VSS (American Water Works Association 1998).

4.2.4.2 Inductively coupled plasma-mass spectroscopy (ICP-MS)

Concentrations of several elements in the samples, generated using sequential extractions and filtration experiments utilizing filters with varying sizes, were determined by inductively coupled plasma-mass spectroscopy (ICP-MS) (PerkinElmer ELAN DRC-e ICP-MS). The elements quantified in these measurements included iron (Fe), calcium (Ca), and manganese (Mn). Quality control samples, including laboratory-fortified blanks and laboratory-fortified

samples, were performed for every 10 samples analyzed. Average elemental recoveries ranged from 85.2 to 92.8% for the laboratory-fortified samples.

4.2.4.3 Adenosine triphosphate (ATP)

To study the biological properties of collected particles, the suspension obtained after the above-described pre-treatment was analyzed according to adenosine triphosphate (ATP) content. The ATP of particles was defined as attached ATP (A-ATP) and measured as previously described (Liu et al., 2013a). In short, the released ATP from cells by nucleotide-releasing buffer (NRB, Celsis) was measured by the intensity of the emitted light in a luminometer (Celsis Advance^{TM}) calibrated with solutions of free ATP (Celsis) in autoclaved tap water following the procedure as given by the manufacturer.

4.2.5 DNA extraction and 454 Pyrosequencing

DNA was extracted from the suspension using the FastDNA Spin Kit for Soil (Q-Biogene/MP Biomedicals, Solon, OH, USA) according to the manufacturer's instructions (Hwang et al., 2011; Tamaki et al., 2011) and was amplified with the bacterium-specific forward primer 27F and the reverse primer 534R (Hong et al., 2010). DNA extraction were formed on unused filters to be used as blank, none of which contained sufficient DNA performing downstream sequencing analysis. The 454 pyrosequencing was performed with a 454 Life Sciences GS FLX series genome sequencer (Roche, Switzerland). The obtained DNA sequences were deposited in the DDBJ sequence read archive (Accession Number: PRJNA498802).

4.2.6 Sequencing data processing

The sequences generated from pyrosequencing were processed by removing low quality sequence ends (threshold: Q = 20), primers, and singleton. UCHIME software was used to identify and remove chimeras (Edgar et al., 2011). Afterwards, the sequences were trimmed, resulting in an average sequence length of 230 bp. The merged alignments of the sequences were obtained via the infernal aligner from the Ribosomal Database Project (RDP) pyrosequencing pipeline (http://pyro.cme.msu.edu/) and the NAST alignment tool from Greengenes, based on the software developed by the Biotechnology Center at the University of Illinois (UI) (http://acai.igb.uiuc.edu/bio/merge-nast-infernal.html). The RDP Classifier was used for the taxonomical assignments of the aligned 454 pyrosequences at the 97% sequence similarity cut-off. The total PAB communities from the different sampling points were analyzed for the number of operational taxonomic units (OTUs), species richness, and biodiversity using

the Quantitative Insights INTO Microbial Ecology (QIIME) program (Caporaso et al., 2010).

Core OTUs were defined as the OTUs with a cutoff of relative abundance (> 1%) in each sampling period. The core genus is defined corresponded to taxonomy information of the core OTUs. Alpha-diversity indices were calculated based on the rarefied OTU table at a depth of 5000 sequences per sample (rarefaction analysis). Beta diversity comparison was calculated at sequence depth of 1046, which could cover all the sequenced samples. The unweighted and weighted UniFrac distance matrices were constructed from the phylogenetic tree and used to conduct the principal coordinate analyses (PCoA) using R vegan package (Noyce et al., 2016). Venn diagrams were drawn using R VennDiagram package to analyze overlapped and unique OTUs among different sampling locations at each sampling period (Chen and Boutros, 2011). Heatmap was implemented by R heatmap packages (Kolde, 2013).

4.2.7 Statistically analysis

Different statistical tools were applied using Past and R (vegan package), including: 1) one-way analysis of variance (ANOVA) tests to determine the significance of differences on physicochemical and microbiological parameters; 2) one-way permutational analysis of variance (PERMANOVA) based on Bray-Curtis similarity matrices to test the significance of differences regarding the beta diversity of bacterial communities (Anderson and Walsh, 2013). The differences were considered significant when the p-value was lower than 0.05 ($P < 0.05$).

4.3 Results

4.3.1 Particles in the bulk water

In this drinking water supply system, up to 40 μg l^{-1} TSS was detected (Figure 4-1). At the treatment plant, the value of TSS decreased slightly after introducing the additional treatments ($T_{3\text{-weeks}}$, by 11% comparing to T_0, $P > 0.05$), followed by a statistically significant decrease after 6 months ($T_{6\text{-months}}$, by 91% comparing to T_0, $P < 0.05$). Differently, in the distribution system, a remarkable initial increase in TSS was observed after introducing the additional treatments ($T_{3\text{-weeks}}$, by 50-260% comparing to T_0, $P < 0.05$), although TSS reduction was achieved after 6 months at the three locations in the distribution system ($T_{6\text{-months}}$, by 3-13% comparing to T_0, $P < 0.05$). During distribution, the TSS decreased along the distribution network from treatment plant (~ 40 μg l^{-1}) to DN3 (~ 10 μg l^{-1}) at T_0. However, at $T_{3\text{-weeks}}$, the TSS levels were comparable between treatment plants and distribution sites, and by $T_{6\text{-months}}$, there was a slight increase in TSS levels from treatment plant to distribution sites (not

significant, $P > 0.05$). Considering the reduction in TSS at the treatment plant at $T_{3\text{-weeks}}$, the elevated TSS levels in distribution systems at the same time point suggest the release of particles from the distribution networks rather than contributions from the treatment plant. Looking into the fractions of TSS (FSS and VSS, Figure 4-1), at the treatment plant, a decrease in VSS was decreased at $T_{3\text{-weeks}}$ compared to T_0, followed by a significant reduction at $T_{6\text{-months}}$. Nevertheless, in distribution system, the VSS fraction at $T_{3\text{-weeks}}$ is higher than at T_0 and $T_{6\text{-months}}$, indicating the biological nature of the released particles during the transitional period.

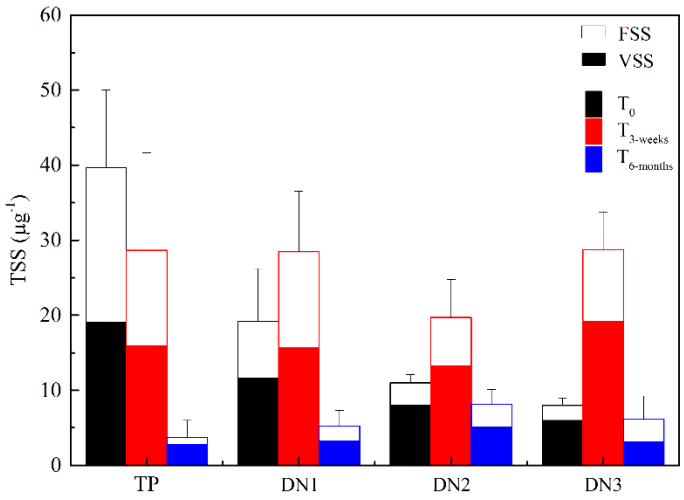

Figure 4-1. *Particle load before (T_0, black), during ($T_{3\text{-weeks}}$, red) and after ($T_{6\text{-months}}$, blue) upgrading the treatments measured by total suspended solids (TSS), volatile suspended solids (VSS) at treatment plant (TP) and distribution network (DN1, DN2 and DN3). Data are presented as mean ± s.d. (n = 3).*

In terms of elemental composition results (Figure 4-2), compared to regular distribution conditions (T_0), no significant changes were observed in Mn concentration at treatment plant, while increases were found in Fe and Ca concentrations during the introduction of additional treatments ($T_{3\text{-weeks}}$). Conversely, all concentrations (i.e., Mn, Fe, Ca) decreased significantly after 6 months of operation with the introduced treatments ($T_{6\text{-months}}$, $P < 0.05$). In the distribution system, clear improvements were evident at $T_{6\text{-months}}$, with decreases of Fe, Mn and Ca concentrations observed at all distribution sites. However, at $T_{3\text{-weeks}}$, Mn concentration increased by 130-250% compared to T_0 ($P < 0.05$), while Fe and Ca concentrations remained stable. Consistent with TSS changes, elemental analysis showed a similar decrease along the distribution system under regular distribution conditions at T_0 (sum of Fe, Mn and Ca, showed as concentrations for each element in Figure 4-2). The elemental composition results revealed

that the decreased TSS may relate to the decrease of Fe from treatment plant to DN3, where Ca and Mn remained the comparable concentrations. Similar to T_0, at $T_{6\text{-months}}$, concentration of Fe decreased, while the concentrations of Mn and Ca remained similar from treatment plant to locations in distribution system. At $T_{3\text{-weeks}}$, concentrations of Fe and Ca decreased from the treatment plant to the distribution system. However, significant increases in Mn concentration were observed at DN1, more than 3 times higher than at treatment plant. Although the Mn concentration decreased to similar levels as the treatment plant at DN2 and DN3, it remained much higher than the Mn concentration at the same location at T_0 and $T_{6\text{-months}}$.

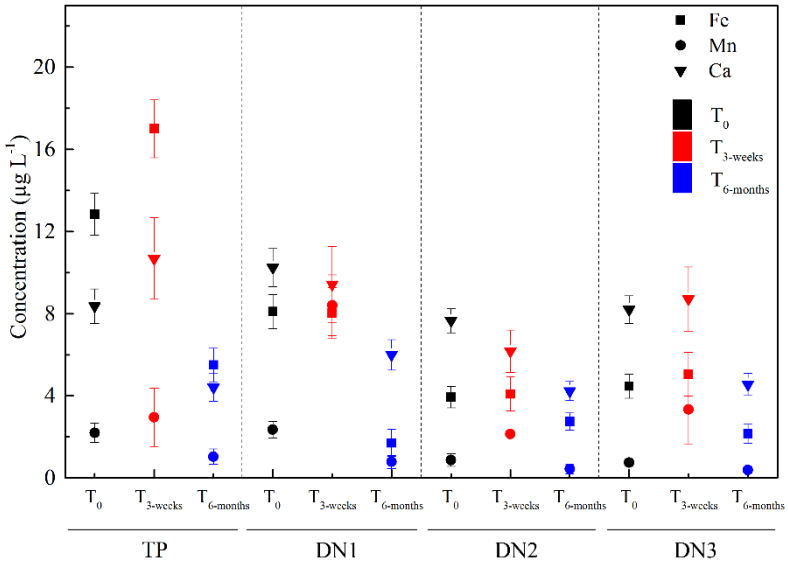

Figure 4-2. *Elemental composition of particles from treatment plant (TP) to locations in distribution network (DN1, DN2 and DN3) before (T_0, black), during ($T_{3\text{-weeks}}$, red) and after ($T_{6\text{-months}}$, blue) upgrading the treatments. Data are presented as mean ± s.d. (n = 3). The vertical dotted lines were added to differentiate between different locations.*

4.3.2 Quantification of particle-associated bacteria (A-ATP)

The active biomass associated with suspended particles were measured by ATP and represented as attached ATP (A-ATP) per mass of suspended particles (ng mg^{-1}) (Figure 4-3). The A-ATP concentration increased during distribution at the three time slots. Generally, A-ATP initially increased at $T_{3\text{-weeks}}$ (by 95-230% compared to T_0, $P < 0.05$) and then decreased at $T_{6\text{-months}}$ below its original values (by 25-46% compared to T_0, $P < 0.05$). Regardless of the sampling period, it was observed that the further going into the distribution system, the higher the A-ATP of the suspended particles. At the treatment plant, the changes of A-ATP in time (T_0, $T_{3\text{-weeks}}$ and $T_{6\text{-months}}$) were different from observations on TSS that the A-ATP already showed an

increase at $T_{3\text{-weeks}}$ when TSS slightly decreased (not significant). While, the changes of A-ATP at the distribution sites were consistent with that of TSS. In space, the constant and significant increases of A-ATP from treatment plant to distribution sites were also different from the changes of TSS, which was especially true for the observations at T_0.

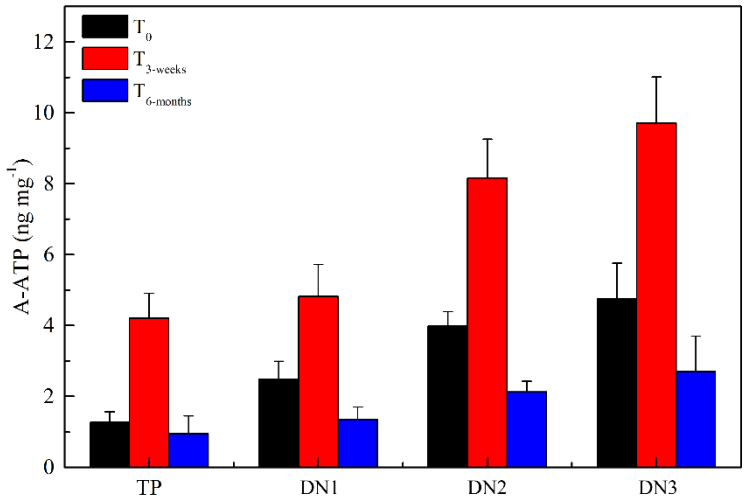

Figure 4-3. *Active biomass of suspended particles measured by ATP from treatment plant (TP) to locations in distribution network (DN1, DN2 and DN3) before (T_0, black), during ($T_{3\text{-weeks}}$, red) and after ($T_{6\text{-months}}$, blue) upgrading the treatments. Data are presented as mean ± s.d. (n = 3).*

4.3.3 Communities of particle-associated bacteria

In total, 148,922 16S rRNA gene pyrosequences were obtained and further assigned as 4918 OTUs based on a similarity cutoff of 97%. The rarefaction curves for some samples did not reach a plateau, indicating that further sequencing efforts would be required to achieve a comprehensive taxonomic representation of the microbial communities (Figure 4-S2). The obtained sequences were assigned to 20 phyla (Figure 4-S3). *Proteobacteria* was the most abundant phylum, which accounted for 42-93% of the total OTUs across all samples. Within *Proteobacteria*, *Alphaproteobacteria* (4-78%), *Gammaproteobacteria* (4-53%) and *Betaproteobacteria* (1-41%) were the most abundant classes. At the genus level, the detected OTUs were mainly composed of *Sphingomonas* spp. (0-43%), *Polaromonas* spp. (0-35%), *Legionella* spp. (0-29%), *Nitrospira* spp. (0-27%), *Sphingobium* spp. (0-22%) and *Pseudomonas* spp. (0-21%) (Figure 4-4).

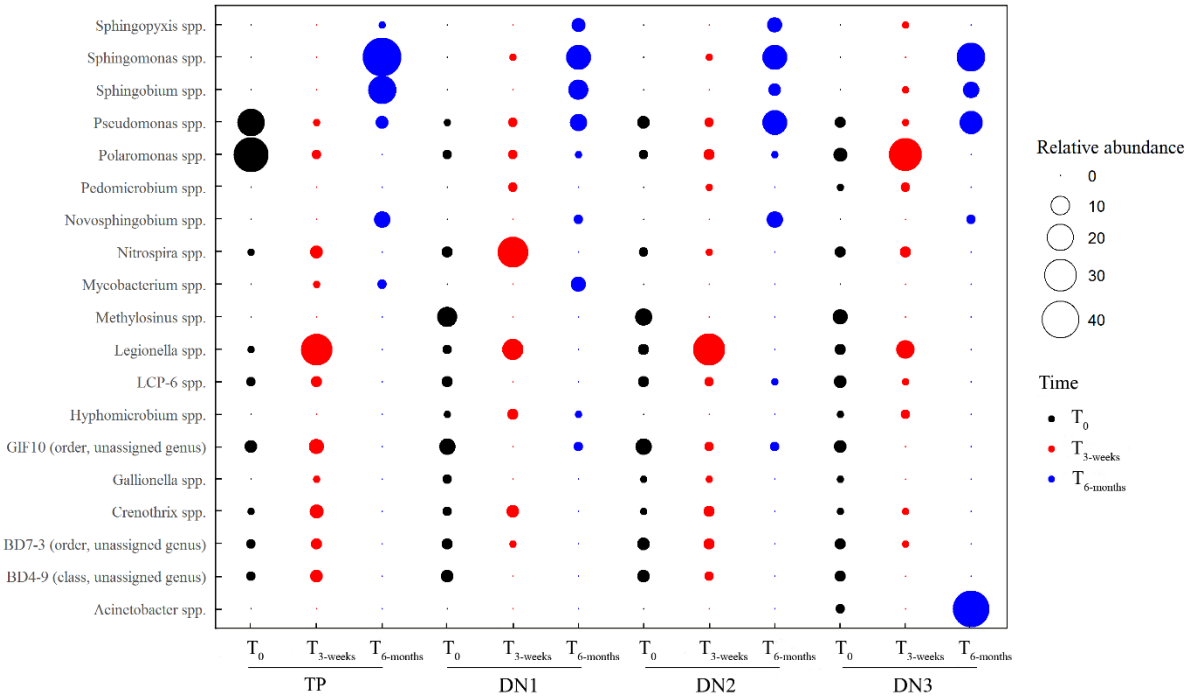

Figure 4-4. *Genera that accounted for > 5% relative abundance (%) in all sites from treatment plant (TP) to locations in distribution network (DN1, DN2 and DN3) before (T_0, black), during ($T_{3\text{-weeks}}$, red) and after ($T_{6\text{-months}}$, blue) upgrading the treatments. Complete heatmap for all core genera (> 1%) is shown in Figure S5.*

At T_0 before upgrading the treatments, *Polaromonas* spp. (35%) and *Pseudomonas* spp. (21%) were the most abundant genera at the treatment plant. The microbial community remained relatively stable during distribution, within which *Methylosinus* spp. (6-10%) was the main member. When it comes to the core OTUs (defined as OTUs with relative abundance greater than 1%), 23 OTUs were found across all samples. Among the core OTUs at DN1, DN2 and DN3, 9/17, 10/17 and 9/18 OTUs were present, respectively, in the treated water (11 core OTUs) (Figure 4-S4a). In the distribution system, 14/17 core OTUs were shared by all locations (DN1, DN2 and DN3).

In contrast, at $T_{3\text{-weeks}}$ during the treatment upgrading, *Legionella* spp. (28%) was the most abundant genus at the treatment plant. Comparing this to T_0, the microbial community of suspended particle-associated bacteria in the distribution system showed a wider variation. *Nitrospira* spp. (27%), *Legionella* spp. (29%) and *Polaromonas* spp. (31%) were the dominating genera at DN1, DN2 and DN3, respectively (Figure 4-4). In total, 33 core OTUs were found in all samples, among which 6/18, 12/16 and 5/17 core OTUs at DN1, DN2 and

DN3 were present at the treatment plant (15 core OTUs) (Figure 4-S4b). However, only 7/17 core OTUs were shared by the three locations.

At $T_{6\text{-months}}$, *Sphingomonas* spp. (43%) and *Sphingobium* spp. (22%) were dominant at the treatment plant. Compared to $T_{3\text{-weeks}}$, the bacterial communities became relatively stable after 6 months' operation of the upgraded treatments. Among the 3 locations, *Sphingomonas* spp. (17-23%) was the main member, except *Acinetobacter* spp. (38%) accounted for the highest abundance at DN3. Regarding the core OTUs, 23 core OTUs were found in all samples, 11/19, 9/13 and 6/8 core OTUs at DN1, DN2 and DN3 were present at treatment plant (11 core OTUs), respectively (Figure 4-S4c). Moreover, 6 core OTUs were shared by the three locations in the distribution system (average 13 core OTUs).

The principal coordinates analysis (PCoA), using unweighted and weighted UniFrac distance, showed clear differences among the three periods of T_0, $T_{3\text{-weeks}}$ and $T_{6\text{-months}}$ (PERMANOVA, $F = 9.643$, $P = 0.001$), which fell into three clusters (Figure 4-5 and Figure 4-S6). The cluster of $T_{6\text{-months}}$ showed an undeniable distance from the other two clusters ($D_{T0\text{-}T3\text{-weeks}} = 0.34 \pm 0.06$, $D_{T0\text{-}T6\text{-months}} = 0.47 \pm 0.05$, $D_{T3\text{-weeks}\text{-}T6\text{-months}} = 0.47 \pm 0.05$). Noticeably, the communities of bacteria associated with suspended particles at the treatment plant at T_0 were similar to that of $T_{3\text{-weeks}}$ (PERMANOVA, $F = 22.71$, $P > 0.100$), which were significantly different from those of $T_{6\text{-months}}$ (PERMANOVA, $F = 18.06$, $P = 0.003$). Moreover, across the three locations in the distribution system, high similarity was found for bacterial communities before treatment upgrades at T_0 (PERMANOVA, $F = 2.002$, $P > 0.05$) and 6 months after treatment upgrades at $T_{6\text{-months}}$ (PERMANOVA, $F = 1.671$, $P > 0.05$), while sharp variations were observed right after treatment upgrading at $T_{3\text{-weeks}}$ (PERMANOVA, $F = 8.381$, $P = 0.003$).

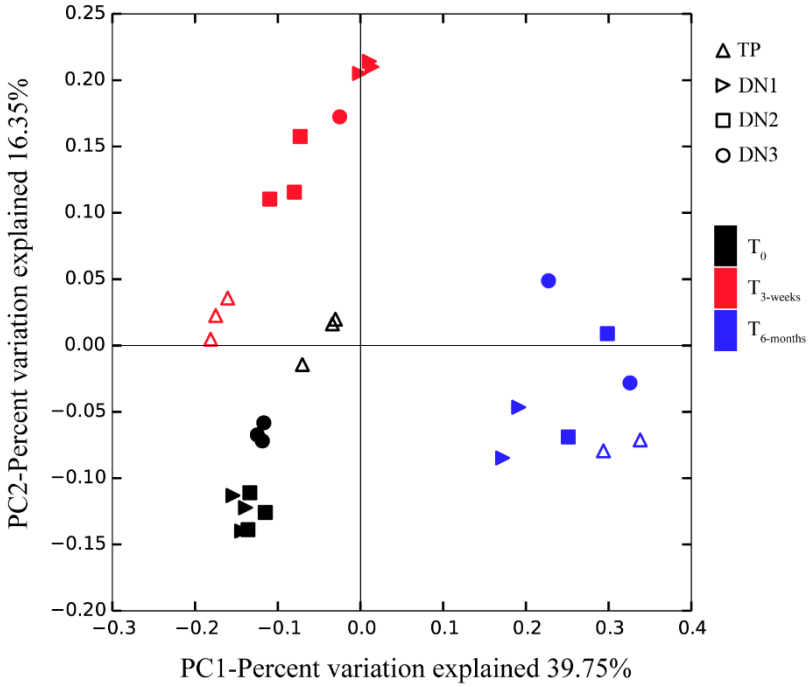

Figure 4-5. *PCoA based on weighted UniFrac distance for samples taken from treatment plant (TP) to locations in distribution network (DN1, DN2 and DN3) before (T_0, black), during ($T_{3\text{-}weeks}$, red) and after ($T_{6\text{-}months}$, blue) upgrading the treatments were included. The microbial communities of PAB at treatment plant are indicated by open triangles. Communities of PAB during distribution are marked by solid triangles (DN1), squares (DN2), and circles (DN3).*

4.4 Discussion

From a long perspective, in this case after 6 months, the upgrading of treatments clearly improved the water quality. However, it is important to notice the so-called transition effects during the initial stage of switching (i.e. during the first 3 weeks), which is defined as water quality deterioration caused by the physiochemical and microbiological characteristic changes of the supply water quality (Liu et al., 2017b; Wu et al., 2015). For the very first time, this study captured the effects of changing supply water quality on the water quality deterioration indirectly through studying the particles over three periods: T_0 (before upgrade treatments), $T_{3\text{-}weeks}$ (during upgrade treatments) and $T_{6\text{-}months}$ (after upgrade treatments).

4.4.1 T_0: particles from treatment plant settled during distribution

Comparing the particle-associated bacteria (PAB) at the treatment plant and distribution sites, the sharing of core membership (up to 75%) and high similarity of the bacterial community (PCoA, Figure 5) revealed that under regular operation at T_0 the PAB present in the distribution system mainly originated from the PAB in the treated water. This finding is consistent with

those previous studies in the Dutch unchlorinated drinking water supply system that assessed the formation of different niches in the distribution system (Liu et al., 2014) and the origin of bacteria in drinking water (Liu et al., 2018), illustrating that the suspended particles in the distribution system are part of the suspended particles entering and flowing through the distribution networks. Meanwhile, the total suspended solids (TSS) decreased from the treatment plant along the distance in the distribution system. This indicated that the particles in the treated water entering the distribution system partly settled in the network because of the precipitation of metal oxides or calcium carbonates, post-flocculation or biological growth that led to particle aggregation (Gauthier et al., 1999). The elemental composition results revealed the possible precipitation of Fe and Mn by a decrease in Fe and Mn concentrations, while the A-ATP results revealed the possible biological growth by an increase of ATP when going further into the distribution system from treatment plant to DN3.

4.4.2 $T_{3\text{-weeks}}$: changing supply water quality and transition effects

During changes to the supply water quality ($T_{3\text{-weeks}}$), previously reported discolored water events (Li et al., 2010) and public health problems (Hanna-Attisha et al., 2016) were not found in the present study. The transition effects caused by the changing of supply water quality and the destabilization of established physiochemical and microbiological equilibrium in DWDS were captured by monitoring the pre-concentrated particles. Regarding the timeline of destabilization, it happened right after the introduction of the new treatments (within 1st week), which lasted three weeks or longer.

4.4.2.1 Physicochemical deterioration

At $T_{3\text{-weeks}}$, after introducing upgraded treatments, one of the clear improvements was the decreased TSS at the treatment plant compared to the TSS at T_0. When there is slightly less TSS entering the distribution system, it is remarkable to observe that more TSS were collected in the distribution system compared to TSS collected at T_0, suggesting the release of suspended particles from the distribution system. Such release of suspended particles may come from destabilization of biofilm, loose deposits or pipe scales caused by changes in the water characteristics (Liu et al., 2017b; Makris et al., 2014). The loss of clear trend of TSS in space from treatment plant to DN3 and the large variations of TSS values measured at each distribution site at $T_{3\text{-weeks}}$ might be caused by the destabilization of uneven distributed loose deposits and biofilm in the network and the variable local hydraulics (Douterelo et al., 2013; Liu et al., 2014).

Regarding the chemical parameters, the same trend as seen for the TSS was observed for Mn: less particulate Mn entered the distribution system, but an increase in particulate Mn was observed in the distribution system at $T_{3\text{-weeks}}$ compared to at T_0 (especially at DN1). Together, the increase of TSS and particulate Mn in the distribution system indicates that the release of suspended particles from the distribution system likely comes from the resuspension of loose deposits and/or the detachment of biofilm, as previous studies have found that loose deposits and biofilms were hotspots for Mn accumulation (Cerrato et al., 2006; Liu et al., 2017a).

4.4.2.2 Microbiological deterioration

At each location in the distribution system, the A-ATP was much higher at $T_{3\text{-weeks}}$ than at T_0, which is consistent with the observation on TSS and Mn, as mentioned above. However, because the A-ATP at the treatment plant was also increased due to the destabilization of treatments (e.g. last step sand filtration), it is difficult to distinguish the observed increases of A-ATP at distribution sites at $T_{3\text{-weeks}}$ were caused by either higher A-ATP in the treated water or the release of A-ATP from the distribution system. The latter should be the case because the community of bacteria associated with suspended particles at the treatment plant remained very similar to T_0 both of which may originate from the release of particles from the last step sand filters, but the increased A-ATP in the distribution system has a totally different community compared to that of T_0 (PCoA clusters, Figure 5, $P < 0.05$), which contributed by the release of biomass from loose deposits or biofilm. This can also be supported by the fact that *Legionella* spp., which was commonly detected in drinking water biofilms (Richards et al., 2015; Rodríguez-Martínez et al., 2015), was most abundant in the treated water at $T_{3\text{-weeks}}$. Regarding the increase of A-ATP at the treatment plant, most likely it was caused by biomass detachment from the sand filters during the application of new treatments (Pinto et al., 2012). While, the high similarity of bacterial communities was not indicating no changes on the bacterial community composition, because the changes of certain member in the community might not be revealed by the similarity analysis of PCoA (Legendre and Anderson, 1999).

The community of particle-associated bacteria across different locations clustered together demonstrated stable microbial community composition and structure at T_0. However, at $T_{3\text{-weeks}}$, the observation of different dominant genera and the dissimilarity across different locations in the distribution system, especially the dissimilarity observed for each location between T_0 and $T_{3\text{-weeks}}$, indicated the occurrence of pronounced disturbances because of the distribution of quality-improved water. This is because the microbial communities in drinking water are

sensitive to water quality changes (i.e. disinfectants, nutrients concentration and composition), which inducing different selection pressures on microbial population and community diversification (Gomez-Alvarez et al., 2016). Following the treatment changes, there was a noticeable reduction in elements such as iron (Fe), manganese (Mn), and sulfate concentrations. Furthermore, the introduction of additional softening and rapid sand filtration may contribute to a decrease in AOC concentration (Chen et al., 2022c; Chien et al., 2008). In this context, extracellular polymeric substances (EPS) could potentially act as a carbon and energy source, supporting the metabolic activity of microorganisms facing nutrient scarcity (Chen et al., 2019; Zhang and Bishop, 2003). Moreover, the reduced nutrients might lead to a decrease of biological activity and a loss of viable cells in biofilm (Kooij, 1992; Liu et al., 2013c; van der Wielen and van der Kooij, 2010). Taken together, these alterations carry the potential to disrupt the biofilm matrix, leading to the release of biofilm into the bulk water. Such release of biofilm into drinking water can be problematic, since biofilm is reservoir for pathogens in drinking water (Wingender and Flemming, 2011).

Although the loose deposits and biofilm sampling was not included in this study, the changes in core community members at $T_{3\text{-weeks}}$ gives a possible indication for the destabilization of DWDS microbial ecology (e.g. *Legionella* spp. *Polaromona*s spp. and *Nitrospira* spp.). *Legionella* spp. was commonly detected in drinking water biofilms (Richards et al., 2015; Rodríguez-Martínez et al., 2015), the increase in its relative abundance and A-ATP at $T_{3\text{-weeks}}$ indicates the possible release of biofilm from the distribution system into bulk water subjected to the changes in supply water quality. *Legionella* spp., a member of this genus widely known to be an opportunistic pathogen (i.e. *Legionella pneumphila*) (Falkinham et al., 2015; Richards et al., 2015), however, the detection of *Legionella* spp. at the genus level does not indicate bio-safety problems, especially in the case in the Netherlands, because the detected member may not be the pathogenic species as scanned earlier in Dutch drinking water systems (van der Wielen and van der Kooij, 2013).

*Polaromona*s spp. have been widely observed in ultraoligotrophic freshwater environments (Magic-Knezev et al., 2009). At T_0, *Polaromonas* spp. was detected in high abundance (35%) at the treatment plant, while they decreased to below 5% in the distribution system. A previous study of the Dutch unchlorinated drinking water system found that *Polaromonas* spp. in bulk water, in which study it is also found that *Polaromonas* spp. was detected in loose deposits (sampled by flushing distribution pipes through hydrant), but not in pipe wall biofilms in terms of core genus (Liu et al., 2014). When it comes to $T_{3\text{-weeks}}$, the relative abundance of

Polaromonas spp. lessened (2%) at the treatment plant, but was much greater (2-31%) in the distribution system compared to T_0 (especially at DN3), confirming the potential contribution/release of loose deposits to the increase in TSS at the taps. Similarly, *Nitrospira* spp., which accounted for an abundance in the distribution system at $T_{3\text{-weeks}}$ (especially at DN1), was only detected in loose deposits and particles as core genus (Liu et al., 2014), indicating the possible resuspension of loose deposits contributing to the increase in TSS after introducing quality-improved supply water.

4.4.3 $T_{6\text{-months}}$: re-stabilizing of microbial water quality in DWDS

At $T_{6\text{-months}}$, after 6 months' operation of the upgraded treatments, the spike in TSS at $T_{3\text{-weeks}}$ was no longer present together with the related particulate Mn, turbidity, A-ATP and the sudden changes in the community composition and structure. Comparing the results from $T_{6\text{-months}}$ to T_0, clear improvements were observed with the decrease in TSS, particulate Mn and A-ATP. The less particle load entering distribution system will limit the accumulation of loose deposits in distribution system, which will reduce the flushing frequency (Jan Vreeburg et al., 2008). The achieved stable improvements, together with the stable bacterial community associated with particles from the treatment plant to the locations across the distribution systems, indicated that the dependence among treatment plant and distribution sites and the stabilization of microbial water quality in DWDS has been re-established. It is known that the destabilization and re-stabilization of microbial ecology may take time (Allison and Martiny, 2008; Liu et al., 2017b), but no information is available from real cases on how long it will take. Based on the present study, it is clear that the destabilization occurred right after introducing new treatments, lasting for more than three weeks. Although the re-stabilization of microbial drinking water quality was achieved after 6 months, it remains uncertain whether microbial ecology in DWDS was fully established, as no biofilm samples were collected in this study, and the re-stabilization of biofilm may take a longer duration (Li et al., 2016). Further research is necessary to determine if a shorter period for re-stabilization of microbial water quality is feasible. Importantly, incorporating biofilm samples into the assessment is crucial for an integral understanding of microbial ecology re-stabilization in DWDS, and further studies are needed to investigate whether a longer period is needed for the complete re-stabilization of microbial ecology in DWDSs.

In contrast to the trend of TSS decrease along the distances at T_0, the TSS became slightly higher while going further into the distribution system. The different trends observed may be

because of the better removal of particles after introducing new treatments. When the particles in the treated water reduced in size and number, the dominating process during distribution was no longer particle sedimentation but the growing of attached bacteria on the particles (Liu et al., 2014). This is consistent with the corresponding slight increase in A-ATP and a similar community of particle-associated bacteria from the treatment plant to different sampling sites in the distribution system.

At $T_{6\text{-months}}$ in the re-stabilized water supply system, the top five dominant genera became *Sphingomonas* spp., *Pseudomonas* spp., *Sphinobium* spp., *Sphingopyxis* spp. and *Novosphingobium* spp. (in descending order), all of which are commonly found in drinking water systems (Douterelo et al., 2017; Ling et al., 2016; Liu et al., 2014; Liu et al., 2016a). The different core genera can be explained by the new treatments and different operations of the treatment steps (filters) (Pinto et al., 2012), which further indicate the possibility of managing drinking water microbes through engineering approaches (Liu et al., 2018; Pinto et al., 2012; Wang et al., 2013).

4.4.4 Capture and investigate transition effects through studying particles in the bulk water

Based on this study, the transitional effects can be generally summarized as: 1) de-stabilization: observed as a spike in the TSS after switching to upgraded treatments, which might associate with the release from biofilm and/or loose deposits in a distribution system; 2) re-stabilization: observed as improvements after operating the upgraded treatments for a period of six months. Special attention should be given to the de-stabilization and release of loose deposits and biofilm into bulk water because both niches are hotspots for heavy metals and (opportunistic) pathogens (Torvinen et al., 2004; Wang et al., 2012). The analysis on (opportunistic) pathogens was not included in this study, it is highly recommended to be investigated in future studies.

Worldwide, changing supply water quality may cause transitional effects which could lead to serious water quality problems: from an esthetic quality perspective (e.g. discoloration) to biological and chemical safety issues (e.g. Pb and Legionnaires' disease) (Liu et al., 2017b; Zahran et al., 2018). Such transitional effects deserve more attention. Yet, there is no methodology illustrating how the transition effects can be captured and investigated. The present study demonstrated an indirect approach by studying the physiochemical and microbiological characteristics of particles over the different periods (T_0, $T_{3\text{-weeks}}$ and $T_{6\text{-months}}$) from treatment plant to distribution sites in a full scale drinking water supply system, which

successfully overcame the challenges of field distribution network accessibility (non-destructive) and dilution effects (concentrated) (Liu et al., 2017b).

From a broader perspective, this methodology can be adapted and applied for transitional effects evaluation in other drinking water supply systems subjected to changes of either source water or treatment processes. By characterizing suspended particles in time (T_0, $T_{3\text{-weeks}}$, $T_{6\text{-months}}$) and space (from treatment plant to distribution sites), the following critical questions that correlated with important drinking water quality issues for customers can be answered:

1) Whether transitional effects occur? Have the distribution system loose deposits and biofilm destabilized and released into bulk water, and how much?

   These questions can be answered by comparing the load of suspended particles (TSS).

2) What has been released into bulk water? Will the release lead to serious water quality problems/risks (e.g. Pb, opportunistic pathogens)? Are there any suggestions should be given to water utility managers and/or customers?

   These questions can be answered by analyzing the changes on physiochemical and microbiological composition regarding the particles in the bulk water.

3) Where the released TSS may originate from? How should the problem be managed?

   Finding the origin of released TSS will be very important for the utility to find proper managing strategy to prevent unwanted water quality problems at customers' taps. The source of released TSS can be tracked using the bacterial community fingerprint by SourceTracker method. The application of SourceTracker method to assess the origin of bacteria in distribution system and tap water has been demonstrated in an early work (Liu et al., 2018).

For future applications, it is recommended that when the distribution system is accessible, studying the particles generated by de-stabilization together with the sampling of loose deposits and biofilm from the target distribution network. By such complete study, the spiked TSS can be source tracked to its origin, based on which the corresponding strategy can be selected, such as flushing the distribution system if the TSS originated from loose deposits, or ice pigging if the TSS originated from pipe wall biofilm. Another recommendation is that the particles in the bulk water should be monitored and sampled online (online filtration every 1 hour, or 2-3 hours), because both the quantity and characteristics of particles in the distribution system are highly dependent on the hydraulic conditions (Fish et al., 2017; Matsui et al., 2007; Sekar et al., 2012). It has been reported that the diurnal hydraulic changes had significant effects on the bulk water bacterial community (Bautista-de Los Santos et al., 2016a). Besides, the obtained online results

will be able to offer high resolution background to distinguish the irregular de-stabilization from regular hydraulic disturbances. Considering the non-periodic release of biofilm and loose deposits, the online system will increase the success rate and avoid the possibility of missing the release events comparing to take particle samples offline.

4.5 Conclusions

Through characterizing the particles before, during and after introducing additional treatment steps, the transitional effects were indirectly investigated. The following conclusions were drawn from this study. Despite the difficulties for conducting field studies, it is encouraged to have more sampling locations for a global understanding throughout the network.

- The water quality significantly improved after 6 months' time operation of the additional treatments, though transition effects occurred right after the treatment upgrade;
- Remarkably, water quality deterioration was observed at the initial stage when the quality-improved treated water distributed into the network at $T_{3\text{-weeks}}$, observed as a spike of total suspended solids (TSS, 50-260%), active biomass (ATP, 95-230%) and inorganic elements (e.g. Mn, 130-250%).
- Pyrosequencing results revealed sharp differences in microbial community composition and structure for the bacteria associated with suspended particles between T_0 and $T_{3\text{-weeks}}$, which re-stabilized after 6 months at $T_{6\text{-months}}$.
- Though the transitional effects were captured, the study shows that the introduction of softening and additional filtration did not have an effect on water quality (no customer complaints regarding the water color, taste, and odor), nor water safety (no pathogenic species detected), which improved considerably after 6-months' period. The methodology of monitoring particles with MuPFiSs and additional analysis is capable of detecting transitional effects by monitoring the dynamics of particles and its physiochemical and microbiological composition.

Supporting information

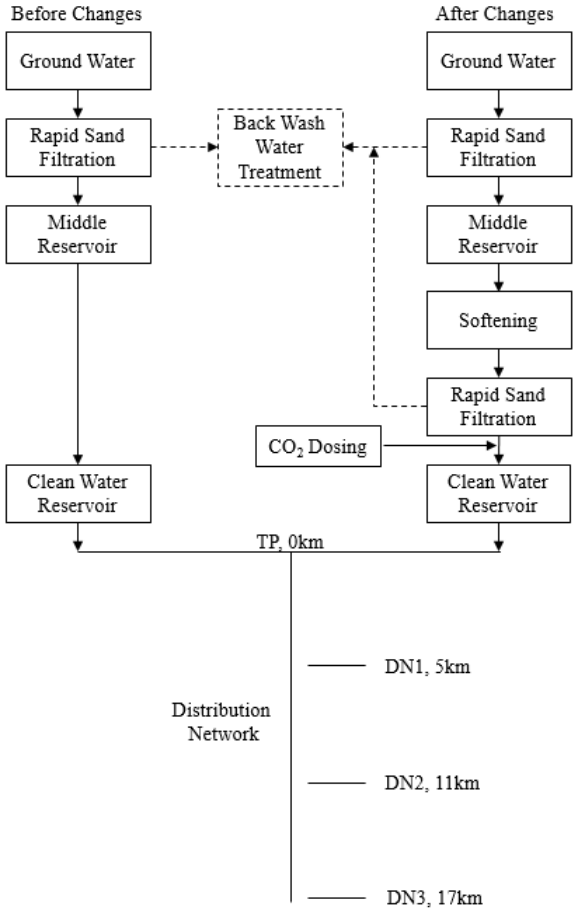

Figure 4-S1. Layout of the treatment processes before and after upgrading. Samples were taken at treatment plant (TP, 0km), DN1 (5km), DN2 (11km) and DN3 (17km).

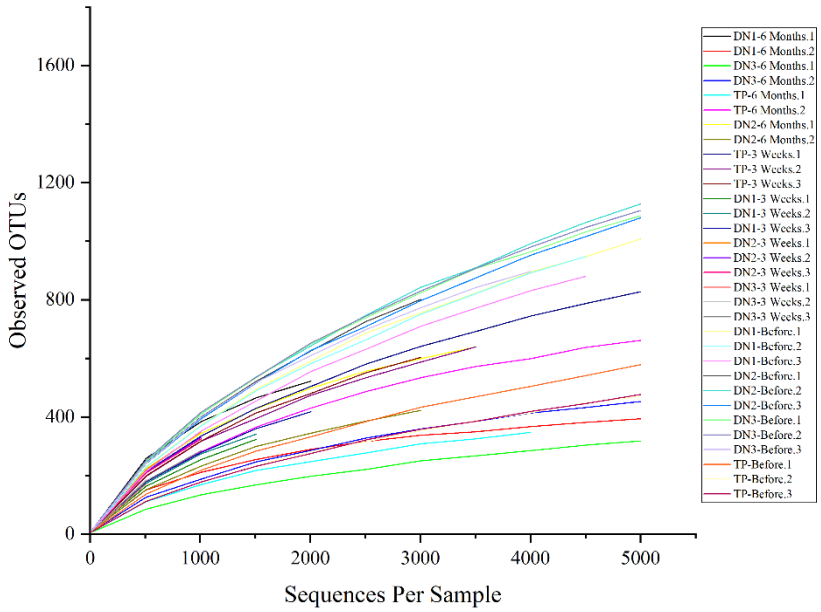

Figure 4-S2. Rarefaction curve of 16S rRNA gene sequences generated by pyrosequencing on the 32 samples at treatment plant and in distribution system before, during and after the treatment upgrading.

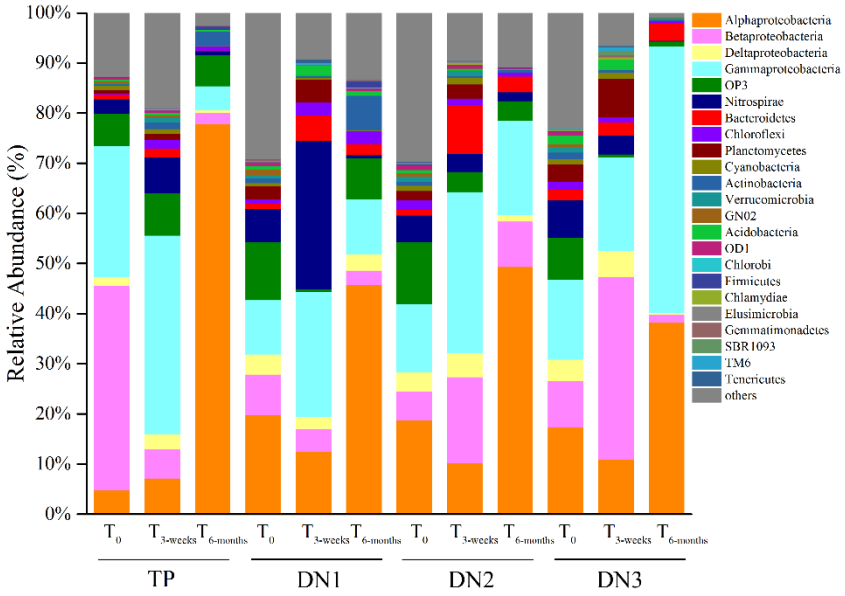

Figure 4-S3. The major phylum (relative abundance > 0.5%) types of bacterial associated with suspended particles at treatment plant and in the distribution system detected over different periods. Data are presented as mean values (n = 3).

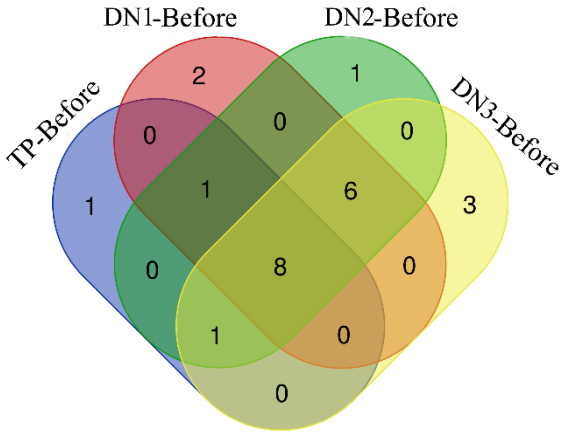

a)

Names	Total	Elements
DN1-Before DN2-Before DN3-Before TP-Before	8	LCP-6 spp. BD4-9 (class, unassigned genus) Alphaproteobacteria (class, unassigned genus) BD7-3 (order, unassigned genus) GIF10 (order, unassigned genus) GIF10 (order, unassigned genus) Legionellaceae (family, unassigned genus) Polaromonas spp. Crenothrix spp.
DN1-Before DN2-Before TP-Before	1	Methylophilaceae (family, unassigned genus)
DN2-Before DN3-Before TP-Before	1	Pseudomonas spp.
DN1-Before DN2-Before DN3-Before	6	Rickettsiales (order, unassigned genus) Nitrospira spp. BPC076 (order, unassigned genus) Legionellales (order, unassigned genus) Coxiellaceae (family, unassigned genus) Methylosinus spp.
TP-Before	1	Comamonadaceae (family, unassigned genus)
DN1-Before	2	Gallionella spp. Legionella spp.
DN2-Before	1	Dehalococcoidaceae (family, unassigned genus)
DN3-Before	3	Acinetobacter spp. Verrucomicrobia (phylum, unassigned genus) Pirellulaceae (family, unassigned genus)

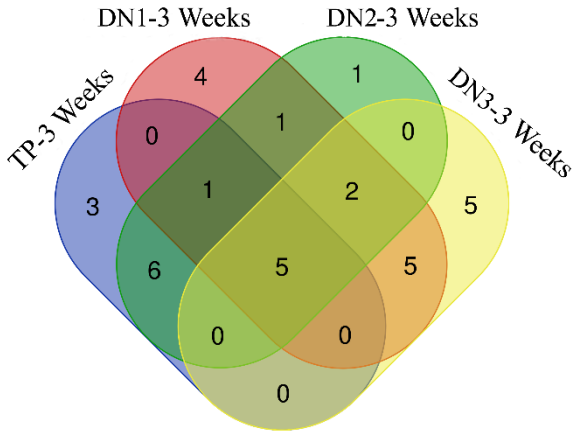

b)

Names	Total	Elements
DN1-3 Weeks DN2-3 Weeks DN3-3 Weeks TP-3 Weeks	5	Nitrospira spp. Legionella spp. Legionellales (order, unassigned genus) Legionellaceae (family, unassigned genus) Polaromonas spp.
DN1-3 Weeks DN2-3 Weeks TP-3 Weeks	1	Crenothrix spp.
DN1-3 Weeks DN2-3 Weeks DN3-3 Weeks	2	Coxiellaceae (family, unassigned genus) Flavobacterium spp.
DN2-3 Weeks TP-3 Weeks	6	LCP-6 spp. BD4-9 (class, unassigned genus) BPC076 (order, unassigned genus) BD7-3 (order, unassigned genus) GIF10 (order, unassigned genus) Rickettsiales (order, unassigned genus)
DN1-3 Weeks DN2-3 Weeks	1	Pseudomonas spp.
DN1-3 Weeks DN3-3 Weeks	5	Pedomicrobium spp. Proteobacteria (phylum, unassigned genus) Pirellulaceae (family, unassigned genus) Hyphomicrobium spp. Sinobacteraceae (family, unassigned genus)
TP-3 Weeks	3	Dehalococcoidaceae (family, unassigned genus) Gallionella spp. Procabacteriaceae (family, unassigned genus)
DN1-3 Weeks	4	Ellin6075 (family, unassigned genus) Gemmata spp. Rhizobiales (order, unassigned genus) Chitinophagaceae (family, unassigned genus)
DN2-3 Weeks	1	Alphaproteobacteria (class, unassigned genus)
DN3-3 Weeks	5	CCM11a (order, unassigned genus) iii1-15 (order, unassigned genus) Rhodocyclaceae (family, unassigned genus) Gemmataceae (family, unassigned genus) Syntrophobacteraceae (family, unassigned genus)

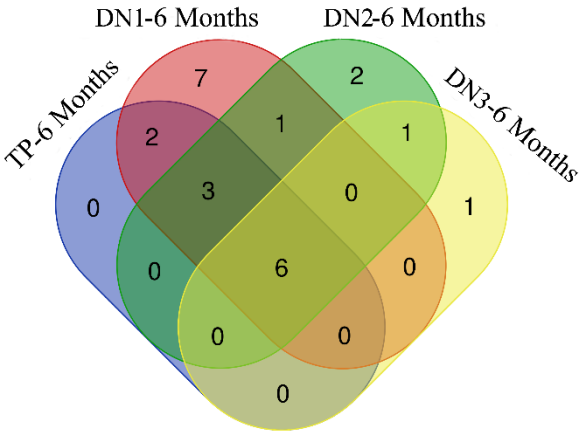

c)

Names	Total	Elements
DN1-6 Months	6	Novosphingobium spp.
DN2-6 Months		Sphingomonadales (order, unassigned genus)
DN3-6 Months		Sphingobium spp.
TP-6 Months		Pseudomonas spp.
		Sphingomonas spp.
		Sphingomonadaceae (family, unassigned genus)
DN1-6 Months	3	Sphingopyxis spp.
DN2-6 Months		Sphingomonadaceae;Other
TP-6 Months		koll11 (class, unassigned genus)
DN1-6 Months	2	Mycobacterium spp.
TP-6 Months		Dechloromonas spp.
DN1-6 Months	1	GIF10 (order, unassigned genus)
DN2-6 Months		
DN2-6 Months	1	Flavobacterium spp.
DN3-6 Months		
DN1-6 Months	7	VC2_1_Bac22 (class, unassigned genus) Ellin6529 (class, unassigned genus)
		Clostridium spp.
		BS119 (class, unassigned genus)
		Syntrophobacteraceae (family, unassigned genus)
		Polaromonas spp.
		Caldilineaceae (family, unassigned genus)
DN2-6 Months	2	LCP-6 spp.
		Comamonadaceae (family, unassigned genus)
DN3-6 Months	1	Acinetobacter spp.

Figure 4-S4. The shared and unique core OTUs of bacteria associated with suspended particles at the treatment plant and in distribution system illustrated by Venn diagram: a) before the treatment upgrading, T_0; b) at the first 3 weeks after upgrading the treatments, $T_{3\text{-weeks}}$; c) 6 months after upgrading the treatments, $T_{6\text{-months}}$. The taxonomy information shared OTUs is given in the table below each figure.

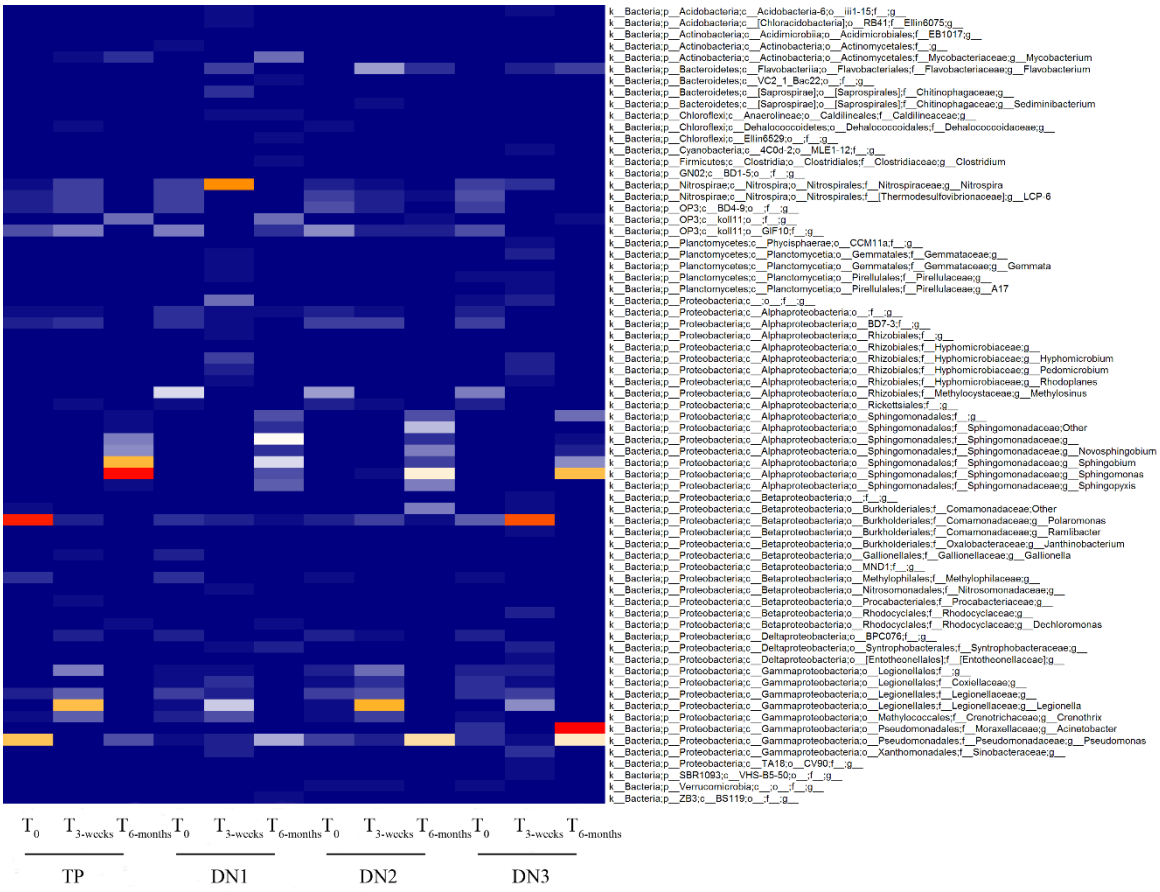

Figure 4-S5. Heatmap showing the complete list of core OTUs (relative abundance > 1%) and their relative abundance in all samples from treatment plant (TP) to locations in distribution network (DN1, DN2 and DN3) before (T_0), during ($T_{3\text{-weeks}}$) and after ($T_{6\text{-months}}$) upgrading the treatments.

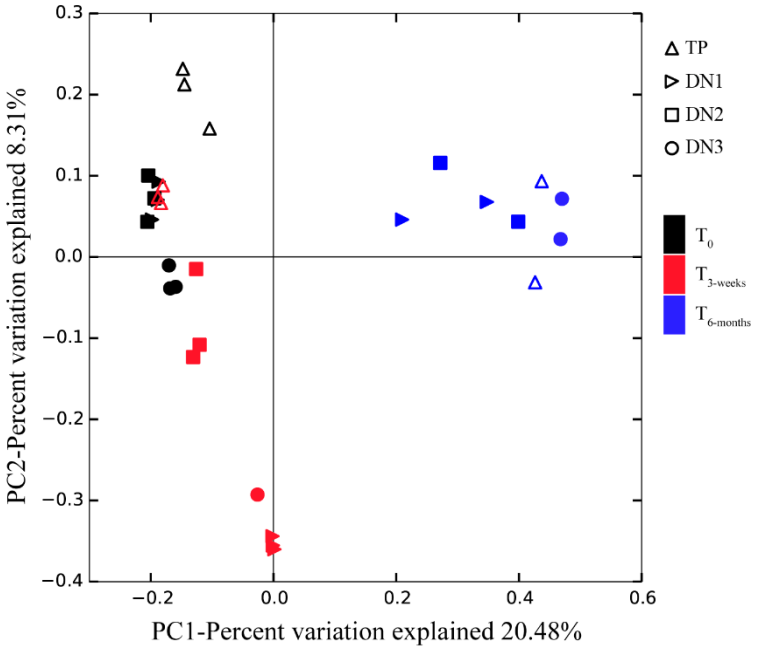

Figure 4-S6. PCoA based on unweighted UniFrac distance for samples taken from treatment plant (TP) to locations in distribution network (DN1, DN2 and DN3) before (T_0, black), during ($T_{3\text{-weeks}}$, red) and after ($T_{6\text{-months}}$, blue) upgrading the treatments were included. The microbial communities of PAB at treatment plant were indicated by open triangles. Communities of PAB during distribution were marked by solid triangles (DN1), squares (DN2), and circles (DN3), respectively.

Chapter 5

Transition Effects in an Unchlorinated Drinking Water System Following the Introduction of Partial Reverse Osmosis

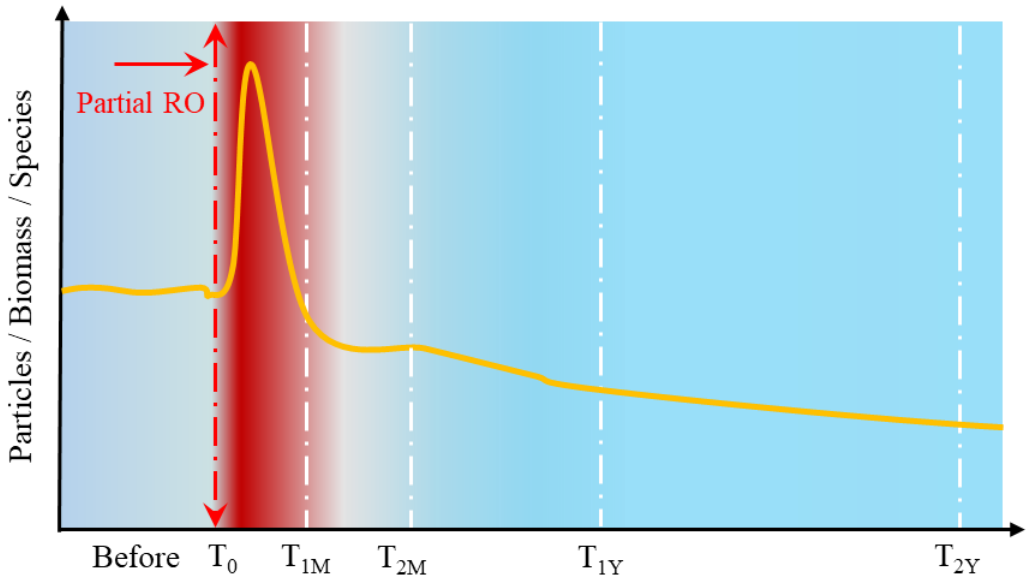

This chapter is based on: Chen, L., Li, X., Medema, G., van der Meer, W., & Liu, G. (2023). Transition effects in an unchlorinated drinking water system following the introduction of partial reverse osmosis. *Nature Water*, 1-10.

Abstract

It is an increasingly common practice that drinking water distribution system (DWDS) may have to deliver new-quality water after decades of services. However, the so called "transition effects" when old DWDS receiving new water remains unclear. In this 2 years' longitudinal study, transition effects induced by introducing partial reverse osmosis (RO) in drinking water production were investigated by combining online monitoring and sampling with 16S rRNA gene amplicon sequencing. Bulk water and suspended particles were collected using the online monitoring and sampling system at different stages: before, during, and after the introduction of RO (1 month, 2 months, 1 year, 2 years). Biofilm and loose deposit samples obtained before and after 1 year and 2 years of RO introduction served as sources in the study. Observed as increase of particle load (+118%), elemental concentrations (e.g., Ca, Fe, Mn), quantity of biomass (+200%), number of observed amplicon sequence variants (ASVs, +57), the occurrence of transition effects was captured as soon as new-quality water enters distribution system. It lasted for 1 month, then started to fade away since 2nd month. The peak transition window is about 1-month time, while the re-stabilization of microbial ecology and improvements of water quality takes much longer till one and two years later, which were attributed to the changes/improvements in treated water quality rather than contributions from biofilm and/or loose deposits. The number of immigrants from loose deposits and biofilm increased by 17.9% during the transition period and decreased by 79.0% two years later. Overall, the study provides valuable insights on the occurrence and possible managing strategies of transition effects, based on which proper monitoring and managing plans could be developed.

Keywords: Drinking water distribution system, partial RO treatments, transition effects, high-resolution sampling, longitudinal study

5.1 Introduction

Transition effects are defined as physicochemical and microbiological water quality problems resulting from irregular changes in supply-water quality (e.g., treatment upgrades), which may lead to the destabilization, mobilization, and release of particles and microbes harbored by drinking water distribution system (e.g., biofilm, loose deposits, pipe scales) (Liu et al., 2017b). Driving by increasingly stricter water quality regulations and the development of water purification technologies, it has become common practice that drinking water distribution system (DWDS) to deliver new-quality water after decades of services (Shannon et al., 2008). However, the transition effects remain unclear, and most switches have been conducted without proper consideration.

Although the definition was proposed in 2017, the observation of transition effects can be traced back to 1990s or even earlier. For example, discoloration occurred during switching source water at Tucson, U.S. in 1992 (Basefsky, 2006), and high concentrations of As, Cu and Fe along with discoloration occurred in the midwestern United States when starting up chlorination in 1996 (Reiber and Dostal, 2000). The small amount of knowledge on transition effects gathered thus far can be partly attributed to lack of attention, methods, and regulations. Moreover, certain characteristics make it difficult to capture and study transition effects, such as uncertainty in the timing of transition effects and the fact that its occurrence cannot be replicated; in addition, the release of particles and microbes will be diluted by large volumes of water continuously being flushed out (Liu et al., 2017b; Makris et al., 2014). Recently, researchers have successfully captured and characterized transition effects during the introduction of softening and rapid sand filtration in a Dutch system by sampling suspended particles before, during (3 weeks) and after (6 months) the switching (Chen et al., 2020). In the study, the authors observed a significant increase of particles, biomass and inorganic elements during the transition, while clear improvements after 6 months. However, no loose deposits or biofilm samples were included in the study. The methodology, period, and frequency of sampling in the study offer insights neither the speed and longevity of transition effects nor where the transition effects originated and how to prevent potential aesthetic and health problems.

The development of sensors and online monitoring/sampling in drinking water offers unprecedented opportunities for high-resolution studies that are real-time, labor-free, and, at the same time, minimize measurement deviations (Banna et al., 2014; Besmer et al., 2016; Favere et al., 2020; Ikonen et al., 2017). Combining sensors of online monitoring and suspended

particles pre-concentration used in a previous study, the authors have developed and applied an online monitoring and sampling system (OMSS) to investigate spatiotemporal variations of planktonic and particle-associated bacteria in Dutch DWDS (Chen et al., 2022b). The study demonstrated regular peaks of particle/cell during the peaks of daily water demand. Combining with integral sampling of biofilm and loose deposits, the proportional contribution of biofilm and loose deposits to the daily peaks were tracked and quantified. The OMSS would be especially valuable for studying transition effects because it can overcome the above-mentioned challenges of aperiodic occurrence and mass dilution.

The objective of this longitudinal study is to investigate transition effects by applying OMSS (high-resolution) for a period of two years (long-term) after the drinking water treatment plant introduced partial reverse osmosis in production. Sampling was conducted before (T_B), during (T_0), and after RO introduction (1 month-T_{1M}; 2 months-T_{2M}; 1 Year-T_{1Y}; 2 years-T_{2Y}). Loose deposits and biofilm samples were taken to track and quantify their contributions using Bayesian-based source tracker (SourceTracker2) and the neutral community model (NCM). This study provides valuable insights into the occurrence of transition effects (e.g., when, how long, where, etc.), based on which proper monitoring, managing actions, and regulations could be developed.

5.2 Materials and Methods

5.2.1 Drinking water treatment plant

The study was conducted at one of the drinking water treatment plants of Oasen in the Netherlands, with a production capacity of 6500-7500 m^3/day. To enhance drinking water quality, reverse osmosis has been introduced into the existing treatment stream since June 2017. The treatment processes before and after RO introduction are illustrated in Figure 5-1A. The riverbank filtrated groundwater was abstracted from well fields A and B followed by aeration, double sand filtration, activated carbon filtration and ultraviolet (UV) disinfection before being delivered to customers. Since June 2017, groundwater abstracted from well field-A (50% capacity) was first treated by RO and blended with groundwater abstracted from well field-B, whereafter it is treated through the original treatment processes.

5.2.2 Sampling locations and water quality improvements

To study improvements of treated and distributed water quality and the dynamics of microbial ecology changes in distribution system, locations were selected at treatment plant (TP) and in

distribution network (DN). The sampling point at TP was right before water enters DN, and locations in DN were selected based on distances to TP (1 km, 4.5 km, 6 km). The two years of water quality monitoring results showed marked improvements achieved by the introduction of RO in both TP and DN (Figure 5-1B and 5-S1). For example, concentrations of Ca decreased by 48%, and electrical conductivity (EC) decreased by 40%, with no observed differences between TP and DN, and between 1 year (T_{1Y}) and 2 year (T_{2Y}). Regarding dissolved organic carbon (DOC), the achieved reduction further increased from 44% at T_{1Y} to 57% at T_{2Y} at both TP and DN compared to before introducing RO (T_B), with no differences among locations in DN. To reveal the responses and dynamics of microbial ecology in DN to water quality improvements, long-term and high-resolution analysis focused on the comparison between TP and DN (combined).

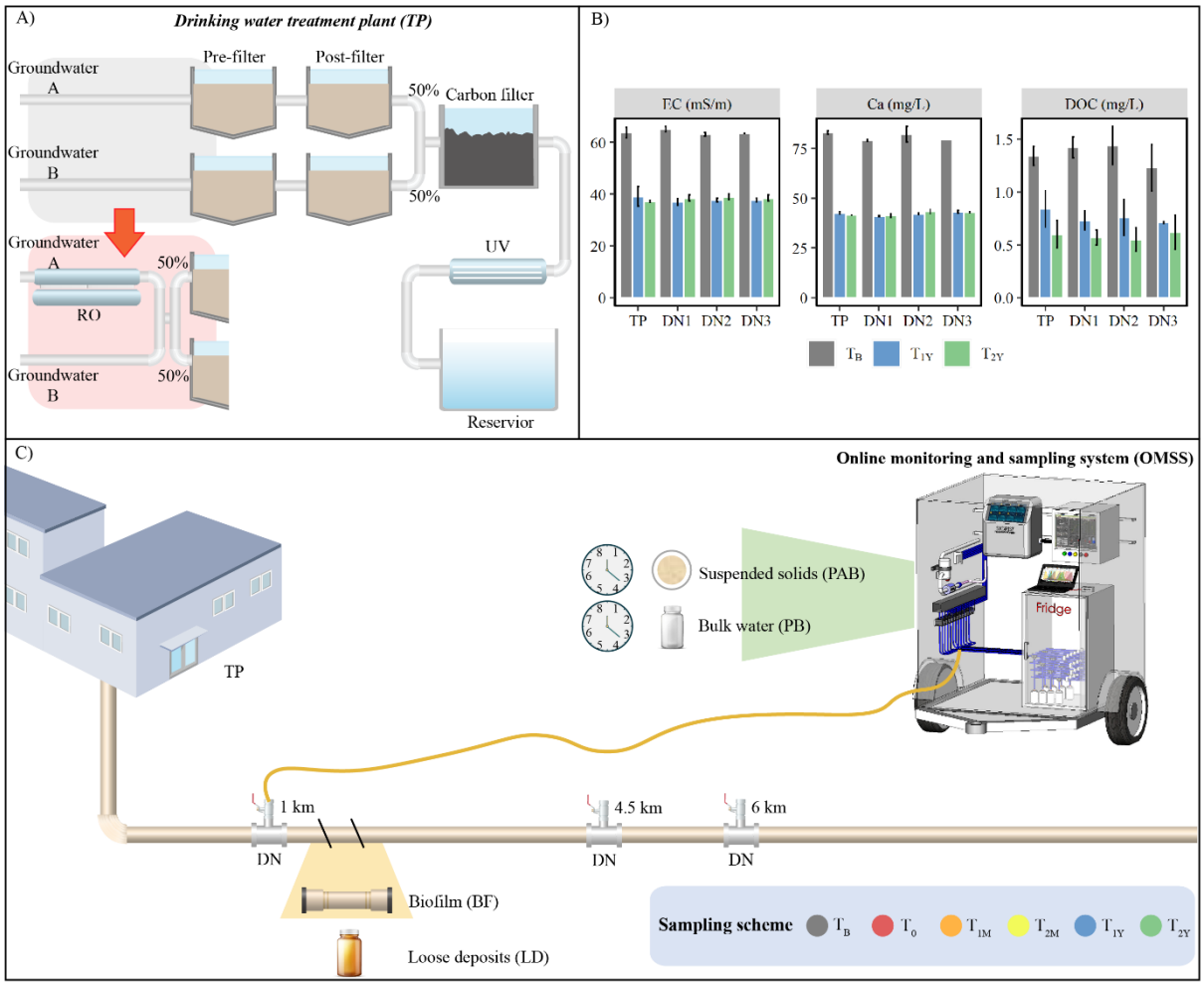

Figure 5-1. *A) Water treatment processes before and after introducing RO; B) EC, Ca, and DOC values before (T_B), and one year (T_{1Y}), 2 years (T_{2Y}) after RO introduction at treatment plant (TP) and in distribution network (DN). DN1, DN2 and DN3 stand for locations in*

distribution network which are 1, 4.5, and 6 km to TP; C) Illustration of sampling program: water (Planktonic bacteria, PB) and particles (particle-associated bacteria, PAB) were taken by online monitoring and sampling system at TP and DN every 3 hours per day. Biofilm (BF) and loose deposits (LD) were sampled at DN after OMSS sampling. Water and particles were sampled before (T_B), immediately after (T_0), one month (T_{1M}), 2 months (T_{2M}), one year (T_{1Y}), and 2 years (T_{2Y}) after introducing RO in production. BF and LD were sampled at T_B, T_{1Y} and T_{2Y}.

5.2.3 Sampling program

Online sampling of water and suspended particles. The online monitoring and sampling system (OMSS, Figure 5-1C) developed was previously applied for continuously sampling of water and suspended particles (Chen et al., 2022b). In short, the system integrated water quality monitoring sensors, data loggers, water sampling bottles, and particle sampling filters (Whatman 1822–047, 1.2 µm), which were controlled and operated by a preprogramed PLC for 24 h. For suspended particles, a filter pore size of 1.2 µm was selected based on the results of a previous study (Liu et al., 2013a). The trans-filter pressure was monitored and logged online, and the pressure differences per volume of water (Δ P/V) were used as an index of particle load in water. Water and suspended particles were sampled every 3 hours continuously for a day at 0–3 h, 3–6 h, 6–9 h, 9–12 h, 12–15 h, 15–18 h, 18–21 h, and 21–24 h. The water bottles and filters were kept in refrigerator to guarantee the sample quality for downstream microbiological analysis. Samples were collected and transported on ice, and processed in the lab immediately within 24 h after sampling. Online sampling of water and particles at TP (water, n = 48; suspended particles, n = 48) and DN (water, n = 48 × 3; suspended particles, n = 48 × 3) were conducted before (T_B) introducing RO, immediately (T_0), 1 month (T_{1M}), 2 months (T_{2M}), 1 year (T_{1Y}), and 2 years (T_{2Y}) after introducing RO. Specifically, the monthly sampling frequency for the first two months (T_0, T_{1M}, T_{2M}) was strategically designed based on observations from our previous study to capture and analyze the short-term transition effects (Chen et al., 2020). Meanwhile, to cover long-term transition effects, samples were collected at 1 year (T_{1Y}) and 2 years (T_{2Y}) after the implementation of the RO treatment.

Biofilm and loose deposits sampling. Together with online sampling of suspended particles at T_B, T_{1Y}, and T_{2Y}, biofilm (BF, n = 12) and loose deposits (LD, n = 6) were sampled in DN as previously described (Liu et al., 2017a). In brief, LD was sampled in duplicates at corresponding hydrants in DN by fully opening the fire hydrant. Subsequently, the flushed pipes

(PVC-U, D = 110 mm) were cut to a length of 30 cm for the purpose of biofilm sampling. During the cutting process, chlorine spray was used to disinfect both the exposed cleaned pipes and cutting tools to minimize the potential for contaminations. After cutting, the pipe sections with BF inside were closed by sterile caps and filled with DNA-free water to keep the inner side wet during transportation. Filters with suspended particles, flushed loose deposits, and cut pipe specimens were transported on ice to the laboratory and pre-treated by low energy ultrasonic treatment performed 3 times, for 2 min each (Branson ultrasonic water bath, 43 kHz, 180 W power output, 10 L sonication chamber). The obtained suspension was used for downstream physiochemical and biological analysis. All samples (n = 402) were processed within 24 hours after collection.

5.2.4 Inductively coupled plasma-mass spectroscopy (ICP-MS)

Concentrations of several elements in the samples, generated using sequential extractions and filtration experiments with filters of varying sizes, were determined by inductively coupled plasma-mass spectroscopy (ICP-MS) (PerkinElmer ELAN DRC-e ICPMS). The elements quantified in these measurements included iron (Fe), calcium (Ca), arsenic (As), aluminum (Al) and manganese (Mn). Quality control samples, including laboratory-fortified blanks and laboratory-fortified samples, were performed for every 10 samples analyzed. Average elemental recoveries ranged from 85.2 to 92.8% for the laboratory fortified samples.

5.2.5 Adenosine triphosphate

Active biomass was quantified by measuring adenosine triphosphate (ATP). Briefly, the ATP was first released from cells by nucleotide-releasing buffer (NRB, Celsis). Afterwards, the released ATP was measured by the intensity of the emitted light in a luminometer (Celsis Advance^{TM}) calibrated with solutions of free ATP (Celsis) in autoclaved tap water following the standard procedure given by the manufacturer (Magic-Knezev and Van Der Kooij, 2004).

5.2.6 DNA extraction and 16S rRNA sequencing

The DNA was extracted from all samples using the FastDNA Spin Kit for Soil (Q-Biogene/MP Biomedicals, Solon, OH, USA) according to the manufacturer's instructions. After checking the DNA amount and quality, a total of 363 samples were used for the subsequent 16S rRNA sequencing. The primer set (341F: 5′-CCTACGGGNGGCWGCAG-3′ and 785R: 5′-GACTACHVGGGTATCTAATCC-3′) targeting the V3-V4 hypervariable regions of sequences from both bacterial and archaeal domains was applied for amplification before sequencing.

Paired-end sequencing of the amplicons (2 × 300 bp) was conducted on an Illumina Miseq platform by BaseClear (Leiden, the Netherlands). The sequencing data have been deposited in the NCBI database, with reference code PRJNA967184.

5.2.7 Sequencing analysis

The bacterial 16S rRNA gene amplicons were processed using the Quantitative Insights Into Microbial Ecology (QIIME2, v2020.11) pipeline with the default settings (Caporaso et al., 2010). Raw reads were quality filtered, denoised, paired-end sequence merged, and chimera filtered by using DADA2 (Callahan et al., 2016). Consequently, unique amplicon sequence variants (ASVs), equivalent to 100% similarity operational taxonomic units (OTUs) in conventional practice, were generated. Taxonomy was assigned using q2-feature-classifier, customized for the primer set used in this study with Silva SSU database release 132 (Quast et al., 2012). Multiple sequence alignment and phylogenetic tree construction were performed using the QIIME 2 plugin q2-phylogeny. Alpha and beta diversity analyses were performed using the QIIME 2 plugin q2-diversity with a threshold of 5970. Principal coordinates analysis (PCoA) was conducted based on Bray-Curtis distances to assess community similarity across sampling time periods, phases, and locations. Significant differences in community composition among sampling time periods, phases, and locations were assessed using PERMANOVA (Permutational multivariate analysis of variance) with 999 permutations calculated per test. Differences were considered significant when the p-value was lower than 0.05 ($P < 0.05$).

5.2.8 Bayesian-based SourceTracker2

The Bayesian-based SourceTracker method was performed to quantify the contribution of potential sources to the sinks (Henry et al., 2016). In the present study, particle-associated bacteria (PAB) in DN at each sampling time were identified as sinks, while planktonic bacteria (PB) and PAB from treatment plant and BF and LD in distribution network were defined as potential sources. SourceTracker analysis was conducted using default settings with a rarefaction depth of 1000, burn-in 100, restart 10, alpha (0.001) and beta (0.01). The analysis was performed three times and the average was calculated as previously described (McCarthy et al., 2017).

5.2.9 Neutral community model

The Sloan neutral community model was used to explore the role of neutral processes (i.e.,

dispersal and random growths/deaths) in the assembly of microbial communities (Ling et al., 2018; Sloan et al., 2006; Venkataraman et al., 2015). In this model, the target communities were these communities at DN, while the source communities were communities from TP and DN (harbored by BF, LD). For each taxon shared between the source and target communities, the expected frequency of detection in the local communities from dispersal and random growths/deaths (i.e., neutral processes) was computed from the abundance in the source communities, following a beta function. RMSE is the square root of the mean of the squared differences between observed and predicted values, with 0 indicating that the data perfectly fit the model and higher values indicating a greater divergence from the model predictions (Sprockett et al., 2020). The fitting was performed using a non-linear regression R package (Minpack.lm). With RMSE values spanning from 0.14 to 0.40 (Figure S14-16), it suggests the applicability of the neutral community model in describing the dataset. Based on whether the ASVs occurred within (neutral partition), less frequently than (below partition), or more frequently than (above partition) the 95% confidence intervals of the NCM predictions, all ASVs were categorized into three groups. Especially, the cumulative relative abundance of ASVs within the neutral partition was used to evaluate the contributions of dispersal (∑relative abundance of blue ASVs in target communities) from the source community in shaping the community assembly of DWDS microbiome. Together, ASVs falling into the neutral partition were defined as immigrants from the source communities to the target communities. The term "immigrants" was employed to depict the contributions from these sources to targets, a terminology widely utilized in engineered water systems (Mei and Liu, 2019). Specifically, the immigrants from LD and BF were defined as LD-Immigrants and BF-Immigrants. Finally, linear discriminant analysis Effect Size (LEfSe) was applied to determine the key sensitive immigrants which were significantly enriched at certain times.

5.3 Results

In general, water quality was greatly improved after introducing RO in production, with about 50% reduction in EC, and concentrations of inorganic (e.g., Ca) and organic matter (e.g., DOC) in the treated and distributed water (Figure 5-1B). Microbiologically, significant changes were observed in the quantity and community of planktonic bacteria (PB, bulk water), particle-associated bacteria (PAB, suspended particles), and bacteria harbored by loose deposits (LD) and biofilm (BF), from both long-term (2-years) and daily (24-hours) perspectives. The datasets revealed that PAB can track the de/re-stabilization of the distribution system microbial ecology better than PB, which could be attributed to the variable levels of dilution effects that might

mask the release of particles and bacteria into bulk water. Therefore, the following sections will focus more on PAB than PB. Spatiotemporal variations in the physicochemical and microbiological characteristics of PB were provided in the supplemental materials correspondingly (Figure 5-S1, 5-S5-10, 5-S12-18).

5.3.1 Changes of particle loads (ΔP/V) and elemental composition of suspended particles

Particle loads (ΔP/V). The particle loads decreased significantly at TP immediately after introducing RO at T_0 compared to T_B (ΔP/V, - 34%), which further decreased until T_{1Y} ($p < 0.05$, Figure 5-2A). On the contrary, the ΔP/V at DN increased dramatically from T_B to T_0 at DN (+118%, $p < 0.05$), then decreased from T_{1M} onwards, reaching levels lower than T_B from T_{2M}. Remarkably, the decrease in ΔP/V at TP and increase in ΔP/V at DN observed at T_0 suggest that increased particles might be contributed by the distribution system. During the distribution from TP to DN, the ΔP/V decreased significantly at T_B (- 57%, $p < 0.05$), increased at T_0 (+ 41%, $p < 0.05$), remained stable at T_{1M}, T_{2M}, and T_{1Y}, while decreasing at T_{2Y} (- 44%, $p < 0.05$). Considering the daily ΔP/V variations at DN, morning (6-9h) and evening (18-21h) peaks were sensitively captured. T_B and T_0 showed the same daily patterns, but the evening peak at T_0 was three times higher than that of T_B (Figure 5-2C). When it comes to T_{1Y} and T_{2Y}, not only the daily patterns became smooth and flatting, but the values were also much lower than T_B and T_0.

Elemental composition. Generally, the spatiotemporal patterns of particle-associated elements (i.e., P-Ca, P-Al, P-As, P-Fe, P-Mn) before and after the RO introduction were similar to those of ΔP/V, which increased first at T_0 and/or T_{1M}, decreased afterwards around T_{2M}, and remained stable at T_{1Y} and T_{2Y} (Figure 5-S2 and 5-S3). It is worth noting that the concentrations of P-Ca, P-Al and P-As started to decrease after T_0, while the concentrations of P-Fe and P-Mn did not decrease until T_{2M}, indicating the late release of Fe and Mn from distribution pipes, which might be because of their presence in the inner layer of scales/biofilms/loose deposits.

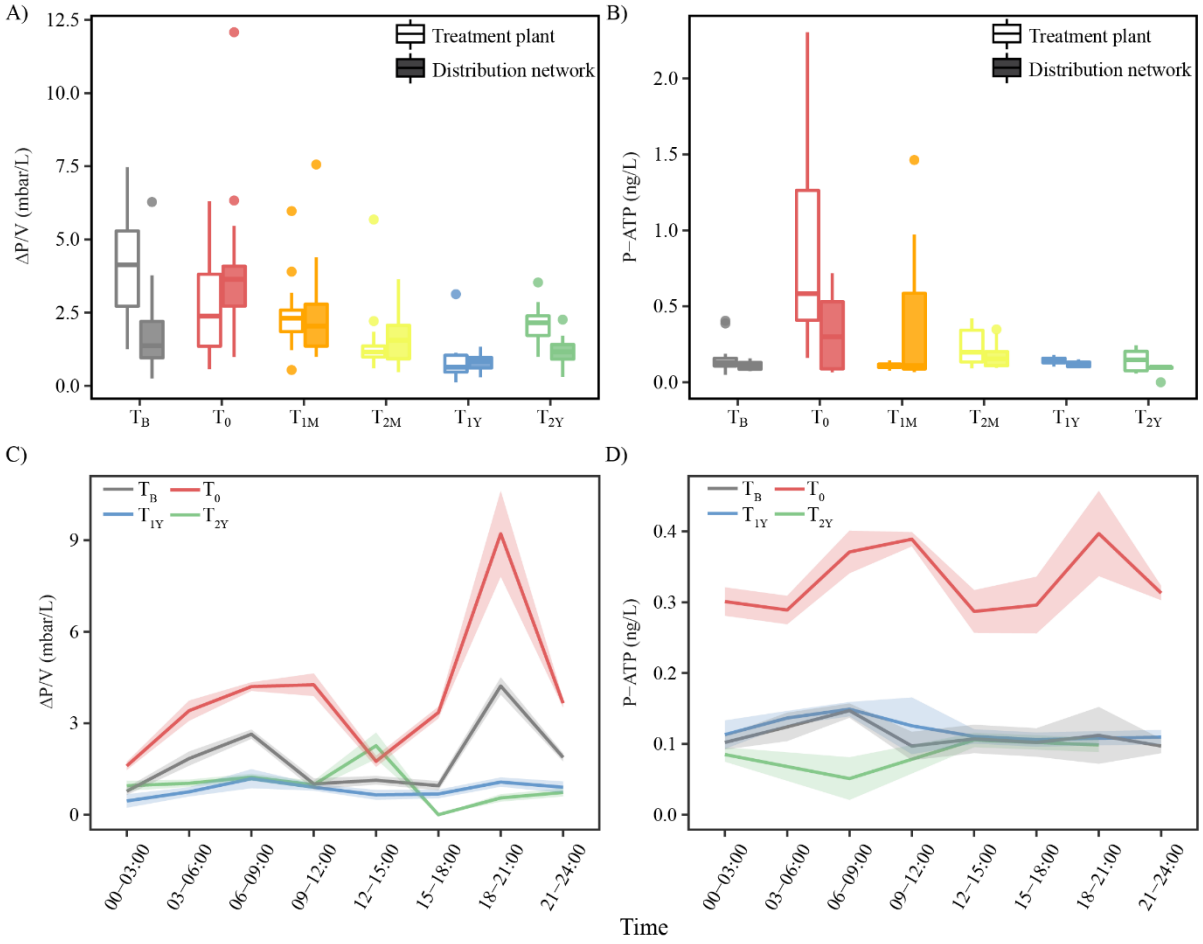

Figure 5-2. *The long-term and daily variations of particle loads (ΔP/V), particle-associated ATP (P-ATP) at treatment plant (TP) and distribution network (DN): A) two-years' changes of ΔP/V at TP and DN; B) two years' changes of P-ATP at TP and DN; C) daily variations of ΔP/V at DN (mean ± s.d., n = 3); D) daily variations of P-ATP at DN (mean ± s.d., n = 3). T_B - before introducing RO in production; T_0 - immediately after RO introduction; T_{1M} - 1 month after RO introduction; T_{2M} - 2 months after RO introduction; T_{1Y} - 1 year after RO introduction; T_{2Y} - 2 years after RO introduction. Box plots show median values (middle line), 25th and 75th percentiles (boxes) and 5th and 95th percentiles (whiskers). Outliers, if present, are shown as individual points beyond the whiskers.*

5.3.2 Changes of particle-associated ATP (P-ATP)

Different from ΔP/V, P-ATP significantly increased at TP from T_B to T_0 (+ 453%, $p < 0.05$) and decreased at T_{1M} to a similar level as T_B (Figure 5-2B and 5-S4), suggesting considerable release of biomass from treatments when introducing RO in production. At DN, a similar increase of P-ATP was observed from T_B to T_0 (+ 200%, $p < 0.05$), which further increased at T_{1M} (+ 209%, $p < 0.05$) and started decreasing since T_{2M}. Comparing TP and DN, P-ATP slightly decreased

during distribution at T_B, while it significantly decreased at T_0 (- 60%, $p < 0.05$), indicating the dominant role of particle sedimentation during distribution from TP to DN at T_B and T_0. Remarkably, at T_{1M}, the P-ATP at DN was dramatically higher than TP (+ 209%, $p < 0.05$). Stable P-ATP was observed afterward from T_{2M} to T_{1Y} and T_{2Y}. The daily variations of P-ATP at DN showed similar patterns as ΔP/V; morning and evening peaks were observed at both T_B and T_0, with peak values at T_0 being 3-4 times higher than that of T_B (Figure 5-2D). When it comes to T_{1Y} and T_{2Y}, not only did the daily patterns become smooth and flatting, but the values were also lower than T_B.

5.3.3 Changes of bacterial community diversity and composition

In total, 7,684,073 sequences were obtained for the 363 samples, including 160 water samples (planktonic bacteria, PB), 185 suspended particles (particle-associated bacteria, PAB), 12 biofilm (BF), and 6 loose deposits (LD) collected before and after introducing RO in the production. The rarefication curves reached a plateau after 4000 sequences, indicating enough sample coverage in this study (Figure 5-S5). Alpha and beta diversity were generated after rarefication to an even sampling depth of 5970 sequences.

5.3.3.1 Bacterial community diversity and composition of PAB

Alpha diversity. The numbers of observed ASVs in the bacterial community of PAB at TP and DN were shown in Figure 5-3A. At TP, the number of observed ASVs increased immediately (T_0, 508 ± 154 ASVs, $P < 0.05$) and 1 month (T_{1M}, 588 ± 92 ASVs, $P < 0.05$) after introducing RO in the production compared to that before introducing RO in the production (T_B, 403 ± 95 ASVs). Afterward, the number of observed ASVs decreased from T_{2M} (512 ± 57 ASVs) till T_{1Y} (535 ± 89 ASVs), which further decreased to 98 ± 36 ASVs at T_{2Y}. At DN, the changes in the number of observed ASVs were even more pronounced ($P < 0.001$). The number of observed ASVs increased from 780 ± 136 ASVs at T_B to 837 ± 140 ASVs at T_0 ($p < 0.05$). Subsequently, the number of observed ASVs continuously decreased to 711 ± 184 ASVs, 484 ± 78 ASVs and 464 ± 110 ASVs at T_{1M}, T_{2M}, and T_{1Y}, respectively, further reaching the lowest level at T_{2Y} (100 ± 42 ASVs). Comparing TP and DN, the number of observed ASVs increased at T_B, T_0, and T_{1M}, while decreased at T_{2M} and T_{1Y} and maintained a stable level at T_{2Y} from TP to DN. This may indicate the re-stabilization of microbial ecology gradually established after a period of two years' time. The daily variations of observed ASVs number at DN showed similar patterns as ΔP/V and P-ATP (Figure 5-3B and 5-S7), with average and peak values at T_0 higher than that of T_B, significantly lower at T_{1Y}, and almost a flat line at T_{2Y}, illustrating high daily stability in

distribution network at T_{2Y}.

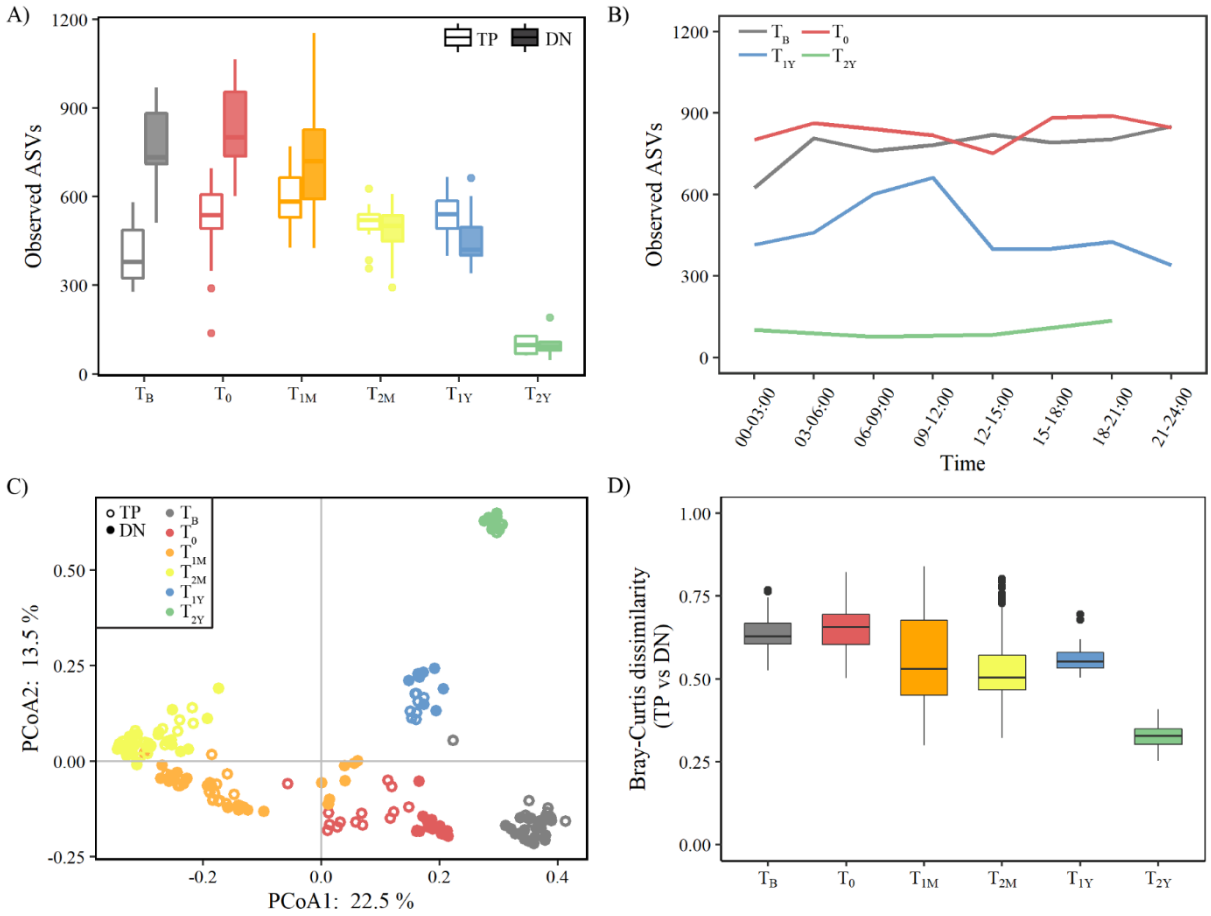

Figure 5-3. *The changes of particle-associated bacteria (PAB) communities at treatment plant (TP) and distribution network (DN): A) the number of observed ASVs at TP and DN at T_B, T_0, T_{1M}, T_{2M}, T_{1Y}, and T_{2Y}; B) daily variations in observed ASVs numbers at DN at T_B, T_{1Y}, and T_{2Y}; C) PCoA plot showing the community similarity of PAB at TP and DN based on Bray-Curtis distances; D) Bray-Curtis distances between PAB communities at TP and DN. T_B - before introducing RO in production; T_0 - immediately after RO introduction; T_{1M} - 1 month after RO introduction; T_{2M} - 2 months after RO introduction; T_{1Y} - 1 year after RO introduction; T_{2Y} - 2 years after RO introduction. Box plots show median values (middle line), 25th and 75th percentiles (boxes) and 5th and 95th percentiles (whiskers). Outliers, if present, are shown as individual points beyond the whiskers.*

Beta diversity. As illustrated by the PCoA plot, samples from different phases formed clear clusters ($p < 0.001$, Figure 5-S8A), with the community of bacteria in BF and LD clustering closer to PAB than PB. For PAB and PB, there were clear pairwise patterns between the TP and DN samples at each sampling time-point (Figure 5-3C and 5-S8B). More specifically, the

dissimilarities in PAB communities between TP and DN increased from T_B to T_0 (different clusters), then decreased from T_{1M} to the lowest dissimilarities at T_{2Y} (highly similar, same cluster, Figure 5-3C). This observation in the PCoA plot was consistent with the Bray-Curtis distances between PAB samples at TP and DN (Figure 5-3D), indicating the re-stabilization of microbial ecology in the distribution network and improved stability of the bacterial community during distribution.

Bacterial community composition. In generally, the bacterial community of PAB was mainly dominated by Proteobacteria (67.5 ± 15.9%) regardless of sampling time and space (Figure 5-S9), with Alphaproteobacteria (17.3 ± 8.2 %) and Gammaproteobacteria (41.6 ± 19.2%) being the dominant classes. At T_B, PAB was dominated by Gammaproteobacteria at both TP (51.4 ± 7.5%) and DN (39.3 ± 6.7%), the relative abundance of which decreased significantly at T_0 at TP (30.6 ± 6.5%) and DN (22.2 ± 2.1%). Consequently, Alphaproteobacteria became dominant at DN (T_0, 28.4 ± 4.0%, Figure 5-S9 and 5-S10). At T_{1M}, Patescibacteria took over and became the most abundant phylum at both TP (35.2 ± 13.6%) and DN (30.4 ± 15.3%), while after T_{2M}, Gammaproteobacteria became the most abundant class again at TP (50.7 ± 8.3% at T_{2M}, 49.4 ± 5.2% at T_{1Y}, 95.3 ± 1.3% at T_{2Y}) and DN (37.6 ± 9.9% at T_{2M}, 51.7 ± 12.6% at T_{1Y}, 96.7 ± 2.1% at T_{2Y}).

5.3.3.2 Bacterial community diversity and composition of LD and BF

For BF, the number of observed ASVs remained the same level with little variations from T_B (827 ± 50 ASVs) to T_{1Y} (855 ± 29 ASVs) and T_{2Y} (832 ± 65 ASVs), indicating the introduction of RO in production had minor impacts on the alpha diversity of BF communities (Figure 5-4A). Differently, there was a significant increase in observed ASVs number at T_{1Y} (1052 ± 127 ASVs), which decreased to the same level as T_B at T_{2Y} (886 ± 83 vs. 855 ± 54 ASVs), indicating the bacterial communities of LD were influenced by changes in supply-water quality.

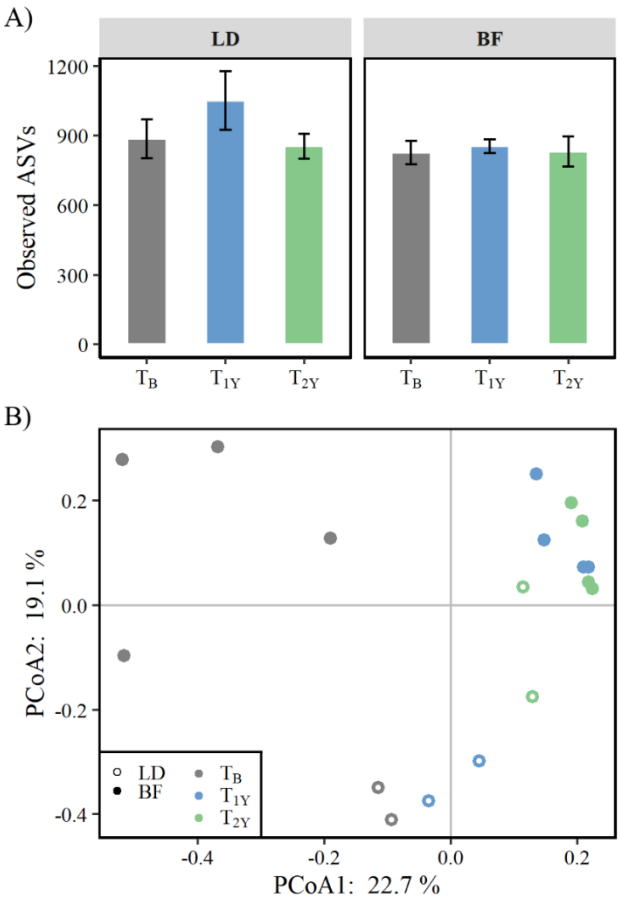

Figure 5-4. *Bacteria community diversity of biofilm (BF) and loose deposits (LD): A) the observed ASVs number of BF (n = 12) and LD (n = 6) from T_B to T_{1Y} and T_{2Y}. Data are presented as mean ± s.d.; B) PCoA plot illustrating the bacterial community similarities of BF and LD from T_B to T_{1Y} and T_{2Y}. T_B - before introducing RO in production; T_{1Y} - 1 year after RO introduction; T_{2Y} - 2 years after RO introduction.*

Regarding the bacterial community similarity, significant changes were observed for both BF and LD from T_B to T_{2Y}. Specifically, the BF at T_{1Y} and T_{2Y} clustered together, clearly different from BF at T_B (Figure 5-4B). Though the number of observed AVSs did not change, the dominant ones and their abundances might be different due to the release of biomass from biofilm. The bacterial community of LD showed the same pattern. Interestingly, it was observed that the LD at T_{2Y} were similar to that of BF at T_{1Y} and T_{2Y}. This may be because of the release of particles and biomass from BF, gradually accumulating in the distribution system and becoming LD. This hypothesis can be supported by the decrease of Patescibacteria (13.2 ± 6.8% to 3.7 ± 2.3%) and increase of Planctomycetes (3.7 ± 1.2% to 14.2 ± 8.1%) in LD from T_{1Y} to T_{2Y}, corresponding well to the bacterial community composition of BF at T_{2Y} (3.9 ± 0.7% for Pateschibacteria; 10.0 ± 5.2% for Planctomycetes) (Figure 5-S11). Besides, the increase of

Gammaproteobacteria in LD from T_B (21.9%) to T_{1Y} (24.9%) might be due to its corresponding decrease/detachment from BF from T_B (39.2%) to T_{1Y} (24.0%).

5.3.4 Quantitative contribution of loose deposits and biofilm to PAB at DN

In terms of the quantitative contribution of loose deposits and biofilm to PAB at DN, both SourceTracker 2 and NCM ($R^2 = 0.79$, $p < 0.05$, Figure 5-S14-18) indicated that PAB from TP was the major contributor to PAB at DN across all sampling times (61.5 ± 14.4%) (Figure 5-S12A), slightly decreasing from T_B (53% ± 7.6) to T_0 (51% ± 6.4) (Figure 5-S12B), significantly decreasing by (up to) 30% (during morning/evening peaks, Figure 5-S13) at T_{1M} (53.1 ± 17.3%), starting to increase since T_{2M} (73.0 ± 4.9%), and remaining stable till T_{1Y} (75.8% ± 5.4) and T_{2Y} (73.6 ± 6.4%). Correspondingly, significant increases in contributions from LD were observed immediately at T_0 (10.3 ± 2.4%, $p < 0.001$) compared to that at T_B (7.4 ± 2.4 %, Figure 5-5A). Although the average contribution from LD slightly decreased at T_{1M} (8.3 ± 5.5%), the peak contributions frequently went above 15% (up to 25%, $p < 0.05$, Figure 5-5B). Clearly, the contribution from LD dramatically decreased since T_{2M} (2.6 ± 1.3%) till T_{1Y} (2.5 ± 1.5%) and further decreased at T_{2Y} (0.4 ± 0.3%). The contribution of BF followed the same pattern as LD, whereas the values were much lower than that of LD, ranging between 1.7% (T_B, T_{1M}, T_{2M}, T_{1Y}) to 3.3% (T_0), which further decreased to 0.1% at T_{2Y} (Figure 5-5A), indicating less contribution and threats lies in BF than LD. The decreased contributions of PAB from TP paired with the increased contributions from LD and BF at T_0 and T_{1M}, were direct evidence of microbial ecology destabilization and bacteria release from LD and BF induced by introducing RO in production. The stable contributions of different sources since T_{2M} suggested possible re-stabilization started to be established. Moreover, the higher contribution from TP, lower contribution of LD and BF, and the flatter daily pattern of T_{2Y} compared to T_B clearly illustrated higher quality and better stability gradually achieved by introducing RO in production.

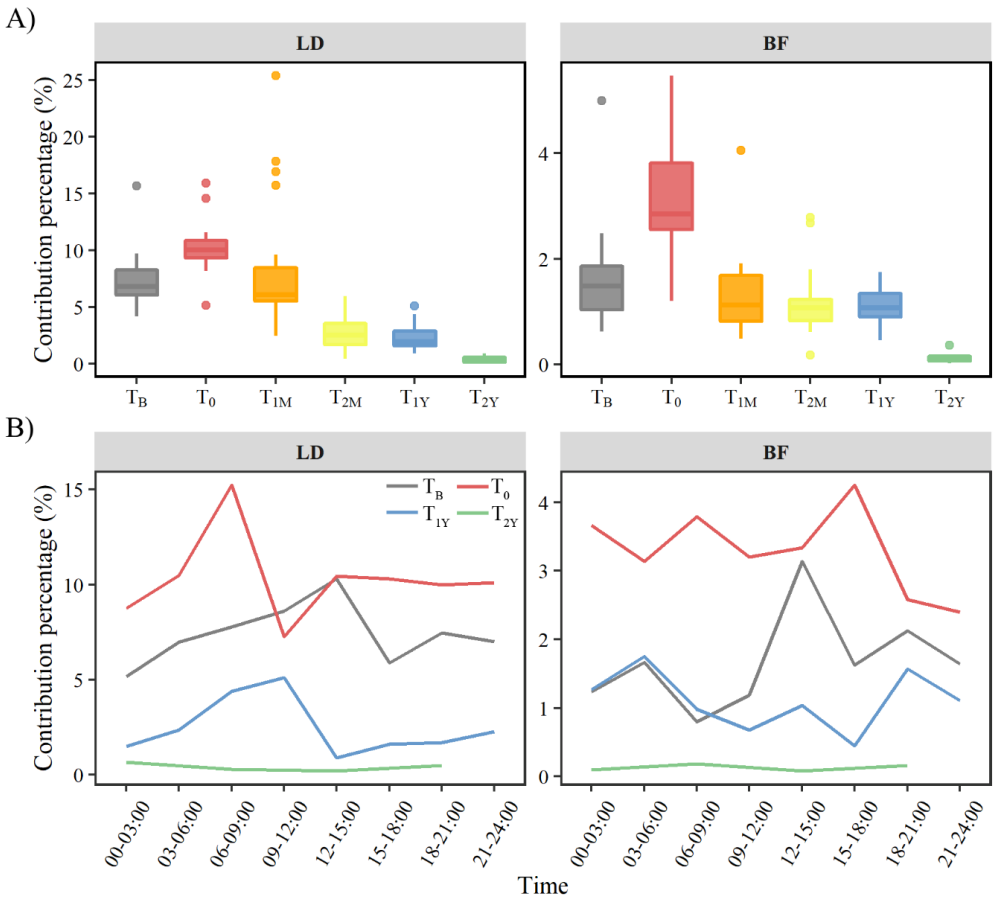

Figure 5-5. *Sources apportion results by SourceTracker2: A) contributions from loose deposits (LD) and biofilm (BF) to particle-associated bacteria (PAB) in distribution network (DN) over time; B) daily variations in contributions from LD and BF to PAB at DN. T_B - before introducing RO in production; T_0 - immediately after RO introduction; T_{1M} - 1 month after RO introduction; T_{2M} - 2 months after RO introduction; T_{1Y} - 1 year after RO introduction; T_{2Y} - 2 years after RO introduction. Box plots show median values (middle line), 25th and 75th percentiles (boxes) and 5th and 95th percentiles (whiskers). Outliers, if present, are shown as individual points beyond the whiskers.*

5.3.5 Key immigrants (ASVs) from LD and BF and their contributions

As identified by NCM, the number of LD-immigrants increased from 391 ASVs to 464 and 462 ASVs at T_0 and T_{1M}, then started to decrease at T_{2M} (427) and further decreased to 345 and 96 ASVs at T_{1Y} and T_{2Y} (Table 5-S1). The trend for BF-immigrants followed exactly the same trend but with much lower numbers compared to LD-immigrants, e.g. 194, 226, 232, 185,,101, and 27 ASVs for T_B, T_{1M}, T_{2M}, T_{1Y}, and T_{2Y}, respectively (Table 5-S1). Such pattern of changes in the number of LD-immigrants and BF-immigrants agreed well with the above-mentioned

changes in P-ATP, the number of observed ASVs, and the contribution of LD and BF to PAB at DN from T_0 to T_{2Y}.

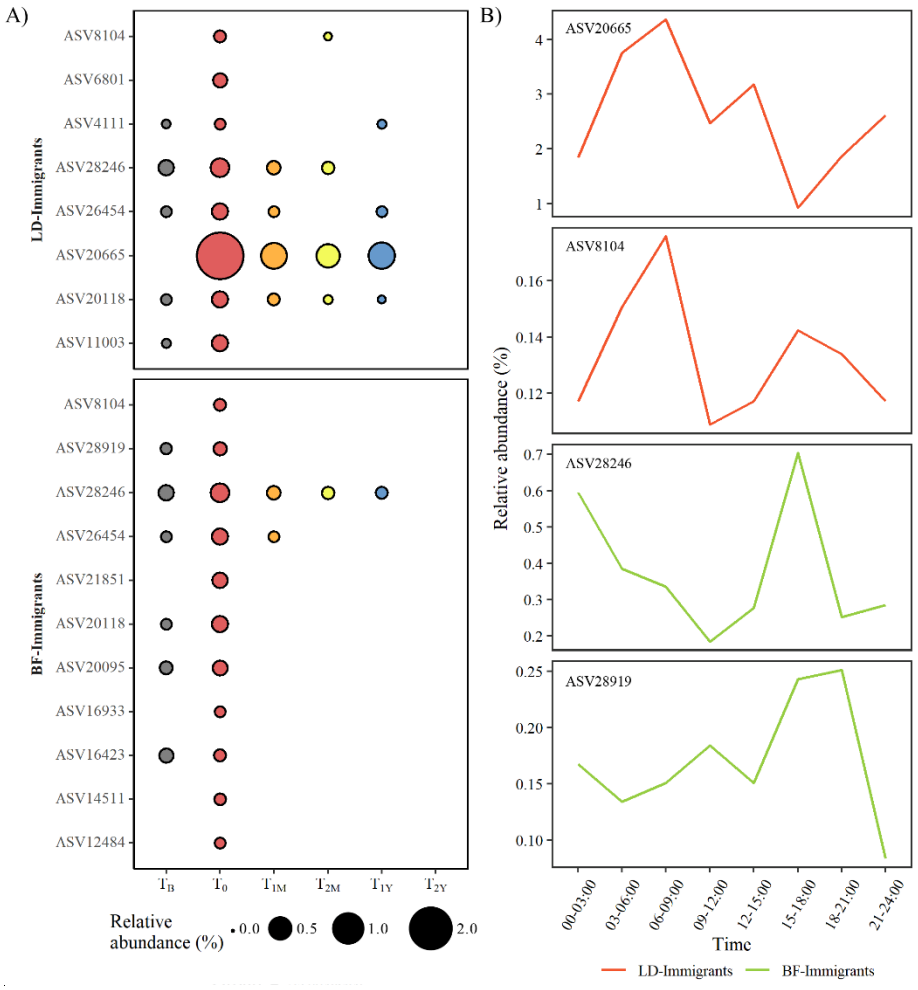

Figure 5-6. *Changes of LD-Immigrants and BF-Immigrants picked by neutral community model (NCM): A) bubble plot showing the variations in relative abundance of LD-Immigrants and BF-Immigrants in particle-associated bacteria (PAB) community,, the circle size stands for the relative abundance and the circle colour stands for sampling periods; B) daily variations of key LD- and BF-Immigrants. Detailed taxonomy information of these immigrants were shown in table 5-S2.*

Considering the key immigrants with relative abundances in PAB at DN > 0.01%, there were 24 (17), 30 (17), 16 (4), 8 (2), and 13 (1) key LD (BF) immigrants at T_0, T_{1M}, T_{2M}, and T_{1Y}, respectively (Figure 5-S19). Key immigrants were not found at T_{2Y} neither from LD nor BF. Focusing on T_0, where both the number and abundances of key immigrants were high, there were 8 LD-immigrants and 11 BF-immigrants significantly discriminative with other sampling times (Figure 5-6A and 5-S20, LDA score > 2, $p < 0.001$). Interestingly, there were 4 shared

ASVs between immigrants from LD and BF: ASV20118 (F_Acetobacter), ASV26454 (O_Rhizobiales), ASV28246 (C_Delproteobacteria), ASV8104 (O_Betaproteobacteriales). For LD-immigrants, the release of dominated ASV20665 (G_Bradyrhizobium) lasted till T_{1Y}. The BF-immigrants, such as ASV16933 (C_Parcubacteria), ASV14511 (C_Parcubacteria), ASV28919 (G_ Nitrospira), were only presented at T_0. For those ASVs, clear daily patterns were observed, with relative abundances spiking at morning (ASV20665, ASV8104) or evening/afternoon peaks (ASV28246, ASV28919) (Figure 5-6B and Table 5-S3).

5.4 Discussion

To understand when and where the transition effects may occur during the starting up of new water treatments, a long-term, high-resolution study in an unchlorinated drinking water distribution system was conducted over 2 years. The longitudinal online monitoring and sampling was combined with micro-ecological models to capture and characterize the responses of the DWDS microbial ecology to changes in water quality and hydrology. This study offered an exceptional opportunity to further explore the mechanism of transition effects.

5.4.1 Peak transition effects occurred within the 1st month of switching

Regarding the timing of transition effects occurrence, the present study reveals that it happened immediately after new-quality water entered the DWDS (Figure 5-2 and 5-3). This observation is consistent with previous reports of sharp transition effects right after supply-water quality changes, such as discoloration, heavy metal, and opportunistic pathogen problems during Flint Water Crisis (Hanna-Attisha et al., 2016; Schwake et al., 2016; Zahran et al., 2018). It should be noted that although transition effects were successfully captured in this study, there was neither detectable water quality deterioration nor customer complains, which can be explained by the highly biostable water (AOC) and little biofilm in the studied system (ATP). Meanwhile, it also means that characterizing bacteria associated with preconcentrated suspended particles is sensitive enough as early warning tool before noticeable problems occur (Chen et al., 2020). In a step beyond previous study, it was found the peak transition effects started fading away after T_{1M} (1 month), while the improvements can be seen since T_{2M} (2 months). This shortens the transition window to 1-month, and intensive monitoring and managing activities should and could be taken during the first month of supply water quality switching. However, regarding improvements, the water quality was increasingly improved till T_{1Y} and further to T_{2Y}, which means the re-stabilization of DWDS microbial ecology takes much longer than the problematic transition period.

The high-resolution online monitoring in distribution system illustrated that both the average and peaks were much higher at T_0 compared to all other periods (T_{1M} to T_{2Y}). Interestingly, the extra variations induced by switching were three times higher at T_0 than at T_B (e.g., particle load revealed by ΔP/V at 06:00-09:00 and 18:00-21:00, Figure 5-2). This suggests the possibility of underestimating the transition effects and underscores the importance of employing high-resolution monitoring, particularly during the peak transition period. Moreover, the exceptionally high values during peak hours may be attributed to changes in water quality (new-quality with half reducing nutrients). Such changes may result in the loss of viable cells within the biofilm (de Vries et al., 2021; Schleheck et al., 2009) and prompt nutrient-deprived microorganisms to utilize extracellular polymeric substances (EPS) as a source of carbon and energy to sustain their metabolic activity (Chen et al., 2019; Zhang and Bishop, 2003). This may disrupt the biofilm matrix, consequently enabling the same hydraulic shear force to generate a higher particle load and biomass.

5.4.2 Loose deposits contributed more than biofilm to transition effects

Both SourceTracker2 and NCM results revealed release of loose deposits and biofilm into bulk water, especially at the beginning stage of switching. The low-level contributions of loose deposits and biofilm to particle-associated bacteria in the distribution system during regular operation agree with the previous study (~ 5%) (Chen et al., 2022b). The 2.5-3 times higher contributions during the transition period (T_0 and T_{1M}) complied with the level of increased particle loads (Figure 5-2), directly confirming the origin of the increased particle load. Moreover, the release of loose deposits and biofilm accompanied by increased immigrants from loose deposits and biofilm into bulk water. This agrees with previous findings that loose deposits and biofilm in distribution system are reservoirs for bacteria and keep releasing microbes into bulk water, especially during disturbances (Flemming et al., 2002; Mackay et al., 1998; Torvinen et al., 2004; Wingender and Flemming, 2011). Besides, the sharp decrease of immigrants at T_{2Y} (from 585 at T_B to 123 at T_{2Y}, -79.0%) indicated the exchange of microbes between distribution pipes and water could be managed by improving treatments.

Comparing the contributions between loose deposits and biofilm, the SourceTracker2 results showed that loose deposits contributed much more than biofilm during the transition window (T_0: 10.3% vs. 3.3%, Figure 5-5). Similarly, the NCM results revealed that there were more immigrants from loose deposits than biofilm (T_0: 73 LD-immigrants vs. 32 BF-immigrants). This conflicts with previous agreements that most of problems are associated with biofilm,

whereas it agrees with previous findings that loose deposits is hotspot for water quality deterioration (Carrière et al., 2005; Echeverría et al., 2009; Gauthier et al., 1999; Liu et al., 2014; Zacheus et al., 2001). Lehtola et al. reported that removing loose deposits by flushing decreased microbial growth and improved water quality in the distribution system (Lehtola et al., 2004). Quantitatively, more than 70% (10.3/13.6, 73/105) release could be avoided if the distribution area is flushed before distributing new-quality water. Taking the information mentioned above, the cleaning benefits could be further enhanced if new-quality water is used to pre-flush the distribution network before distributing it to customers.

5.4.3 Practical Implication

This study observed that the transition effects occurred immediately after receiving new-quality water (T_0), lasting for a month (T_{1M}) and fading away since T_{2M}. The re-stabilization of microbial ecology and improvements of water quality took much longer to be seen (T_{1Y}, T_{2Y}). The timing and window for the occurrence of transition effects are critical for both water utility and customers, based on which proper monitoring and managing actions can be planned to make sure the safe and smooth switching of supply water quality. For example, intensive monitoring should be carried out shortly before the switching and during the first month of switching. However, there is currently no regulation or guideline for water utilities to follow. Most introductions of new treatments and switching of sources have been carried out directly without considering possible transition effects. Based on the results from the present study, it is highly recommended environmental agency (e.g., US EPA) or governmental department (e.g., China CDC), overseeing drinking water quality supervision and administration, take the lead in developing standard protocols and official documents for proper regulation. Moreover, this study highlights the absolute predominant contribution from loose deposits in the transition effects. Therefore, major risks and problems can be avoided by simply flushing the distribution system before distributing new-quality water to clean up loose deposits.

Overall, the study provides valuable insights into the occurrence and possible managing strategies of transition effects. It should be noted that the timing, duration, and level of transition effects might differ from case to case. The actual situation will be highly dependent on the differences between old and new water quality, the level of biofilm formed, and the amount of loose deposits accumulated in distribution system.

5.5 Conclusions

In this study, a longitudinal investigation into the transition effects (refer to the water quality deteriorations caused by the release of biofilm and/or loose deposits) induced by the introduction of RO in production was conducted over a substantial 2-year duration. The investigation systematically addressed the timing, duration, and sources of these transition effects. The following conclusions were drawn from this study.

- The transition effects occurred as soon as new-quality water enters distribution system at T_0, which were observed as significant increases of particle load ($\Delta P/V$, +118%), elemental concentrations (e.g., Ca, Fe, Mn), quantity of ATP (+200%), number of observed bacterial species (+57 ASVs).
- The transition effects lasted for 1 month till T_{1M}, started to fade away since T_{2M}. Notably, though the peak transition window is about 1-month time, the re-stabilization of microbial ecology and improvements of water quality takes much longer till one (T_{1Y}) and two years (T_{2Y}) later, which were attributed to the changes/improvements in treated water quality rather than contributions from biofilm and/or loose deposits.
- Both SourceTracker2 and NCM results revealed the release of loose deposits and biofilm into bulk water, particularly in the earlier stages. Specifically, the contributions of loose deposits and biofilm were 2.5-3 times higher during the transition period (T_0 and T_{1M}) than during other time periods.
- Notably, loose deposits exhibited a greater contribution to the particle-associated bacteria than biofilm throughout the entire study period, with the most pronounced distinctions in their contributions observed at T_0 and T_{1M}.

Supporting information

Table 5-S1. The number of LD- and BF-immigrants determined by neutral community model before (T_B), immediately after (T_0), after 1 month (T_{1M}), 2 months (T_{2M}), 1 year (T_{1Y}), and 2 years (T_{2Y}) of the RO introduction.

	LD-immigrants	**BF-immigrants**
T_B	391	194
T_0	464	226
T_{1M}	462	232
T_{2M}	427	185
T_{1Y}	345	101
T_{2Y}	96	27

Table 5-S2. Detailed LD- and BF-immigrants taxa information.

	ASV	Phylum	Class	Order	Family	Genus	Species
LD-Immigrants	ASV10304	Proteobacteria	Gammaproteobacteria	Betaproteobacteriales	Burkholderiaceae	Rhodoferax	
	ASV10465	Planctomycetes	Phycisphaerae	Phycisphaerales	Phycisphaeraceae	SM1A02	uncultured Planctomycetales bacterium
	ASV10521	Proteobacteria	Alphaproteobacteria	Reyranellales	Reyranellaceae	Reyranella	uncultured alpha proteobacterium
	ASV11003	Proteobacteria	Alphaproteobacteria	Acetobacterales	Acetobacteraceae	uncultured	
	ASV13994	Proteobacteria	Deltaproteobacteria	Bdellovibrionales	Bdellovibrionaceae	Bdellovibrio	uncultured bacterium
	ASV1478	Nitrospirae	Nitrospira	Nitrospirales	Nitrospiraceae	Nitrospira	
	ASV15736	Patescibacteria	Parcubacteria	Candidatus Kaiserbacteria	groundwater metagenome	groundwater metagenome	groundwater metagenome
	ASV16423	Proteobacteria	Alphaproteobacteria	Rhizobiales	A0839		
	ASV18908	Patescibacteria	Parcubacteria	Candidatus Kaiserbacteria			
	ASV19603	Proteobacteria	Alphaproteobacteria	Rhodospirillales	uncultured	uncultured soil bacterium	uncultured soil bacterium
	ASV1995	Proteobacteria	Alphaproteobacteria	Rhizobiales	Xanthobacteraceae	uncultured	
	ASV20118	Proteobacteria	Alphaproteobacteria	Acetobacterales	Acetobacteraceae	uncultured	
	ASV20665	Proteobacteria	Alphaproteobacteria	Rhizobiales	Xanthobacteraceae	Bradyrhizobium	
	ASV22622	Proteobacteria	Alphaproteobacteria	uncultured			
	ASV2274	Proteobacteria	Alphaproteobacteria	Acetobacterales	Acetobacterales Incertae Sedis	uncultured	uncultured bacterium

Table 5-S2. Continued.

	ASV	Phylum	Class	Order	Family	Genus	Species
	ASV24113	Patescibacteria	Parcubacteria	Candidatus Kaiserbacteria	uncultured bacterium	uncultured bacterium	
	ASV24454	Proteobacteria	Gammaproteobacteria	Acidiferrobacterales	Acidiferrobacteraceae	Sulfurifustis	uncultured Planctomycetales bacterium
	ASV24515	Proteobacteria	Alphaproteobacteria	Rhizobiales	KF-JG30-B3	metagenome	uncultured alpha proteobacterium
	ASV24645	Proteobacteria	Alphaproteobacteria	Micavibrionales	uncultured		
	ASV25321	Proteobacteria	Deltaproteobacteria				uncultured bacterium
	ASV25361	Proteobacteria	Gammaproteobacteria	PLTA13			
	ASV2631	Patescibacteria	Parcubacteria	Candidatus Kaiserbacteria	uncultured bacterium	uncultured bacterium	groundwater metagenome
	ASV26454	Proteobacteria	Alphaproteobacteria	Rhizobiales	Rhizobiales Incertae Sedis	uncultured	
	ASV26482	Proteobacteria	Gammaproteobacteria	Betaproteobacteriales	Burkholderiaceae		
	ASV26926	Proteobacteria	Gammaproteobacteria	Betaproteobacteriales	TRA3-20		uncultured soil bacterium
	ASV27189	Chloroflexi	Anaerolineae	Caldilineales	Caldilineaceae	uncultured	
	ASV27552	Dadabacteria	Dadabacteriia	Dadabacteriales	uncultured candidate division SBR1093 bacterium	uncultured candidate division SBR1093 bacterium	
	ASV28246	Proteobacteria	Deltaproteobacteria				
	ASV29480	Patescibacteria	Parcubacteria	Candidatus Adlerbacteria	metagenome	metagenome	

Table 5-S2. Continued.

ASV	Phylum	Class	Order	Family	Genus	Species
ASV30873	Cyanobacteria	Melainabacteria	Obscuribacterales	uncultured bacterium	uncultured bacterium	uncultured bacterium
ASV3659	Patescibacteria	Parcubacteria	Candidatus Adlerbacteria			
ASV4111	Patescibacteria	Parcubacteria	Candidatus Kaiserbacteria	Ambiguous_taxa	Ambiguous_taxa	Ambiguous_taxa
ASV4239	Patescibacteria	Parcubacteria	Candidatus Nomurabacteria	uncultured bacterium	uncultured bacterium	uncultured bacterium
ASV4279	Omnitrophicaeota	uncultured beta proteobacterium	uncultured beta proteobacterium	uncultured beta proteobacterium	uncultured beta proteobacterium	uncultured beta proteobacterium
ASV5704	Proteobacteria	Gammaproteobacteria	Betaproteobacteriales	Burkholderiaceae	Polaromonas	Ambiguous_taxa
ASV6514	Proteobacteria	Alphaproteobacteria	Rhizobiales	Xanthobacteraceae	uncultured	
ASV6801	Proteobacteria	Gammaproteobacteria	Betaproteobacteriales	TRA3-20	Ambiguous_taxa	Ambiguous_taxa
ASV7595	Patescibacteria	Parcubacteria	Candidatus Kaiserbacteria	uncultured bacterium	uncultured bacterium	uncultured bacterium
ASV8104	Proteobacteria	Gammaproteobacteria	Betaproteobacteriales	TRA3-20		
ASV8855	Proteobacteria	Alphaproteobacteria	Reyranellales	Reyranellaceae	Reyranella	
ASV9921	Actinobacteria	Actinobacteria	Corynebacteriales	Nocardiaceae	Rhodococcus	

Table 5-S2. Continued.

	ASV	Phylum	Class	Order	Family	Genus	Species
BF-Immigrants	ASV10304	Proteobacteria	Gammaproteobacteria	Betaproteobacteriales	Burkholderiaceae	Rhodoferax	
	ASV12484	Proteobacteria	Alphaproteobacteria	Micavibrionales	uncultured	metagenome	metagenome
	ASV1478	Nitrospirae	Nitrospira	Nitrospirales	Nitrospiraceae	Nitrospira	
	ASV15369	Patescibacteria	Parcubacteria	Candidatus Kaiserbacteria			
	ASV15736	Patescibacteria	Parcubacteria	Candidatus Kaiserbacteria	groundwater metagenome	groundwater metagenome	groundwater metagenome
	ASV16423	Proteobacteria	Alphaproteobacteria	Rhizobiales	A0839		
	ASV16933	Patescibacteria	Parcubacteria				
	ASV20095	Proteobacteria	Alphaproteobacteria	Rhizobiales	Rhizobiales Incertae Sedis	Bauldia	
	ASV20118	Proteobacteria	Alphaproteobacteria	Acetobacterales	Acetobacteraceae	uncultured	
	ASV20456	Omnitrophicaeota	uncultured bacterium	uncultured bacterium	uncultured bacterium	uncultured bacterium	uncultured bacterium
	ASV21585	Proteobacteria	Alphaproteobacteria	Rhizobiales	Xanthobacteraceae	uncultured	
	ASV21851	Proteobacteria	Alphaproteobacteria	Micavibrionales	uncultured	Ambiguous_taxa	Ambiguous_taxa
	ASV22797	Patescibacteria	Parcubacteria	Candidatus Kaiserbacteria			
	ASV24211	Omnitrophicaeota	uncultured bacterium	uncultured bacterium	uncultured bacterium	uncultured bacterium	uncultured bacterium
	ASV26454	Proteobacteria	Alphaproteobacteria	Rhizobiales	Rhizobiales Incertae Sedis	uncultured	Ambiguous_taxa

Table 5-S2. Continued.

	ASV	Phylum	Class	Order	Family	Genus	Species
	ASV27552	Dadabacteria	Dadabacteriia	Dadabacteriales	uncultured candidate division SBR1093 bacterium	uncultured candidate division SBR1093 bacterium	uncultured candidate division SBR1093 bacterium
	ASV28246	Proteobacteria	Deltaproteobacteria				
	ASV28721	Proteobacteria	Alphaproteobacteria	uncultured			
	ASV28919	Nitrospirae	Nitrospira	Nitrospirales	Nitrospiraceae	Nitrospira	
	ASV4385	Proteobacteria	Alphaproteobacteria	Rhizobiales	Xanthobacteraceae	Rhodoplanes	
	ASV5615	Proteobacteria	Deltaproteobacteria	Bdellovibrionales	Bdellovibrionaceae	Bdellovibrio	
	ASV654	Proteobacteria	Deltaproteobacteria	Sva0485	uncultured delta proteobacterium	uncultured delta proteobacterium	uncultured delta proteobacterium
	ASV8104	Proteobacteria	Gammaproteobacteria	Betaproteobacteriales	TRA3-20		
	ASV14511	Patescibacteria	Parcubacteria	Candidatus Kaiserbacteria	Parcubacteria bacterium OLB19	Parcubacteria bacterium OLB19	Parcubacteria bacterium OLB19

Table 5-S3. The correlations between the relative abundance in specific LD- and BF-Immigrants affiliated to particle-associated bacteria (PAB) and LD- and BF-contributions to PAB in distribution network (DN) at T_0. T_0: immediately after the RO introduction.

	ASV number	**r (Pearson's)**	**p**
LD-Immigrants vs LD-contribution	ASV20665	0.48	0.06
	ASV6801	0.05	0.84
	ASV20118	0.32	0.22
	ASV28246	0.0005	1.00
	ASV8104	0.53	0.04
	ASV26454	-0.22	0.42
	ASV11003	0.15	0.58
	ASV4111	0.47	0.07
BF-Immigrants vs BF-contribution	ASV8104	0.26	0.34
	ASV28919	0.29	0.28
	ASV28246	0.60	0.01
	ASV26454	0.22	0.41
	ASV21851	-0.21	0.43
	ASV20118	-0.17	0.54
	ASV20095	0.12	0.67
	ASV16933	0.03	0.91
	ASV16423	0.01	0.97
	ASV14511	-0.16	0.56
	ASV12484	0.01	0.98

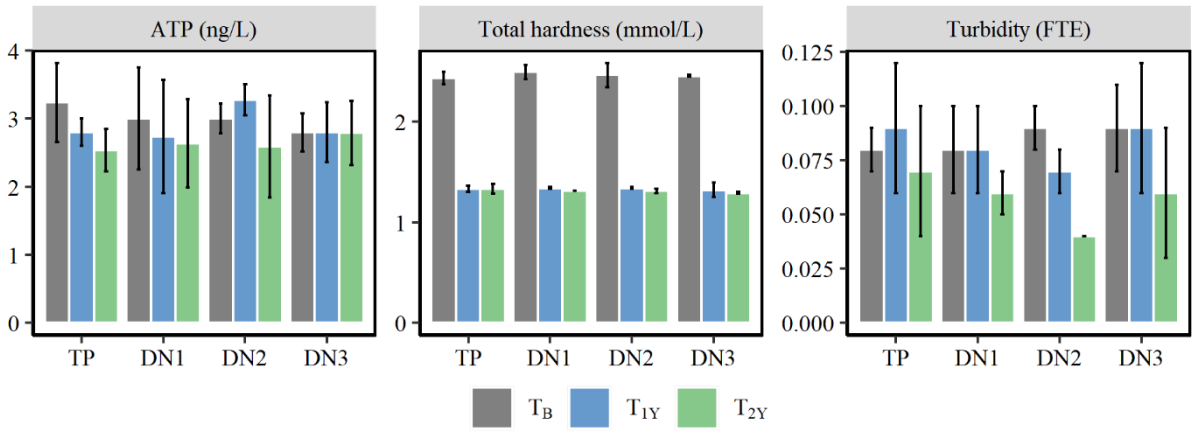

Figure 5-S1. ATP concentration, total hardness, and turbidity in bulk water before (T_B), after 1 year (T_{1Y}), and 2 years (T_{2Y}) of the RO introduction at treatment plant (TP) and in distribution network (DN). DN1, DN2 and DN3 stand for locations in distribution network which are 1, 4.5, and 6 km to TP. Data are presented as mean ± s.d. (n = 3).

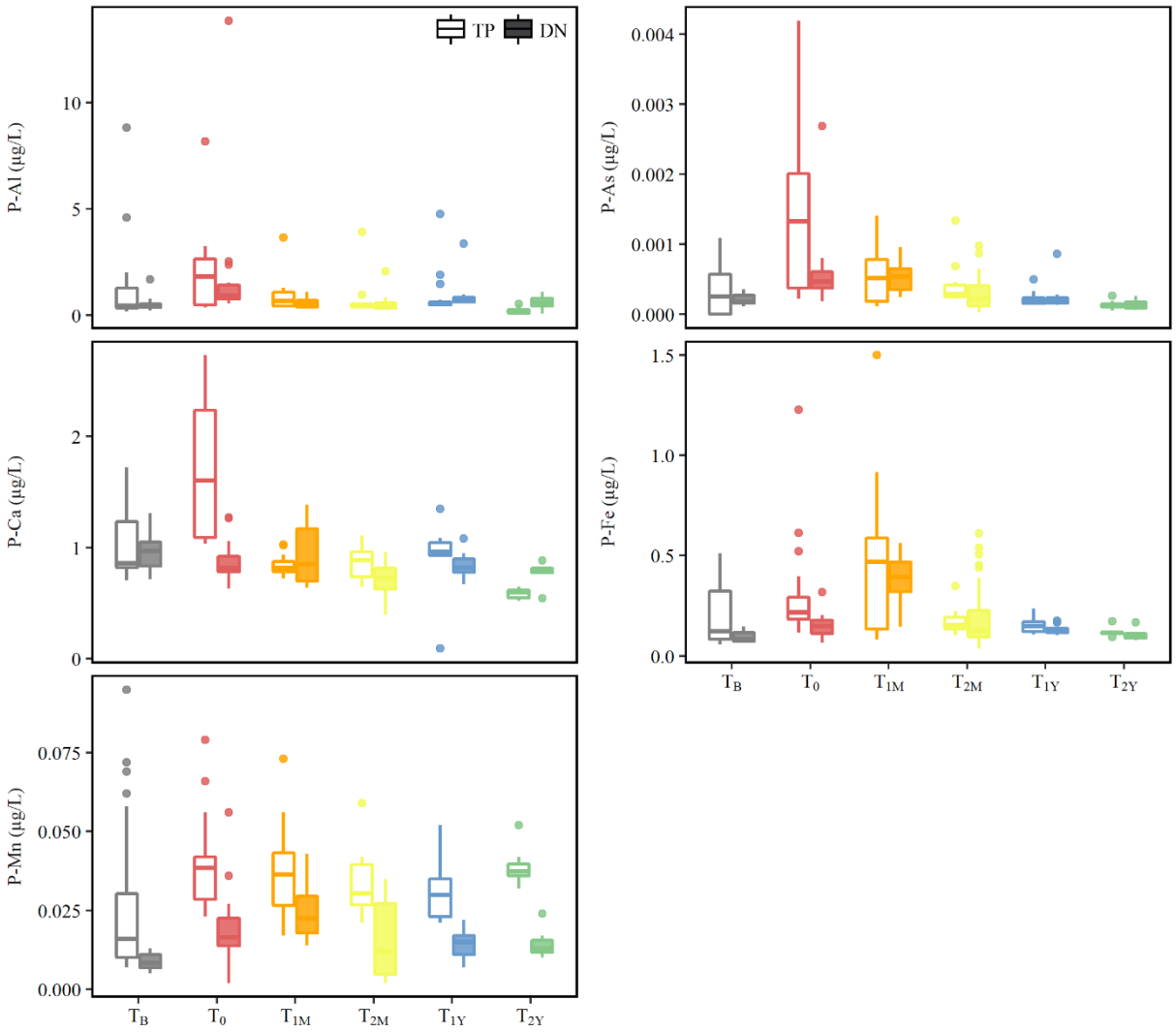

Figure 5-S2. Spatial and temporal variations in particle-associated elements (i.e., P-Al, P-As, P-Ca, P-Fe, P-Mn) at treatment plant (TP) and in distribution network (DN) before (T_B), immediately after (T_0), after 1 month (T_{1M}), 2 months (T_{2M}), 1 year (T_{1Y}), and 2 years (T_{2Y}) of the RO introduction. Box plots show median values (middle line), 25th and 75th percentiles (boxes) and 5th and 95th percentiles (whiskers). Outliers, if present, are shown as individual points beyond the whiskers.

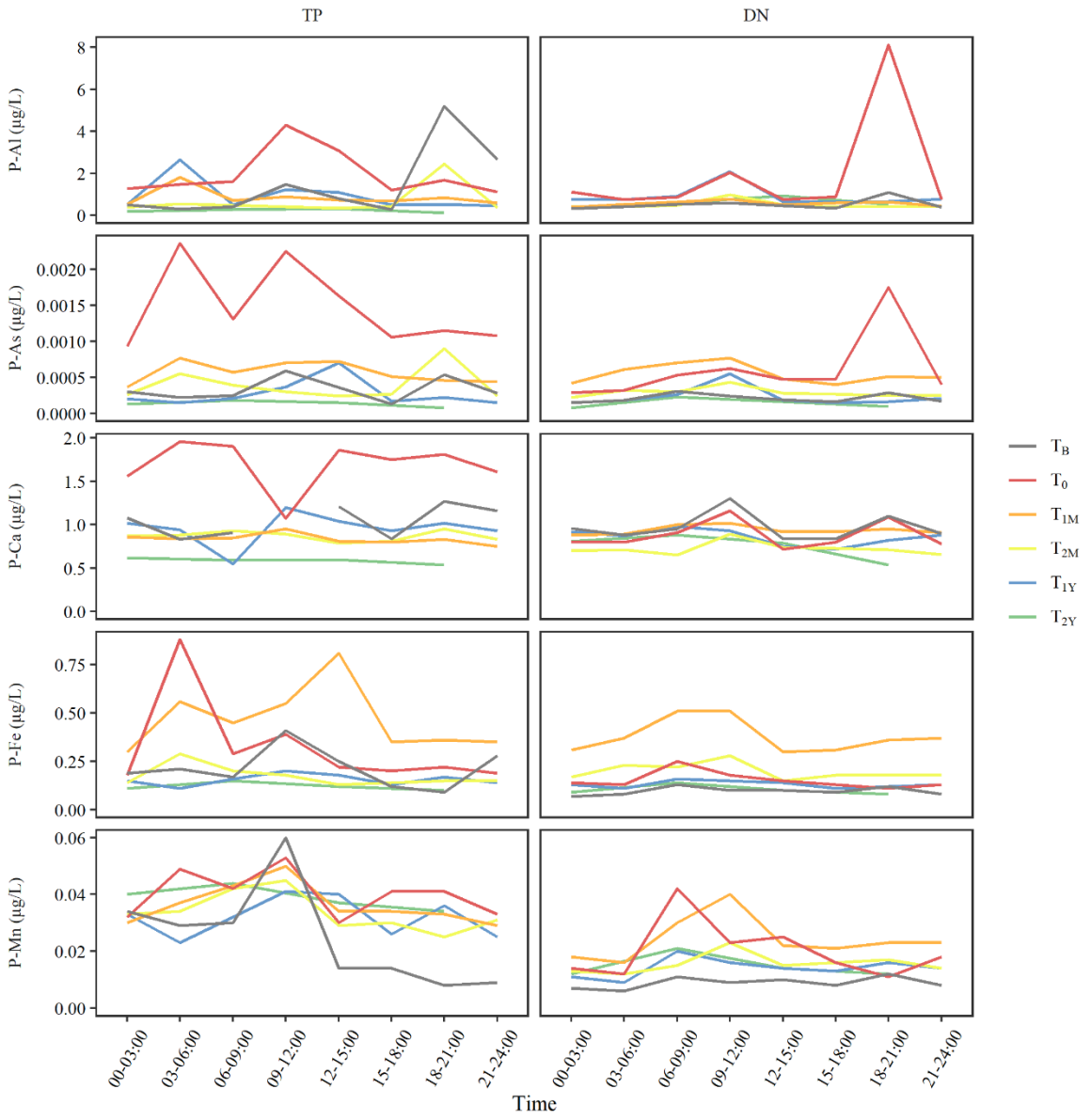

Figure 5-S3. Daily variations in particle-associated elements (i.e., P-Al, P-As, P-Ca, P-Fe, P-Mn) at treatment plant (TP) and in distribution network (DN). T_B: before the RO introduction; T_0: immediately after the RO introduction; T_{1M}: 1 month after the RO introduction; T_{2M}: 2 months after the RO introduction; T_{1Y}: 1 year after the RO introduction; T_{2Y}: 2 years after the RO introduction.

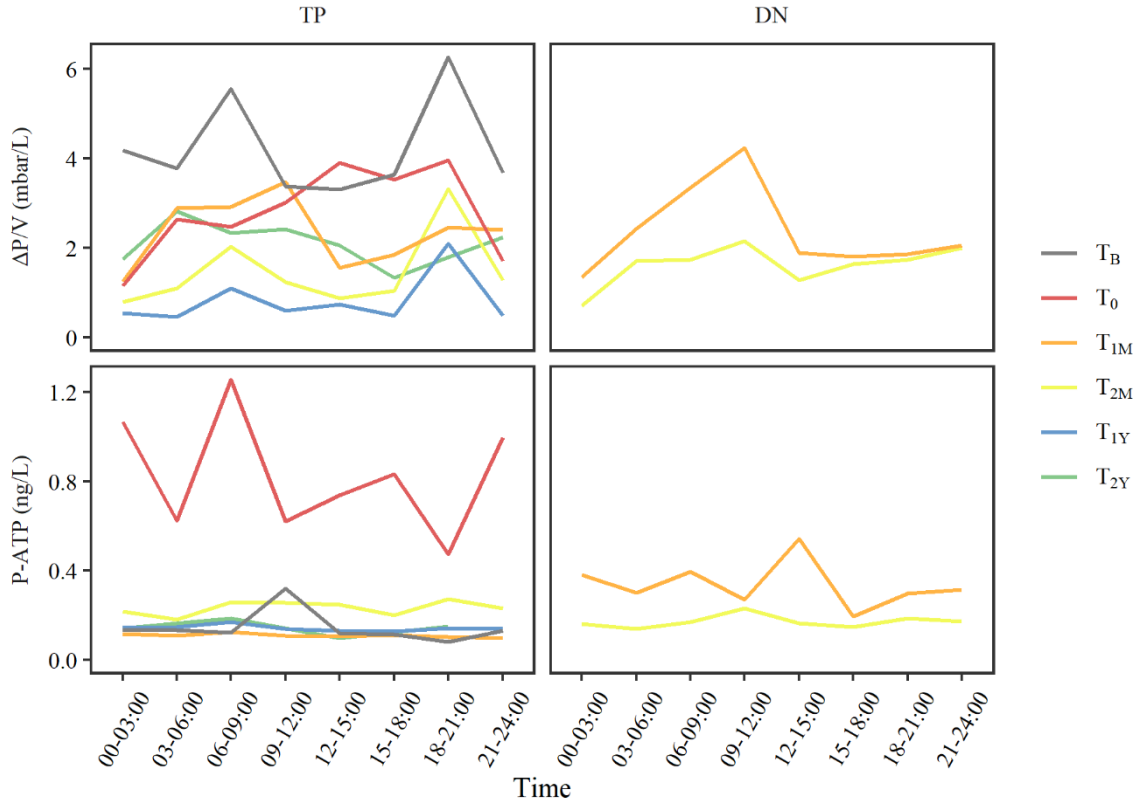

Figure 5-S4. Daily variations in particle loads (ΔP/V) and particle-associated ATP (P-ATP) at treatment plant (TP) and in distribution network (DN). The data of ΔP/V and P-ATP at T_B, T_0, T_{1Y}, and T_{2Y} were presented in Figure 5-2. T_B: before the RO introduction; T_0: immediately after the RO introduction; T_{1M}: 1 month after the RO introduction; T_{2M}: 2 months after the RO introduction; T_{1Y}: 1 year after the RO introduction; T_{2Y}: 2 years after the RO introduction.

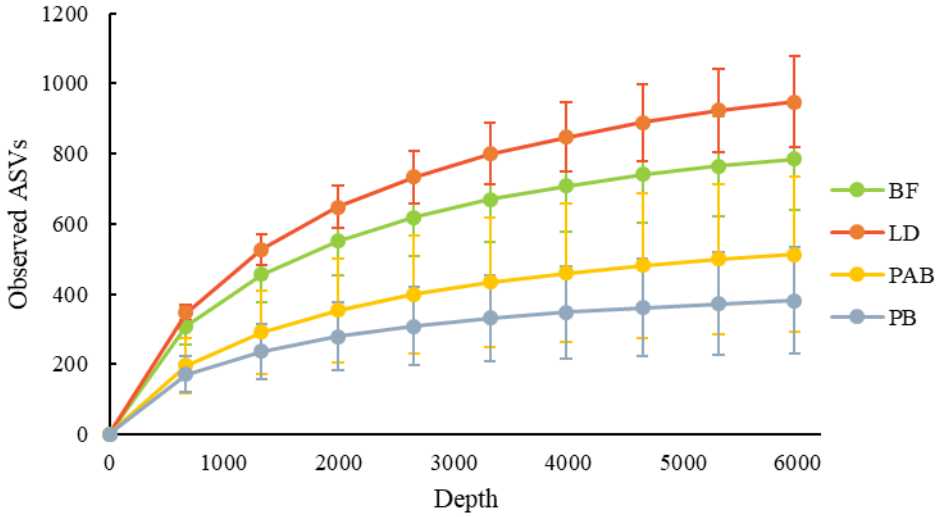

Figure 5-S5. Rarefication curves across all samples grouped by different phases. BF stands for biofilm, LD stands for loose deposits, PAB stands for particle-associated bacteria, and PB stands for planktonic bacteria.

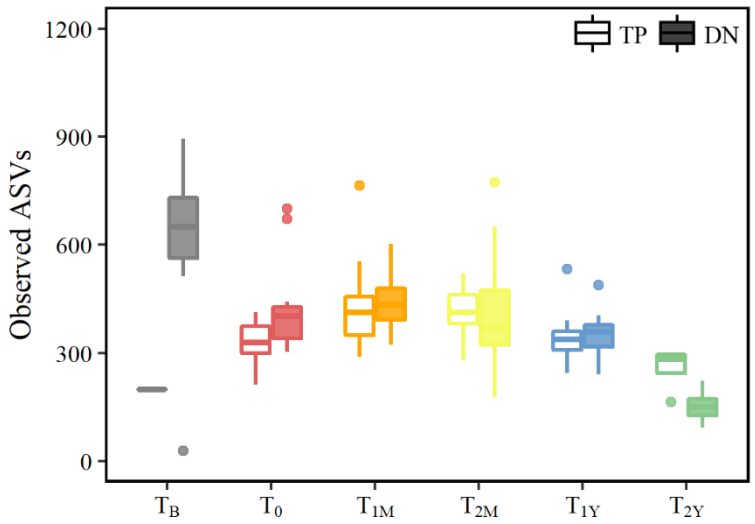

Figure 5-S6. The long-term changes in alpha diversity in planktonic bacterial (PB) communities at treatment plant (TP) and in distribution network (DN). T_B: before the RO introduction; T_0: immediately after the RO introduction; T_{1M}: 1 month after the RO introduction; T_{2M}: 2 months after the RO introduction; T_{1Y}: 1 year after the RO introduction; T_{2Y}: 2 years after the RO introduction. Box plots show median values (middle line), 25^{th} and 75^{th} percentiles (boxes) and 5^{th} and 95^{th} percentiles (whiskers). Outliers, if present, are shown as individual points beyond the whiskers.

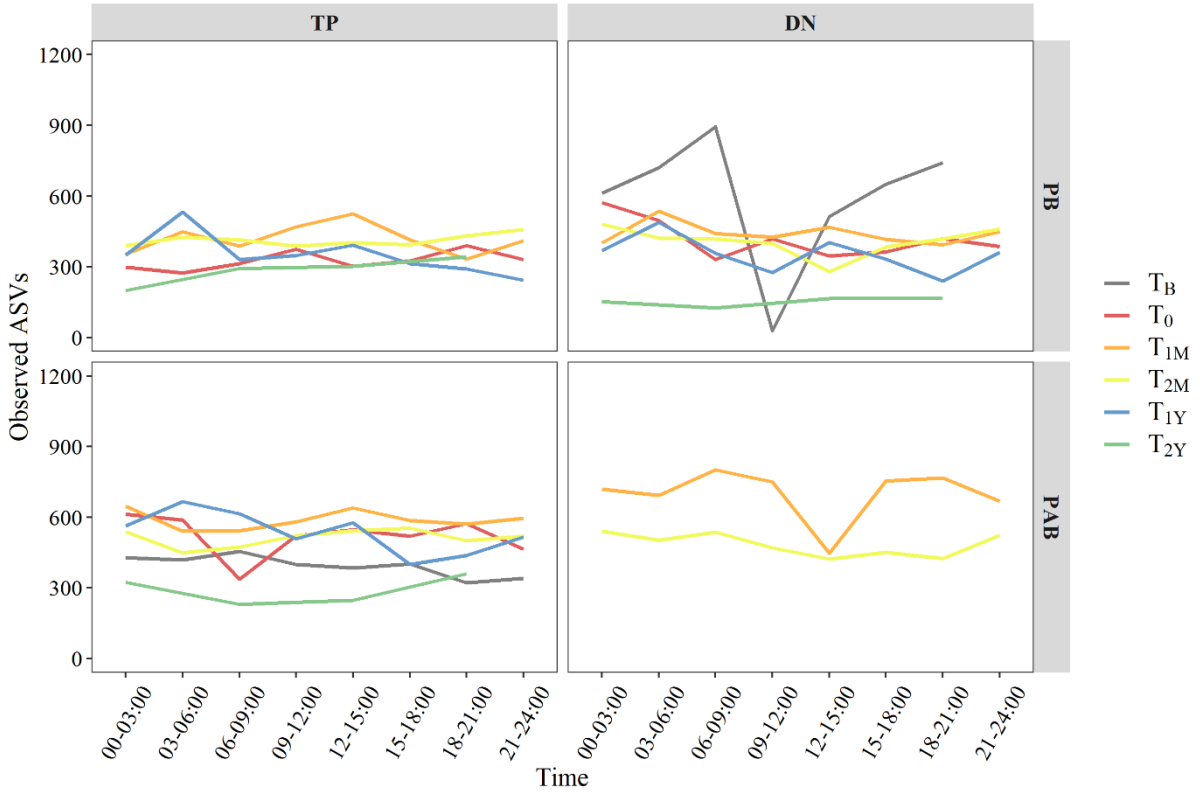

Figure 5-S7. Daily variations in alpha diversity (i.e., the number of observed ASVs) in planktonic bacteria (PB) and particle-associated bacteria (PAB) at treatment plant (TP) and in distribution network (DN). T_B: before the RO introduction; T_0: immediately after the RO introduction; T_{1M}: 1 month after the RO introduction; T_{2M}: 2 months after the RO introduction; T_{1Y}: 1 year after the RO introduction; T_{2Y}: 2 years after the RO introduction.

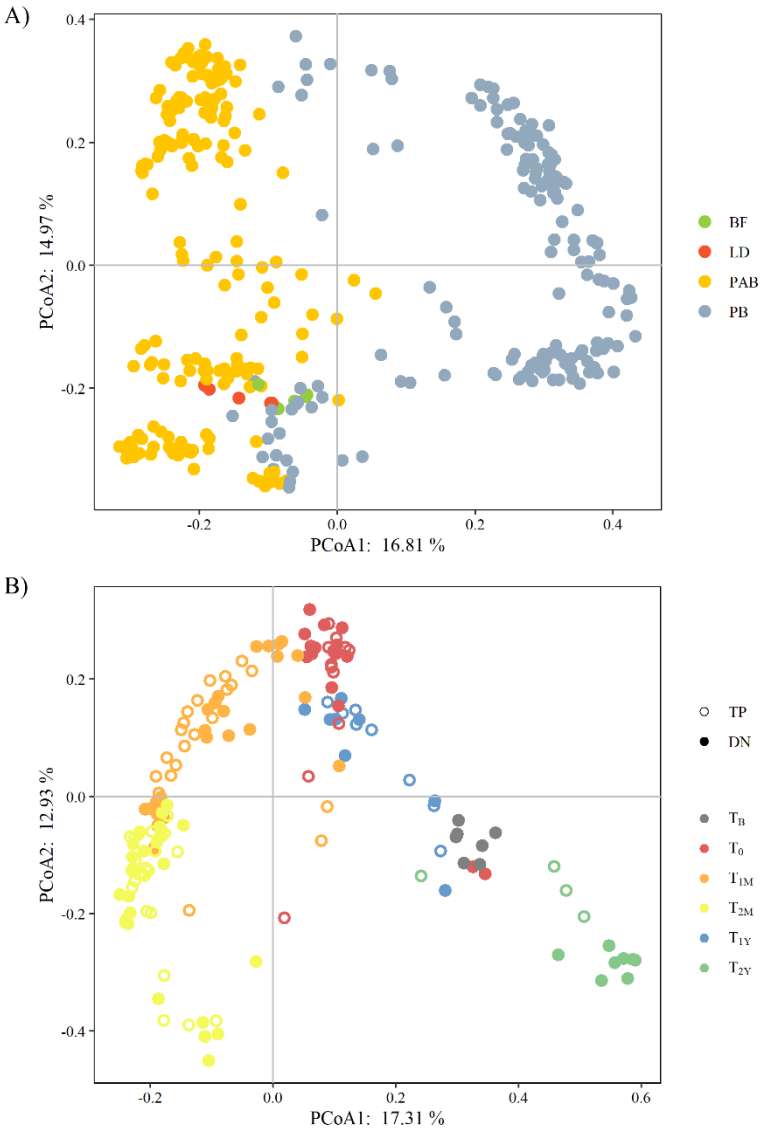

Figure 5-S8. A) PCoA plot based on Bray-Curtis distances across all samples at treatment plant (TP) and in distribution network (DN) coloured by different phases; B) PCoA plot based on Bray-Curtis distances within planktonic bacteria (PB) at TP and DN over time. T_B: before the RO introduction; T_0: immediately after the RO introduction; T_{1M}: 1 month after the RO introduction; T_{2M}: 2 months after the RO introduction; T_{1Y}: 1 year after the RO introduction; T_{2Y}: 2 years after the RO introduction.

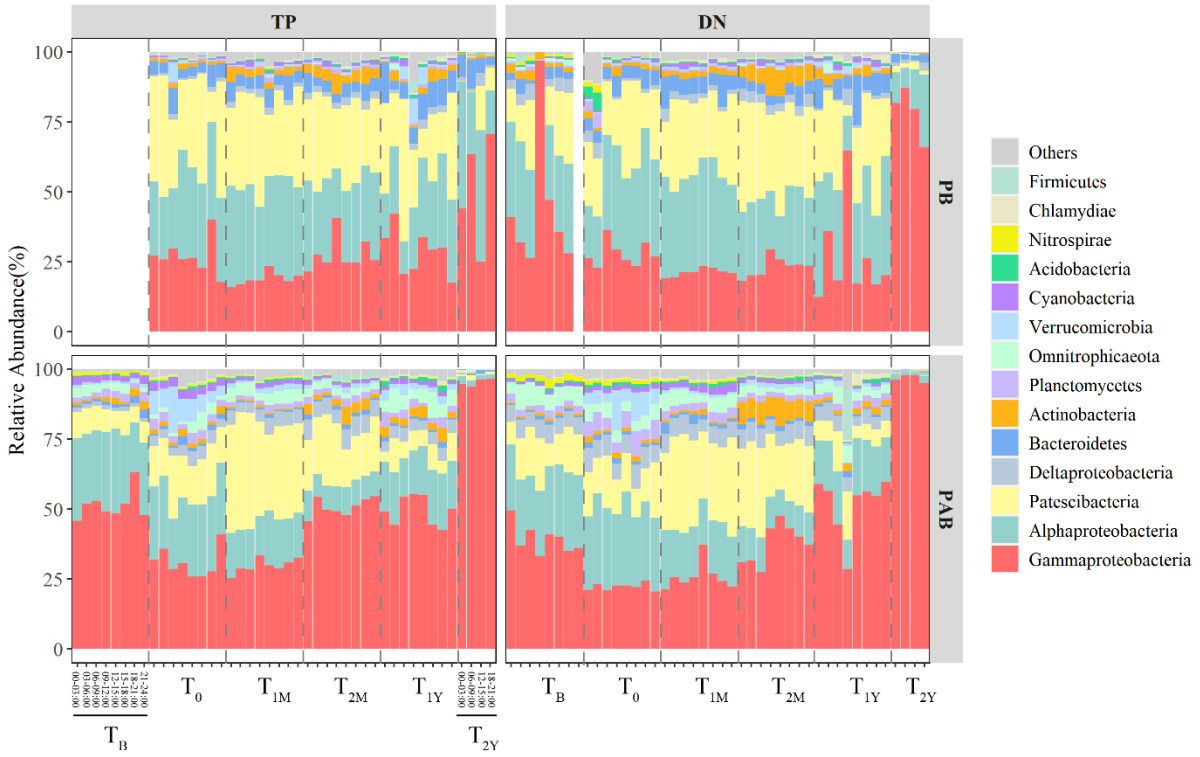

Figure 5-S9. The variations in community composition within planktonic bacteria (PB) and particle-associated bacteria (PAB) at treatment plant (TP) and in distribution network (DN) at phylum level over time. T_B: before the RO introduction; T_0: immediately after the RO introduction; T_{1M}: 1 month after the RO introduction; T_{2M}: 2 months after the RO introduction; T_{1Y}: 1 year after the RO introduction; T_{2Y}: 2 years after the RO introduction.

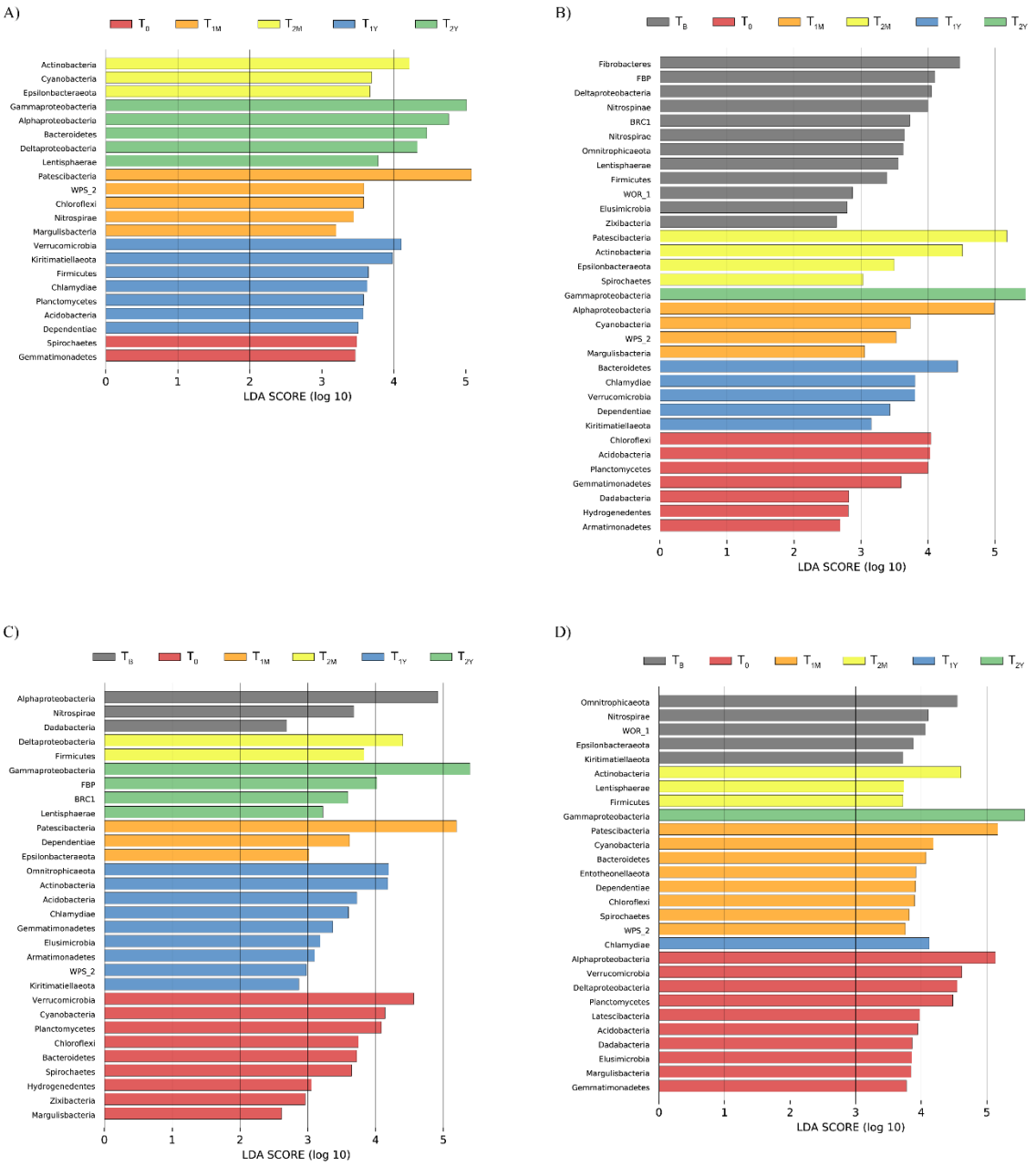

Figure 5-S10. Significantly enriched taxa at phylum level among different time periods within planktonic bacteria (PB) and particle-associated bacteria (PAB) at TP (A, C) and DN (B, D) based on Lefse LDA analysis. T_B: before the RO introduction; T_0: immediately after the RO introduction; T_{1M}: 1 month after the RO introduction; T_{2M}: 2 months after the RO introduction; T_{1Y}: 1 year after the RO introduction; T_{2Y}: 2 years after the RO introduction. TP stands for treatment plant, while DN stands for distribution network.

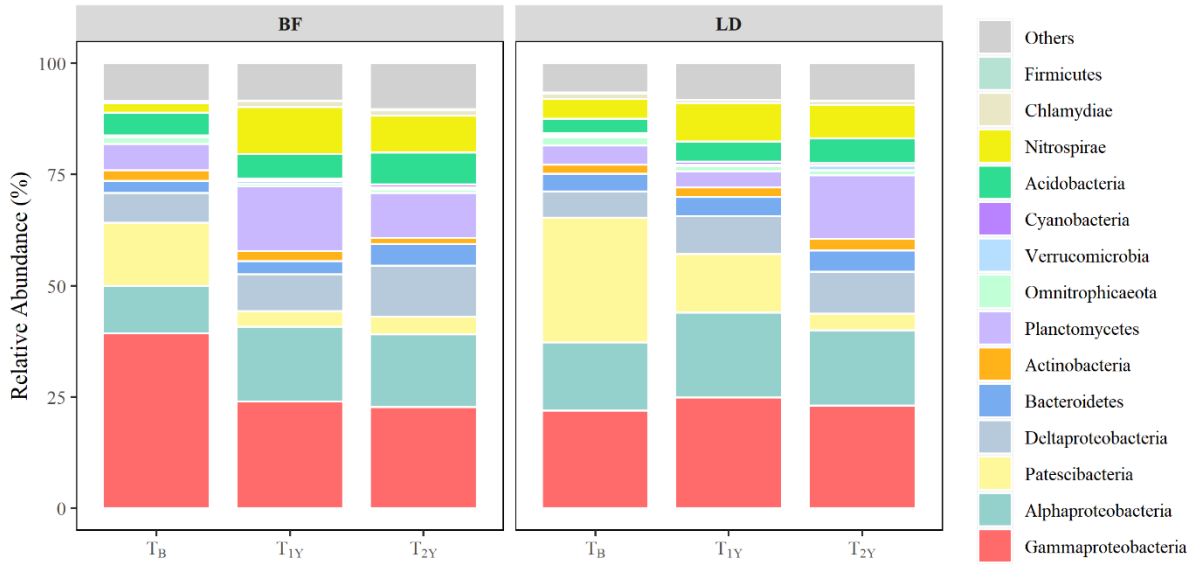

Figure 5-S11. The variations in taxonomy composition at phylum level in distribution network (DN) within biofilm (BF) and loose deposits (LD) over time. T_B: before the RO introduction; T_{1Y}: 1 year after the RO introduction; T_{2Y}: 2 years after the RO introduction.

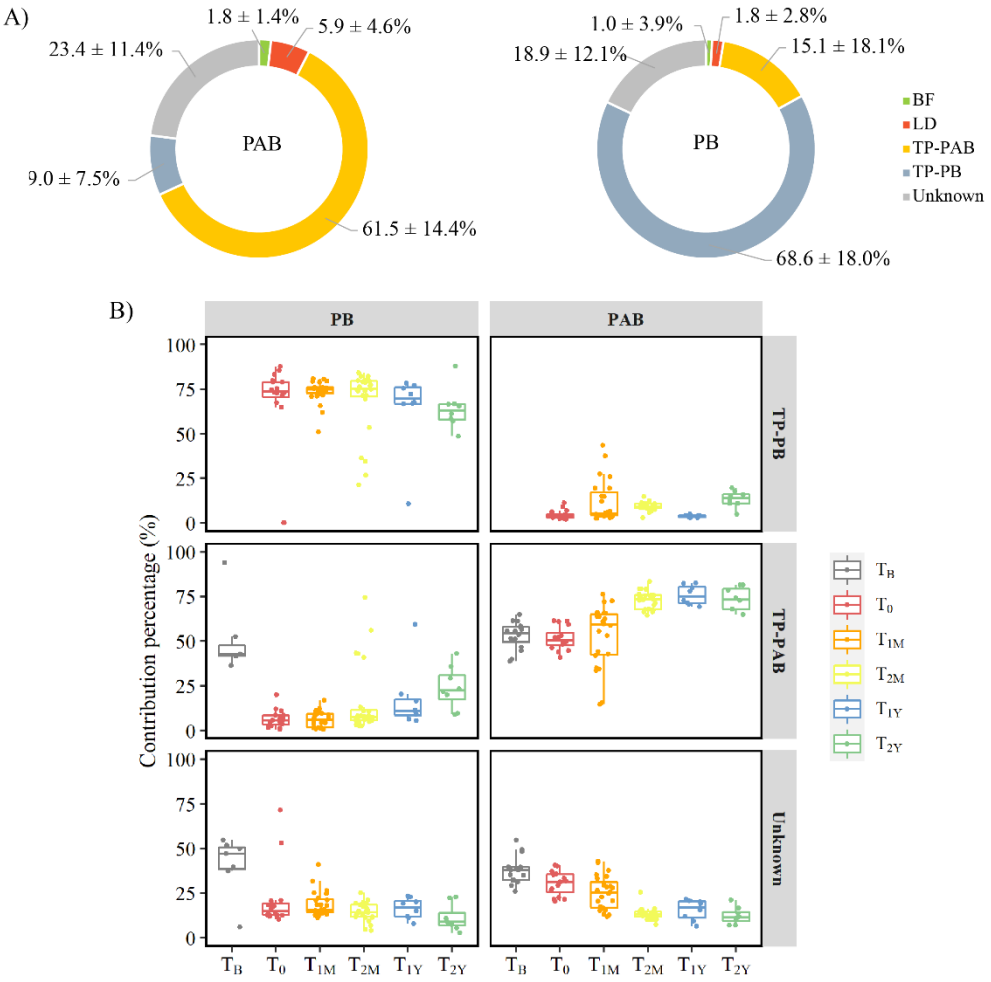

Figure 5-S12. A) The percentage of contributions from all the sources (BF, LD, TP-PAB, TP-PB, Unknown) to particle-associated bacteria (PAB) and planktonic bacteria (PB) in distribution network (DN); B) The percentage of contributions from PB and PAB from treatment plant to PB and PAB at DN over time. BF and LD stand for biofilm and loose deposits. TP-PB stands for planktonic bacteria from treatment plant, while TP-PAB stands for particle-associated bacteria from treatment plant. T_B: before the RO introduction; T_0: immediately after the RO introduction; T_{1M}: 1 month after the RO introduction; T_{2M}: 2 months after the RO introduction; T_{1Y}: 1 year after the RO introduction; T_{2Y}: 2 years after the RO introduction. TP stands for treatment plant, while DN stands for distribution network. Box plots show median values (middle line), 25th and 75th percentiles (boxes) and 5th and 95th percentiles (whiskers). Outliers, if present, are shown as individual points beyond the whiskers.

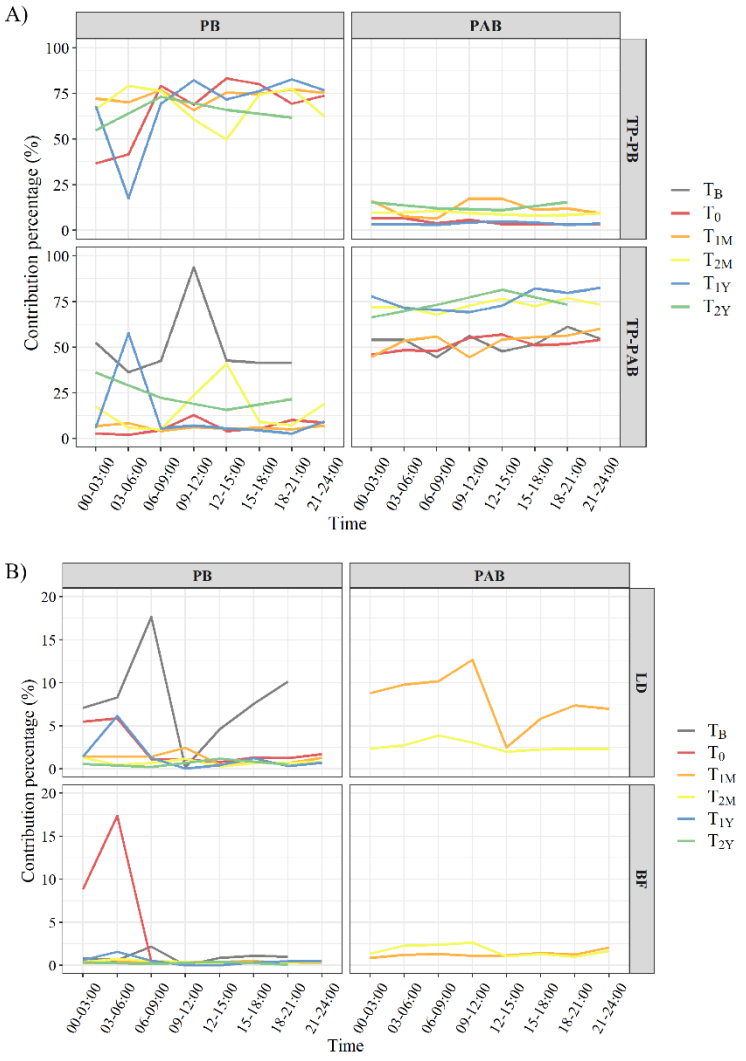

Figure 5-S13. A) Daily variations in the percentage of contributions from TP-PB and TP-PAB to PB and PAB in distribution network (DN); B) Daily variations in the percentage of contributions from loose deposits (LD) and biofilm (BF) to PB and PAB at DN. TP-PB stands for planktonic bacteria from treatment plant, while TP-PAB stands for particle-associated bacteria from treatment plant.

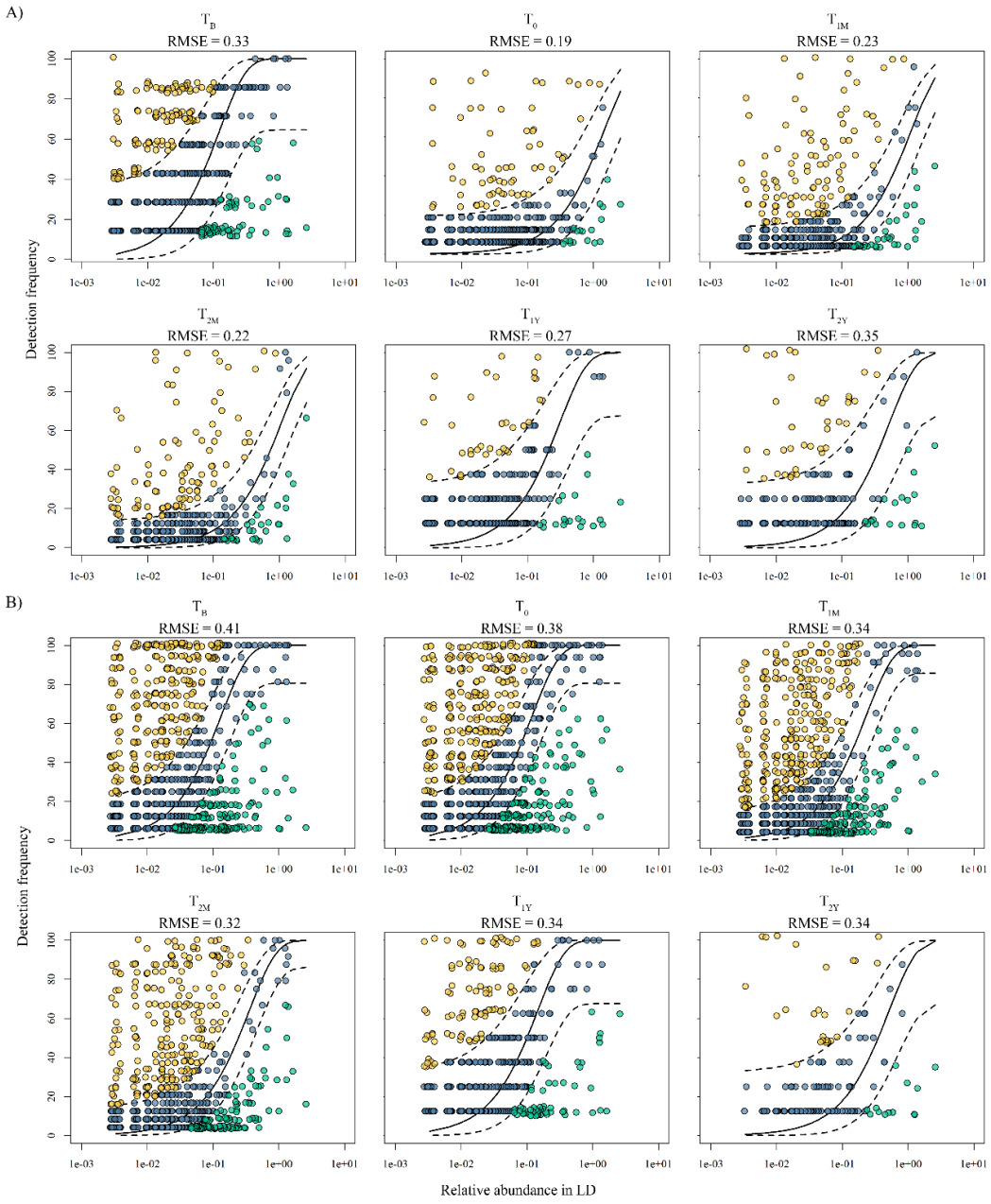

Figure 5-S14. Neutral processes explain microbial community assembly across time. Scatterplot of the prevalence of each ASV in PB (A) and PAB (B) in distribution network (DN) versus its mean relative abundance in loose deposits (LD) for each time period. The gray line is their predicted distribution (shaded area is 95% confidence interval) based on the neutral community model. Points are colored by the ASV's fit to the model: above prediction – yellow, as prediction – blue, below prediction – green. Average RMSE was calculated from 1000 bootstrap resamplings.

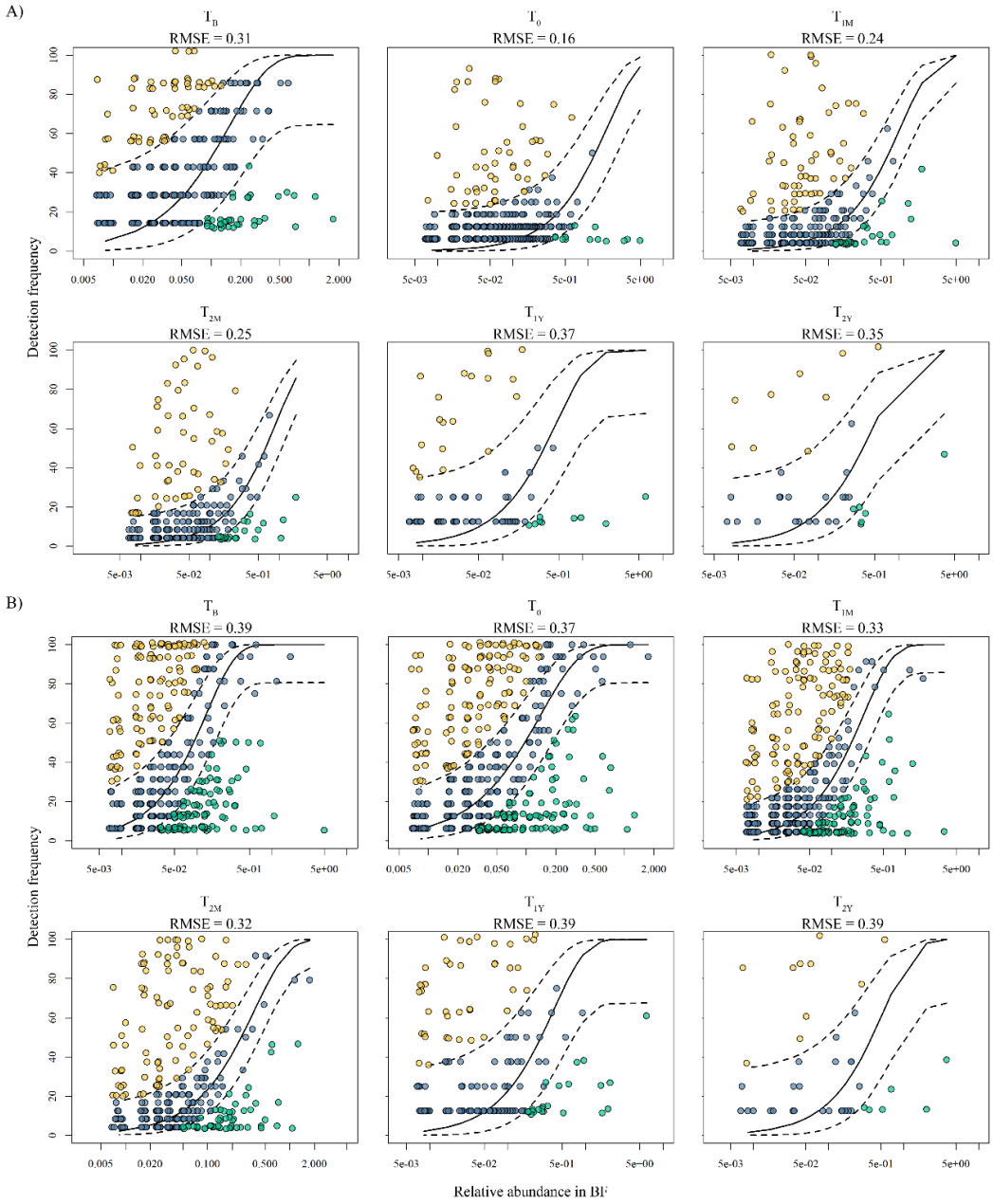

Figure 5-S15. Neutral processes explain microbial community assembly across time. Scatterplot of the prevalence of each ASV in PB (A) and PAB (B) in distribution network (DN) versus its mean relative abundance in biofilm (BF) for each time period. The gray line is their predicted distribution (shaded area is 95% confidence interval) based on the neutral community model. Points are colored by the ASV's fit to the model: above prediction – yellow, as prediction – blue, below prediction – green. Average RMSE was calculated from 1000 bootstrap resamplings.

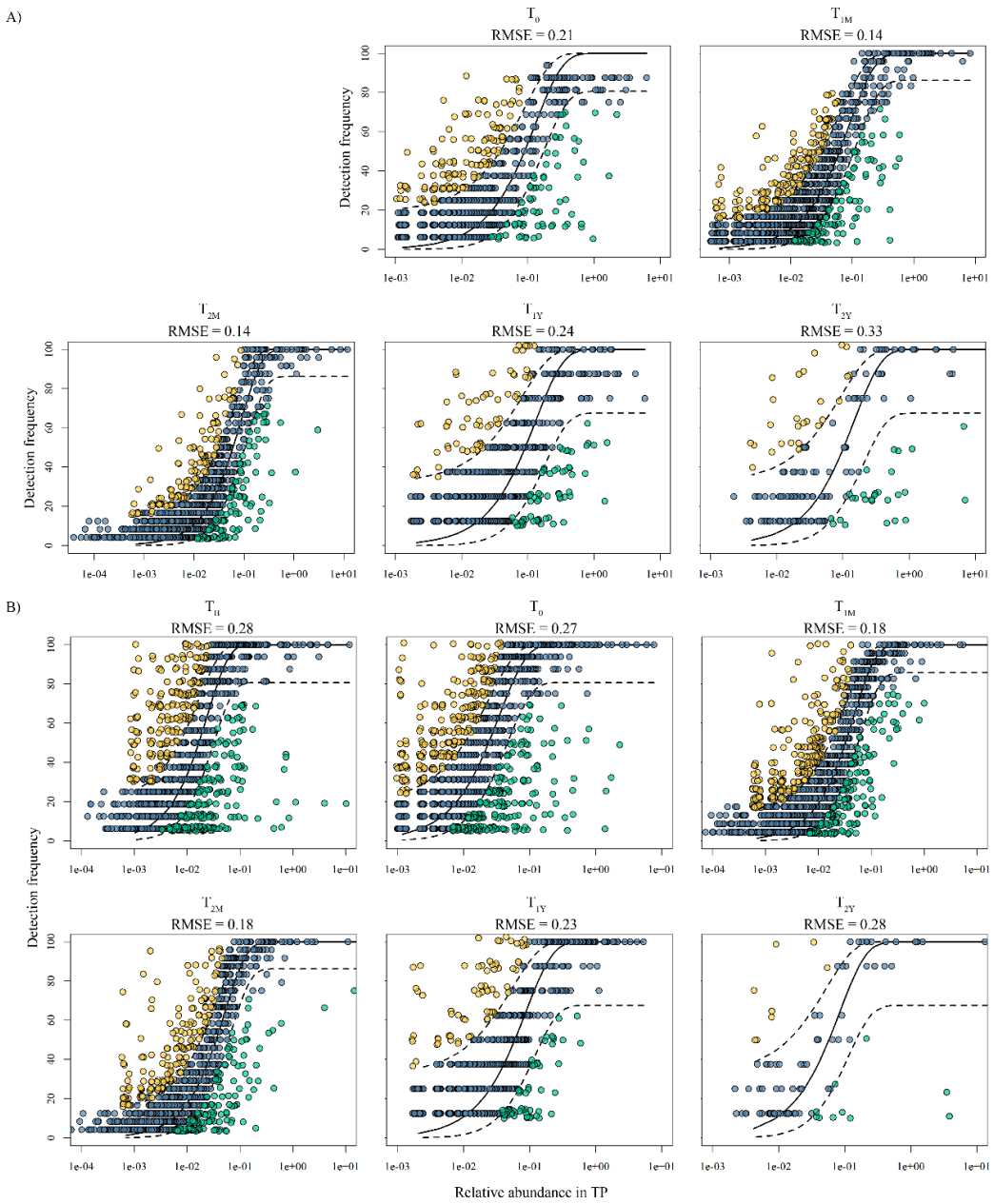

Figure 5-S16. Neutral processes explain microbial community assembly across time. Scatterplot of the prevalence of each ASV in PB (A) and PAB (B) in distribution network (DN) versus its mean relative abundance in PB and PAB at treatment plant (TP) for each time period. The gray line is their predicted distribution (shaded area is 95% confidence interval) based on the neutral community model. Points are colored by the ASV's fit to the model: above prediction – yellow, as prediction – blue, below prediction – green. Average RMSE was calculated from 1000 bootstrap resamplings.

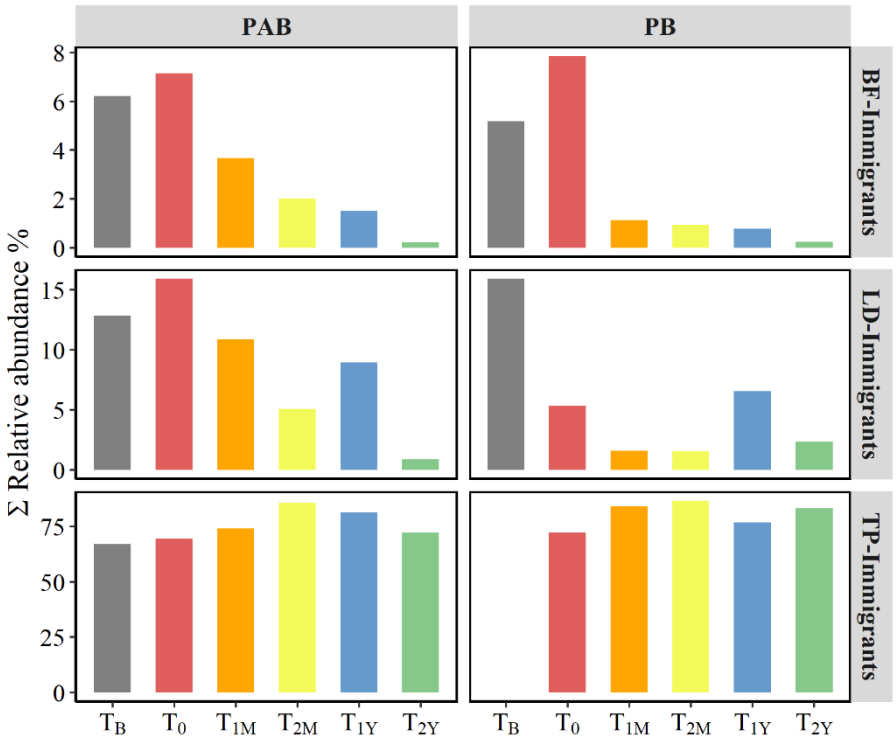

Figure 5-S17. The cumulative relative abundance in immigrants affiliated to particle-associated bacteria (PAB) and planktonic bacteria (PB) from biofilm (BF), loose deposits (LD) and treatment plant (TP) to PAB and PB in distribution network (DN). T_B: before the RO introduction; T_0: immediately after the RO introduction; T_{1M}: 1 month after the RO introduction; T_{2M}: 2 months after the RO introduction; T_{1Y}: 1 year after the RO introduction; T_{2Y}: 2 years after the RO introduction. TP stands for treatment plant, while DN stands for distribution network.

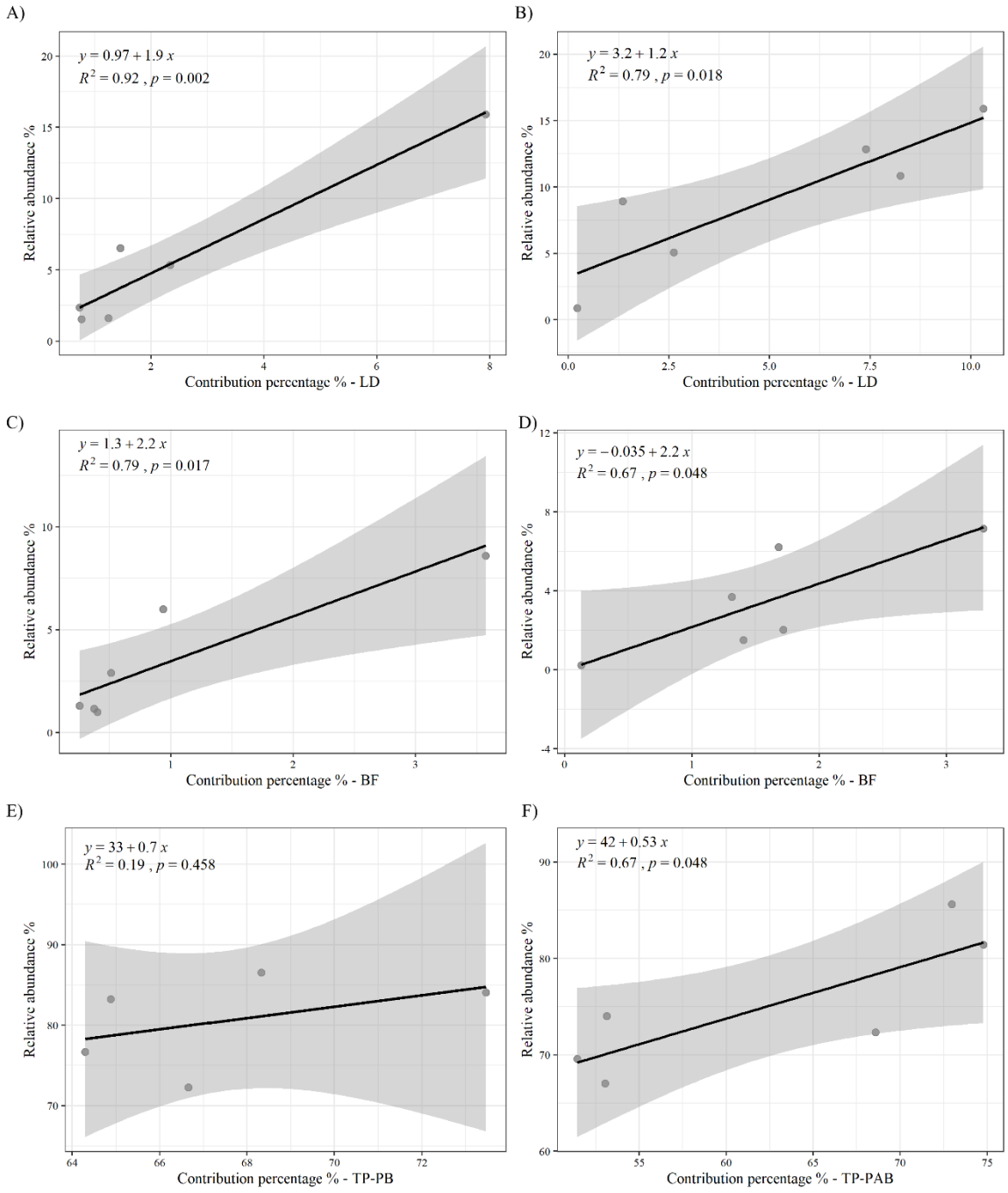

Figure 5-S18. The correlations between contribution percentage from different sources (TP-PB, TP-PAB, LD, BF) and the cumulative relative abundances in PB (A, C, E) and PAB (B, D, F) predicted using neutral community model. TP-PB stands for planktonic bacteria from treatment plant, while TP-PAB stands for particle-associated bacteria from treatment plant. LD and BF stand for loose deposits and biofilm.

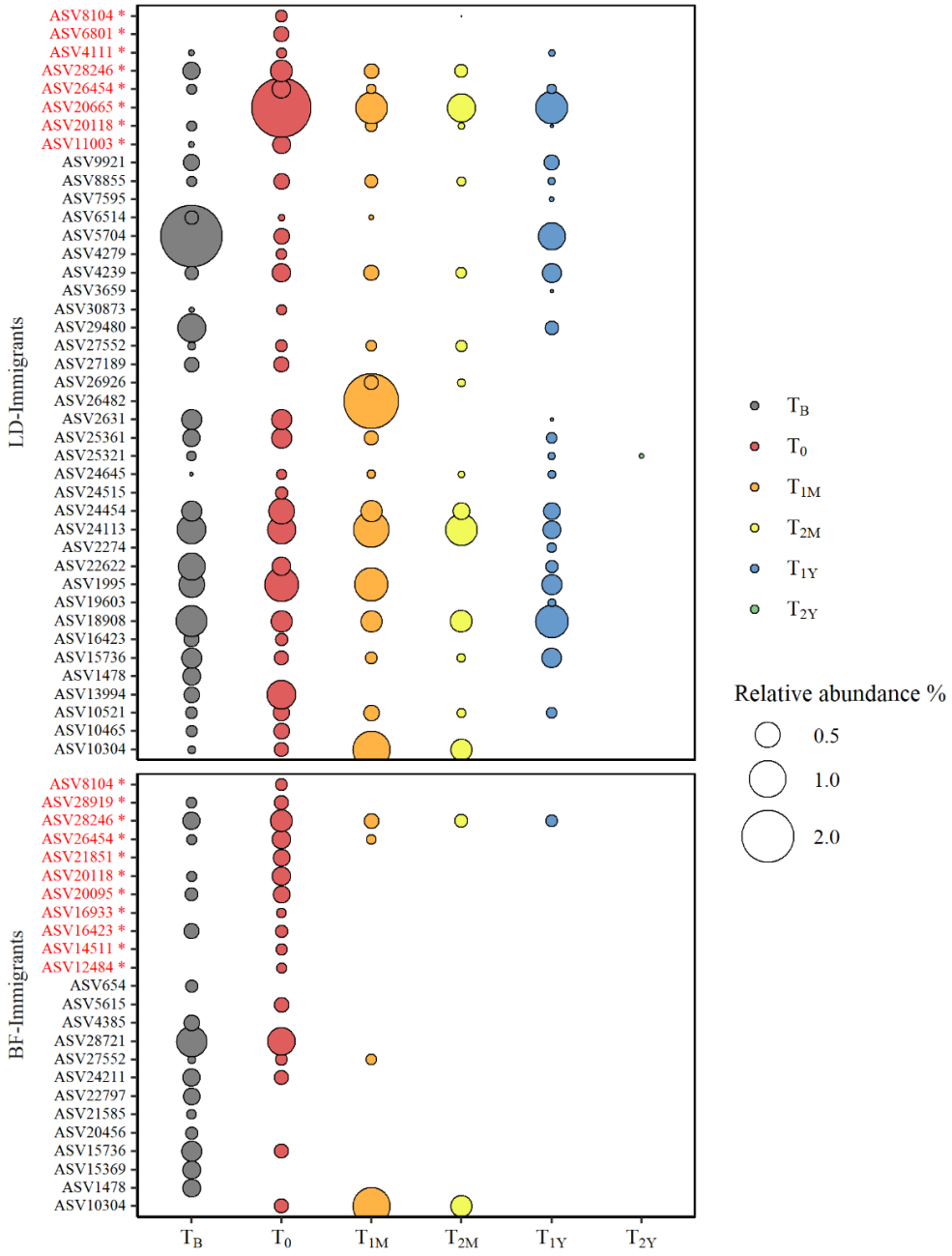

Figure 5-S19. Bubble plot showing the variations in relative abundance of LD- and BF-Immigrants (relative abundance > 0.01%) affiliated to particle-associated bacteria (PAB) over time. Different size stands for the relative abundance, while different colours stand for different sampling periods. T_B: before the RO introduction; T_0: immediately after the RO introduction; T_{1M}: 1 month after the RO introduction; T_{2M}: 2 months after the RO introduction; T_{1Y}: 1 year after the RO introduction; T_{2Y}: 2 years after the RO introduction. TP stands for treatment plant, while DN stands for distribution network.

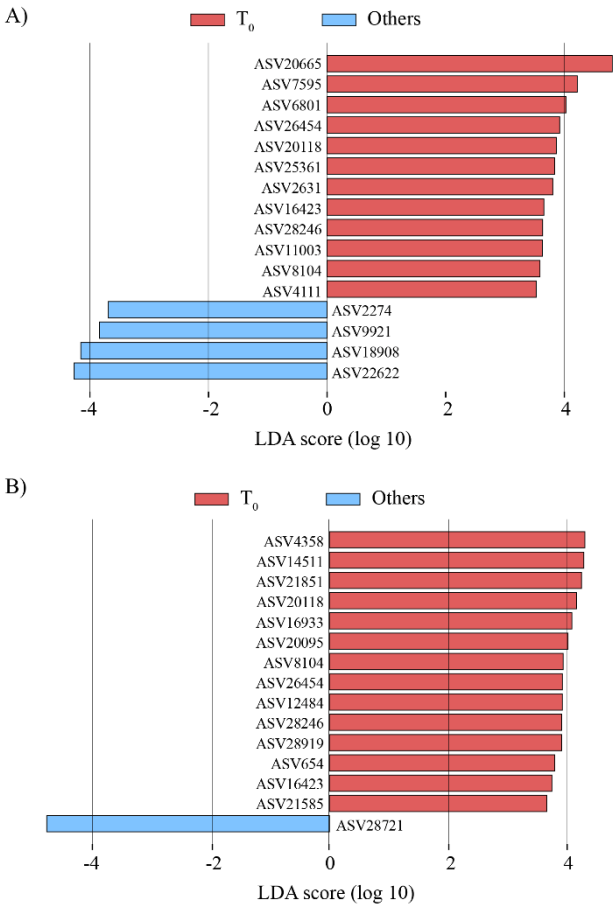

Figure 5-S20. Significantly enriched LD- and BF-Immigrants (relative abundance > 0.01%) affiliated to particle-associated bacteria (PAB) at T_0 in distribution network based on Lefse LDA analysis. T_0: immediately after the RO introduction.

Chapter 6

Conclusions and Outlook

6.1 Overall conclusions

Ensuring microbial quality in drinking water is crucial for public health, and drinking water distribution systems (DWDSs) serve as the ultimate safeguards in delivering and maintaining the biosafety of drinking water. However, there is a common consensus that the drinking water quality may deteriorate during distribution, which is closely linked to the established biofilm and/or loose deposits in DWDSs (Fish et al., 2017; Vreeburg and Boxall, 2007). The water leaves from the treatment plant, encompassing certain amount of cells, nutrients, and particles, contributing to the formation of biofilm and/or loose deposits. Simultaneously, the release of cells or particles can occur due to changes in hydraulics or variations in supply water quality, resulting in a deterioration of drinking water quality. These ongoing processes significantly impact the quality of drinking water during distribution. As stated in the Introduction of this thesis, there is a lack of knowledge regarding the dynamics of biofilm development and detachment, ongoing issues in microbial drinking water quality monitoring, and a dearth of understanding of microbial ecology in DWDSs. These knowledge gaps significantly hinder effective drinking water quality management. To address these knowledge gaps, both pilot and field studies were conducted in this thesis.

6.1.1 Dynamics of biofilm development and detachment

In DWDSs, the presence of biofilm and loose deposits is unavoidable. The prevention of biofilm formation in DWDSs poses a distinct challenge compared to mitigating loose deposit accumulation. Loose deposits, encompassing materials such as mineral particles, organic matters, and other non-cohesive substances settling loosely on pipe surfaces, can be efficiently managed through practical measures such as reducing particle entry or implementing routine flushing processes (Carrière et al., 2005; Friedman et al., 2002). In contrast, biofilm is a complex matrix of microorganisms, organic matter, and extracellular polymeric substances (EPS) that adhere tightly to pipe surfaces (Liu et al., 2016b), which cannot be simply removed by flushing the distribution systems. To devise successful biofilm prevention measures, it is essential to comprehend the conditions that promote its growth and detachment.

Clear changes in ATP/ICC content and microbial communities in biofilm developed with or without disinfectants (i.e., free chlorine and monochloramine) were observed over time (Chapter 2). In general, it is found that the biofilm developed in the absence of disinfectants exhibited a range of $0 – 4 \times 10^2$ pg ATP/cm^2 and $0 – 10^6$ ICC/cm^2 during the 64-week development period. It is expected that the biofilm grows over time as the feed water continues

to flow. The observed ATP/ICC content fall within the ranges typically observed in field distribution networks supplied with the same water and composed of the same pipe materials (i.e., PVC) (Liu et al., 2014; Liu et al., 2017a; Liu et al., 2020) (Chapter 3, data not shown in this thesis). Regarding the biofilm communities, it is observed that Proteobacteria dominated at the early stage, whereas Pastecibacteria progressively became dominant together with Proteobacteria at the later stages. The prevalence of Proteobacteria in biofilm communities was consistently observed in both chlorinated and unchlorinated field distribution networks (Douterelo et al., 2018b; Douterelo et al., 2014; Liu et al., 2014; Liu et al., 2017a; Liu et al., 2020; Revetta et al., 2013) (Chapter 3), whereas the dominance of Pastecibacteria in drinking water biofilms was infrequent. Patescibacteria is a newly defined superphylum and has been found to be prevalent in nutrient-limited aquifer environments, such as the groundwater and drinking water (Dai et al., 2020; Tian et al., 2020). Similarly, Patescibacteria was found to be a dominant phylum in both treated and distributed water in the field distribution network supplied with the same water (Chapter 3). The dominance of Pastecibacteria in the pilot-biofilm indicates the contributions of treated water to the biofilm. Nevertheless, notable variations in the relative abundance of Pastecibacteria were observed between the pilot-biofilm (Chapter 2, over one-year age, relative abundance ~ 35%) and field-biofilm (Chapter 3, over 20-years age, relative abundance < 10%). This discrepancy might be primarily attributed to differences in biofilm ages (Douterelo et al., 2018b; Martiny et al., 2003) and the complex hydraulic conditions within the field distribution networks (Cowle et al., 2019; Fish et al., 2017), given that both systems utilized the same PVC pipes, and considering the absence of significant effects related to surface-to-volume ratio due to different pipe diameters on biofilm communities observed in Chapter 3 (TN-110 mm PVC vs DN-63 mm PVC). The biofilm ages are likely the key determinant, as it was observed that even though the biofilm communities exhibit significant differences under steady and varied flow rate (Fish et al., 2017), the dominance of the Proteobacteria phylum persists across different hydraulic conditions (Douterelo et al., 2013). As the biofilm matures, Pastecibacteria might be progressively overtaken by other species predominantly affiliated with the Proteobacteria phylum. These observations hints that the simulation study in Chapter 2 is representative on the early stages of biofilm development, emphasizing that longer time periods, even years, is needed to fully develop mature microbial communities in DWDS (Martiny et al., 2003).

The presence of disinfectants (i.e., free chlorine and monochloramine) significantly limited biofilm growth and shaped the biofilm communities. The suppression effects of both free

chlorine and monochloramine on biofilm growth have been widely demonstrated (Clayton et al., 2021; Shen et al., 2017), while there is a lack of knowledge regarding the effects of these disinfectants on biofilm succession, especially from a long-term perspective. The significant changes in microbial community structure under different disinfection strategies and throughout developmental period are likely to be derived from the different bacterial sensitivity to disinfectants, where chlorine/monochloramine-resistant species outcompeted others in biofilms. For example, the dominant species detected in biofilm communities in free chlorine applied condition, belonging to Gammaproteobacteria (i.e., f_Burkholderiaceae, *Rhizobacter* spp., *Pseudomonas* spp.) and Alphaproteobacteria (*Hyphomicrobium* spp.), have been frequently reported as chlorine-resistant (Chen et al., 2023; Douterelo et al., 2018b; Douterelo et al., 2017; Fish and Boxall, 2018; Ke et al., 2023), whereas the dominant species found in biofilm communities in monochloramine applied condition, *Sphingobium* spp. affiliated with Alphaproteobacteria, has been identified as monochloramine-resistant (Ke et al., 2023; Potgieter et al., 2020). Furthermore, free chlorine exerted significant selective pressure on biofilm communities, resulting in a less complex community in comparison to monochloramine. This selection pressure was evident from the initial stages of biofilm development.

In contrast to the pilot-scale system (i.e., under steady state), there are daily variations in the field distribution systems, which will create hydraulic variations during the biofilm development. Attachment and detachment may continuously occur. The daily dynamics in the interactions between biofilm and bulk water were sensitively captured using a novel online monitoring and sampling system (OMSS, Chapter 3), with peaks in biofilm contribution detected at morning (6-9h) and evening (18-21h) hours, and an average contribution of around 5%. However, it was observed that contributions from biofilm into bulk water significantly increased when there are supply water quality changes (Chapter 4 & 5), reaching levels as high as 25%. The increased contributions from biofilm were likely attributed to the changes in supply water quality induced disturbances in the established equilibrium in DWDSs after the treatment upgrading and introduction of RO. Especially, after the introduction of RO, there is a notable reduction of approximately 50% in nutrient levels (e.g., DOC, metal elements). Under these conditions, EPS could serve as the source of carbon and energy for nutritionally deprived microorganisms to guarantee their metabolic activity (Chen et al., 2019; Zhang and Bishop, 2003). In addition, the reduced nutrients after RO introduction might induce a reduction of biological activity and a loss of viable cells in biofilm (Kooij, 1992; Liu et al., 2013b; Schleheck et al., 2009). Collectively, these changes have the potential to disrupt the biofilm matrix,

resulting in the release of biofilm into bulk water. Likewise, starvation treatments have been employed to enhance the control of membrane biofouling (de Vries et al., 2021) and the removal of drinking water biofilm (Chen et al., 2022a), often in conjunction with flushing. However, it should be noted that the magnitude of the biofilm responses to the changes differed between observations in Chapter 4 (e.g., a 95% increase in P-ATP) and Chapter 5 (e.g., a 200% increase in P-ATP). This variation could be attributed to differences in the changes in treated water quality resulting from distinct operations. A notable distinction lies in the substantial decrease (47%) in DOC subsequent to the implementation of RO. Conversely, TOC reduction was insignificant (15%) immediately after the integration of softening and sand filtration, despite a 100% reduction in sulphate (SO_4^{2-}), iron (Fe), and manganese (Mn). This is in line with previous studies, which suggest that carbon nutrients play a crucial role as limiting factors for microbial growth (Liu et al., 2013b; Pick et al., 2021; Smeets et al., 2009). A reduction in these nutrients may disrupt the equilibrium in DWDSs, resulting in the release of biofilm into the bulk water.

Given the insights from Chapter 2-5, it is concluded that the biofilm growth is significantly influenced by the types of disinfectants and nutrient concentration. As observed in Chapter 2, both free chlorine and monochloramine exhibited strong suppression effects on biofilm growth and shaped the biofilm community. Following a reduction in nutrients levels (Chapter 4 and 5), the biofilm responded immediately through releasing cells/particles into bulk water. Additionally, it is evident that the biofilm detachment might exhibit a daily pattern under regular operations (Chapter 3), while the extent of the biofilm detachment might be enhanced by the changed water quality, manifested by increased contributions of biofilm to the bulk water (Chapter 4 & 5).

It is evident that the biofilm age and the types of disinfectants play a crucial role in the development of biofilm in DWDSs. Understanding the succession of biofilm is essential for determining biofilm ages, as the composition and structure of biofilms change over time. This information is pivotal for effective biofilm management in DWDSs, allowing for adjustments in the frequency of cleaning procedures, selection of disinfectants based on biofilm age-related vulnerabilities, or optimization of hydraulic conditions to impede biofilm formation during its early stages. Younger biofilms, for instance, may exhibit higher susceptibility to specific disinfection methods or preventive measures and respond differently to alterations in water quality or hydraulic conditions when compared to mature biofilms (Fish et al., 2017; Singla et al., 2013; Stojicic et al., 2013). This might be especially beneficial in scenarios involving the introduction of new pipelines. It is important to proactively address biofilm formation from the

outset. From a sustainability and by-product formation perspective, there is a clear rationale for discontinuing the use of disinfectants. However, in instances where disinfection is deemed necessary, both free chlorine and monochloramine prove effective in limiting biofilm growth within DWDSs. Notably, the use of free chlorine may have advantages in predicting biofilm dynamics compared to monochloramine, given its ability to establish highly homogeneous biofilm communities and promote biofilm stabilization. This is particularly beneficial for biofilm management, as the predictability of microbial activities allows for effective control through precise strategies, such as targeted dosing of antimicrobial agents, regular monitoring, and implementation of tailored maintenance protocols. Nevertheless, it is important to note that when formulating disinfection strategies, additional factors in DWDSs should be taken into account, including the generation of disinfection by-products, the decay of residual disinfectants, and the potential enrichment of specific pathogens and antibiotic resistance genes (Fielding and Farrimond, 1999; Ling et al., 2018; Loret and Dumoutier, 2019; Richardson, 2003; Zhang et al., 2019). Future studies should incorporate these factors to offer a thorough evaluation for the choice of disinfectants in DWDSs. Additionally, given the immediately elevated contributions from biofilm attributed to the changes in supply water quality, flushing the distribution area with new-quality water might be an efficient way for cleaning of the distribution network.

6.1.2 Influence of drinking water distribution system microbial ecology on biological water quality

From a systematic perspective, if the microbial ecology in drinking water distribution system remain stable, the microbial water quality at customers' taps would ideally be the same as produced at the treatment plant. In other words, the contribution from loose deposits and biofilm will be minor, this is exactly what we see under the regular operation condition (Chapter 3). However, once the equilibrium is disturbed, deteriorations in the drinking water quality might occur. This becomes particularly significant for the high bio-stable drinking water in the Netherlands, where deteriorations must be attributed to the release of the biofilm/loose deposits from the DWDSs. The qualitative and quantitative demonstration of this phenomenon is evident in Chapters 4 and 5, where changes in supply water quality occurred as a result of treatment upgrades (i.e., adding extra softening and sand filter) and the introduction of partial RO.

Drawing insights from Chapter 3-5, it can be concluded that the key factor for preserving equilibrium in microbial ecology in DWDSs is maintaining the stability in both hydraulic

conditions and water quality. Under normal operation (Chapter 3), the daily variations in water quality are proposed as a baseline for evaluating the potential of the water quality deterioration and the extent of the contamination. In situations where destabilization is anticipated, as explored in Chapters 4 and 5, the focus should be on the potential for water quality deterioration and how loose deposits and biofilm respond to these changes. Though deteriorations were detected immediately after the supply water quality changes, the extent of the deterioration and the time required for re-stabilization differed between the observations in Chapter 4 and 5. As mentioned above, this discrepancy in the extent of the deterioration (200% increases in P-ATP in Chapter 5 v.s. 95% increases in P-ATP in Chapter 4) might be attributed to the extent of the nutrients reduction. One notable distinction is the significant decrease in DOC by 47% after the introduction of RO (Chapter 5). The higher extent of disturbances and the significant reduction in nutrients may necessitate a longer time for re-stabilization after the introduction of RO. This aligns with the typical strategies to limit the microbial growth through controlling nutrient levels, especially carbon-related nutrients (Liu et al., 2013b; Pick et al., 2021; Smeets et al., 2009). The observations suggest that smaller/shorter changes in nutrient levels, especially for carbon related nutrients, may lead to a swifter re-stabilization process.

6.1.3 Importance of loose deposits in DWDSs

Loose deposits are gaining increasing attention due to their identified role as hotspots for microbes and metal elements (Liu et al., 2017a; Ma et al., 2019), and their contributions to water quality deterioration in DWDS, such as the occurrence of water discoloration (Mussared et al., 2019; Vreeburg and Boxall, 2007). Unlike biofilm, loose deposits, comprising materials such as mineral particles, organic matters, and other non-cohesive substances settling loosely on pipe surfaces, possess the characteristic of being removable and can be resuspended during hydraulic disturbances (Carrière et al., 2005; Rubulis et al., 2008). However, there was limited understanding of how loose deposits respond to daily hydraulics and their reactions to changes in water quality. Utilizing source tracker, the contributions of loose deposits to bulk water have been quantified, exhibiting daily peaks in their contributions under normal operation (Chapter 3) and increased contributions during transition periods (Chapter 5). The notable contributions from loose deposits underscore their significant role in influencing drinking water quality within DWDSs.

In both field distribution systems (Chapter 3 and 5), significantly higher contributions from loose deposits, when compared to biofilm, were observed. Notably, during the transition period,

the contributions from loose deposits were exceptionally greater than those from biofilm. This challenges conventional perspectives, which attribute most water quality deteriorations to biofilms (Liu et al., 2016b), while it is in agreement with previous findings that loose deposits are hotspots for water quality deterioration (Carrière et al., 2005; Liu et al., 2017a; Zacheus et al., 2001). The heightened contributions from loose deposits relative to biofilm suggest that loose deposits are more responsive than biofilm to the varying hydraulics and changes in supply water quality. This sensitivity may be attributed to the loosely associated particulate matter and microbes, making it easier for new-quality water to diffuse, penetrate, and react with these particles. In contrast, the compact structure of biofilm, coupled with protection from extracellular polymeric substances, could contribute to its resilience to water quality changes.

These findings underscore the importance of considering loose deposits, particularly during transitional phases. Major risks and problems in DWDSs could be avoided simply by flushing the distribution system before distribution of new-quality water. Given the heightened responsiveness of loose deposits to water quality changes, flushing with new-quality water before officially distributing it to customers for consumption will be an effective and affordable method of precleaning. Notably, the role of loose deposits could be particularly noteworthy in chlorinated systems, as their presence may lead to chlorine depletion, potentially impacting water disinfection efficacy and overall water quality.

6.1.4 Importance of particle-associated bacteria in DWDSs

The traditional assessment of microbial drinking water quality predominantly focuses on planktonic bacteria (Ling et al., 2018; Prest et al., 2016b), often overlooking the crucial role of particle-associated bacteria. However, insights gained from chapters 3 and 5 underscore the higher contribution of biofilm and loose deposits to particle-associated bacteria (up to 25%) compared to planktonic bacteria (up to 5%). This parallels findings from a prior study that source-tracked contributions from biofilm and loose deposits to particle-associated bacteria in an unchlorinated distribution system (Liu et al., 2018). The high contributions of biofilm and/or loose deposits to particle-associated bacteria highlight that particles can serve as efficient indicators of biofilm detachment and loose deposit resuspension in comparison to planktonic bacteria. Specifically, the significance of particle-associated bacteria was notably demonstrated in Chapters 4 and 5, where through the direct characterization of particles in bulk water, the transition effects were successfully captured.

In summary, the monitoring of particles in the distribution systems can serve as a valuable

means to detect water quality deteriorations arising from the impacts of biofilm and loose deposits. This method has the ability to overcome the challenges of field distribution network accessibility (non-destructive) and dilution effects (concentrated). Hence, it is strongly recommended for the assessment of microbial drinking water quality.

6.1.5 Drinking water quality monitoring strategies

Grab sampling, a conventional method for monitoring drinking water quality, has inherent limitations that may impede its effectiveness in providing comprehensive insights into water quality dynamics. The constraints of grab sampling in monitoring drinking water quality include potential inaccuracies in capturing temporal variations, susceptibility to dilution effects, and limited representation of spatial differences. Online monitoring systems have the capacity to provide a more comprehensive and accurate assessment, capturing real-time variations and enhancing our ability to respond to potential water quality issues effectively. This is exemplified in Chapters 3 and 5, where the spatiotemporal changes in drinking water quality were sensitively captured by applying the Online Microbial Sampling System (OMSS) that was developed in this study. The captured daily peaks in the drinking water quality emphasizes the importance of considering these periodic variations to avoid misleading comparisons of spatiotemporal data in daily water quality management. The OMSS developed proves to be a valuable instrument in setting a baseline for daily drinking water quality. Moreover, it aids in microbial drinking water quality assessment by characterizing both planktonic and particle-associated bacteria, which have been demonstrated to be valuable messengers for determining local dominant processes within DWDS in this thesis.

With the development of advanced microbial community profiling techniques, the application of Bayesian-based source tracking has successfully contributed to tracking the origin of water quality changes in distribution systems (Liu et al., 2018). This sophisticated approach utilizes Bayesian statistical methods to analyze microbial community data (Knights et al., 2011), offering valuable insights into the sources influencing water quality dynamics. Utilizing source tracker, the contributions from biofilm and loose deposits to bulk water phases were quantitatively assessed in this thesis (Chapter 3 and 5). The combination of OMSS and source tracking enables the capture of daily dynamics in the contributions from biofilm and loose deposits (Chapter 3) and addresses challenges related to the aperiodic occurrence of transition effects (Chapter 5). This integrated approach is particularly useful in transition effects studies, aiding in determining the origin of water quality deterioration and suggesting corresponding

cleaning procedures. For example, if deteriorations are attributed to biofilm, interventions like ice pigging may be recommended, while if the deteriorations are primarily from loose deposits, flushing may suffice.

Additionally, the synergistic application of OMSS with other strategies, such as online ATP (de Vera and Wert, 2019), online FCM (Besmer et al., 2014), and nanopore sequencing, holds promise in realizing real-time microbial water quality assessment with sequencing capabilities. This innovative combination opens avenues for more comprehensive and timely insights into microbial dynamics, enhancing our understanding and management of drinking water quality.

6.2 Specific conclusions

(1) Biofilm formation and the effects of disinfection regimes on biofilm development (Chapter 2)

Research question: How does biofilm form in DWDSs? And how do disinfection regimes affect the biofilm development in DWDSs?

- Disinfectants significantly suppressed biofilm growth and shaped the biofilm communities. Remarkably, MC expressed better suppression effects on the biofilm activity (i.e., ATP), whereas FC exerted more intense selection pressure, resulting in a more homogenous and less complex biofilm community.
- The temporal results highlighted that biofilm formation underwent fundamental stages from initial colonization to accumulation and selection and stabilization at different rates under each of the conditions. Reaching the stabilization stage took the longest in the MC condition (> 64 weeks), followed by the NC (~ 36 weeks) and FC conditions (~ 19 weeks).

(2) Dynamics in the interactions between biofilm and bulk water phases (Chapter 3, 4, and 5)

- **Regular operational conditions (Chapter 3)**

Research question: What's the spatiotemporal dynamic in DWDS microbial water quality under regular conditions?

- Spatially, increases in the particle loads were observed from the treatment plant to distribution networks, while the quantity of the particle-associated bacteria decreased from the treatment plant to the transportation network but increased in the distribution

networks. In terms of the diversity of planktonic and particle-associated bacteria, the trend was similar to that of the particle-associated bacterial quantity, except that the diversity of both planktonic and particle-associated bacteria was larger at the distribution networks than that at the treatment plant. According to the SourceTracker2 results, the observed increases in the particles and the bacteria (i.e., planktonic and particle-associated bacteria) mainly originated from the biofilm and loose deposits.

- Temporally, the OMSS allowed to capture the daily peaks in the quantity of particle-associated bacteria, the observed OTU number in both planktonic and particle-associated bacteria, and contributions of loose deposits and biofilms during morning (6-9h) or evening (18-21h) hours. The temporal trends revealed clear dynamic interactions between the water phase (i.e., planktonic and particle-associated bacteria) and solid phase (i.e., biofilm and loose deposits) during the distribution.
- Methodologically, this study highlights that the combination of OMSS and the microbial fingerprint-based SourceTracker2 is a powerful tool for studying spatiotemporal water quality variations in an unchlorinated drinking water distribution system. Furthermore, the particles and associated bacteria can be valuable messengers revealing the physiochemical and microbiological processes occurring in distribution systems.

- **Irregular operational conditions (Chapter 4 & 5)**

Research question: Will transition effects (i.e., water quality deteriorations caused by contributions of biofilm/loose deposits) happen when water treatment is upgraded and treated water quality changes accordingly? How to capture and characterise transition effects? When will the disturbed system be re-stabilized? How to manage the transition effects?

- In Chapter 4, the results showed that the water quality significantly improved after 6 months' operation of the additional treatments. Remarkably, water quality deterioration was observed at the initial stage when the quality-improved treated water distributed into the network at $T_{3\text{-weeks}}$, reflected by a spike of total suspended solids (TSS, 50-260%), active biomass (ATP, 95-230%) and inorganic elements (e.g. Mn, 130-250%). Additionally, pyrosequencing results revealed sharp shifts in microbial community composition and structure for the bacteria associated with suspended particles between T_0 and $T_{3\text{-weeks}}$, which re-stabilized at $T_{6\text{-months}}$. This study highlights the potential water quality deterioration caused by changing the supply water quality, which can be

captured and assessed by monitoring the suspended particles throughout distribution networks.

- In comparison to Chapter 4, critical research questions regarding "how fast/how long the transition effects will occur/last, where the deteriorations originate from, and what actions should be carried out to mitigate the transition effects" were addresses in Chapter 5. The results showed that significant transition effects were captured right after the introduction of RO at T_0, where the particle loads, elements concentrations (e.g., Ca, Fe, Mn), quantity of biomass, and the number of observed species increased strongly. This was attributed to contributions from biofilm and loose deposits. The deteriorations lasted 1 month till T_{1M}, thereafter started to fade away from T_{2M}. Though the peak transition window is about 1-month time, the re-stabilization of the microbial ecology and improvements of water quality takes much longer till one (T_{1Y}) and two (T_{2Y}) years later, which were primarily attributed to the changes/improvements in treated water quality rather than contributions from biofilm and/or loose deposits. Furthermore, enhanced peaks in the water quality deterioration were observed during morning (6-9h) and evening (18-21h) hours, suggesting that the extent of water quality deterioration may have been underestimated. Based on the observations in this study, it is commended to perform cleaning procedures, such as flushing, before implementing treatment upgrades, and to conduct intensive monitoring of drinking water quality in DWDSs both before and within the initial month of the transition.

6.3 Limitations and further research

Though the findings in this thesis collectively contribute to a better understanding of the microbial drinking water quality dynamics, it is also important to acknowledge the limitations in this thesis. The lack of understanding of microbial viability and activity in drinking water using next generation sequencing (NGS) technology and the need for further exploration of biofilm responses under typical or irregular conditions in chlorinated systems worldwide hinder a comprehensive understanding of microbial drinking water quality across various scenarios. Methods such as proteomics or metabolomics may help to better understand the activity of the microbial community in the different phases in the DWDS (Franzosa et al., 2015). Future research efforts should prioritize these aspects to advance our knowledge and contribute to more effective drinking water management practices.

6.3.1 Challenges in utilizing NGS technology for microbial analysis in DWDSs

NGS technology was frequently used in this thesis to analyse the microbial community in drinking water under various conditions, which greatly contributed to our understandings on the microbial drinking water quality. A significant limitation of NGS technology pertains to viability assessment, as it lacks the capability to distinguish between live and dead cells (Garner et al., 2021; Tan et al., 2015). However, discerning viability is crucial for accurately evaluating microbial drinking water quality. To address this deficiency, it is advisable to complement NGS data with other methods such as transcriptomics, metaproteomics, metabolomics or functional assays that provide insights into microbial activity and metabolic processes, allowing for a more comprehensive understanding of the microbial community's functional dynamics (Cao et al., 2017; Garner et al., 2021; Zhang and Liu, 2019).

6.3.2 Exploration on microbial drinking water quality in chlorinated systems

Throughout this thesis, the majority of investigations, spanning Chapters 3-5, were conducted in unchlorinated systems with plastic pipes. However, in many countries, disinfectants are commonly used to ensure the microbiological safety of drinking water (Dai et al., 2020), and iron-based pipe materials (ductile iron, stainless steel, and galvanized steel) remain prevalent (Zhang et al., 2022). The potential interplay between disinfectants and these metal pipe materials introduces a scenario where disinfectants may react with the metal, altering pipe surfaces and creating uneven pipe walls that facilitate bacterial adhesion. Consequently, this phenomenon may lead to chlorine decay, further promoting bacterial regrowth within DWDSs. Altogether, the spatiotemporal dynamics in drinking water quality within chlorinated systems may be more intricate compared to those in non-chlorinated systems. The developed OMSS can be applied to offer comprehensive insights into the spatiotemporal variations in drinking water quality in chlorinated systems without deviations. This exploration allows for an in-depth understanding of the complex interplay among various engineering factors (such as chlorine concentration, hydraulic conditions, and pipe materials) and how these interactions impact DWDS biofilms and overall drinking water quality in chlorinated systems.

Additionally, recognizing the potential transition effects may become more crucial when changes in supply water quality occur in chlorinated systems compared to unchlorinated systems. While the principle of transition effects remains the same, physiochemical and microbiological processes may vary significantly due to the influences of chlorine decay. For instance, the reduction of organic matter in treated water will result in reduced chlorine demand

at the treatment plant, but the release of organic matter from the distribution system may deplete chlorine much faster than in regular operation. An unexpectedly rapid reduction in chlorine levels poses challenges, especially considering that released microbes might be pathogenic. In chlorinated systems, chlorine decay may play key roles in the occurrence of transition effects.

6.4 Recommendations for water utilities

Based on the observations in this thesis, management strategies for ensuring higher water quality were proposed from the perspective of daily water quality management and transition effects management.

- The captured daily peaks in the drinking water quality emphasizes the importance of considering these periodic variations to avoid misleading comparisons of spatiotemporal data in daily water quality management. The OMSS developed proves to be a valuable instrument in setting a baseline for daily drinking water quality. Furthermore, the integration of OMSS with a Bayesian-based source tracker allows for tracing the origins of variations in drinking water quality. This becomes particularly advantageous in situations involving transitional effects, enabling the assessment of deterioration risks and the tracking of contamination sources.
- Given the insights from Chapter 4 and 5, it is highly advisable to recognize the potential occurrence of transition effects in DWDSs when there is a change in the quality of the supply water and to acknowledge that the re-stabilization of the microbial ecology in DWDSs may take a long time. Performing cleaning procedures, such as flushing or ice pigging, before transitioning to the new-quality water is deemed essential. Moreover, a robust recommendation is made to intensively monitor the quality of drinking water in distribution systems before and during the initial month. In such circumstances, it is advisable to utilize online sampling to ensure accurate water quality assessment and prevent any deviations. Furthermore, the implementation of a Bayesian-based source tracker facilitates the identification of contamination sources in drinking water, enabling the optimization of cleaning processes. For example, if most deteriorations are attributed to loose deposits, flushing the distribution systems will be adequate. However, in cases where deteriorations stem from biofilm, it is recommended to employ more robust removal methods like ice pigging or similar approaches.

Bibliography

Agudelo-Vera, C., Avvedimento, S., Boxall, J., Creaco, E., De Kater, H., Di Nardo, A., Djukic, A., Douterelo, I., Fish, K.E. and Rey, P.L.I. 2020. Drinking water temperature around the globe: understanding, policies, challenges and opportunities. Water 12(4), 1049.

Allison, S.D. and Martiny, J.B. 2008. Resistance, resilience, and redundancy in microbial communities. Proceedings of the National Academy of Sciences 105(Supplement 1), 11512-11519.

Anderson, M.J. and Walsh, D.C.I. 2013. PERMANOVA, ANOSIM, and the Mantel test in the face of heterogeneous dispersions: What null hypothesis are you testing? Ecological Monographs 83(4), 557-574.

Ashbolt, N.J. 2015. Microbial contamination of drinking water and human health from community water systems. Current Environmental Health Reports 2, 95-106.

AWWA 2002 Effects of water age on distribution system water quality, p. 19.

Banna, M.H., Imran, S., Francisque, A., Najjaran, H., Sadiq, R., Rodriguez, M. and Hoorfar, M. 2014. Online drinking water quality monitoring: review on available and emerging technologies. Critical Reviews in Environmental Science and Technology 44(12), 1370-1421.

Basefsky, M. 2006. Issues of aging infrastructure: the tucson experience. Southwest Hydrology, March/April 2.

Batté, M., Appenzeller, B.M.R., Grandjean, D., Fass, S., Gauthier, V., Jorand, F., Mathieu, L., Boualam, M., Saby, S. and Block, J.C. 2003. Biofilms in drinking water distribution systems. Reviews in Environmental Science and Biotechnology 2(2), 147-168.

Bautista-de Los Santos, Q.M., Schroeder, J.L., Blakemore, O., Moses, J., Haffey, M., Sloan, W. and Pinto, A.J. 2016a. The impact of sampling, PCR, and sequencing replication on discerning changes in drinking water bacterial community over diurnal time-scales. Water Research 90, 216-224.

Bautista-de los Santos, Q.M., Schroeder, J.L., Sevillano-Rivera, M.C., Sungthong, R., Ijaz, U.Z., Sloan, W.T. and Pinto, A.J. 2016b. Emerging investigators series: microbial communities in full-scale drinking water distribution systems – a meta-analysis. Environmental Science: Water Research & Technology 2(4), 631-644.

Bell, G. 2000. The distribution of abundance in neutral communities. The American Naturalist 155(5), 606-617.

Berry, D., Xi, C. and Raskin, L. 2006. Microbial ecology of drinking water distribution systems. Current Opinion in Biotechnology 17(3), 297-302.

Besmer, M.D., Epting, J., Page, R.M., Sigrist, J.A., Huggenberger, P. and Hammes, F. 2016. Online flow cytometry reveals microbial dynamics influenced by concurrent natural and operational events in groundwater used for drinking water treatment. Scientific Reports 6, 38462.

Besmer, M.D. and Hammes, F. 2016. Short-term microbial dynamics in a drinking water plant treating groundwater with occasional high microbial loads. Water Research 107, 11-18.

Besmer, M.D., Weissbrodt, D.G., Kratochvil, B.E., Sigrist, J.A., Weyland, M.S. and Hammes, F. 2014. The feasibility of automated online flow cytometry for in-situ monitoring of microbial dynamics in aquatic ecosystems. Frontiers in Microbiology 5, 265.

Bian, K., Wang, C., Jia, S., Shi, P., Zhang, H., Ye, L., Zhou, Q. and Li, A. 2021. Spatial dynamics of bacterial community in chlorinated drinking water distribution systems supplied with two treatment plants: An integral study of free-living and particle-associated bacteria. Environment International 154, 106552.

Biggs, C.A., Boxall, J.B., Sekar, R. and Ramalingam, B. 2013. Aggregation and biofilm formation of bacteria isolated from domestic drinking water. Water Supply 13(4), 1016-1023.

Bokulich, N.A., Kaehler, B.D., Rideout, J.R., Dillon, M., Bolyen, E., Knight, R., Huttley, G.A. and Caporaso, J.G. 2018. Optimizing taxonomic classification of marker-gene amplicon sequences with QIIME 2's q2-feature-classifier plugin. Microbiome 6(1), 1-17.

Bolyen, E., Rideout, J.R., Dillon, M.R., Bokulich, N.A., Abnet, C., Al-Ghalith, G.A., Alexander, H., Alm, E.J., Arumugam, M. and Asnicar, F. 2018. QIIME 2: Reproducible, interactive, scalable, and extensible microbiome data science. PeerJ Preprints.

Buse, H.Y., Lu, J., Struewing, I.T. and Ashbolt, N.J. 2013. Eukaryotic diversity in premise drinking water using 18S rDNA sequencing: implications for health risks. Environmental Science and Pollution Research 20, 6351-6366.

Callahan, B.J., McMurdie, P.J., Rosen, M.J., Han, A.W., Johnson, A.J.A. and Holmes, S.P. 2016. DADA2: high-resolution sample inference from Illumina amplicon data. Nature Methods 13(7), 581-583.

Cao, Y., Fanning, S., Proos, S., Jordan, K. and Srikumar, S. 2017. A review on the applications of next generation sequencing technologies as applied to food-related microbiome studies. Frontiers in Microbiology 8, 1829.

Caporaso, J.G., Kuczynski, J., Stombaugh, J., Bittinger, K., Bushman, F.D., Costello, E.K., Fierer, N., Pena, A.G., Goodrich, J.K. and Gordon, J.I. 2010. QIIME allows analysis of high-throughput community sequencing data. Nature Methods 7(5), 335-336.

Carragher, B.J., Stewart, R.A. and Beal, C.D. 2012. Quantifying the influence of residential water appliance efficiency on average day diurnal demand patterns at an end use level: A precursor to optimised water service infrastructure planning. Resources, Conservation and Recycling 62, 81-90.

Carrière, A., Gauthier, V., Desjardins, R. and Barbeau, B. 2005. Evaluation of loose deposits in distribution

systems through: unidirectional flushing. Journal - American Water Works Association 97(9), 82-92.
Cerrato, J.M., Reyes, L.P., Alvarado, C.N. and Dietrich, A.M. 2006. Effect of PVC and iron materials on Mn(II) deposition in drinking water distribution systems. Water Research 40(14), 2720-2726.
Chan, S., Pullerits, K., Keucken, A., Persson, K.M., Paul, C.J. and Radstrom, P. 2019. Bacterial release from pipe biofilm in a full-scale drinking water distribution system. NPJ Biofilms Microbiomes 5(1), 9.
Chaves Simões, L. and Simões, M. 2013. Biofilms in drinking water: problems and solutions. RSC Advances 3(8), 2520-2533.
Chen, H. and Boutros, P.C. 2011. VennDiagram: a package for the generation of highly-customizable Venn and Euler diagrams in R. BMC Bioinformatics 12, 35.
Chen, J.-J., Yeh, H.-H., Tseng, I.-C., Lin, T.-F. and Lai, W.-L. 2002. Upgrading conventional treatment processes for water quality improvement - a pilot study. Water Supply 2(5-6), 165-171.
Chen, J., Li, W., Tan, Q., Sheng, D., Li, Y., Chen, S. and Zhou, W. 2022a. Effect of disinfectant exposure and starvation treatment on the detachment of simulated drinking water biofilms. Science of The Total Environment 807, 150896.
Chen, J., Lu, Y., Cheng, J. and Zhang, J. 2019. Effect of starvation on the nitrification performance of constructed rapid infiltration systems. Environmental Technology 40(11), 1408-1417.
Chen, L., Li, X., van der Meer, W., Medema, G. and Liu, G. 2022b. Capturing and tracing the spatiotemporal variations of planktonic and particle-associated bacteria in an unchlorinated drinking water distribution system. Water Research 219, 118589.
Chen, L., Ling, F., Bakker, G., Liu, W.T., Medema, G., van der Meer, W. and Liu, G. 2020. Assessing the transition effects in a drinking water distribution system caused by changing supply water quality: an indirect approach by characterizing suspended solids. Water Research 168, 115159.
Chen, L., Zhai, Y., van der Mark, E., Liu, G., van der Meer, W. and Medema, G. 2021. Microbial community assembly and metabolic function in top layers of slow sand filters for drinking water production. Journal of Cleaner Production 294.
Chen, S., Li, X., Wang, Y., Zeng, J., Ye, C., Li, X., Guo, L., Zhang, S. and Yu, X. 2018. Induction of Escherichia coli into a VBNC state through chlorination/chloramination and differences in characteristics of the bacterium between states. Water Research 142, 279-288.
Chen, W., Chien, C., Ho, W., Ou, J., Chen, S. and Kao, C. 2022c. Effects of treatment processes on AOC removal and changes of bacterial diversity in a water treatment plant. Journal of Environmental Management 311, 114853.
Chen, X., Xiao, L., Niu, J., Wang, Y., Zhang, X., Gong, L., Yao, F. and Xu, K. 2023. Early succession of biofilm bacterial communities in newly built drinking water pipelines via multi-area analysis. Applied Microbiology and Biotechnology, 1-12.
Chesson, P. 2000. Mechanisms of maintenance of species diversity. Annual Review of Ecology and Systematics 31(1), 343-366.
Chien, C., Kao, C., Chen, C., Dong, C. and Wu, C. 2008. Application of biofiltration system on AOC removal: Column and field studies. Chemosphere 71(9), 1786-1793.
Choi, Y. and Morgenroth, E. 2003. Monitoring biofilm detachment under dynamic changes in shear stress using laser-based particle size analysis and mass fractionation. Water Science and Technology 47(5), 69-76.
Clayton, G.E., Thorn, R.M.S. and Reynolds, D.M. 2021. The efficacy of chlorine-based disinfectants against planktonic and biofilm bacteria for decentralised point-of-use drinking water. npj Clean Water 4(1).
Cowle, M.W., Webster, G., Babatunde, A.O., Bockelmann-Evans, B.N. and Weightman, A.J. 2019. Impact of flow hydrodynamics and pipe material properties on biofilm development within drinking water systems. Environmental Technology.
Cruz, M.C., Woo, Y., Flemming, H.C. and Wuertz, S. 2020. Nitrifying niche differentiation in biofilms from full-scale chloraminated drinking water distribution system. Water Research 176, 115738.
Dai, Z., Sevillano-Rivera, M.C., Calus, S.T., Bautista-de Los Santos, Q.M., Eren, A.M., van der Wielen, P., Ijaz, U.Z. and Pinto, A.J. 2020. Disinfection exhibits systematic impacts on the drinking water microbiome. Microbiome 8(1), 42.
de Vera, G.A. and Wert, E.C. 2019. Using discrete and online ATP measurements to evaluate regrowth potential following ozonation and (non) biological drinking water treatment. Water Research 154, 377-386.
de Vries, H.J., Kleibusch, E., Hermes, G.D.A., van den Brink, P. and Plugge, C.M. 2021. Biofouling control: the impact of biofilm dispersal and membrane flushing. Water Research 198, 117163.
Douterelo, I., Calero-Preciado, C., Soria-Carrasco, V. and Boxall, J.B. 2018a. Whole metagenome sequencing of chlorinated drinking water distribution systems. Environmental Science: Water Research & Technology 4(12), 2080-2091.
Douterelo, I., Fish, K.E. and Boxall, J.B. 2018b. Succession of bacterial and fungal communities within biofilms of a chlorinated drinking water distribution system. Water Research 141, 74-85.
Douterelo, I., Jackson, M., Solomon, C. and Boxall, J. 2016. Microbial analysis of in situ biofilm formation in

drinking water distribution systems: implications for monitoring and control of drinking water quality. Applied Microbiology and Biotechnology 100, 3301-3311.

Douterelo, I., Jackson, M., Solomon, C. and Boxall, J. 2017. Spatial and temporal analogies in microbial communities in natural drinking water biofilms. Science of the Total Environment 581, 277-288.

Douterelo, I., Sharpe, R. and Boxall, J. 2013. Influence of hydraulic regimes on bacterial community structure and composition in an experimental drinking water distribution system. Water Research 47(2), 503-516.

Douterelo, I., Sharpe, R. and Boxall, J. 2014. Bacterial community dynamics during the early stages of biofilm formation in a chlorinated experimental drinking water distribution system: implications for drinking water discolouration. Journal of Applied Microbiology 117(1), 286-301.

Dumbrell, A.J., Nelson, M., Helgason, T., Dytham, C. and Fitter, A.H. 2010. Relative roles of niche and neutral processes in structuring a soil microbial community. The ISME Journal 4(3), 337-345.

Echeverría, F., Castaño, J.G., Arroyave, C., Peñuela, G., Ramírez, A. and Morató, J. 2009. Characterization of deposits formed in a water distribution system. Ingeniare. Revista Chilena de Ingeniería 17(2), 275-281.

Edgar, R.C., Haas, B.J., Clemente, J.C., Quince, C. and Knight, R. 2011. UCHIME improves sensitivity and speed of chimera detection. Bioinformatics 27(16), 2194-2200.

Edwards, M. and Dudi, A. 2004. Role of chlorine and chloramine in corrosion of lead ‐ bearing plumbing materials. Journal ‐ American Water Works Association 96(10), 69-81.

Eijkman, C. 1904. Die Gärungsprobe bei 46 C als Hilfsmittel bei der Trinkwasseruntersuchung. Cbl. Bakteriol. Abth I. Orog 37, 742-752.

Falkinham, J.O., 3rd, Hilborn, E.D., Arduino, M.J., Pruden, A. and Edwards, M.A. 2015. Epidemiology and ecology of opportunistic premise plumbing pathogens: Legionella pneumophila, Mycobacterium avium, and Pseudomonas aeruginosa. Environmental Health Perspectives 123(8), 749-758.

Farhat, N., Kim, L.H. and Vrouwenvelder, J.S. 2020. Online characterization of bacterial processes in drinking water systems. npj Clean Water 3(1).

Favere, J., Buysschaert, B., Boon, N. and De Gusseme, B. 2020. Online microbial fingerprinting for quality management of drinking water: Full-scale event detection. Water Research 170, 115353.

Favere, J., Waegenaar, F., Boon, N. and De Gusseme, B. 2021. Online microbial monitoring of drinking water: How do different techniques respond to contaminations in practice? Water Research 202, 117387.

Feazel, L.M., Baumgartner, L.K., Peterson, K.L., Frank, D.N., Harris, J.K. and Pace, N.R. 2009. Opportunistic pathogens enriched in showerhead biofilms. Proceedings of the National Academy of Sciences of the United States of America 106(38), 16393-16398.

Ferrebee, M., Osborne, E. and Garner, E. 2023. Spatiotemporal trends in particle-associated microbial communities in a chlorinated drinking water distribution system. PLOS Water 2(11), e0000183.

Fielding, M. and Farrimond, M. 1999. Disinfection by-products in drinking water: current issues. Elsevier.

Fish, K., Osborn, A.M. and Boxall, J.B. 2017. Biofilm structures (EPS and bacterial communities) in drinking water distribution systems are conditioned by hydraulics and influence discolouration. Science of the Total Environment 593, 571-580.

Fish, K.E. and Boxall, J.B. 2018. Biofilm microbiome (re) growth dynamics in drinking water distribution systems are impacted by chlorine concentration. Frontiers in Microbiology 9, 2519.

Fish, K.E., Collins, R., Green, N.H., Sharpe, R.L., Douterelo, I., Osborn, A.M. and Boxall, J.B. 2015. Characterisation of the physical composition and microbial community structure of biofilms within a model full-scale drinking water distribution system. PLoS One 10(2), e0115824.

Fish, K.E., Reeves-McLaren, N., Husband, S. and Boxall, J. 2020. Unchartered waters: the unintended impacts of residual chlorine on water quality and biofilms. NPJ Biofilms Microbiomes 6(1), 34.

Fish, K.E., Sharpe, R.L., Biggs, C.A. and Boxall, J.B. 2022. Impacts of temperature and hydraulic regime on discolouration and biofilm fouling in drinking water distribution systems. PLOS Water 1(8), e0000033.

Flemming, H.-C. 1998. Relevance of biofilms for the biodeterioration of surfaces of polymeric materials. Polymer Degradation and Stability 59(1-3), 309-315.

Flemming, H.-C., Percival, S. and Walker, J. 2002. Contamination potential of biofilms in water distribution systems. Water Science and Technology: Water Supply 2(1), 271-280.

Franzosa, E.A., Hsu, T., Sirota-Madi, A., Shafquat, A., Abu-Ali, G., Morgan, X.C. and Huttenhower, C. 2015. Sequencing and beyond: integrating molecular'omics' for microbial community profiling. Nature Reviews Microbiology 13(6), 360-372.

Friedman, M., Kirmeyer, G.J. and Antoun, E. 2002. Developing and implementing a distribution system flushing program. Journal ‐ American Water Works Association 94(7), 48-56.

Garner, E., Davis, B.C., Milligan, E., Blair, M.F., Keenum, I., Maile-Moskowitz, A., Pan, J., Gnegy, M., Liguori, K. and Gupta, S. 2021. Next generation sequencing approaches to evaluate water and wastewater quality. Water Research 194, 116907.

Gauthier, V., Gérard, B., Portal, J.M., Block, J.C. and Gatel, D. 1999. Organic matter as loose deposits in a drinking water distribution system. Water Research 33(4), 1014-1026.

Gomez-Alvarez, V., Pfaller, S., Pressman, J.G., Wahman, D.G. and Revetta, R.P. 2016. Resilience of microbial communities in a simulated drinking water distribution system subjected to disturbances: role of conditionally rare taxa and potential implications for antibiotic-resistant bacteria. Environmental Science: Water Research & Technology 2(4), 645-657.

Gomez-Alvarez, V., Revetta, R.P. and Santo Domingo, J.W. 2012. Metagenomic analyses of drinking water receiving different disinfection treatments. Applied and Environmental Microbiology 78(17), 6095-6102.

Gomez-Alvarez, V., Schrantz, K.A., Pressman, J.G. and Wahman, D.G. 2014. Biofilm community dynamics in bench-scale annular reactors simulating arrestment of chloraminated drinking water nitrification. Environmental Science & Technology 48(10), 5448-5457.

Gomez-Smith, C.K., LaPara, T.M. and Hozalski, R.M. 2015. Sulfate reducing bacteria and mycobacteria dominate the biofilm communities in a chloraminated drinking water distribution system. Environmental Science & Technology 49(14), 8432-8440.

Guo, X.P., Yang, Y., Lu, D.P., Niu, Z.S., Feng, J.N., Chen, Y.R., Tou, F.Y., Garner, E., Xu, J., Liu, M. and Hochella, M.F., Jr. 2018. Biofilms as a sink for antibiotic resistance genes (ARGs) in the Yangtze Estuary. Water Research 129, 277-286.

Hammes, F., Broger, T., Weilenmann, H.U., Vital, M., Helbing, J., Bosshart, U., Huber, P., Peter Odermatt, R. and Sonnleitner, B. 2012. Development and laboratory‐scale testing of a fully automated online flow cytometer for drinking water analysis. Cytometry Part A 81(6), 508-516.

Hanna-Attisha, M., LaChance, J., Sadler, R.C. and Champney Schnepp, A. 2016. Elevated blood lead levels in children associated with the Flint drinking water crisis: a spatial analysis of risk and public health response. American Journal of Public Health 106(2), 283-290.

Hargesheimer, E.E., Conio, O. and Popovicova, J. (2002) Online monitoring for drinking water utilities. American Water Works Association.

Henry, R., Schang, C., Coutts, S., Kolotelo, P., Prosser, T., Crosbie, N., Grant, T., Cottam, D., O'Brien, P. and Deletic, A. 2016. Into the deep: evaluation of SourceTracker for assessment of faecal contamination of coastal waters. Water Research 93, 242-253.

Hong, P.Y., Hwang, C., Ling, F., Andersen, G.L., LeChevallier, M.W. and Liu, W.T. 2010. Pyrosequencing analysis of bacterial biofilm communities in water meters of a drinking water distribution system. Applied and Environmental Microbiology 76(16), 5631-5635.

Huang, G., Ng, T.W., Chen, H., Chow, A.T., Liu, S. and Wong, P.K. 2020. Formation of assimilable organic carbon (AOC) during drinking water disinfection: A microbiological prospect of disinfection byproducts. Environmental International 135, 105389.

Husband, P., Boxall, J. and Saul, A. 2008. Laboratory studies investigating the processes leading to discolouration in water distribution networks. Water Research 42(16), 4309-4318.

Hwang, C., Ling, F., Andersen, G.L., Lechevallier, M.W. and Liu, W.T. 2011. Evaluation of methods for the extraction of DNA from drinking water distribution system biofilms. Microbes and Environments 27(1), 9-18.

Ikonen, J., Pitkanen, T., Kosse, P., Ciszek, R., Kolehmainen, M. and Miettinen, I.T. 2017. On-line detection of Escherichia coli intrusion in a pilot-scale drinking water distribution system. Journal of Environmental Management 198(Pt 1), 384-392.

Ke, Y., Sun, W., Chen, Z., Zhu, Y., Chen, X., Yan, S., Li, Y. and Xie, S. 2023. Effects of disinfectant type and dosage on biofilm's activity, viability, microbiome and antibiotic resistome in bench-scale drinking water distribution systems. Water Research, 120958.

Kim, E.J., Herrera, J.E., Huggins, D., Braam, J. and Koshowski, S. 2011. Effect of pH on the concentrations of lead and trace contaminants in drinking water: a combined batch, pipe loop and sentinel home study. Water Research 45(9), 2763-2774.

Knights, D., Kuczynski, J., Charlson, E.S., Zaneveld, J., Mozer, M.C., Collman, R.G., Bushman, F.D., Knight, R. and Kelley, S.T. 2011. Bayesian community-wide culture-independent microbial source tracking. Nature Methods 8(9), 761-763.

Kolde, R. 2013. A package for drawing pretty heatmaps in R. Pheatmap: Pretty Heatmaps.

Kooij, D.v.d. 1992. Assimilable organic carbon as an indicator of bacterial regrowth. Journal‐American Water Works Association 84(2), 57-65.

Lautenschlager, K., Boon, N., Wang, Y., Egli, T. and Hammes, F. 2010. Overnight stagnation of drinking water in household taps induces microbial growth and changes in community composition. Water Research 44(17), 4868-4877.

Lee, W.H., Pressman, J.G. and Wahman, D.G. 2018. Three-dimensional free chlorine and monochloramine biofilm penetration: correlating penetration with biofilm activity and viability. Environmental Science & Technology 52(4), 1889-1898.

Lee, W.H., Wahman, D.G., Bishop, P.L. and Pressman, J.G. 2011. Free chlorine and monochloramine application to nitrifying biofilm: comparison of biofilm penetration, activity, and viability. Environmental Science &

Technology 45(4), 1412-1419.
Legendre, P. and Anderson, M.J. 1999. Distance-based redundancy analysis: testing multispecies responses in multifactorial ecological experiments. Ecological Monographs 69(1), 1-24.
Lehtola, M.J., Laxander, M., Miettinen, I.T., Hirvonen, A., Vartiainen, T. and Martikainen, P.J. 2006. The effects of changing water flow velocity on the formation of biofilms and water quality in pilot distribution system consisting of copper or polyethylene pipes. Water Research 40(11), 2151-2160.
Lehtola, M.J., Nissinen, T.K., Miettinen, I.T., Martikainen, P.J. and Vartiainen, T. 2004. Removal of soft deposits from the distribution system improves the drinking water quality. Water Research 38(3), 601-610.
Li, D., Li, Z., Yu, J., Cao, N., Liu, R. and Yang, M. 2010. Characterization of bacterial community structure in a drinking water distribution system during an occurrence of red water. Applied and Environmental Microbiology 76(21), 7171-7180.
Li, H., Yu, H., Liang, Y., Zhang, X., Yang, D., Wang, L., Shi, D., Chen, T., Zhou, S., Yin, J., Yang, Z., Li, J. and Jin, M. 2023. Extended chloramination significantly enriched intracellular antibiotic resistance genes in drinking water treatment plants. Water Research 232, 119689.
Li, W., Wang, F., Zhang, J., Qiao, Y., Xu, C., Liu, Y., Qian, L., Li, W. and Dong, B. 2016. Community shift of biofilms developed in a full-scale drinking water distribution system switching from different water sources. Science of the Total Environment 544, 499-506.
Liao, X., Chen, C., Zhang, J., Dai, Y., Zhang, X. and Xie, S. 2015. Operational performance, biomass and microbial community structure: impacts of backwashing on drinking water biofilter. Environmental Science and Pollution Research 22(1), 546-554.
Liebana, R., Modin, O., Persson, F., Szabo, E., Hermansson, M. and Wilen, B.M. 2019. Combined deterministic and stochastic processes control microbial succession in replicate granular biofilm reactors. Environmental Science & Technology 53(9), 4912-4921.
Lin, H., Zhang, S., Zhang, S., Lin, W. and Yu, X. 2017. The function of advanced treatment process in a drinking water treatment plant with organic matter-polluted source water. Environmental Science and Pollution Research 24(10), 8924-8932.
Ling, F., Hwang, C., LeChevallier, M.W., Andersen, G.L. and Liu, W.T. 2016. Core-satellite populations and seasonality of water meter biofilms in a metropolitan drinking water distribution system. The ISME Journal 10(3), 582-595.
Ling, F., Whitaker, R., LeChevallier, M.W. and Liu, W.T. 2018. Drinking water microbiome assembly induced by water stagnation. The ISME Journal 12(6), 1520-1531.
Liu, G., Bakker, G.L., Li, S., Vreeburg, J.H., Verberk, J.Q., Medema, G.J., Liu, W.T. and Van Dijk, J.C. 2014. Pyrosequencing reveals bacterial communities in unchlorinated drinking water distribution system: an integral study of bulk water, suspended solids, loose deposits, and pipe wall biofilm. Environmental Science & Technology 48(10), 5467-5476.
Liu, G., Ling, F., van der Mark, E., Zhang, X., Knezev, A., Verberk, J., van der Meer, W., Medema, G., Liu, W. and van Dijk, J. 2016a. Comparison of particle-associated bacteria from a drinking water treatment plant and distribution reservoirs with different water sources. Scientific Reports 6, 20367.
Liu, G., Ling, F.Q., Magic-Knezev, A., Liu, W.T., Verberk, J.Q. and Van Dijk, J.C. 2013a. Quantification and identification of particle-associated bacteria in unchlorinated drinking water from three treatment plants by cultivation-independent methods. Water Research 47(10), 3523-3533.
Liu, G., Lut, M.C., Verberk, J.Q. and Van Dijk, J.C. 2013b. A comparison of additional treatment processes to limit particle accumulation and microbial growth during drinking water distribution. Water Research 47(8), 2719-2728.
Liu, G., Tao, Y., Zhang, Y., Lut, M., Knibbe, W.J., van der Wielen, P., Liu, W., Medema, G. and van der Meer, W. 2017a. Hotspots for selected metal elements and microbes accumulation and the corresponding water quality deterioration potential in an unchlorinated drinking water distribution system. Water Research 124, 435-445.
Liu, G., Verberk, J. and Van Dijk, J. 2013c. Bacteriology of drinking water distribution systems: an integral and multidimensional review. Applied Microbiology and Biotechnology 97, 9265-9276.
Liu, G., Zhang, Y., Knibbe, W.J., Feng, C., Liu, W., Medema, G. and van der Meer, W. 2017b. Potential impacts of changing supply-water quality on drinking water distribution: A review. Water Research 116, 135-148.
Liu, G., Zhang, Y., Liu, X., Hammes, F., Liu, W.-T., Medema, G., Wessels, P. and Van der Meer, W.G. 2020. 360-degrees distribution of biofilm quantity and community in an operational unchlorinated drinking water distribution pipe. Environmental Science & Technology.
Liu, G., Zhang, Y., van der Mark, E., Magic-Knezev, A., Pinto, A., van den Bogert, B., Liu, W., van der Meer, W. and Medema, G. 2018. Assessing the origin of bacteria in tap water and distribution system in an unchlorinated drinking water system by SourceTracker using microbial community fingerprints. Water Research 138, 86-96.
Liu, L., Xing, X., Hu, C. and Wang, H. 2019. O3-BAC-Cl2: A multi-barrier process controlling the regrowth of

opportunistic waterborne pathogens in drinking water distribution systems. Journal of Environmental Sciences 76, 142-153.

Liu, S., Gunawan, C., Barraud, N., Rice, S.A., Harry, E.J. and Amal, R. 2016b. Understanding, monitoring, and controlling biofilm growth in drinking water distribution systems. Environmental Science & Technology 50(17), 8954-8976.

Loret, J.-F. and Dumoutier, N. 2019. Non-tuberculous mycobacteria in drinking water systems: A review of prevalence data and control means. International Journal of Hygiene and Environmental Health 222(4), 628-634.

Lucas, S., Coombes, P. and Sharma, A. 2010. The impact of diurnal water use patterns, demand management and rainwater tanks on water supply network design. Water Science and Technology: Water Supply 10(1), 69-80.

Luo, C., Tsementzi, D., Kyrpides, N., Read, T. and Konstantinidis, K.T. 2012. Direct comparisons of Illumina vs. Roche 454 sequencing technologies on the same microbial community DNA sample. PLoS One 7(2), e30087.

Ma, X., Li, G., Yu, Y., Chen, R., Zhang, Y., Tao, H., Zhang, G. and Shi, B. 2019. Spatial variation of loose deposit characteristics in a 40 km long operational drinking water distribution system. Environmental Science: Water Research & Technology 5(10), 1689-1698.

Mackay, W.G., Gribbon, L.T., Barer, M.R. and Reid, D.C. 1998. Biofilms in drinking water systems - A possible reservoir for Helicobacter pylori. Water Science and Technology 38(12), 181-185.

Magic-Knezev, A. and Van Der Kooij, D. 2004. Optimisation and significance of ATP analysis for measuring active biomass in granular activated carbon filters used in water treatment. Water Research 38(18), 3971-3979.

Magic-Knezev, A., Wullings, B. and Van der Kooij, D. 2009. Polaromonas and Hydrogenophaga species are the predominant bacteria cultured from granular activated carbon filters in water treatment. Journal of Applied Microbiology 107(5), 1457-1467.

Makris, K.C., Andra, S.S. and Botsaris, G. 2014. Pipe scales and biofilms in drinking-water distribution systems: undermining finished water quality. Critical Reviews in Environmental Science and Technology 44(13), 1477-1523.

Manickum, T. 2020. Total colony counts (TCC) by flow cytometry (FCM) should replace the Heterotrophic Plate Count (HPC) test for bacteriological enumeration of water-some recent developments in flow cytometry: A review. Hydrology: Current Research 11(3).

Martiny, A.C., Jorgensen, T.M., Albrechtsen, H.J., Arvin, E. and Molin, S. 2003. Long-term succession of structure and diversity of a biofilm formed in a model drinking water distribution system. Applied and Environmental Microbiology 69(11), 6899-6907.

Matsui, Y., Yamagishi, T., Terada, Y., Matsushita, T. and Inoue, T. 2007. Suspended particles and their characteristics in water mains: developments of sampling methods. Journal of Water Supply: Research and Technology—AQUA 56(1), 13-24.

McCarthy, D.T., Jovanovic, D., Lintern, A., Teakle, I., Barnes, M., Deletic, A., Coleman, R., Rooney, G., Prosser, T., Coutts, S., Hipsey, M.R., Bruce, L.C. and Henry, R. 2017. Source tracking using microbial community fingerprints: Method comparison with hydrodynamic modelling. Water Research 109, 253-265.

McDaniel, E.A., Wahl, S.A., Ishii, S., Pinto, A., Ziels, R., Nielsen, P.H., McMahon, K.D. and Williams, R.B.H. 2021. Prospects for multi-omics in the microbial ecology of water engineering. Water Research 205, 117608.

McGill, B.J., Maurer, B.A. and Weiser, M.D. 2006. Empirical evaluation of neutral theory. Ecology 87(6), 1411-1423.

Mei, R. and Liu, W.T. 2019. Quantifying the contribution of microbial immigration in engineered water systems. Microbiome 7(1), 144.

Mi, Z., Dai, Y., Xie, S., Chen, C. and Zhang, X. 2015. Impact of disinfection on drinking water biofilm bacterial community. Journal of Environmental Sciences 37, 200-205.

Miller, H.C., Wylie, J., Dejean, G., Kaksonen, A.H., Sutton, D., Braun, K. and Puzon, G.J. 2015. Reduced efficiency of chlorine disinfection of Naegleria fowleri in a drinking water distribution biofilm. Environmental Science & Technology 49(18), 11125-11131.

Mounce, S., Gaffney, J., Boult, S. and Boxall, J. 2015. Automated data-driven approaches to evaluating and interpreting water quality time series data from water distribution systems. Journal of Water Resources Planning and Management 141(11), 04015026.

Mussared, A., Fabris, R., Vreeburg, J., Jelbart, J. and Drikas, M. 2019. The origin and risks associated with loose deposits in a drinking water distribution system. Water Supply 19(1), 291-302.

Ng, W.J., Tan, C.T. and Bae, S. 2021. Effects of monochloramine on culturability, viability and persistence of Pseudomonas putida and tap water mixed bacterial community. Applied Microbiology and Biotechnology

105(9), 3799-3810.
Niederdorfer, R., Fragner, L., Yuan, L., Hausherr, D., Wei, J., Magyar, P., Joss, A., Lehmann, M.F., Ju, F. and Burgmann, H. 2021. Distinct growth stages controlled by the interplay of deterministic and stochastic processes in functional anammox biofilms. Water Research 200, 117225.
Ning, D., Deng, Y., Tiedje, J.M. and Zhou, J. 2019. A general framework for quantitatively assessing ecological stochasticity. Proceedings of the National Academy of Sciences 116(34), 16892-16898.
Noyce, G.L., Fulthorpe, R., Gorgolewski, A., Hazlett, P., Tran, H. and Basiliko, N. 2016. Soil microbial responses to wood ash addition and forest fire in managed Ontario forests. Applied Soil Ecology 107, 368-380.
Ntushelo, K. 2013. Identifying bacteria and studying bacterial diversity using the 16S ribosomal RNA gene-based sequencing techniques: A review. African Journal of Microbiology Research 7, 5533-5540.
Ofiteru, I.D., Lunn, M., Curtis, T.P., Wells, G.F., Criddle, C.S., Francis, C.A. and Sloan, W.T. 2010. Combined niche and neutral effects in a microbial wastewater treatment community. Proceedings of the National Academy of Sciences 107(35), 15345-15350.
Ohkouchi, Y., Ly, B.T., Ishikawa, S., Kawano, Y. and Itoh, S. 2013. Determination of an acceptable assimilable organic carbon (AOC) level for biological stability in water distribution systems with minimized chlorine residual. Environmental Monitoring and Assessment 185, 1427-1436.
Paul, E., Ochoa, J.C., Pechaud, Y., Liu, Y. and Line, A. 2012. Effect of shear stress and growth conditions on detachment and physical properties of biofilms. Water Research 46(17), 5499-5508.
Pérez-Cobas, A.E., Gomez-Valero, L. and Buchrieser, C. 2020. Metagenomic approaches in microbial ecology: an update on whole-genome and marker gene sequencing analyses. Microbial Genomics 6(8).
Pick, F.C., Fish, K.E. and Boxall, J.B. 2021. Assimilable organic carbon cycling within drinking water distribution systems. Water Research 198, 117147.
Pinto, A.J., Xi, C. and Raskin, L. 2012. Bacterial community structure in the drinking water microbiome is governed by filtration processes. Environmental Science & Technology 46(16), 8851-8859.
Poças, A. 2014. Discolouration loose deposits in distribution systems: composition, behaviour and practical aspects.
Polanska, M., Huysman, K. and van Keer, C. 2005. Investigation of assimilable organic carbon (AOC) in flemish drinking water. Water Research 39(11), 2259-2266.
Potgieter, S., Pinto, A., Sigudu, M., du Preez, H., Ncube, E. and Venter, S. 2018. Long-term spatial and temporal microbial community dynamics in a large-scale drinking water distribution system with multiple disinfectant regimes. Water Research 139, 406-419.
Potgieter, S.C., Dai, Z., Venter, S.N., Sigudu, M. and Pinto, A.J. 2020. Microbial nitrogen metabolism in chloraminated drinking water reservoirs. Msphere 5(2).
Preciado, C.C., Husband, S., Boxall, J., Del Olmo, G., Soria-Carrasco, V., Maeng, S.K. and Douterelo, I. 2021. Intermittent water supply impacts on distribution system biofilms and water quality. Water Research 201, 117372.
Prest, E.I., El-Chakhtoura, J., Hammes, F., Saikaly, P.E., van Loosdrecht, M.C. and Vrouwenvelder, J.S. 2014. Combining flow cytometry and 16S rRNA gene pyrosequencing: a promising approach for drinking water monitoring and characterization. Water Research 63, 179-189.
Prest, E.I., Hammes, F., van Loosdrecht, M.C. and Vrouwenvelder, J.S. 2016a. Biological Stability of Drinking Water: Controlling Factors, Methods, and Challenges. Frontiers in Microbiology 7, 45.
Prest, E.I., Schaap, P.G., Besmer, M.D. and Hammes, F. 2021. Dynamic hydraulics in a drinking water distribution system influence suspended particles and turbidity, but not microbiology. Water 13(1), 109.
Prest, E.I., Weissbrodt, D.G., Hammes, F., van Loosdrecht, M.C. and Vrouwenvelder, J.S. 2016b. Long-term bacterial dynamics in a full-scale drinking water distribution system. PLoS One 11(10), e0164445.
Quast, C., Pruesse, E., Yilmaz, P., Gerken, J., Schweer, T., Yarza, P., Peplies, J. and Glöckner, F.O. 2012. The SILVA ribosomal RNA gene database project: improved data processing and web-based tools. Nucleic Acids Research 41(D1), D590-D596.
Reiber, S. and Dostal, G. 2000. Arsenic and old pipes—a mysterious liaison: well water disinfection sparks surprises. Opflow 26(3), 1-14.
Revetta, R.P., Gomez-Alvarez, V., Gerke, T.L., Curioso, C., Santo Domingo, J.W. and Ashbolt, N.J. 2013. Establishment and early succession of bacterial communities in monochloramine-treated drinking water biofilms. FEMS Microbiology Ecology 86(3), 404-414.
Richards, C.L., Broadaway, S.C., Eggers, M.J., Doyle, J., Pyle, B.H., Camper, A.K. and Ford, T.E. 2015. Detection of pathogenic and non-pathogenic bacteria in drinking water and associated biofilms on the crow reservation, Montana, USA. Microbial Ecology 76, 52-63.
Richardson, S.D. 2003. Disinfection by-products and other emerging contaminants in drinking water. TrAC Trends in Analytical Chemistry 22(10), 666-684.
Riesenfeld, C.S., Schloss, P.D. and Handelsman, J. 2004. Metagenomics: genomic analysis of microbial communities. Annual Review of Genetics 38, 525-552.

Rodríguez-Martínez, S., Sharaby, Y., Pecellín, M., Brettar, I., Höfle, M. and Halpern, M. 2015. Spatial distribution of Legionella pneumophila MLVA-genotypes in a drinking water system. Water Research 77, 119-132.

Roeder, R.S., Lenz, J., Tarne, P., Gebel, J., Exner, M. and Szewzyk, U. 2010. Long-term effects of disinfectants on the community composition of drinking water biofilms. International Journal of Hygiene and Environmental Health 213(3), 183-189.

Rubulis, J., Verberk, J., Vreeburg, J., Gruškevica, K. and Juhna, T. 2008 Chemical and microbial composition of loose deposits in drinking water distribution systems. Proceedings of the, 7th International Conference on Environmental Engineering, pp. 22-23.

Sanger, F., Nicklen, S. and Coulson, A.R. 1977. DNA sequencing with chain-terminating inhibitors. Proceedings of the National Academy of Sciences 74(12), 5463-5467.

Sauer, K., Stoodley, P., Goeres, D.M., Hall-Stoodley, L., Burmølle, M., Stewart, P.S. and Bjarnsholt, T. 2022. The biofilm life cycle: expanding the conceptual model of biofilm formation. Nature Reviews Microbiology 20(10), 608-620.

Scharfenaker, M.A. 2002. White papers set stage for regulating distribution system water quality. Journal AWWA 94(10), 14-24.

Schleheck, D., Barraud, N., Klebensberger, J., Webb, J.S., McDougald, D., Rice, S.A. and Kjelleberg, S. 2009. Pseudomonas aeruginosa PAO1 preferentially grows as aggregates in liquid batch cultures and disperses upon starvation. PLoS One 4(5), e5513.

Schuster, S.C. 2008. Next-generation sequencing transforms today's biology. Nature Methods 5(1), 16-18.

Schwake, D.O., Garner, E., Strom, O.R., Pruden, A. and Edwards, M.A. 2016. Legionella DNA markers in tap water coincident with a spike in Legionnaires' disease in Flint, MI. Environmental Science & Technology Letters 3(9), 311-315.

Sekar, R., Deines, P., Machell, J., Osborn, A.M., Biggs, C.A. and Boxall, J.B. 2012. Bacterial water quality and network hydraulic characteristics: a field study of a small, looped water distribution system using culture-independent molecular methods. Journal of Applied Microbiology 112(6), 1220-1234.

Servais, P., Laurent, P. and Randon, G. 1995. Comparison of the bacterial dynamics in various French distribution systems. Aqua-London Then Oxford-Journal of the International Water Supply Association- 44, 10-10.

Sevillano, M., Dai, Z., Calus, S., Bautista-de Los Santos, Q.M., Eren, A.M., van der Wielen, P., Ijaz, U.Z. and Pinto, A.J. 2020. Differential prevalence and host-association of antimicrobial resistance traits in disinfected and non-disinfected drinking water systems. Science of the Total Environment 749, 141451.

Shannon, M.A., Bohn, P.W., Elimelech, M., Georgiadis, J.G., Marinas, B.J. and Mayes, A.M. 2008. Science and technology for water purification in the coming decades. Nature 452(7185), 301-310.

Shen, Y., Huang, C., Lin, J., Wu, W., Ashbolt, N.J., Liu, W.T. and Nguyen, T.H. 2017. Effect of disinfectant exposure on Legionella pneumophila associated with simulated drinking water biofilms: release, inactivation, and infectivity. Environmental Science & Technology 51(4), 2087-2095.

Shendure, J. and Ji, H. 2008. Next-generation DNA sequencing. Nature Biotechnology 26(10), 1135-1145.

Shi, P., Jia, S., Zhang, X.X., Zhang, T., Cheng, S. and Li, A. 2013. Metagenomic insights into chlorination effects on microbial antibiotic resistance in drinking water. Water Research 47(1), 111-120.

Singla, S., Harjai, K. and Chhibber, S. 2013. Susceptibility of different phases of biofilm of Klebsiella pneumoniae to three different antibiotics. The Journal of Antibiotics 66(2), 61-66.

Sloan, W.T., Lunn, M., Woodcock, S., Head, I.M., Nee, S. and Curtis, T.P. 2006. Quantifying the roles of immigration and chance in shaping prokaryote community structure. Environmental Microbiology 8(4), 732-740.

Sly, L.I., Hodgkinson, M.C. and Arunpairojana, V. 1990. Deposition of manganese in a drinking water distribution system. Applied and Environmental Microbiology 56(3), 628-639.

Smeets, P.W.M.H., Medema, G.J. and van Dijk, J.C. 2009. The Dutch secret: how to provide safe drinking water without chlorine in the Netherlands. Drinking Water Engineering and Science 2(1), 1-14.

Sousi, M., Liu, G., Salinas-Rodriguez, S.G., Chen, L., Dusseldorp, J., Wessels, P., Schippers, J.C., Kennedy, M.D. and van der Meer, W. 2020. Multi-parametric assessment of biological stability of drinking water produced from groundwater: Reverse osmosis vs. conventional treatment. Water Research 186, 116317.

Sprockett, D.D., Martin, M., Costello, E.K., Burns, A.R., Holmes, S.P., Gurven, M.D. and Relman, D.A. 2020. Microbiota assembly, structure, and dynamics among Tsimane horticulturalists of the Bolivian Amazon. Nature Communications 11(1), 3772.

Stegen, J.C., Lin, X., Fredrickson, J.K., Chen, X., Kennedy, D.W., Murray, C.J., Rockhold, M.L. and Konopka, A. 2013. Quantifying community assembly processes and identifying features that impose them. The ISME Journal 7(11), 2069-2079.

Stojicic, S., Shen, Y. and Haapasalo, M. 2013. Effect of the source of biofilm bacteria, level of biofilm maturation, and type of disinfecting agent on the susceptibility of biofilm bacteria to antibacterial agents. Journal of Endodontics 39(4), 473-477.

Storey, M.V., van der Gaag, B. and Burns, B.P. 2011. Advances in on-line drinking water quality monitoring and

early warning systems. Water Research 45(2), 741-747.
Sze, M.A. and Schloss, P.D. 2019. The impact of DNA polymerase and number of rounds of amplification in PCR on 16S rRNA gene sequence data. Msphere 4(3), 10-1128.
Tamaki, H., Wright, C.L., Li, X., Lin, Q., Hwang, C., Wang, S., Thimmapuram, J., Kamagata, Y. and Liu, W.T. 2011. Analysis of 16S rRNA amplicon sequencing options on the roche/454 next-generation titanium sequencing platform. PLoS ONE 6(9).
Tan, B., Ng, C., Nshimyimana, J.P., Loh, L.L., Gin, K.Y. and Thompson, J.R. 2015. Next-generation sequencing (NGS) for assessment of microbial water quality: current progress, challenges, and future opportunities. Frontiers in Microbiology 6, 1027.
Tang, Z., Hong, S., Xiao, W. and Taylor, J. 2006. Characteristics of iron corrosion scales established under blending of ground, surface, and saline waters and their impacts on iron release in the pipe distribution system. Corrosion Science 48(2), 322-342.
Ternes, T., Joss, A. and Oehlmann, J. 2015. Occurrence, fate, removal and assessment of emerging contaminants in water in the water cycle (from wastewater to drinking water). Water Research 72, 1-2.
Tian, R., Ning, D., He, Z., Zhang, P., Spencer, S.J., Gao, S., Shi, W., Wu, L., Zhang, Y. and Yang, Y. 2020. Small and mighty: adaptation of superphylum Patescibacteria to groundwater environment drives their genome simplicity. Microbiome 8, 1-15.
Tokeshi, M. 1990. Niche apportionment or random assortment: species abundance patterns revisited. The Journal of Animal Ecology, 1129-1146.
Torvinen, E., Suomalainen, S., Lehtola, M.J., Miettinen, I.T., Zacheus, O., Paulin, L., Katila, M.L. and Martikainen, P.J. 2004. Mycobacteria in water and loose deposits of drinking water distribution systems in Finland. Applied and Environmental Microbiology 70(4), 1973-1981.
Tsvetanova, Z.G. and Hoekstra, E.J. 2010. The effect of the surface-to-volume contact ratio on the biomass production potential of the pipe products in contact with drinking water. Water Science and Technology: Water Supply 10(1), 105-112.
Van Der Wende, E., Characklis, W.G. and Smith, D.B. 1989. Biofilms and bacterial drinking water quality. Water Research 23(10), 1313-1322.
van der Wielen, P.W. and van der Kooij, D. 2010. Effect of water composition, distance and season on the adenosine triphosphate concentration in unchlorinated drinking water in the Netherlands. Water Research 44(17), 4860-4867.
van der Wielen, P.W. and van der Kooij, D. 2013. Nontuberculous mycobacteria, fungi, and opportunistic pathogens in unchlorinated drinking water in the Netherlands. Applied and Environmental Microbiology 79(3), 825-834.
Venkataraman, A., Bassis, C.M., Beck, J.M., Young, V.B., Curtis, J.L., Huffnagle, G.B. and Schmidt, T.M. 2015. Application of a neutral community model to assess structuring of the human lung microbiome. MBio 6(1).
Verberk, J., Hamilton, L., O'halloran, K., Van Der Horst, W. and Vreeburg, J. 2006. Analysis of particle numbers, size and composition in drinking water transportation pipelines: results of online measurements. Water Science and Technology: Water Supply 6(4), 35-43.
Verberk, J.Q.J.C., Vreeburg, J.H.G., Rietveld, L.C. and Van Dijk, J.C. 2009. Particulate fngerprinting of water quality in the distribution system. Water SA 35(2), 192-199.
Vreeburg, I.J. and Boxall, J.B. 2007. Discolouration in potable water distribution systems: A review. Water Research 41(3), 519-529.
Vreeburg, J., Schippers, D., Verberk, J. and Van Dijk, J. 2008. Impact of particles on sediment accumulation in a drinking water distribution system. Water Research 42(16), 4233-4242.
Waak, M.B., Hozalski, R.M., Halle, C. and LaPara, T.M. 2019a. Comparison of the microbiomes of two drinking water distribution systems-with and without residual chloramine disinfection. Microbiome 7(1), 87.
Waak, M.B., LaPara, T.M., Halle, C. and Hozalski, R.M. 2019b. Nontuberculous mycobacteria in two drinking water distribution systems and the role of residual disinfection. Environmental Science & Technology 53(15), 8563-8573.
Walker, A.W., Martin, J.C., Scott, P., Parkhill, J., Flint, H.J. and Scott, K.P. 2015. 16S rRNA gene-based profiling of the human infant gut microbiota is strongly influenced by sample processing and PCR primer choice. Microbiome 3(1), 1-11.
Wang, H., Edwards, M., Falkinham, J.O., III and Pruden, A. 2012. Molecular survey of the occurrence of Legionella spp., Mycobacterium spp., Pseudomonas aeruginosa, and amoeba hosts in two chloraminated drinking water distribution systems. Applied and Environmental Microbiology 78(17), 6285-6294.
Wang, H., Edwards, M.A., Falkinham III, J.O. and Pruden, A. 2013. Probiotic approach to pathogen control in premise plumbing systems? A review. Environmental Science & Technology 47(18), 10117-10128.
Wang, H., Masters, S., Edwards, M.A., Falkinham, J.O., 3rd and Pruden, A. 2014a. Effect of disinfectant, water age, and pipe materials on bacterial and eukaryotic community structure in drinking water biofilm.

Environmental Science & Technology 48(3), 1426-1435.
Wang, H., Proctor, C.R., Edwards, M.A., Pryor, M., Santo Domingo, J.W., Ryu, H., Camper, A.K., Olson, A. and Pruden, A. 2014b. Microbial community response to chlorine conversion in a chloraminated drinking water distribution system. Environmental Science & Technology 48(18), 10624-10633.
Williams, M.M., Domingo, J.W., Meckes, M.C., Kelty, C.A. and Rochon, H.S. 2004. Phylogenetic diversity of drinking water bacteria in a distribution system simulator. Journal of Applied Microbiology 96(5), 954-964.
Wingender, J. and Flemming, H.C. 2011. Biofilms in drinking water and their role as reservoir for pathogens. International Journal of Hygiene and Environmental Health 214(6), 417-423.
Wu, H., Zhang, J., Mi, Z., Xie, S., Chen, C. and Zhang, X. 2015. Biofilm bacterial communities in urban drinking water distribution systems transporting waters with different purification strategies. Applied Microbiology and Biotechnology 99(4), 1947-1955.
Xing, X., Wang, H., Hu, C. and Liu, L. 2018a. Characterization of bacterial community and iron corrosion in drinking water distribution systems with O3-biological activated carbon treatment. Journal of Environmental Sciences 69, 192-204.
Xing, X., Wang, H., Hu, C. and Liu, L. 2018b. Effects of phosphate-enhanced ozone/biofiltration on formation of disinfection byproducts and occurrence of opportunistic pathogens in drinking water distribution systems. Water Research 139, 168-176.
Zacheus, O.M., Lehtola, M.J., Korhonen, L.K. and Martikainen, P.J. 2001. Soft deposits, the key site for microbial growth in drinking water distribution networks. Water Research 35(7), 1757-1765.
Zahran, S., McElmurry, S.P., Kilgore, P.E., Mushinski, D., Press, J., Love, N.G., Sadler, R.C. and Swanson, M.S. 2018. Assessment of the Legionnaires' disease outbreak in Flint, Michigan. Proceedings of the National Academy of Sciences 115(8), E1730-E1739.
Zhang, H., Chang, F., Shi, P., Ye, L., Zhou, Q., Pan, Y. and Li, A. 2019. Antibiotic resistome alteration by different disinfection strategies in a full-scale drinking water treatment plant deciphered by metagenomic assembly. Environmental Science & Technology 53(4), 2141-2150.
Zhang, H., Xu, L., Huang, T., Yan, M., Liu, K., Miao, Y., He, H., Li, S. and Sekar, R. 2021. Combined effects of seasonality and stagnation on tap water quality: Changes in chemical parameters, metabolic activity and co-existence in bacterial community. Journal of Hazardous Materials 403, 124018.
Zhang, Q. 2009. The South-to-North Water Transfer Project of China: environmental implications and monitoring strategy. JAWRA Journal of the American Water Resources Association 45(5), 1238-1247.
Zhang, X. and Bishop, P.L. 2003. Biodegradability of biofilm extracellular polymeric substances. Chemosphere 50(1), 63-69.
Zhang, X., Lin, T., Jiang, F., Zhang, X., Wang, S. and Zhang, S. 2022. Impact of pipe material and chlorination on the biofilm structure and microbial communities. Chemosphere 289, 133218.
Zhang, Y. and Liu, W.-T. 2019. The application of molecular tools to study the drinking water microbiome–Current understanding and future needs. Critical Reviews in Environmental Science and Technology 49(13), 1188-1235.
Zhou, J. and Ning, D. 2017. Stochastic community assembly: does it matter in microbial ecology? Microbiology and Molecular Biology Reviews 81(4), e00002-00017.
Zhou, L.-l., Zhang, Y.-j. and Li, G.-b. 2009. Effect of pipe material and low level disinfectants on biofilm development in a simulated drinking water distribution system. Journal of Zhejiang University-SCIENCE A 10(5), 725-731.
Zhu, Z., Wu, C., Zhong, D., Yuan, Y., Shan, L. and Zhang, J. 2014. Effects of pipe materials on chlorine-resistant biofilm formation under long-term high chlorine level. Applied Biochemistry and Biotechnology 173(6), 1564-1578.
Zlatanovic, L., van der Hoek, J.P. and Vreeburg, J.H.G. 2017. An experimental study on the influence of water stagnation and temperature change on water quality in a full-scale domestic drinking water system. Water Research 123, 761-772.

Acknowledgement

致谢

The PhD journey is a big adventure, which is full of unknown, exciting moments, and challenging time. It took me six years to get there. During this journey, there are so many people who have helped, supported and encouraged me. Without their support and encouragement, I cannot complete this adventure successfully. At this time point, I would like to extend my heartfelt thanks to them.

First of all, a special thanks to my daily supervisor (also one of my promoters) Prof. Gang Liu. Gang, thank you for always being so supportive and patient. I did enjoy the time that we worked together in the first two years of my PhD, before you went back to China to start your own research group. I am very grateful that you've never diminished your support for me as I could understand you must be fully occupied during the first stage of team-building. Your passion, confidence, and critical thinking towards research and life deeply affect me. From you, I know how important the communication is for being a good researcher apart from hard work.

I would like to thank my promoters Prof. Walter van der Meer and Prof. Gertjan Medema. Walter, you are always kind and supportive. Without your great support, we wouldn't be able to conduct so much interesting research and get to where we are. I cherish the travel time to China with you in 2019. At that time, I was impressed by your sense of humor. Gertjan, thank you for being my promoter, and I am so proud to be one of your PhD students. I was greatly expressed by your critical thinking. Many times, your question "what's your research question?" and "what's the storyline here" reminds me of the direction I should go forward.

My appreciation also goes to my students (Master & Bachelor), who contributed so much to my PhD work. Certainly, I learned a lot as well from them. Xinyue, Kongwei, I did enjoyed the time that we worked together in the Waterlab and the lab at Leiden University, and also the discussions about the exploration of the applications on the nanopore sequencing in drinking water systems. Haoran, Fei, Chen, Ziyan, Rayen, Jeffery, Cherry, Elif, Divvay, Xinquan, thank you all for helping me with the field and pilot work. We did so much filtration work, and drove across every streets. Without your help, I cannot finish so much work during my PhD.

My thanks also go to my colleagues from Oasen, Maarten, Irene, Sara. With so many field and pilot studies in my PhD, I cannot make the systems (OMSS, pilot) work so successfully without your support and timely help.

I also very appreciate the short visiting time to Prof. Amy pruden's group in the US. Through this trip, I know Joyce, songyang, Abe. I greatly appreciated the discussions about the pilot study with them.

I would also like to acknowledge Yujia, who helped me and my students work in their lab. I treasured our roommate's time, the Den Haag beach time, the BBQ time, and also the girls' conversation time. Qi, thank you very much for encouraging and also 'getting' me to finalize these courses needed for the graduation when I was struggling with the pilot system running. Gratitude also should go to my colleagues, 'big brothers and sisters' - Xuedong, Ran, Jenny, Peng, Cuijie, Feifei, Nan (Zheyi), Hongxiao, Ka Leung, Liangfu, Ruxin; 'friends from the big office (4.96)' - Mingliang, Bin, Max, Zhe, Hongbo, Shuo (Dengxiao), Jian, Bruno, Carina, Lenno, Emiel, Sara…; big family from Gang's group in China. Without your accompany, my PhD life wouldn't be that colourful.

Finally, I would like to express my greatest thanks to my family. Thanks to my father and mother, their selfless love accompanied me during my whole PhD journey. Thanks to my brother and my sister-in-law, and their daughter for accompanying my parents, and bringing us so much happiness. Greatest thanks also to my husband, Linfei, for your great patience, support, and love.

May, 14th, 2023

Beijing

Lihua Chen

List of Publications

Peer reviewed journal papers

Chen, L., Li, X., Medema, G., van der Meer, W., & Liu, G. (2023). Transition effects in an unchlorinated drinking water system following the introduction of partial reverse osmosis. Nature Water, 1-10.

Chen, L., Li, X., van der Meer, W., Medema, G., & Liu, G. (2022). Capturing and tracing the spatiotemporal variations of planktonic and particle-associated bacteria in an unchlorinated drinking water distribution system. Water Research, 219, 118589.

Chen, L., Zhai, Y., van der Mark, E., Liu, G., van der Meer, W., & Medema, G. (2021). Microbial community assembly and metabolic function in top layers of slow sand filters for drinking water production. Journal of Cleaner Production, 294, 126342.

Zhai, Y., **Chen, L.**, Liu, G., Song, L., Arenas-Lago, D., Kong, L., ... & Vijver, M. G. (2021). Compositional and functional responses of bacterial community to titanium dioxide nanoparticles varied with soil heterogeneity and exposure duration. Science of the Total Environment, 773, 144895. (Co-first author)

Chen, L., Ling, F., Bakker, G., Liu, W. T., Medema, G., van der Meer, W., & Liu, G. (2020). Assessing the transition effects in a drinking water distribution system caused by changing supply water quality: an indirect approach by characterizing suspended solids. Water research, 168, 115159.

Sousi, M., Liu, G., Salinas-Rodriguez, S. G., **Chen, L.**, Dusseldorp, J., Wessels, P., ... & van der Meer, W. (2020). Multi-parametric assessment of biological stability of drinking water produced from groundwater: Reverse osmosis vs. conventional treatment. Water research, 186, 116317.

Chen, L., Medema, G., van der Meer, W., & Liu, G. (2024) Long-term Successional Dynamics in Drinking Water Distribution System Biofilms with and without Residual Disinfectants. To be submitted.

Peer reviewed journal papers in preparation:

Chen, L., Medema, G., van der Meer, W., & Liu, G. (2024) Characterizing drinking water microbiome by Nanopore metagenomic sequencing.

Chen, L., Medema, G., van der Meer, W., & Liu, G. (2024) Profiling of antibiotic resistance genes and their hosts in drinking water distribution systems by Oxford Nanopore MinION^{TM} Sequencing.

Chen, L., Medema, G., van der Meer, W., & Liu, G. (2024) Effects of disinfection strategies changes on microbial communities, pathogens, and antibiotic resistance genes: an integral study in simulated unchlorinated, chlorinated, and chloraminated DWDSs.

Chen, L., Medema, G., van der Meer, W., & Liu, G. (2024) High-throughput profiling and tracing the antibiotic resistance genes from raw water to tap water in two unchlorinated drinking water supply systems.

Chen, L., Medema, G., van der Meer, W., & Liu, G. (2024) Evaluation of DNA extraction methods for filtered drinking water.

Curriculum Vitae

Family name: Chen (陈)
Given name: Lihua (利华)
Email: lhchen91@gmail.com

Lihua Chen was born on the 10th of April, 1991, in Jiyuan, Henan Province, China. In 2014, she finished her bachelor study at Zhengzhou University of Aeronautics and started her master study in Environmental Engineering at Institute of Urban Environment, Chinese Academy of Sciences. After obtained her MSc degree in 2017, she started her PhD project at Delft University of Technology, under the supervision of Prof. Gertjan Medema, Prof. Walter van der Meer and Prof. Gang Liu. Her PhD study focused on the effects of water quality on biofilm in drinking water distribution systems.